Working Group on the Ecosystem Effects of Fishing Activities (WGECO)

Calderwood, Julia; Collie, Jeremy; Croll, Jasper; Greenstreet, Simon P. R.; Griffiths, Christian; Kenchington, Ellen; Kooten, Tobias van; Lynam, Christopher P.; Moriarty, M.; Ragnarsson, Stefán Áki

Total number of authors:
17

Link to article, DOI:
10.17895/ices.pub.4981

Publication date:
2019

Document Version
Publisher's PDF, also known as Version of record

Citation (APA):
Calderwood, J., Collie, J., Croll, J., Greenstreet, S. P. R., Griffiths, C., Kenchington, E., Kooten, T. V., Lynam, C. P., Moriarty, M., Ragnarsson, S. Á., Reid, D. G., Rindorf, A., Savina-Rolland, M., Sarrazin, V., Shephard, S., Smith, B., & Thompson, M. (2019). *Working Group on the Ecosystem Effects of Fishing Activities (WGECO)*. International Council for the Exploration of the Sea (ICES). ICES Scientific Report Vol. 1 No. 27
https://doi.org/10.17895/ices.pub.4981

WORKING GROUP ON THE ECOSYSTEM EFFECTS OF FISHING ACTIVITIES (WGECO)

VOLUME 1 | ISSUE 27

ICES SCIENTIFIC REPORTS

RAPPORTS
SCIENTIFIQUES DU CIEM

ICES INTERNATIONAL COUNCIL FOR THE EXPLORATION OF THE SEA
CIEM CONSEIL INTERNATIONAL POUR L'EXPLORATION DE LA MER

International Council for the Exploration of the Sea
Conseil International pour l'Exploration de la Mer

H.C. Andersens Boulevard 44-46
DK-1553 Copenhagen V
Denmark
Telephone (+45) 33 38 67 00
Telefax (+45) 33 93 42 15
www.ices.dk
info@ices.dk

ISSN number: 2618-1371 I

ICES Scientific Reports

Volume 1 | Issue 27

WORKING GROUP ON THE ECOSYSTEM EFFECTS OF FISHING ACTIVITIES (WGECO)

Recommended format for purpose of citation:

ICES. 2019. Working Group on the Ecosystem Effects of Fishing Activities (WGECO).
ICES Scientific Reports. 1:27. 148 pp. http://doi.org/10.17895/ices.pub.4981

Editors

Jeremy Collie • Stefán Áki Ragnarsson

Authors

Julia Calderwood • Jeremy Collie • Simon Greenstreet • Jasper Croll • Chris Griffiths • Ellen Kenchington • Tobias van Kooten • Chris Lynam • Meadhbh Moriarty • Stefán Ragnarsson • David Reid • Anna Rindorf • Marie Savina-Rolland • Victoria Sarrazin • Sam Shephard • Brian Smith • Murray Thompson

ICES International Council for the Exploration of the Sea
CIEM Conseil International pour l'Exploration de la Mer

Contents

i Executive summary

The 2019 meeting of WGECO was held at the International Council for the Exploration of the Sea, Copenhagen, Denmark from 8–16 April 2019. The meeting was attended by 16 delegates from eight countries and was chaired by Stefán Ragnarsson (Iceland) and Jeremy Collie (USA). The work conducted centred on three Terms of Reference that had been made by WGECO. In addition, a list of sensitive species prepared by WGBYC was reviewed.

WGECO continued the work initiated in 2018 to examine the ecological consequences of stock rebuilding, with emphasis on benthivorous fish (ToRa). Two case studies were carried out to estimate the predation pressure of fish on benthos. In one, the consumption of benthic invertebrates by demersal fish on the US continental shelf regions was compared with their biomass in sediments. The estimated annual consumption of benthic organisms was a small proportion (<5%) of total abundance for most taxa but as high as 25% for some prey. Benthic food resources do not appear to be limiting the feeding of benthivorous fishes. The second study examined the temporal trends in diet composition and consumption rates of haddock, which has experienced a northerly shift in abundance in Icelandic waters. Some prey types showed clear trends from 2006 to 2019, while others had more variable patterns. Consumption rates of benthic invertebrates, fish and zooplankton/natantia prey types were calculated. The much greater consumption of fish prey relative to the other two prey groups was of interest.

WGECO scrutinized methods to estimate density-dependent effects on fish growth and made suggestions on its estimation from stock assessment or survey data. A simulation study showed that the age-specific growth increment may not be a useful variable to test for density-dependent growth, because it depends on body size. In the WGECO 2018 report, the case had been made that North Sea plaice show density-dependent growth reduction. In 2019, we conducted a more thorough analysis of the spatial and temporal trends in distribution, growth and status of plaice in the North Sea. As the plaice population increased in abundance, the spatial distribution did not expand, apart from an increased occupancy of marginal areas. The observed reduction in plaice weight-at-length may thus be explained by the metabolic stress associated with the effects of rising sea temperature on plaice growth rates. However, the two mechanisms, temperature and density, that can explain reduced weight-at-age are not mutually exclusive.

As part of ToR b, WGECO compiled fisheries-dependent size composition data from four regions: West of Scotland, Irish Sea, West of Ireland, and the Northern Celtic Sea. This novel dataset was used to examine changes in the length composition of the catch in relation to changes in total catch (used as a proxy for fishing pressure). In the Irish Sea, for example, the commercial fishery now catches larger individuals of larger demersal species as the total catch has declined. Size composition of the landings was compared with size composition in the surveys. In the northern Celtic Sea and West of Scotland, the commercial fleets generally take fish of a much larger size than those caught by the survey. By contrast, in the Irish Sea the commercial fleets tend to capture fish across the whole size range available in the environment.

Demersal fish community indicators of species composition and size–structure were investigated for several sea areas, using survey data for state, and fisheries-dependent data for pressure. Together, these indicators can be used to track the wider impacts of fisheries on the ecosystem and monitor the evolving nature of the relationship between pressure and state. Simple empirical approaches for setting targets and baselines for demersal fish communities were tested with sensitivity analyses and applied to additional survey areas. **WGECO recommends** that these indicators be adopted by ICES for evaluating acceptable status for communities and supplemented where possible with risk-based targets from multispecies modelling approaches. A multispecies

model framework was advanced to determine more ambitious risk-based targets for demersal fish community indicators that can be used to minimise the risk that stocks suffer from impaired reproductive capacity consistent with commercial fish stock indicators. Ensemble modelling demonstrated that the fish community in the North Sea is recovering in response to fisheries management.

WGECO reviewed potential indicators of spatial distribution with special attention to the simplicity of use and ease of communicating the results to non-experts (ToRc). Metrics including aspects of latitude, longitude or depth (e.g. range and centre of gravity) and the area containing a fixed percentage of the population (termed core area) were considered simple to use and easy to communicate. Other measures were considered useful for scientific purposes but less easily applied and communicated to managers. The accuracy of selected indicators for spatial distribution were explored in a simulation study. The metrics produced from the simulated raw survey data and modelled data accurately reflected the underlying mean abundance of the simulated data, but more accurately for the more-common species. Changes in the centre of gravity were detected with high accuracy. The percent of occupied area is generally accurate in its trend when there is a strongly aggregated population, whereas classifying occupied area is more complicated when the population is more dispersed. This preliminary analysis provides the context for analysing distributional metrics at the scale of large marine ecosystems. The spatial distributions of three age groups of plaice were analysed as a case study. The observed northerly and easterly movements of plaice distribution and into deeper waters are interpreted as a response to warming sea temperatures. Consistency in area usage over time was examined to identify those areas critical to plaice. This analysis revealed that the proportion of the population using the 'critical areas' (defined as the area holding 75% of the population in 60% of years) was stable over the study period, though some decreases have been noted in recent years.

WGECO compared the list of sensitive species identified by WGBYC with the underlying list of species to be monitored under the protection programmes in the EU, using methods reviewed previously in WGECO as well as the sensitivity ratings carried out by IUCN. A resulting list of sensitive species and vulnerable/endangered/critically endangered species is provided. Halibut (*Hippoglossus hippoglossus*) was the only species suggested by WGBYC which is considered sensitive to fishing. The remaining species, with the exception of the two *Hippocampus* species, are diadromous species likely to be most sensitive to deterioration of their freshwater habitat. Eleven sensitive species are absent from the list of species to be monitored under protection programmes; **WGECO recommends** that these 11 should be added to the Commission list to provide information on sensitive and vulnerable species. Further, **WGECO recommends** that the requirement to return specimens of endangered and critically endangered species to the sea should not be restricted to parts of EU waters and that the status of sensitive species should be monitored on a regular basis, with the aim of providing advice on the adequacy of existing landing restrictions.

ii Expert group information

Expert group name	Working Group on Ecosystem Effects of Fishing Activities (WGECO)
Expert group cycle	Annual
Year cycle started	2019
Reporting year in cycle	1/1
Chair(s)	Jeremy Collie, USA
	Stefán Ragnarsson, Iceland
Meeting venue(s) and dates	8–16 April 2019, Copenhagen, Denmark (16 participants)

1 Opening of the meeting

The 2019 meeting of WGECO was held at the ICES headquarters, Copenhagen, Denmark from 9–16th of April 2019. The meeting was attended by 16 delegates from eight countries and was chaired by Stefán Ragnarsson (Iceland) and Jeremy Collie (USA). The participants' list is included as Annex 1. The work conducted was centred on three Terms of Reference that were made by WGECO in addition to review the list of sensitive fish species list that was prepared by WGBYC. The meeting agenda is included as Annex 2.

2 Terms of Reference for the 2019 meeting

2018/2/ACOM27 The **Working Group on the Ecosystem Effects of Fishing Activities** (WGECO), chaired by Jeremy Collie, US and Stefan Ragnarsson, Iceland, will meet in Copenhagen 9–16 April 2019 to:

a) Investigate the ecological consequences of stock rebuilding, with particular emphasis on benthivorous fish and invertebrates.
   1. Make first-order estimates of predation pressure on benthos;
   2. Examine evidence of food limitation and density-dependent growth;
   3. Compare the footprints of trawling to the footprints of predation pressure on benthos.

b) Use empirical data and available multispecies models to examine how the degree of fisheries balance relates to ecosystem status.
   1. Compare the length composition of total catch (landings and discards) to the length composition in the survey for one region (e.g. Irish Sea);
   2. Use multispecies models (developed by WGSAM) to identify targets for ecological indicators of state (i.e. status) that relate to an acceptable risk of species diversity loss; and
   3. Use output of multispecies models to investigate how proposed management strategies affect fisheries balance.

c) Review the knowledge of spatial distribution indicators for fish and benthos.
   1. Make recommendations on which indicators to develop, considering both how useful/important these are, and also simplicity of use and clarity of communication;
   2. Test several candidate spatial distribution indicators; and
   3. Scope and evaluate methods to integrate indicators.

d) Conduct a "reality check" and horizon scanning survey within WGECO. The aim is to develop a consensus view of the major emerging issues in relation to fisheries and ecosystems, and on which WGECO could focus future work. WGECO members will provide a list of emerging issues (horizon scanning), that would benefit from scrutiny by WGECO. This list will be collated and used as material for a plenary discussion, and with the aim of producing a perspectives paper in the ICES JMS or Fish and Fisheries.

e) Review the sensitive species list prepared by WGBYC. This year, WGBYC evaluated the list of species to be monitored under protection programmes in the Union or under international obligations (COMMISSION IMPLEMENTING DECISION (EU) 2016/1251) to determine which of the bony fish species are considered sensitive bycatch and hence relevant to the work of WGBYC. This list will be included in the fisheries overviews. WGECO is requested to compare the resulting list to sensitive species identified using methods reviewed previously in WGECO and to comment on any discrepancies.

WGECO will report by 30 April 2019 for the attention of the Advisory Committee.

Supporting Information

Priority	The current activities of this Group will enable ICES to respond to advice requests from member countries. Consequently these activities are considered to have a very high priority. It will also lead ICES into issues related to the ecosystem affects of fisheries, especially with regard to the application of the Precautionary Approach. Consequently, these activities are considered to have a very high priority.
Scientific justification	Term of Reference a) Many stocks are rebuilding and will likely have higher abundance and biomass than we have seen in recent times. This in turn will likely have effects through trophic interactions both up and down the foodweb. At ICES, WGECO and WGSAM have been tasked previously with similar ToRs. WGECO will investigate the potential consequences of stock recovery of benthivorous fish and invertebrates, their ensuing risks for fish stock management and the use of MSFD indicators. It is hypothesized that a large increase in benthivorous fish will have an impact on benthic productivity and biodiversity. This ToR requires data on the spatial distribution of benthivorous predators, their prey consumption rates and diet composition. It also requires data on the abundance and production of benthic faunal. This ToR links to ToR c. Term of Reference b) Identifying thresholds and limits for ecosystem indicators remains a central challenge for ecosystem based fisheries management. This ToR will examine if MSY targets implemented in the current management regime will lead to acceptable ecosystem status. This ToR aims to identify reference levels for a range of ecosystem indicators with the use of size-based models. This proposed ToR links to WGSAM. Term of Reference c) WGECO has traditionally had a leading role in developing and testing indicators, and their use for provision of advice. The work of this ToR facilitates operationalization of these indicators, by identifying data sources, refining, evaluating their strengths and weaknesses and gaps in indicator availability. Indicators that are evaluated to be promising will be tested. Term of Reference d) The ICES strategic plan will end in 2018. This initiative is to allow WGECO to contribute strongly to the development of future ICES strategy. We intend to seek input across the national and disciplinary range of WGECO members, many of whom are operating at a high level in the field and in the home institutes. We aim to publish this as a perspective paper in one of the key journals, and this will be available to inform future progress for this important and centrally positioned Expert Group.
Resource requirements	The research programmes which provide the main input to this group are already underway, and resources are already committed. The additional resource required to undertake additional activities in the framework of this group is negligible.
Participants	The Group is normally attended by some 20–25 members and guests.
Secretariat facilities	None.
Financial	No financial implications.
Linkages to advisory committees	There are no current direct linkages with the advisory committees.
Linkages to other committees or groups	There is a very close working relationship with the groups of the Fisheries Technology Committee, WGBIRD, BEWG, WGBIODIV and WGSAM.
Linkages to other organizations	OSPAR, HELCOM

3 ToR a: Investigate the ecological consequences of stock rebuilding, with particular emphasis on benthivorous fish and invertebrates

3.1 General remarks

This is the second year of this term of reference for WGECO, and it is expected it to be finalised in 2020. The work related to "first-order approximations of predation pressure on benthos" received relatively much attention in the previous report. This approach has been extended this year to compare the consumption of benthos with the biomass of benthos in the seafloor. Furthermore, the approach presented last year was applied to the Icelandic haddock stock. The work under "examine evidence of food limitation" this year has taken the form of reviewing the different methods to do so from stock assessment and survey time-series. The work related to "comparing footprints of predation pressure to the footprints of bottom trawling" is largely in the form of exploring ideas and plans for WGECO 2020, WGFBIT and a first collation of prey consumption by plaice in the North Sea and the estimated effect of trawling-induced benthos mortality. A table for the distribution of stomach-content data across species and size classes was presented; this table could help direct future stomach sampling to support the work undertaken in this ToR and other research projects.

3.2 First-order estimates of predation pressure on major benthos of the Northeast US continental shelf and Iceland, and its relation to available benthos and benthic production (US only).

3.2.1 Introduction

Fish diet data from NOAA Fisheries, Northeast Fisheries Science Center (NEFSC), and Iceland bottom-trawl surveys were evaluated for 32 fish of the Northeast US and Icelandic continental shelves (Table 1). The total amount of food eaten, and the type of food eaten were the primary data examined. From these basic diet data, biomass of benthic invertebrate taxa (US) or total benthos, fish and plankton/natantia (Iceland), per capita consumption, and population-level consumption were calculated.

For US waters, biomasses of benthic taxa (g m^{-2}) were estimated for the four major regions of the northeast US continental shelf (i.e. Mid-Atlantic Bight, Southern New England, Georges Bank, and Gulf of Maine; Figure 3.1). The percent of benthic taxa consumed relative to benthic density and production was considered by region for the northeast US continental shelf, based on estimates of benthic density and production (g m^{-2}; derived from literature values of production:biomass ratios),

Haddock (*Melanogrammus aeglefinus*) is a major fishery resource for Iceland and is most common along the south and southwest coasts of Iceland. Over recent decades, there has been a considerable northerly shift in the haddock distribution, and it is likely that these changes are temperature driven. The average mean temperature north of Iceland has increased between 1994 and 2010 and was exceptionally high in 2003 when there was also a very strong inflow of Atlantic

water into the area (Jónsson and Valdimarsson, 2012). These environmental conditions may have increased the survival of the extremely strong 2003-year class and contributed to its northward shift.

Jaworski *et al*. (2006) analysed the diets of various groundfish species based on data collected in an intensive stomach data collection programme in 1992 in the waters around Iceland. They showed that the most important prey items for haddock were polychaetes followed by ophiuroids, amphipods, capelin, and various echinoderm and fish species.

Table 3.1. Thirty-two benthivorous fish from the US (all) and Iceland (*).

Scientific name	Common name
Amblyraja radiate	Thorny skate
Anarhichas lupus	Atlantic wolffish
Brosme	Cusk
Citharichthys arctifrons	Gulf stream flounder
Dipturus laevis	Barndoor skate
Enchelyopus cimbrius	Fourbeard rockling
Gadus morhua	Atlantic cod
Glyptocephalus cynoglossus	Witch flounder
Helicolenus dactylopterus	Blackbelly rosefish
Hemitripterus americanus	Sea raven
Hippoglossoides platessoides	American plaice
Leucoraja erinacea	Little skate
Leucoraja ocellata	Winter skate
Limanda ferruginea	Yellowtail flounder
Macrozoarces americanus	Ocean pout
Malacoraja senta	Smooth skate
*Melanogrammus aeglefinus**	Haddock
Merluccius bilinearis	Silver hake
Morone saxatilis	Striped bass
Mustelus canis	Smooth dogfish
Myoxocephalus octodecemspinosus	Longhorn sculpin
Paralichthys oblongus	Fourspot flounder
Pollachius virens	Pollock
Prionotus carolinus	Northern searobin

Scientific name	Common name
Pseudopleuronectes americanus	Winter flounder
Scophthalmus aquosus	Windowpane
Squalus acanthias	Spiny dogfish
Stenotomus chrysops	Scup
Tautogolabrus adspersus	Cunner
Urophycis chuss	Red hake
Urophycis regia	Spotted hake
Urophycis tenuis	White hake

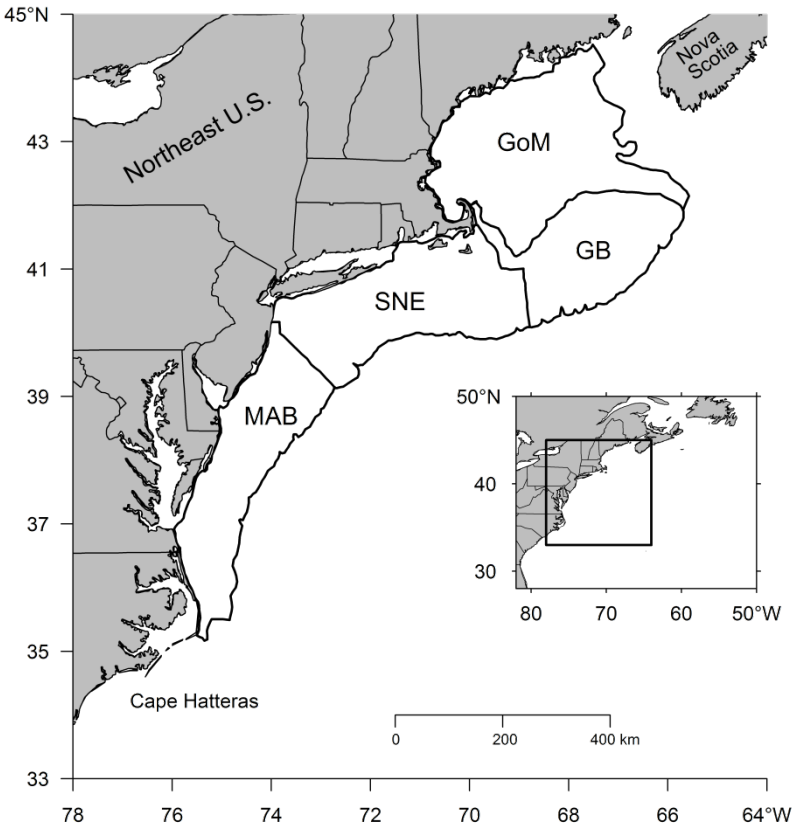

Figure 3.1. Map of sampling regions of the Northeast US continental shelf. GoM: Gulf of Maine, GB: Georges Bank, SNE: Southern New England, and MAB: Mid-Atlantic Bight.

3.2.2 Methods

Every fish predator that contained benthos (defined in Table 3.2; US), and the most common prey items eaten by haddock (Iceland) were considered. From that original list, a subset of the 32 primary predators from US waters (excluding pelagic and other potential predators with incidental benthos predation) were included for estimating benthos consumption and the diet data were aggregated spatially by continental shelf region. For the Iceland data, haddock was chosen for analysis and its consumption was aggregated by year.

Table 3.2. Prey benthos considered for US waters.

Taxonomic name	Common name
Anthozoa	Sea anemones, corals
Asteroidea	Sea stars
Bivalvia	Bivalves
Caprellidae	Caprellids
Echinoidea	Sea urchins, sand dollars
Gammaridea	Gammarids
Isopoda	Isopods
Ophiuroidea	Brittlestars
Paguridae	Hermit crabs
Polychaeta	Bristle worms

US estimates were calculated on a seasonal basis (two 6-month periods) for each predator and summed for each year. Although the diet data collections for these predators started quantitatively in 1973 (mainly Order Gadiformes) and extend to the present (through 2017), not all benthivores were sampled during the full extent of this sampling program. Stomach sampling for the non-Gadiformes considered here began in 1977 and extends through 2017. For more details on the food habits sampling protocols and approaches, see Link and Almeida (2000) and Smith and Link (2010). This sampling programme was part of the NEFSC bottom-trawl survey program; further details of the survey program can be found in Azarovitz (1981), NEFC (1988), and Reid *et al*. (1999).

Haddock diet data obtained by the Icelandic Groundfish Survey were available from 2006 onwards. From each haul, stomachs were obtained from the first five haddock captured and food items were identified on board the research vessel to the lowest taxonomic resolution possible. More information on the sampling approaches can be found in Anon. (2010). No previous analysis has been carried out on the haddock data.

Temporal changes in the diet composition were compared for prey groups (benthos, fish and zooplankton/natantia, for which the latter includes various pelagic and semi-pelagic organisms including zooplankton, euphausiids, mysids and swimming decapods) and for the most common prey types. The mean density of the three prey groups and the dominant prey types, both in terms of number and weight/biomass per year, were calculated. These estimates were derived

by dividing the total sum of each prey group or prey type per year by the total number of stomachs. The temporal trends in the abundance and composition of prey types over time were examined with MDS plots using 4-root transformed data.

Iceland consumption estimates for haddock were calculated for a single season (spring; three months) each year with sampling reoccurring each March.

Basic Diet Data

Mean amounts of benthos eaten ($D_{i,reg,t}$; as observed from US diet sampling) for each predator (i), region (reg), and season (t, fall or spring) were weighted by the number of fish at length per tow and the total number of fish per tow as part of a two-stage cluster design (See Link and Almeida, 2000; Latour *et al*. 2007). These means included empty stomachs, and units for these estimates are grammes (g). For Iceland haddock, mean of the benthos, fish and zooplankton/natantia eaten ($D_{i,yr,t}$) were weighted by the total number of haddock collected per tow and were limited to spring by year (yr, t) irrespective of region.

Numbers of Stomachs

Similar to previous methods of estimating benthos consumption by fishes (WGECO 2018), a minimum sample size approximately equal to 20 stomachs for each predator per season-region (US) or year (Iceland) was used based on trophic diversity curves (e.g. Koen Alonso *et al*., 2002; Belleggia *et al*., 2008). Estimates of diet compositions of benthos were estimated for each predator, region, and season (US) or for the entire continent and year (Iceland).

Consumption Rates

To estimate per capita consumption, the gastric evacuation rate method was used (Eggers, 1977; Elliott and Persson, 1978). Units are in g region^{-1} (US) or g year^{-1} (Iceland). Using the evacuation rate model to calculate consumption requires two variables and two parameters. The daily per capita consumption rate of benthos, $C_{i,reg/yr,t,}$ is calculated as:

$$C_{i,reg/yr,t} = 24 \cdot E_{i,reg/yr,t} \cdot D_{i,reg/yr,t}$$

where 24 is the number of hours in a day. The evacuation rate $E_{i,reg/yr,t}$:

$$E_{i,reg/yr,t} = \alpha e^{\beta T_{i,reg/yr,t}}$$

is formulated such that estimates of mean benthos eaten ($D_{i,reg/yr,t}$) and ambient temperature ($T_{i,reg/yr,t}$) as stratified mean bottom temperature associated with the presence of each predator from the NEFSC bottom-trawl surveys (Taylor and Bascuñán, 2000; Taylor *et al*., 2005) are required. The parameters α and β were set as 0.004 and 0.115 and chosen from the literature (Durbin *et al*., 1983; Tsou and Collie, 2001a, 2001b; Temming and Herrmann, 2003).

Fish Predator Abundance Estimation

Benthos consumption was scaled to the population level by including predator population abundance. Abundance estimates came from survey indices, estimated as swept-area abundance (US), or from stock assessment models (Iceland) for each predator and year. US species assumed a catchability of 1.0, and time-series means were estimated by region.

Scaling Consumption

Following the estimation of consumption rates for each predator, region, and/or temporal (t) scheme, those estimates were scaled up to a seasonal estimate ($C'_{i,reg/yr,t}$) by multiplying the number of days in each half year (182.5; US) or number of days for a single season (91.25; Iceland):

$$C'_{i,reg/yr,t} = C_{i,reg/yr,t} \cdot 182.5 \text{ or } 91.25.$$

For the US data, these were then summed to provide an annual estimate by region, $C'_{i,reg}$:

$$C'_{i,reg} = C_{i,reg,fall} + C_{i,reg,spring}$$

For the Iceland data, $C'_{i,yr}$ consisted of the single spring season per year:

$$C'_{i,yr} = C_{i,yr,spring}$$

and were then scaled by the population abundance (time-series mean by region for US data; annual abundance for Iceland data) to estimate a total annual amount of benthos removed by predator and region or year, $C_{i,reg/yr}$:

$$C_{i,reg/yr} = C'_{i,reg/yr} \cdot N_{i,reg/yr}$$

The total consumption of benthos per predator is presented as annual tonnes per region (US) or tonnes per year for the spring season (Iceland).

US Benthos and Production

Benthic macroinvertebrates of the four regions of the northeast US continental shelf were sampled seasonally from 1956–1965 with Smith-McIntyre and Campbell grab samplers. Sampling followed a non-random, grid design with one sample per 20 minutes latitude by 20 minutes longitude area. A 1-mm mesh screen was used to wash samples, and remaining material was preserved in 5% formalin for laboratory processing. The volume of sediment sampled by each benthic sampler was used to standardize the biomass of benthos sampled. Mean amounts of benthos were presented as biomass per m^{-2} based in each shelf region area. Benthos adequately sampled by the grab samplers included ten taxa (Table 3.2) and included major benthic macroinvertebrate prey across the four continental shelf regions (Smith and Link, 2010). Benthos biomass was assumed to be time invariant given that the four shelf regions were not sampled annually.

Proxy values of benthic production were obtained from P:B ratios for specific benthic taxa detailed in Hermsen *et al*. (2003) and references therein (Table 3.3). When a range of P:B ratios was available per benthic taxon, an average was used. For the benthic taxa considered here, P:B ratios were matched by taxonomic family and/or class of benthos. Proxies of production were generated by multiplying P:B by biomass density (similar to Hermsen *et al*., 2003) and assumed to be static across time and region. This permitted estimates of total percent of benthic production consumed by all fish predators by region.

US Uncertainty

Error associated with consumption, percent benthos consumed per m^2, and percent production consumed per m^2 was quantified with a randomization approach. For consumption by each predator and total consumption (sum of all predators), 1000 random observations were generated for each input parameter (i.e. $D_{i,reg,t}$, α, β, $t_{i,reg,t}$, $N_{i,reg}$) assuming gamma distributions. This randomisation allowed confidence intervals to be assessed from distributions of consumption by fish predator and across all predators. The same methods were applied when calculating the total percent of benthos consumed per m^2 and total percent of benthic production consumed per m^2. Inputs of production were assumed to be without error. For each consumption metric, medians are reported with 95% confidence intervals.

Table 3.3. Biomass, production:biomass (P:B) ratios, and production (P) estimates for benthos derived from empirical and literature sources.

Benthos	Region	Biomass g m^{-2}	P:B	P
Anthozoa	GB	0.43	0.70	0.30
	GoM	30.58	0.70	21.40
	MAB	68.82	0.70	48.17
	SNE	2.91	0.70	2.03
Asteroidea	GB	33.99	0.45	15.29
	GoM	21.39	0.45	9.62
	MAB	4.54	0.45	2.04
	SNE	20.27	0.45	9.12
Bivalvia	GB	742.63	0.98	727.78
	GoM	31.25	0.98	30.62
	MAB	1124.25	0.98	1101.76
	SNE	297.07	0.98	291.13
Caprellidae	GB	4.44	1.10	4.89
	GoM	0.12	1.10	0.13
	MAB	0.57	1.10	0.63
	SNE	2.22	1.10	2.44
Echinoidea	GB	59.85	0.70	41.89
	GoM	361.81	0.70	253.27
	MAB	30.21	0.70	21.15
	SNE	25.48	0.70	17.83
Gammaridea	GB	3.07	1.10	3.38
	GoM	3.80	1.10	4.18
	MAB	0.69	1.10	0.76
	SNE	7.01	1.10	7.71
Isopoda	GB	1.72	1.10	1.89
	GoM	1.63	1.10	1.79
	MAB	0.99	1.10	1.09
	SNE	1.31	1.10	1.44

Benthos	Region	Biomass g m^{-2}	P:B	P
Ophiuroidea	GB	17.25	0.48	8.34
	GoM	11.46	0.48	5.54
	MAB	2.86	0.48	1.38
	SNE	0.63	0.48	0.30
Paguridae	GB	1.54	1.10	1.70
	GoM	21.29	1.10	23.41
	MAB	1.70	1.10	1.87
	SNE	4.86	1.10	5.34
Polychaeta	GB	5.90	2.15	12.69
	GoM	14.65	2.15	31.51
	MAB	2.98	2.15	6.42
	SNE	22.28	2.15	47.91

3.2.3 Results and Conclusions

US Consumption by Region

Total consumption (sum of all predators) per year by region ranged from 100s to greater than 24 000 tonnes of benthic taxa consumed (Figure 3.2). Increased consumption was attributed to the predominant prey taxa by region such as gammarids (Georges Bank, Mid-Atlantic Bight Southern New England), bivalves (Gulf of Maine, Southern New England), echinoids (Gulf of Maine), and ophiuroids, polychaetes, and pagurids (namely in the Gulf of Maine; Table 3.3).

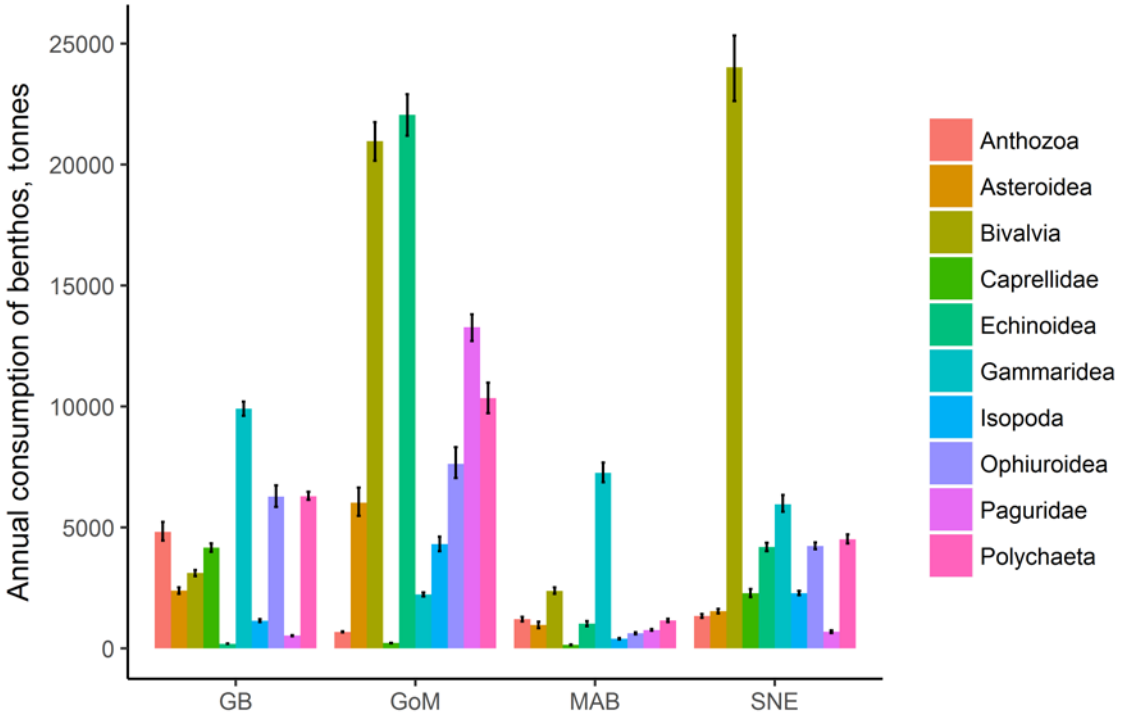

Figure 3.2. Median annual consumption of benthos (tonnes) by continental shelf region. Error represents 95% confidence intervals.

Relative to the amount of benthos available in the environment (g m^{-2}), the annual median percent consumption of benthic taxa by region was variable and suggestive of relative prey preference (Figure 3.3). Regions with relatively high consumption and low density of benthic taxa per m^2 resulted in percent consumption estimates greater than 15 % m^{-2} and as high as approximately 25% m^{-2}; however, less than 5% m^{-2} was typically consumed per benthic taxon for all regions.

Annual median percent of benthic production consumed by the 32 fish predators revealed high variation among benthic taxa and the four regions (Figure 3.4). Interestingly, most benthic taxa by region had less than 5% of their production consumed per m^2; similar to the percent of benthic biomass consumed per shelf region area (Figure 3.3). Production-to-biomass ratios of most benthic taxa, derived from literature values from a broad spectrum of benthic organisms (Table 3.3) were approximately one, yet percent production consumed was generally low. Anthozoans on Georges Bank were an exception with 30% of their production consumed.

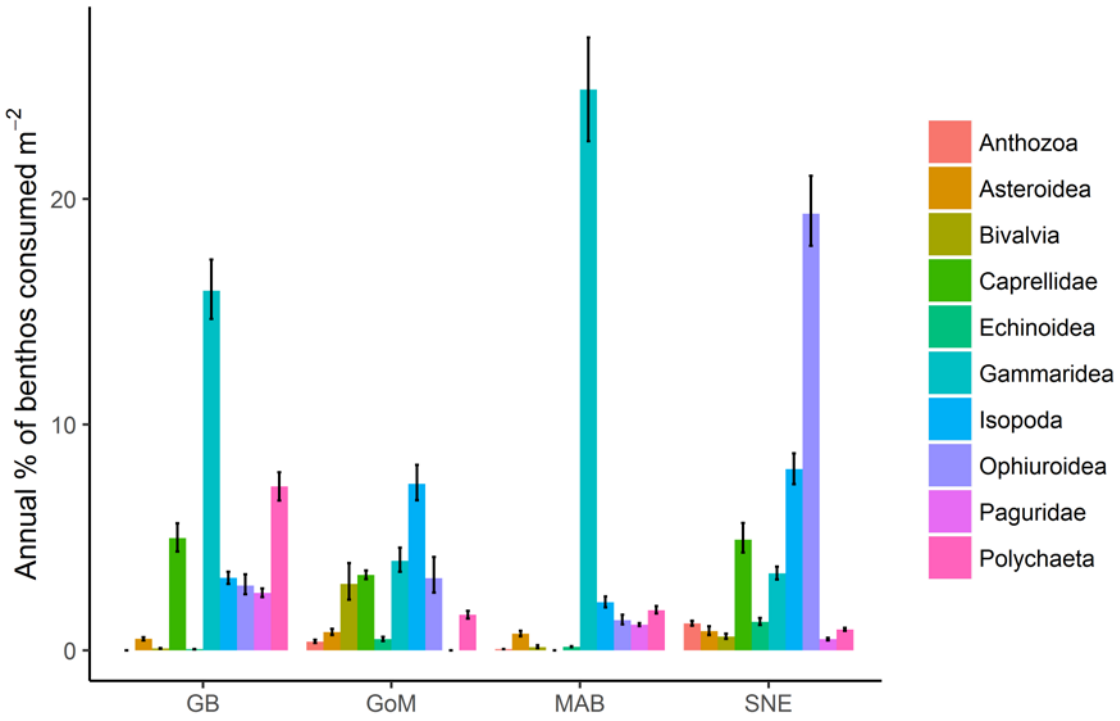

Figure 3.3. Median annual percent of benthos consumed per m² by continental shelf region. Error represents 95% confidence intervals.

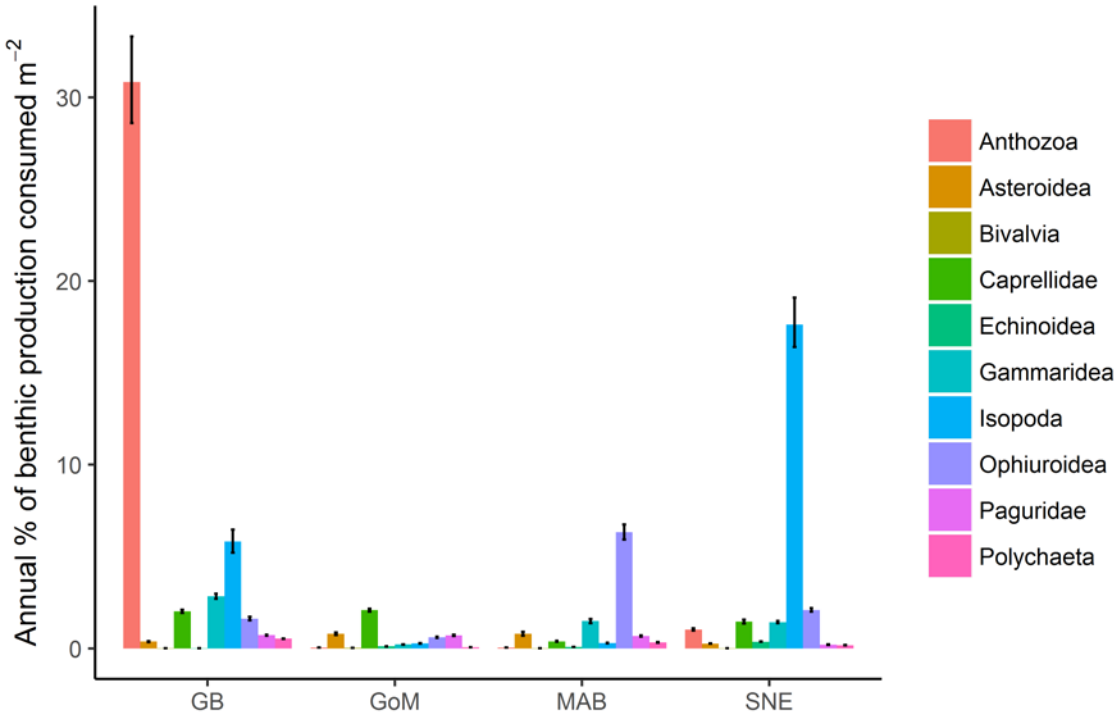

Figure 3.4. Median annual percent of benthic production consumed per m² by continental shelf region. Error represents 95% confidence intervals.

At a regional scale, the many fish predators that forage on benthos of the northeast US waters do not appear to be depleting benthos at or near their productivity levels; thus, benthic food resources particularly for benthivores do not seem to be limited. Prey switching in benthivores of this shelf has been shown in response to harvesting (Smith *et al*., 2013) and invasive species (Smith *et al*., 2014), suggesting that benthivorous fish shift their diet in response to prey abundance. Additionally, many of these fishes are also opportunistic generalist feeders, eating a wide range of benthic invertebrate and benthic fish prey (Smith and Link, 2010). However, the true catchability of these demersal species is <1, meaning that the swept-areas biomass estimates we used are minimum estimates. Also, efforts to rebuild fish stocks and an assumed linear change in population-level consumption with population abundance, would increase predator abundance by one to two orders of magnitude, which in turn would raise the total percent of benthos and benthic production consumed up to or near 100% for several benthic taxa. It would be worthwhile to examine consumption and proportions of benthos removed on a finer scale in areas where fishes may aggregate for specific prey resources (Richardson *et al*., 2014). Additionally, increased monitoring of benthos and their production specifically for this shelf is of interest to better address these concerns.

Temporal Trends in Haddock Diets in Icelandic Waters

A total of 22 227 haddock stomachs have been analysed between 2006 to 2019 with a total of 122 prey types recorded. Euphausiids, ophiuroids, polychaetes, capelin, bivalves, gammarids, natantia, echinoids, gastropods, hyperiids, unidentified fish and *Pandalus borealis* contribute 95% of all prey items recorded in terms of abundance and 63% by weight.

The amount of benthos in haddock diets rose over the period (Figure 3.5), a trend that is largely driven by the increase in ophiuroids, which was the most common benthic invertebrate prey type (Figure 3.6). Other common benthic invertebrate prey types (polychaetes, bivalves, gammarids, echinoids and unidentified benthos) showed variable trends (Figure 3.6). The contribution of fish in diets was highly variable over time (Figure 3.5), but the most common fish preys were capelin (*Mallotus villosus*) and unidentified fish (Figure 3.7). The contribution of zooplankton/natantia decreased markedly after 2007 with a small increase in 2012. The prey items that were mainly contributing to these trends were euphausiids and natantia (Figure 3.7).

The MDS ordination showed clear changes in the prey composition and abundance over time (Figure 3.8). The temporal trends portrayed by the ordination based on abundance and weight of prey items were largely consistent. The diets in 2007 and 2008 appeared to be markedly different from subsequent years.

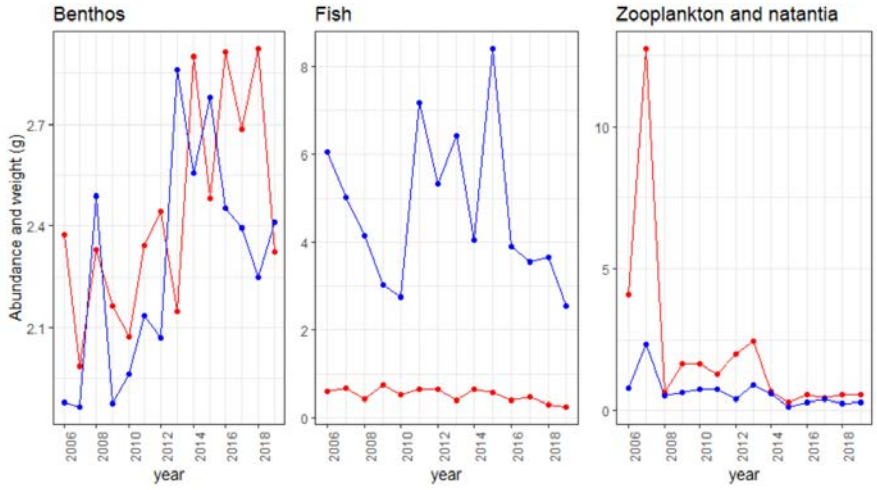

Figure 3.5. Trends in the mean density of benthos, fish and zooplankton/natantia in diets in units of abundance (red lines) and weight in grammes (blue lines) between 2006 and 2019. The mean densities were calculated by dividing the total abundance and weight of each prey group by the total number of stomachs. The y-axis scales are equal for biomass and abundance.

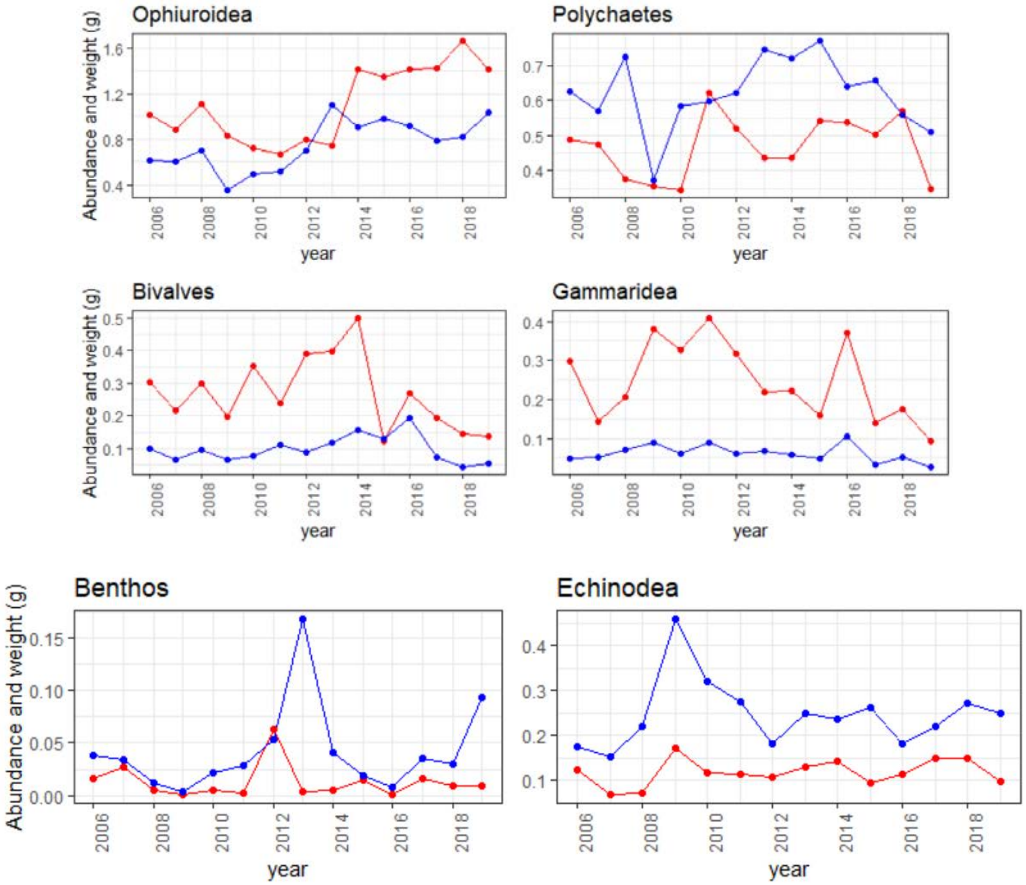

Figure. 3.6. Trends in the mean density of six most common benthic prey types in units of abundance (red lines) and biomass (blue lines). The mean densities were calculated by dividing the total abundance and weight of each prey group by the total number of stomachs. The y-axis scales are equal for biomass and abundance.

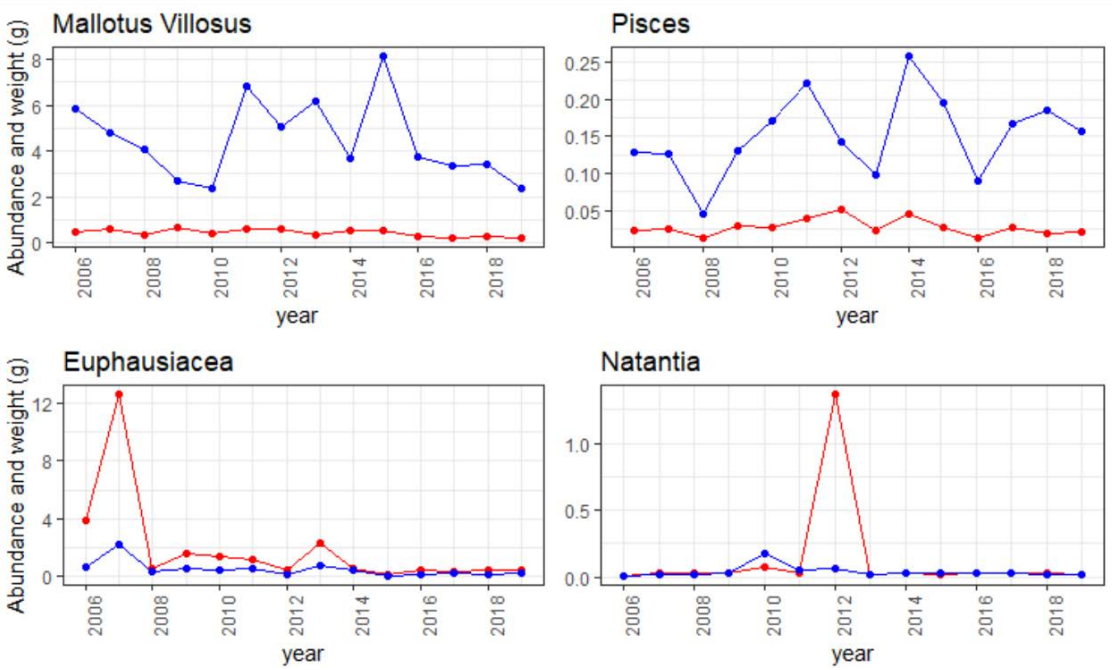

Figure 3.7. Trends in the mean density of capelin (*Mallotus villosus*) and unidentified fish (pisces), (above) and euphausiids and natantia (below) in units of abundance (red lines) and biomass (blue lines). The mean densities were calculated by dividing the total abundance and weight of each prey group by the total number of stomachs. The y-axis scales are equal for biomass and abundance.

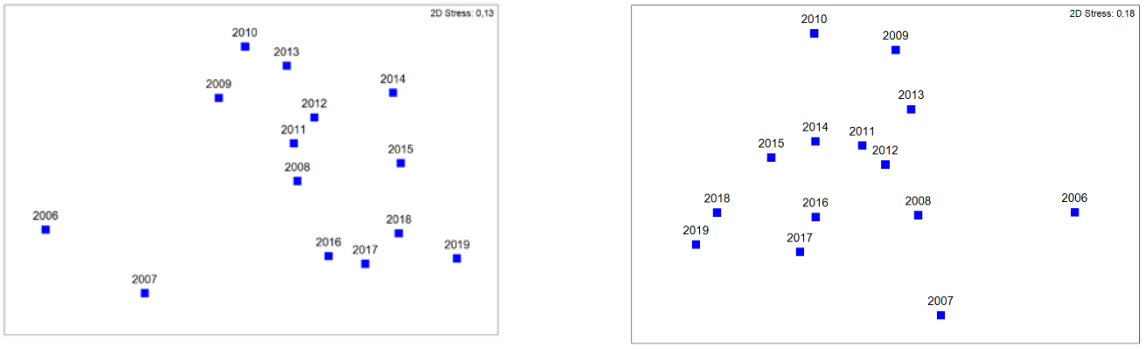

Figure. 3.8. MDS ordination showing the temporal trends in the diet composition and abundance over the period 2006 to 2019 based on abundance (left) and biomass (right).

Iceland Haddock Consumption by Year

The total consumption by haddock decreased over the study period (Figure 3.9). These trends are presumably mostly driven by trends in stock biomass. Haddock was estimated to consume around 25 000 tonnes of benthic invertebrates in spring 2006 but was below 10 000 tonnes in some years (Figure 3.9). The consumption of fish was mostly around 100 000 tonnes but peaked at 500 000 in spring 2006. The consumption of zooplankton and natantia peaked in 2006 and 2013 and was on an order of magnitude of 10 000–70 000 tonnes.

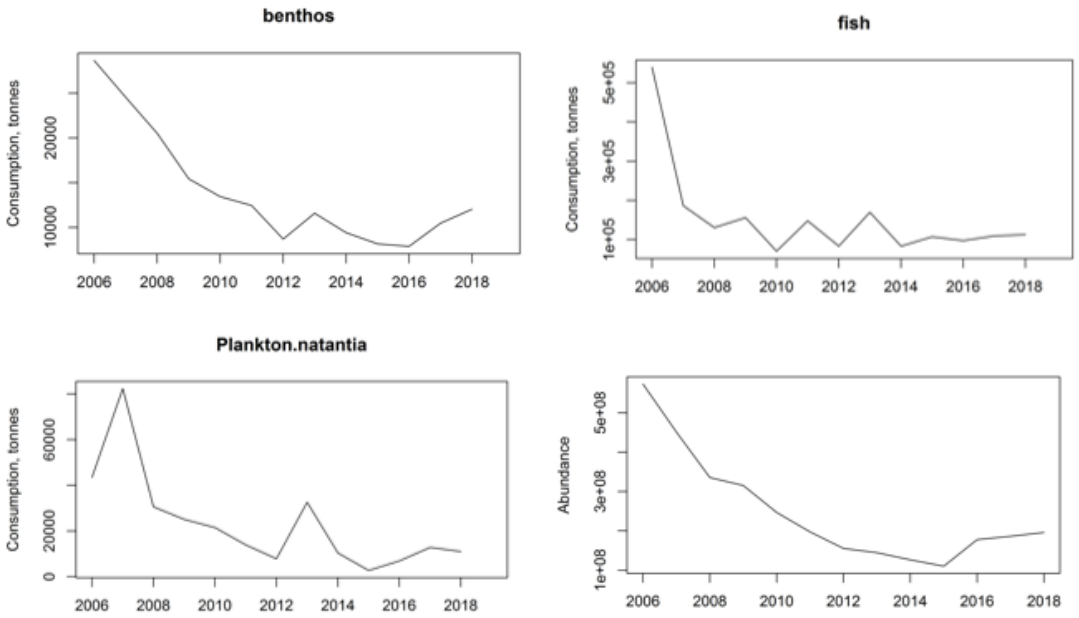

Figure. 3.9. Time-series of total consumption by haddock between 2006 and 2018 on benthic invertebrates (top left), fish (top right) and zooplankton/natantia (bottom left) scaled over a 3-month period. Bottom right: haddock population numbers (hundreds of millions) from 2006 to 2018.

3.3 Detecting density-dependent growth from stock assessment and survey data

WGECO considered the importance of choosing the correct indicators to study the strength and direction of density-dependent growth. There are several issues that require attention, each treated in the proposed steps for analysing density-dependent growth below.

1. Choose the response or dependent variable to use. Consider whether it is necessary to have an indicator that reacts on an annual basis or whether it suffices to have a cohort integrated measure:

General comments: When weight-at-age is estimated from commercial catches, weight-at-age of younger age groups may be biased towards keeping only larger specimens at high density. When estimating weight at younger ages from the survey, rapidly growing cohorts are likely to have higher catchability due to retention in the gear, creating an automatic positive relationship with density. Weight change of an age group depends on mean size when fish grow according to a von Bertalanffy curve. Hence, smaller ages are likely to have greater impact on the indicator than larger age classes, as the relative change in weight of large fish is smaller. This problem could be removed by expressing the weight-at-age in units of standard deviations from the mean.

Table 3.4. Pros and cons of growth metrics used to test for density-dependent growth.

Growth metric	Pros	Cons
A. Weight-at-age *a* in year *t*, w_{at}, including only ages reliably samples (e.g. exclude first and last ages).	Simple to obtain and explain.	If regressing weight-at-age against numbers-at-age for all ages in one model, there is an automatic negative relationship as fish grow and experience mortality. If separate models are made for each age group, the results for different ages may be contradictory.
B. Weights normalised to the mean of each age and analysed separately.	Simple to obtain and explain	Weight relative to the mean of an age group depends on mean size when fish grow according to a von Bertalanffy curve
C. Weights normalised to the mean of each age and averaged for all ages within a year.	Simple to obtain and explain. Likely to show strong results where growth in a year is impacted by a common factor for several ages (e.g. changes in the amount of plankton for planktivorous fish)	Smaller ages are likely to have greater impact on the indicator than larger age classes as the relative change in weight of large fish is smaller (see general comments above). The metric integrates growth over a variable number of year classes depending on the number of age groups for the stock and so is more prone to being impacted by changes in prior years.
D. Weights normalised to the mean of each age and analysed for all ages together within a cohort (Cook *et al.*, 1999, J. Northw. Atl. Fish. Sci., Vol. 25: 91–99).	Simple to obtain and explain. Likely to show strong results where growth of a cohort is impacted by initial cohort density and less by annual common factors.	Smaller ages are likely to have greater impact on the indicator than larger age classes as the relative change in weight of large fish is smaller (see general comments above). This metric integrates growth over a variable number of years depending on the number of age groups for the stock.
E. Weight increments $\Delta w_{at} = w_{a+1,t+1} - w_{at}$ or $\Delta \ln w_{at} = \ln w_{a+1,t+1} - \ln w_{at}$	Frequently used in the literature, these metrics, attempt to assign incremental change to a specific time.	Both measures depend on starting size when fish grow according to a von Bertalanffy curve (see general comments above). The metric is more prone to noise than estimates based on a single age because errors occur in both variables.
F. $\Delta w = w_{t+1}^{\frac{1}{3}} - e^{-K} w_t^{\frac{1}{3}}$ $= Linf * (1 - e^{-K})$	If *K* is constant the metric is proportional to *Linf*. If *K* is constant and correctly estimated, this metric is independent of weight-at-age. The inverse of Δw is linear in time.	Depends on a fixed estimate of *K* and hence assumes all variability to be in *Linf*. If *K* is not constant or incorrectly estimated, the metric is no longer independent of weight-at-age.
H. $\Delta w = \frac{w_{t+1}^{\frac{1}{3}} - w_{\infty}^{\frac{1}{3}}}{w_t^{\frac{1}{3}} - w_{\infty}^{\frac{1}{3}}}$ $= K$	Assuming that $Winf$ is constant in which case the metric is equal to *K*. If $Winf$ is constant and correctly estimated, this metric is independent of weight-at-age.	Depends on a fixed estimate of *Winf* and hence assumes all variability to be in *K*. If *Winf* is not constant or incorrectly estimated, the metric is no longer independent of weight-at-age.

Growth metric	Pros	Cons
I. Average annual residual from a cohort-specific von Bertalanffy growth curve by year.	This gives an annual cohort specific effect. Can be good if there are one-off events impacting growth of all ages (no positive autocorrelation in growth conditions)	Smaller ages are likely to have greater impact on the indicator than larger age classes as the relative change in weight of large fish is smaller (see general comments above). The estimation is prone to random variation as there is only one point for each age and cohort and hence the estimates of von Bertalanffy growth parameters are very uncertain. Disregards effects that the cohort experiences either at recruitment or throughout its lifetime. Therefore, not well suited to determine long-term changes, as they are likely to occur for several years and hence change the cohort von Bertalanffy curve.
J. Average annual or cohort residual from a stock-specific von Bertalanffy growth curve.	Provides an annual cohort effect which is likely to be very similar to weights normalised by dividing by mean weight.	Smaller ages are likely to have greater impact on the indicator than larger age classes as the relative change in weight of large fish is smaller (see general comments above).

2. Choose the (independent) measure of stock abundance

The density metrics of relevance will depend on where in the life history the density-dependence is expected and how it is expected to act. Several studies compare growth of the individual age group to total-stock biomass or total spawning–stock biomass. However, these measures are generally not the most relevant to fish, which are not close to their maximum size as their dietary overlap is not complete with all ages. Furthermore, they are not statistically independent of weight-at-age, as this enters the calculation of both.

If density-dependent growth occurs as fish in the larval or juvenile stage of a demersal fish compete for food, it is likely to impact the size at the very youngest ages. The most relevant density is then the number of fish in the cohort, as the feeding overlap with older ages is likely to be small for the rapidly growing small fish. As fish grow larger, the size and feeding overlap of adjacent year classes is likely to increase, raising the need to look at aspects related to total food consumption of likely predators. As fish predation increases with body mass, the abundance of competitors will depend on whether they are of the same cohort, younger or older. Often this is accounted for by estimating the total biomass of competitors, but this raises the problem of weight-at-age not being statistically independent of biomass. One way to get around this problem is to use the average weight-at-age over the entire time-series when estimating biomass ($\sum N_a \, \overline{w}_a$). As a large part of the variation in biomass is derived from changes in numbers-at-age, this should work reasonably well in most cases. Note also that the positive bias is reduced when using weight increments instead of weight-at-age.

3. Choose a model equation ($\Delta w_{a,t}$ denotes the chosen growth metric):

a) Hyperbolic (Horbowy and Luzenczyk, 2016) $\Delta w_{a,t} = \frac{a}{1+b \times SSB}$

b) Exponential (Zimmerman *et al.*, 2018) $\Delta w_{a,t} = \propto e^{-\beta SSB}$

c) Linearized (Horbowy, work in prep) $(\Delta w)^{-1} = \alpha + \beta * Stock$

d) Non-parametric (including the quadrant method where data are examined to determine the fraction of all years which have above average growth and above average stock size).

4. Choose model application

a) Fit model with a common shape parameter for all ages to increase the power of the estimation.
b) Fit model to a range of stocks, for which growth data are available.
c) Fit a mixed-effect model to "share" data across stocks.

5. Try to explain the results of meta-analyses.

   Why do some stocks exhibit density-dependent growth? e.g. large contrast in stock size, benthic feeders, pelagics, etc. For stocks that appear to have density-dependent growth, examine the potential mechanisms.

In summary, we provide some general guidance, based on the information listed above. To test for density-dependent growth in early life, choose the youngest age that is reliably sampled and regress its weight against cohort abundance. To test for density-dependent growth later in life, choose one of the methods (or all) based on weight increments to remove the potential effect of initial cohort density. Method E does not make any assumptions about whether variability of growth is due to changes in *K* or *Linf*, but the growth increments are not independent of age. The growth increments in methods F and G are independent of age, but make strong assumptions that either *K* or *Linf* is constant. Regress Δw against biomass calculated as $\sum N_a \, \overline{w}_a$, summed over the ages that are expected to have feeding overlap. These methods are expected to have low bias, but they should be simulation tested before drawing firm conclusions.

3.4 A simulation study to test growth and weight-at-age as an indicator of density-dependent growth reduction

One approach to compare density-dependence in growth and recruitment is to use the density-dependent parameter of the Ricker function (β in $R = \alpha e^{\beta \, SSB}$). A negative value of β represents negative density-dependence. It is suggested the Ricker function can be fitted for recruitment per spawning–stock biomass (resulting in β_R), weight-at-age (resulting in β_{W_a}) and size increment at age (resulting in β_{G_a}) as indicators for density-dependence in recruitment and growth respectively (Zimmerman *et al*., 2018). We used simulated data with density-dependence in both growth and recruitment to explore how these indicators for density-dependence respond to different strengths of density-dependence.

We simulated populations using a physiologically structured population model in which both ingestion and maintenance requirements scale with body size (De Roos *et al*., 1990; Jager *et al*., 2013; Croll *et al*., in prep). In the model, both the individual growth rate and the individual reproduction rate are limited by the food intake of an individual. Therefore, density-dependent growth and reproduction arise through the interaction of the stock with the food resource. Individuals follow a von Bertalanffy growth trajectory in which the asymptotic maximum length changes with the resource density. Energy allocated to reproduction is stored and individuals reproduce yearly. On top of the density-dependence in reproduction, we add a Beverton–Holt stock–recruitment relationship ($R = R_{max} \frac{R_p}{R_{max}+R_p}$) to simulate additional density-dependence in the early life stage. In this way, density-dependence in recruitment can be controlled by changing the maximum recruitment (R_{max}) in the Beverton–Holt stock–recruitment relationship. Decreasing R_{max} simultaneously decreases the strength of density-dependent growth, because it reduces the number of individuals entering the population and thus limits population resource consumption.

In this case study, the model is parameterized for Sole (*Solea solea*) using the Dynamics Energy Budget parameters published by Van der Veer *et al*. (2001). The stock dynamics is simulated over a period of 60 years for different values of maximum recruitment. To obtain information on the variation in the stock composition during the simulation, the fishing intensity is gradually increased from 0.1 to 0.6 during the first half of the simulation and gradually decreased from 0.6 to 0.1 during the second half of the simulation (bottom graphs of Figure 3.10). The density-dependent Ricker functions are fitted as described in Zimmermann *et al*. (2018).

At low values of maximum recruitment, density-dependence in recruitment is strong, and the stock dynamics are fully regulated by density-dependence in recruitment. Due to the high-density-dependence in recruitment, individuals experience limited competition and experience high growth rates (Figure 3.10, top left graph). Consequently, density-dependence in growth does not affect the stock structure or population biomass (constant length-at-age in top left graph of Figure 3.10). With increasing maximum recruitment, the density-dependence in recruitment decreases and density-dependence in growth affects the population structure (Figure 3.10, top right). With decreasing density-dependence in recruitment, the population biomass is more determined by growth and less by recruitment, causing a positive relationship between individual growth and population biomass. At very high values of maximum recruitment, the density-dependence in recruitment is very weak. Consequently, the entire stock consists of only a single cohort and the population biomass is fully predicted by the individual growth rate. Because these single cohort cycles are not representative for actuals stocks, these very high maximum recruitment values are not considered further.

Figure 3.10. Cohort dynamics for low and high maximum recruitment (R_{max}): top figures show the cohort growth trajectories per year for the simulated data at low ($R_{max}=5\times10^{9}$) and intermediate ($R_{max}=5\times10^{10}$) maximum recruitment. Bottom figures show the development of fishing effort during the simulation.

With high density-dependence in recruitment (low R_{max}), the indicator for density-dependent recruitment (β_R) gives a negative value (Figure 3.11, dashed line). The indicator for density-dependent recruitment is constant as long as density-dependence in recruitment is the only process limiting the stock. Accordingly, both indicators for density-dependent growth (β_{W_a} and β_{G_a}) are zero, because density-dependence in growth does not affect the stock density (Figure 3.11, solid and dotted coloured lines).

If density-dependence in recruitment is reduced (increasing R_{max}) both density-dependence in recruitment and growth affect the stock structure. The effect of density-dependent growth on the

stock structure is not visible in the density-dependent growth indicator based on the growth rate (β_{G_a}), which remains equal to zero (Figure 3.11, solid lines). In contrast, the density-dependence in growth is visible in the negative values of the density-dependent growth indicator based on weight-at-age (β_{W_a}) (Figure 3.11, dotted lines). Note that the value of the density-dependent growth indicators based on weight-at-age are positive for some values of R_{max}, indicating higher weight-at-age in a larger population (positive density-dependence). This is probably caused by the increasing strength of the positive relationship between growth rate and population biomass, because the biomass is more determined by growth and less by recruitment. This positive relation between the growth rate and population biomass is likely to mask the signal of a negative density effect on growth. Lastly the indicator for density-dependent recruitment (β_R) and the indicator for density-dependent growth based on weight-at-age (β_{W_a}) strongly fluctuate. These fluctuations strongly co-occur with changes in the stock age and size distribution and changes in the number of cohorts in the stock.

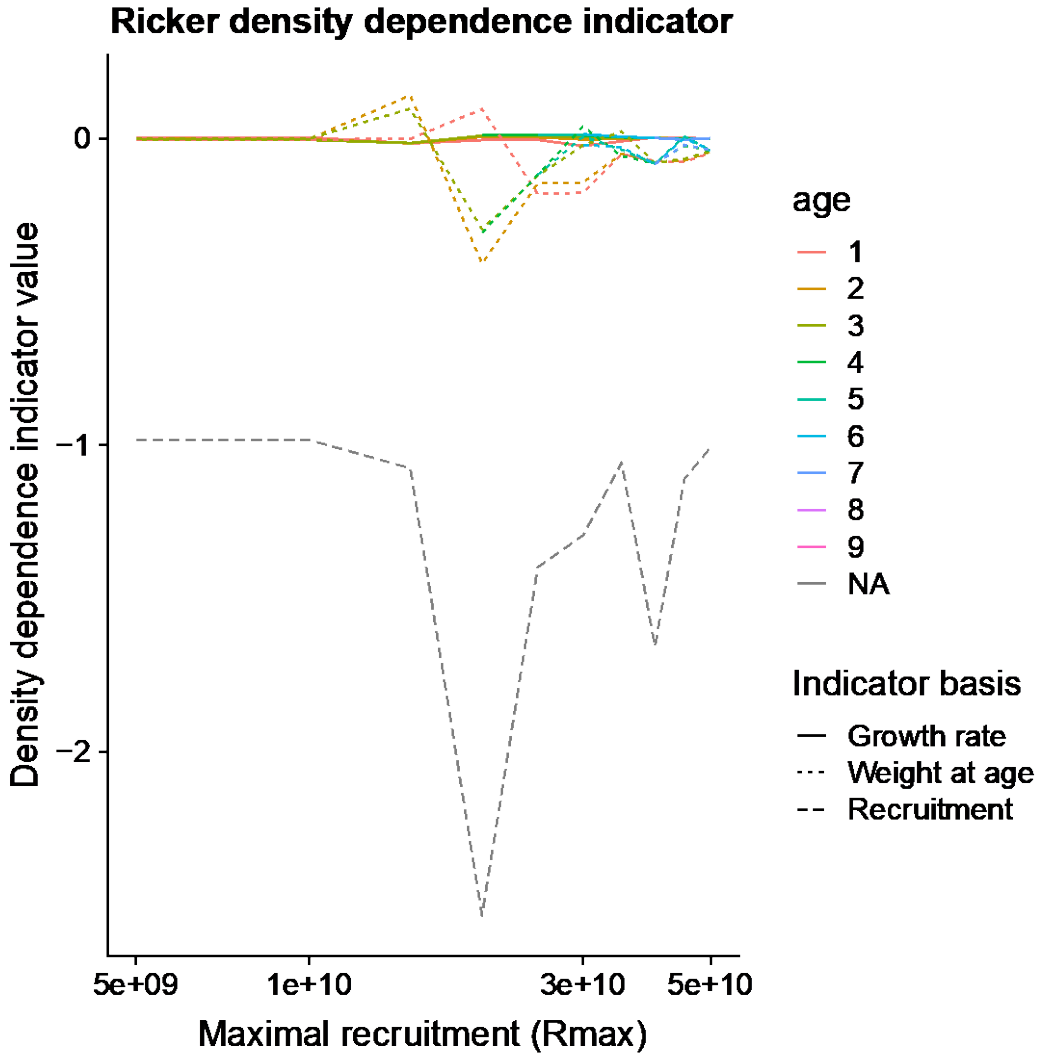

Figure 3.11. Effect of the density-dependence in recruitment on the density-dependence indicators based on the Ricker function. A low value in R_{max} results in high density-dependence in recruitment and vice versa. The dashed grey line is the indicator for density-dependence in recruitment per biomass and is calculated for the entire stock. The solid and dotted lines are the indicators for density-dependent growth based on growth rate and weight-at-age (solid and dotted lines respectively) split per age.

From this simulation we can draw several conclusions about the use of the density-dependent parameter of the Ricker function as indicator for density-dependence in recruitment and growth. Firstly, it is clear these statistical indicators only indicate the strength of density-dependence as it occurred during the period to which the relationship is fitted, and does not indicate the potential of density-dependence to act on the stock. Secondly, the density-dependent growth indicator based on the growth rate (β_{G_a}) is very insensitive to density-dependence in growth. This could be caused by the negative relation between length and growth, which could dampen or even cancel out the signal of density-dependent reduction in growth. Thirdly, the positive relationship between growth rate and stock biomass can mask the signal of density-dependent growth if growth has a strong effect on the population biomass. Lastly, the density-dependence indicators based on the Ricker function are very sensitive to changes in the population structure and the number of cohorts in the population. They might therefore not be a reliable absolute measure for density-dependence.

3.5 Case study: Change in North Sea plaice growth and condition: better management, food limitation or environmental change?

3.5.1 Trends in the plaice stock

From the early 1950s, total stock and spawning–stock biomass of plaice both increased and then maintained relatively high levels throughout the 1960s, 1970s and 1980s (Figure 3.12a). Throughout this 30-y period of plenty, landings steadily increased to unprecedented levels not seen over the previous 100 years. This increase in landings was associated with a marked increase in fishing mortality. Throughout the 1980s and towards the end of this period of plenty, these high levels of fishing mortality were sustained by a period of persistently high recruitment production (Figure 3.12a). Through the 1990s, however, recruitment returned to more normal levels, but fisheries management failed to respond and reduce levels of fishing mortality accordingly. Fishing mortality therefore remained high throughout the 1990s, so consequently, stock biomass declined markedly, and landings tailed off (Figure 3.12a). From 2000 onwards, drastic remedial management was implemented and, by 2010, fishing mortality had been reduced to levels lower than at any time since the Second World War. As a result, from around 2008, total stock and spawning–stock biomass have both increased and are now higher than at any time during the available data time-series (Figure 3.12a).

Long-term trends in weight-at-age indicate declines in body weight in later years (Figure 3.12b). These declines have been linked to the increase in plaice stock biomass, the inference being that increased plaice abundance has resulted in raised levels of intraspecific competition for prey resources, such that plaice have become increasingly food limited. These reductions in weight-at-age commenced at different times for different age classes, starting earlier among older age classes than among younger (Figure 3.12b). The time at which weight-at-age started to decline among age classes 6 and older predated the period of particularly high stock biomass by some years. In fact, these declines commenced at a time when plaice stock biomass was actually at its lowest point since the 1950s (Figure 3.12b). Among the younger age classes, weight-at-age was also lower at the start of the time-series, and not too dissimilar from modern-day weight-at-age (Figure 3.12b). These observations suggest that any explanation for the recent reduction in plaice weight-at-age are likely to be more complicated than simply increased levels of intraspecific competition and food limitation.

Although apparent in all age classes, reductions in weight-at-age are most obvious among the older age classes. If over this time period, the weight-at-length relationship has remained constant, then this infers a decrease in growth rate among North Sea plaice. Alternatively, the observed declines in weight-at-age could reflect reductions in body condition, which implies change in the weight-at-length relationship.

3.5.2 Trends in growth assuming constant weight-at-length

The von Bertalanffy equation, $L_t = L_\infty(1 - \exp[-K(t - t_0)])$, describes the increase in the length (L) of fish over time (t). It requires two species-specific parameters to be known: the asymptotic body-length (L_∞) and a growth term (K), which determines the speed at which a fish approaches its asymptotic body length given its current length (L_t) at time t. The 'Petersen method' provides a means of estimating the two von Bertalanffy equation parameters from data where the mean length of fish at specified age steps is known (Gulland, 1983, Chapter 4). The critical assumption is that the time-steps between each length node are identical; precisely the data provided by the stock assessments, which give stock weights-at-age estimates for the 1st of January in each year.

To examine possible long-term changes in growth pattern, the 'Petersen method' was applied to plaice weight-at-age data for cohorts for which data were deemed sufficiently complete for each time-step as to derive satisfactory linear regression fits to the L_t and L_{t+1} data. Figure 3.13 shows estimated L_∞ and K parameter values for each plaice cohort. For the period 1957 to 2008, data for each cohort were complete. Outside this period, estimates of L_∞ and K were derived from incomplete cohort age data. The start of the weight-at-age time-series only contained data for the later age classes for cohorts that actually started life prior to the start of the time-series. Conversely, cohorts starting life towards the end of the weight-at-age time-series would be missing their later age-class data. The fitted loess smoother suggested a marked decline in L_∞ after 1999. Some coincidental increase in K was apparent, but the relationship between L_∞ and K appeared to differ between the two periods during which different growth patterns were implied.

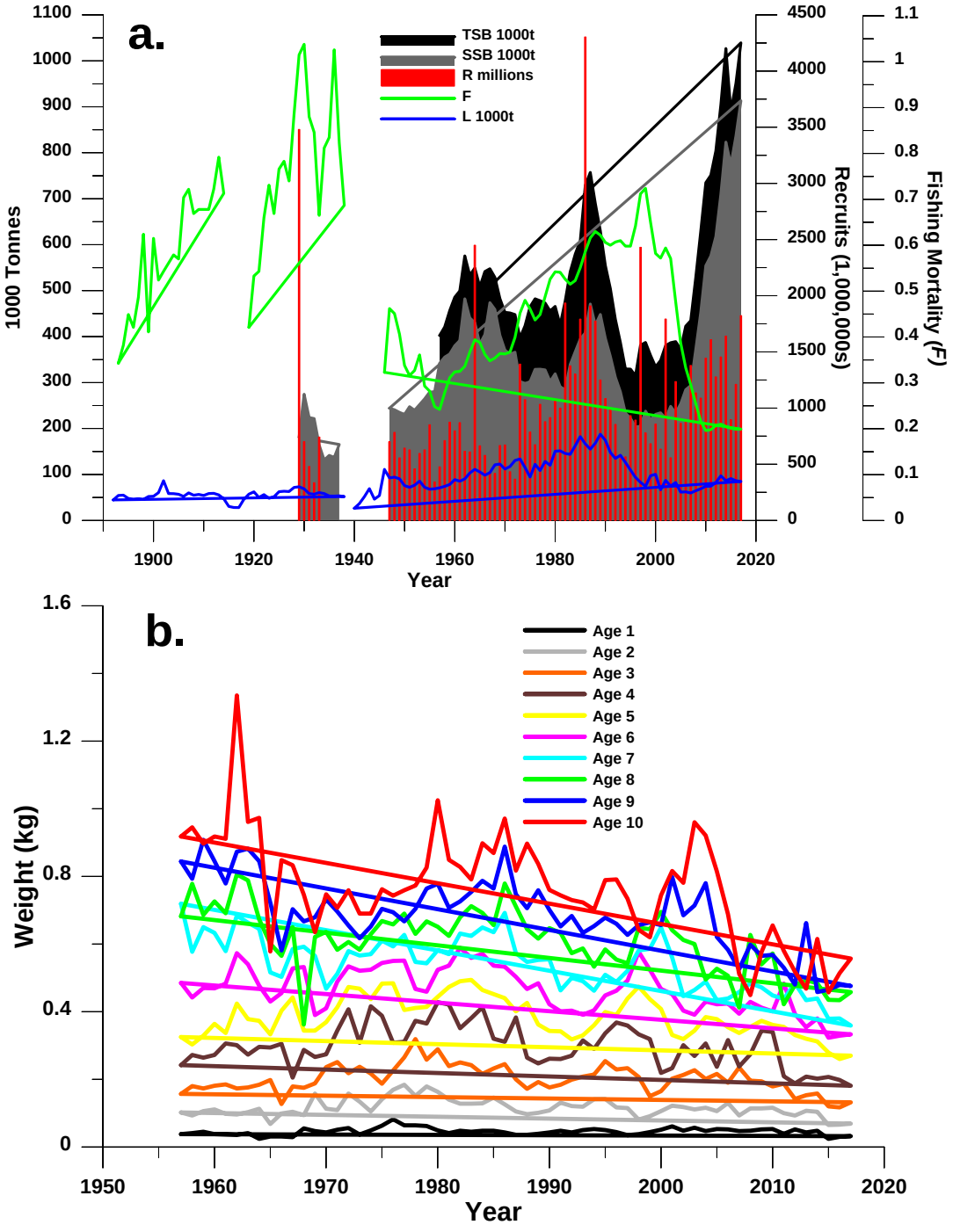

Figure 3.12. a. Long-term trends in plaice total-stock biomass (TSB), spawning–stock biomass (SSB), numbers of recruits (R), fishing mortality (F) and landings (L) in the North Sea. b. Long-term trends in stock assessment weight-at-age in the North Sea plaice stock.

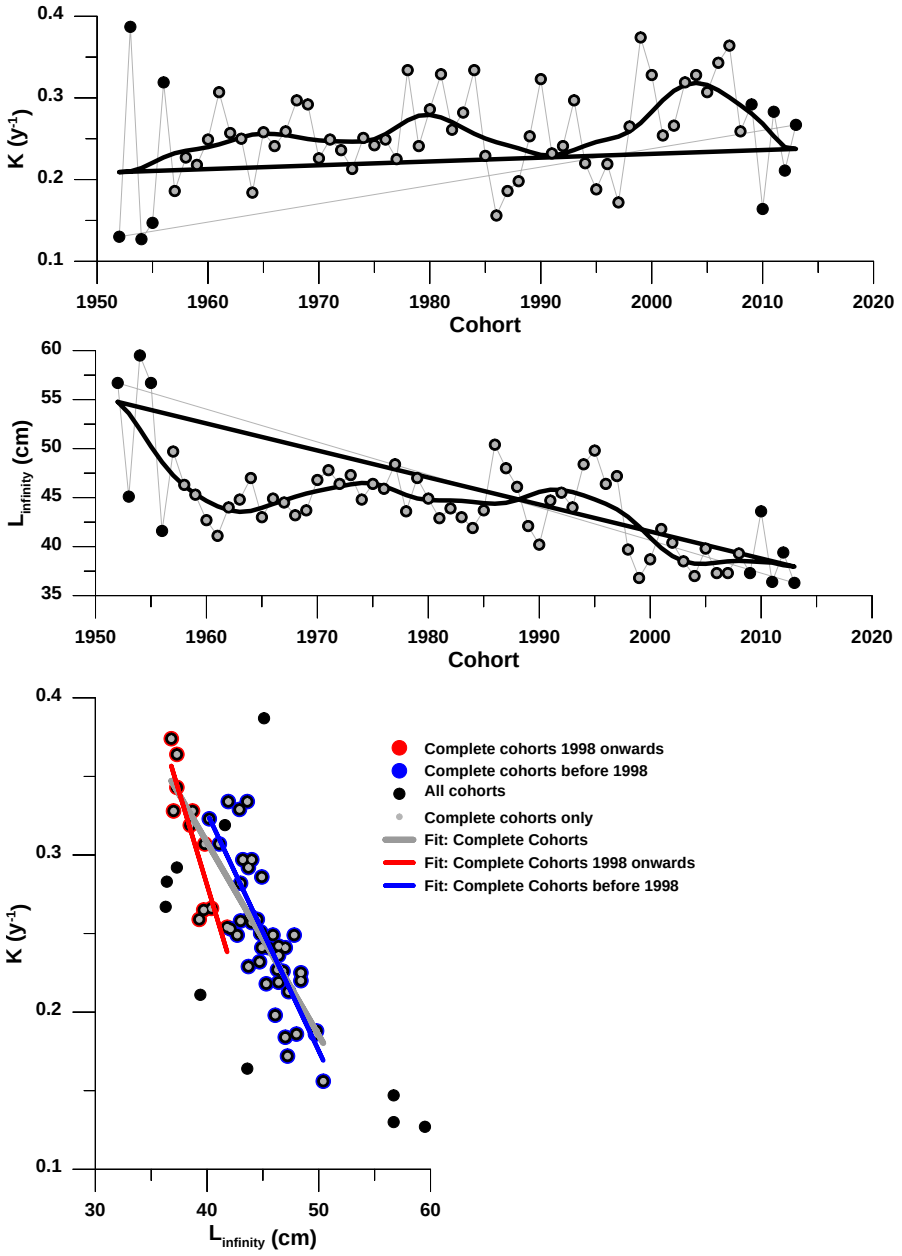

Figure 3.13. Variation in von Bertalanffy growth equation *K* (upper panel) and L_∞ (middle panel) parameter values for plaice cohorts over the period 1952 to 2013. Parameter values for datapoints with a central grey fill are derived from complete weight-at-age data, whilst parameter values for the full black datapoints at the start and end of each time-series are derived from incomplete weight-at-age data. Heavy black lines show fitted loess smooths constructed using a tricubic kernel and second-order polynomial and a fitting window of 40% of the data range. Lower panel shows the relationship between L_∞ and *K*. Linear fits for the whole dataset, and cohorts before and after the apparent change in growth pattern are shown.

3.5.3 Evidence of food limitation and competition for prey resources

Plaice prey almost exclusively on benthic invertebrates, but ontogenetic development of the diet is evident. Data used to parameterise the ERSEM model suggest three principal age groupings (Greenstreet, 1996, based on data in Basimi and Grove, 1985a). Table 3.5 indicates these age groupings according to the biomass of prey consumed daily as a percentage of predator body-mass. Fish in age groupings 1, 2 and 3 had similar diets, so for this analysis, these two categories were combined. Tables 14.2.5 and 14.3.3 in the latest WGNSSK report (ICES, 2018) give respectively, the mean weight-at-age (kg) and the numbers-at-age (1000s) of plaice in the stock in each

year for the period 1957 to 2017. Multiplied together, these tables give estimates of the biomass-at-age (tonnes) of plaice in the stock in each year, which multiplied by daily food consumption estimates as a percentage of biomass (Table 3.5) gives estimates of the quantity of prey consumed daily by each age class of plaice in each year. Fish in any given cohort do not just compete with fish the same age as themselves; they also compete with fish in either older or younger cohorts that have similar diet. Thus in 1972, for example, age-1 plaice in the 1972 cohort (where cohorts are defined as the year that fish were aged as age 1) will also be competing with age-2 fish from the 1971 cohort and age-3 fish from the 1970 cohort, as these age classes of plaice fall into the same dietary grouping. To determine the "prey competition" fields that each age class of each cohort would have to compete with as they grew, the daily consumption estimates of each age class of plaice in each year were summed across the appropriate age groupings. Annual variation in the level of the three different "prey-competition" fields is shown in Figure 3.14, along with the total quantity of prey consumed daily in each year by the entire plaice population.

Table 3.5. Daily food consumption (as % of predator body-mass) for age groups of plaice with similar diet (Greenstreet, 1996).

Prey	Age Groupings			
	1	2 & 3	4 to 6	7+
P. koreni	1.836	1.648	0.559	0.000
Nephtys	0.090	0.117	0.057	0.000
Other Polychaets	0.290	0.197	0.390	0.000
A. alba	2.169	2.246	0.739	0.000
C. Pellucidus	0.120	0.112	0.117	0.000
E. ensis	0.067	0.089	0.121	0.000
Other Moluscs	0.078	0.090	0.094	0.000
Upogebia	0.000	0.000	0.000	2.050
Ann. Avg. D. Cons. (%BW)	**4.650**	**4.500**	**2.075**	**2.050**

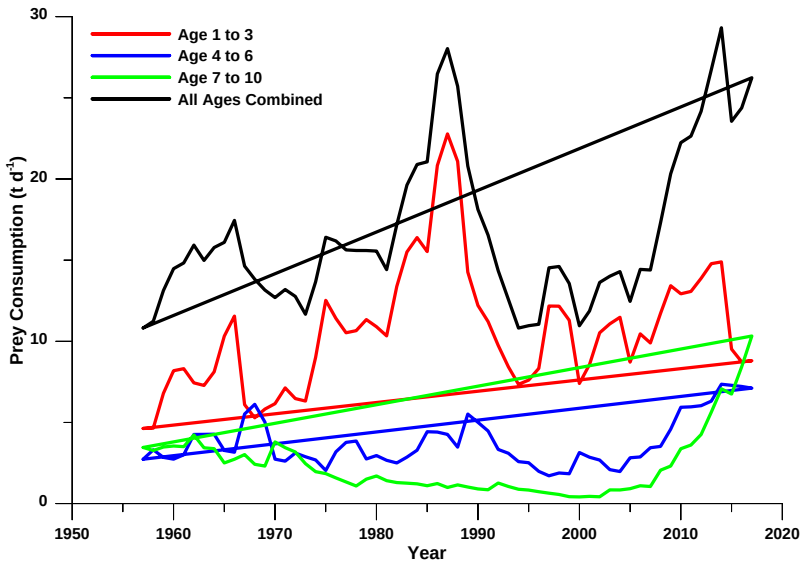

Figure 3.14. Long-term variation in the total quantity of food consumed daily by the whole plaice stock and by fish assigned to three separate dietary age groupings. These trends provide an indication of temporal variation in the extent of competition for prey (the 'prey competition field') experienced by different cohorts of plaice at different stages of their lifespan.

A daily growth coefficient (g) was determined from the differences in weight-at-age at each age increment for each cohort (c) following, $\frac{W_{c,y+1}}{W_{c,y}} = e^{gt}$, where $W_{c,y=y}$ is the mean weight-at-age of plaice of any particular cohort in a given year and $W_{c,y=y+1}$ is the mean weight-at-age of plaice of the same cohort one year later and t is the number of time-steps. Rearranging this equation to

solve for g gives, $g = \ln\left[\frac{W_{c,y+1}}{W_{c,y}}\right] / t$. Since the weights are measured one year apart, t=1 for an annual growth rate estimate and t disappears from the equation, but for daily growth rate measures, t=365. This growth coefficient was used to explore variation in the growth rates of each age class of each cohort of plaice. These coefficients could be related to the strength of the 'prey competition field' experienced by each cohort of plaice through each annual time-step, from age 1 to age 2, age 2 to age 3, through to age 9 to age 10; a total of nine separate annual growth steps for each cohort. These relationships, shown for each age class in Figure 3.15, suggest that the level of competition for prey had no consistent negative impact on the growth of different cohorts of plaice across individual annual growth time-steps.

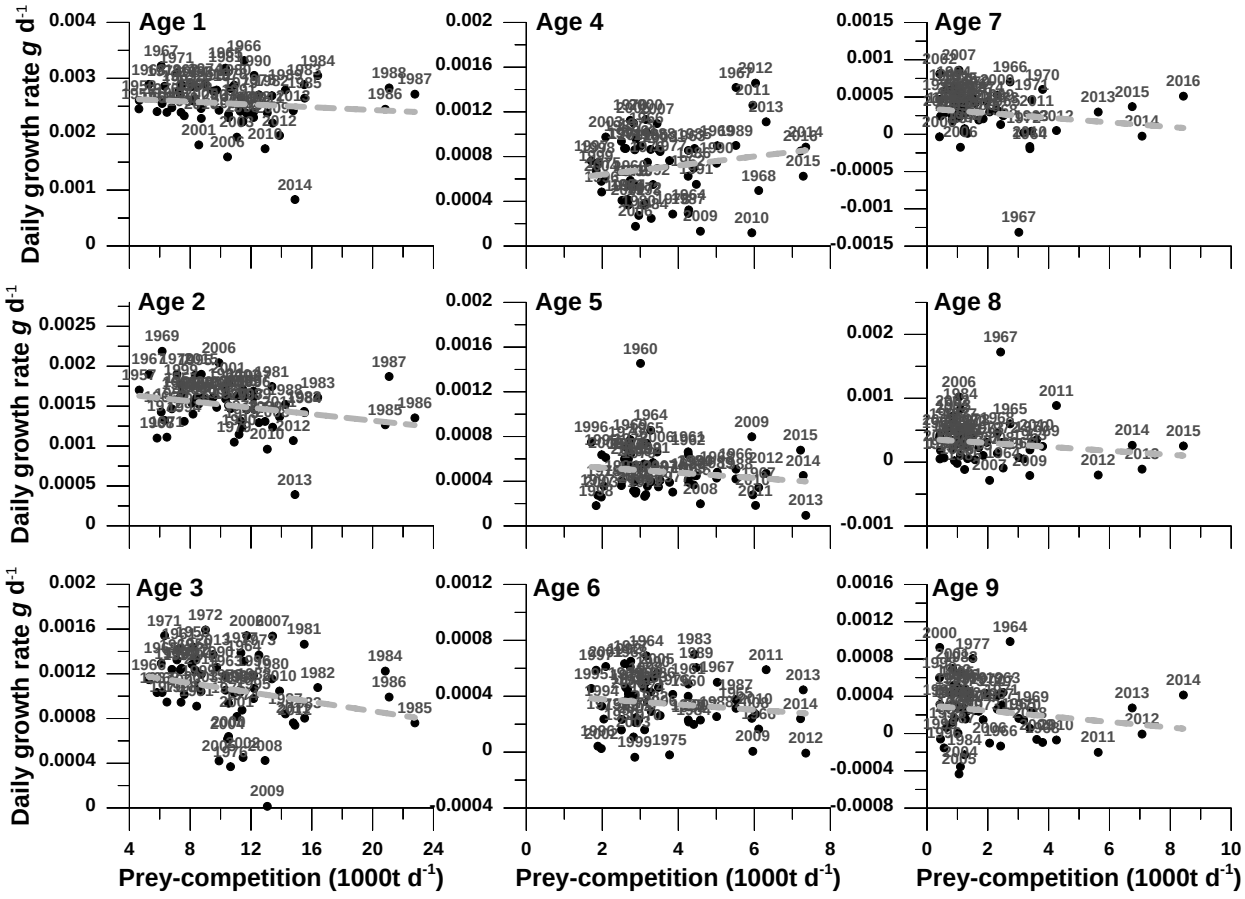

Figure 3.15. Effect of variation in the strength of the 'prey competition field' on the growth of plaice across individual annual growth steps. Growth rate was determined as the log of the growth increment between adjacent years, so the panel labelled Age 1 relates the growth rate ($W_{age\ 2}/W_{age\ 1}$), and the panel labelled Age 2 relates the growth rate ($W_{age\ 3}/W_{age\ 2}$), etc. The growth of each age (indicated by data labels) was related to the strength of the 'prey competition field' experienced by that age class during those time-steps. So for the 1972 cohort, growth from age 1 to age 2 is related to the age 1 to 3 'prey-competition' field estimated for 1972; growth from age 2 to age 3 is related to the age 1 to 3 'prey-competition' field estimated for 1973, and so on. Grey lines show linear functions fitted to each relationship and these are dashed to indicate non-significant relationships.

But, while in any one year, and for any given cohort/age class, the effect of prey competition on annual growth rate might be minimal and not detectable, high levels of prey competition that persist year on year could still have an impact on the growth of particular cohorts that experience such conditions. Figure 3.16a shows variation in prey competition conditions experienced at each age time-step by each cohort throughout its lifetime. Two particular lifetime total peaks are evident: for cohorts starting life in the middle to late 1980s, and for cohorts starting life from 2000 onwards. These peaks differ in that the competition was especially strong during early life for

the 1980s period cohorts, but comparatively much stronger in later life for the 2000 and later cohorts. This marked increase in the level of competition experienced in later life by the 1998 and subsequent cohorts is emphasized in Figures 3.16b, c and d, which show the strength of daily prey competition experienced by each cohort averaged across different age-class groups and the fraction of total cohort lifespan prey competition experienced during ages 7, 8 and 9.

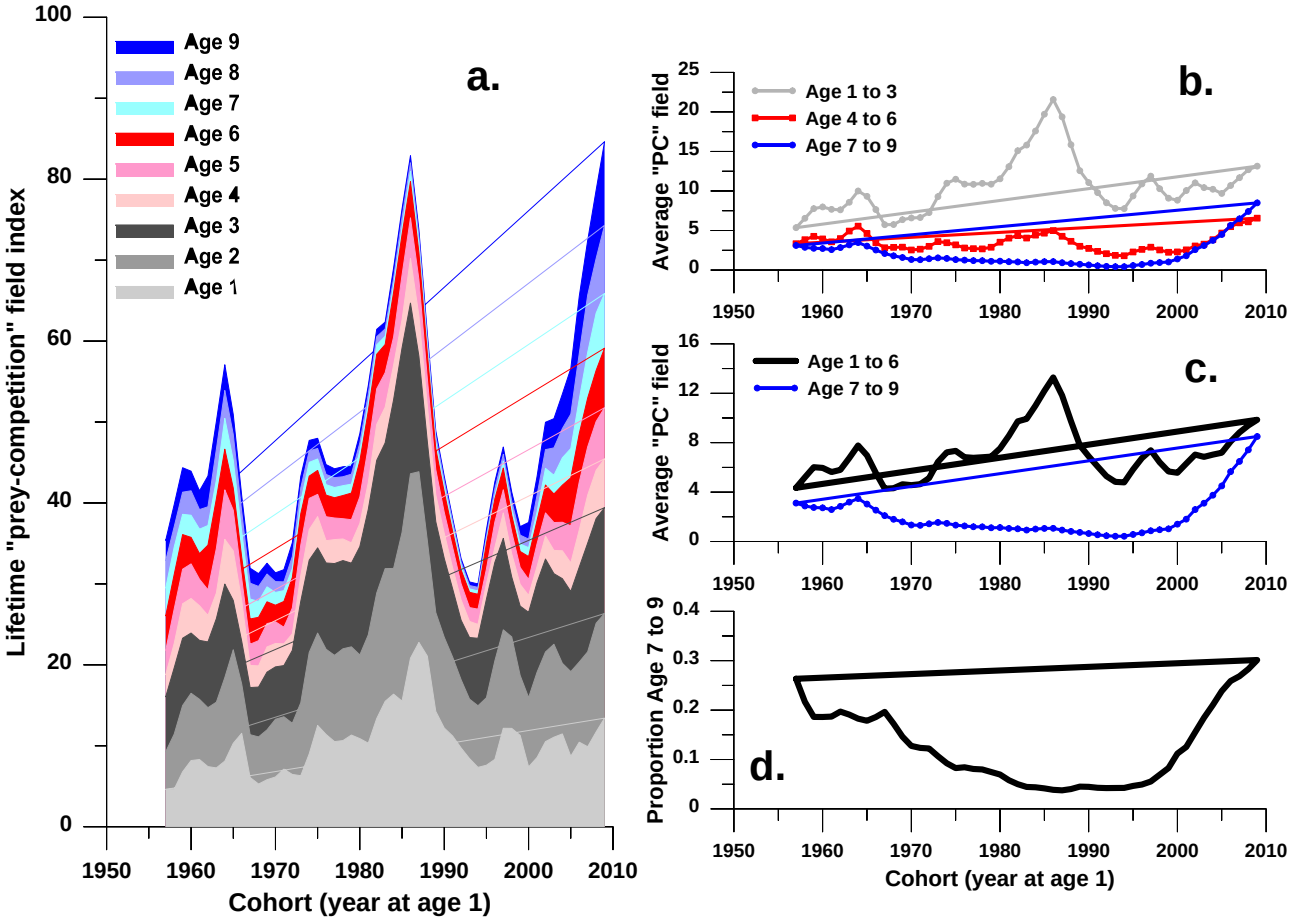

Figure 3.16.a. Variation in the strength of the prey-competition (PC) field (1000t d^{-1}) experienced by each age class of each cohort and summed across age classes to give an index of "lifetime" competition levels. b: Daily prey competition (PC) experienced by each cohort averaged across different age-class components. c: Repeat of analysis depicted in panel b, but this time averaging across age classes 1 to 6. d: Variation in the proportion of lifetime competition for prey experienced by each cohort that was encountered in later life, when age 7 to 9.

It is conceivable that these high levels of competition for prey experienced in later life by the 1998 and later cohorts may have stifled growth at this point in their lifespans, causing the reduction in asymptotic body length (L_∞) observed in Figure 3.13. Alternatively, high levels of competition for prey earlier in life may have stalled growth, which subsequently manifested as lower weight-at-age in later life, again reducing asymptotic body length. This possibility was also examined, as was the possibility that higher levels of competition averaged over each cohort's whole lifetime reduced asymptotic body length. Figure 3.17 examines these various hypotheses, relating variation in asymptotic body length determined for each cohort to variation in prey competition levels experienced by each cohort during different phases of its life. Only one significant correlation was detected, relating asymptotic body length to the strength of the age 7 to 9 'prey competition field'. Highlighting the 1998 to 2009 cohort datapoints clearly suggests that a direct causal relationship was unlikely, and instead infers that some sort of step-change in plaice life-history traits may have occurred. Estimates of asymptotic body length for the 1998 and all subsequent cohorts were lower than equivalent estimates for all but two of the preceding cohorts,

but only the 2005 to 2009 cohorts experienced age 7 to 9 'prey competition fields' stronger than those experienced by all the earlier cohorts. The 1998 to 2004 cohorts experienced competition levels in later life that were unexceptional, in the same range as those experienced by earlier cohorts yet estimates of asymptotic body length for these later cohorts were on average 6 cm smaller.

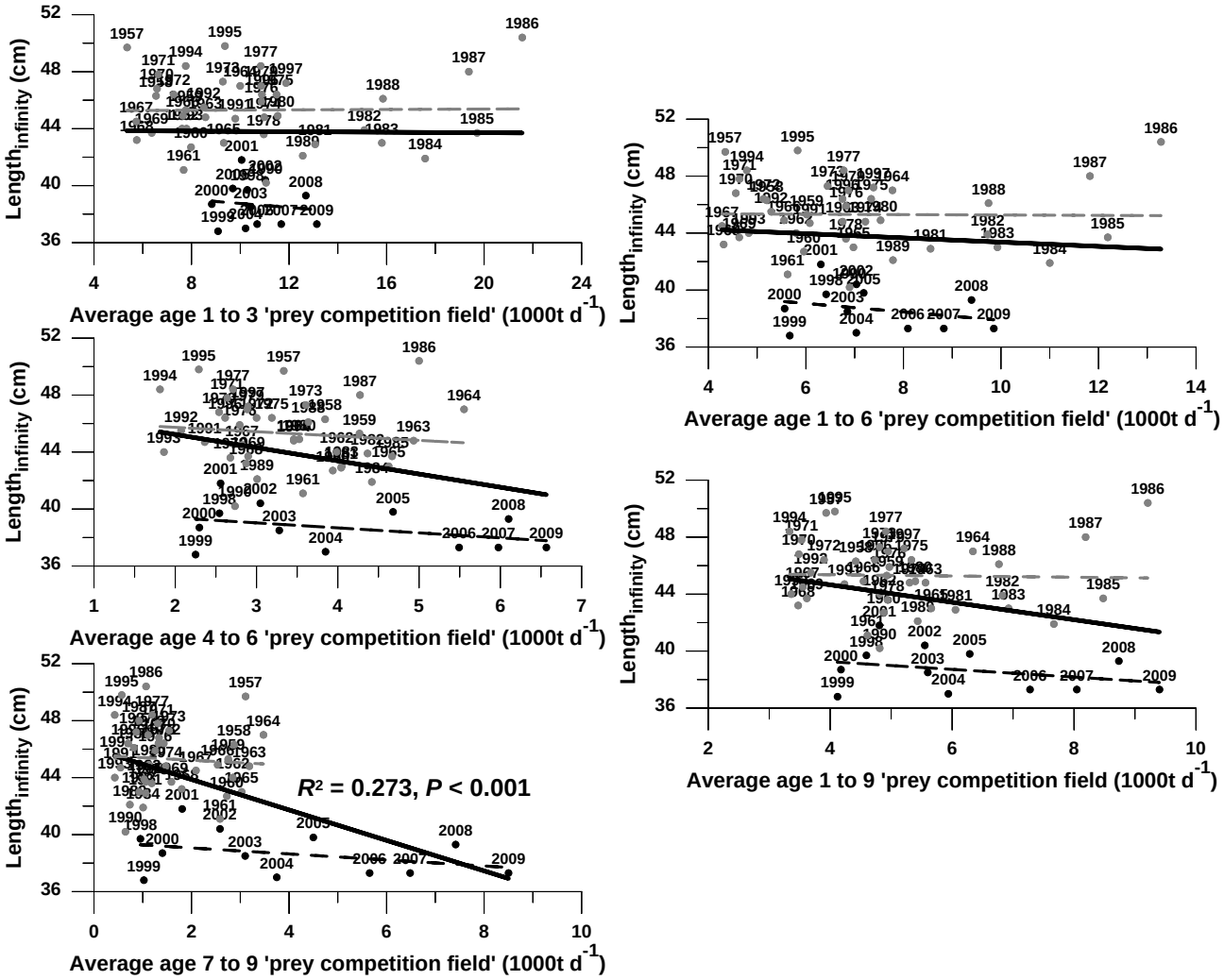

Figure 3.17. Relationships between the strength of the 'prey competition field' experienced by each cohort between the ages of 1y to 3y, 3y to 6y, 7y to 9y, 1y to 6y, and 1y to 9y (i.e. over their whole lifespan), and the estimate of cohort asymptotic body length (L_∞). Data for the 1998 to 2009 cohorts are highlighted (black dots). Heavy black line shows the relationship obtained for all cohorts, dashed lines show the non-significant relationships for early (1957 to 1997, grey) and later (1998 to 2009, black) cohorts. Date labels indicate cohort years (when age 1).

It is conceivable that the reduction in asymptotic body length is erroneous because of the assumption of constant weight-at-length. It may be that the reduction in weight-at-age observed in the stock assessment data (ICES, 2018) is caused by a decline in body condition (weight-at-length), and that there is no associated reduction in length-at-age. The effect of variation in the strength of the 'prey completion field' on cohort daily growth rates was therefore examined directly (Figure 3.18). The results were almost identical with those shown in Figure 3.17 for asymptotic body length. Again, the only significant correlation observed occurred between the strength of the 'prey completion field' at ages 7 to 9 and the daily growth rate at this stage of each cohort's life.

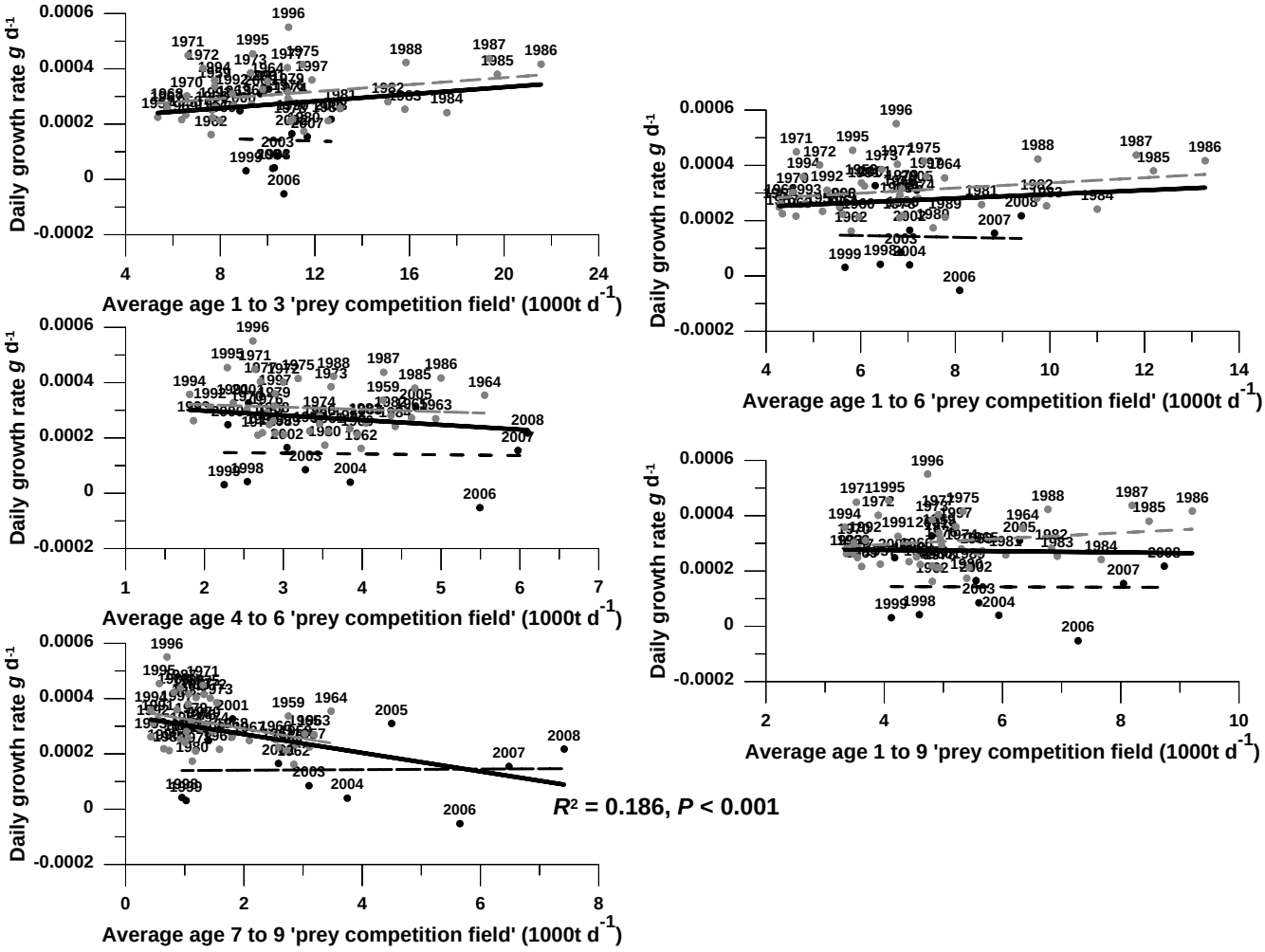

Figure 3.18. Relationships between the strength of the 'prey competition field' experienced by each cohort between the ages of 1 to 3, 3 to 6, 7 to 9, 1 to 6, and 1 to 9 (i.e. over their whole lifespan), and the estimates of cohort daily growth rate over these periods (g d^{-1}). Data for the 1998 to 2009 cohorts are highlighted (black dots). Heavy black line shows the significant relationship obtained for all cohorts, dashed lines show the non-significant relationships for early (1957 to 1997, grey) and later (1998 to 2009, black) cohorts. Date labels indicate cohort years (when age 1).

3.5.4 Testing the assumption of constant weight-at-length

Thus far, a constant weight-at-length relationship has been assumed; the reduction in weight-at-age observed in the stock assessment data consequently reflected a corresponding decline in length-at-age, and this reduction in length-at-age therefore gave rise to the perceived decline in plaice asymptotic body length. However, weight-at-length data collected by the Dutch third-quarter beam trawl survey since 1996 suggest a significant year effect in the weight-at-length relationship (Figure 3.19a), affecting the constant parameter a in the weight-at-length relationship (Figure 3.19b). Setting the body condition in 1996 as the reference condition with a value of 1.0, these data can be used to estimate the average decline in body condition over time (Figure 3.19c). By 2014 to 2016, plaice body condition had declined to about 93% of the 1996 reference level. Figure 3.19d indicates how this change in body condition would change the body mass of a 33 cm plaice, the approximate average length of an age-5 fish across the whole assessment time-series. It is unfortunate that earlier weight-at-length data are not available to allow exploration of variation in body condition prior to 1996, but the marked decline in body condition between 1996 and 1998 corresponds closely in time with the sharp reduction in estimated cohort asymptotic body length shown in Figure 3.13. This agreement suggests that the decline in weight-at-age apparent in the stock assessment data (Figure 3.12) could, at least in part, have been caused

by a reduction in plaice condition, rather than entirely due to a change in growth pattern primarily affecting asymptotic body length.

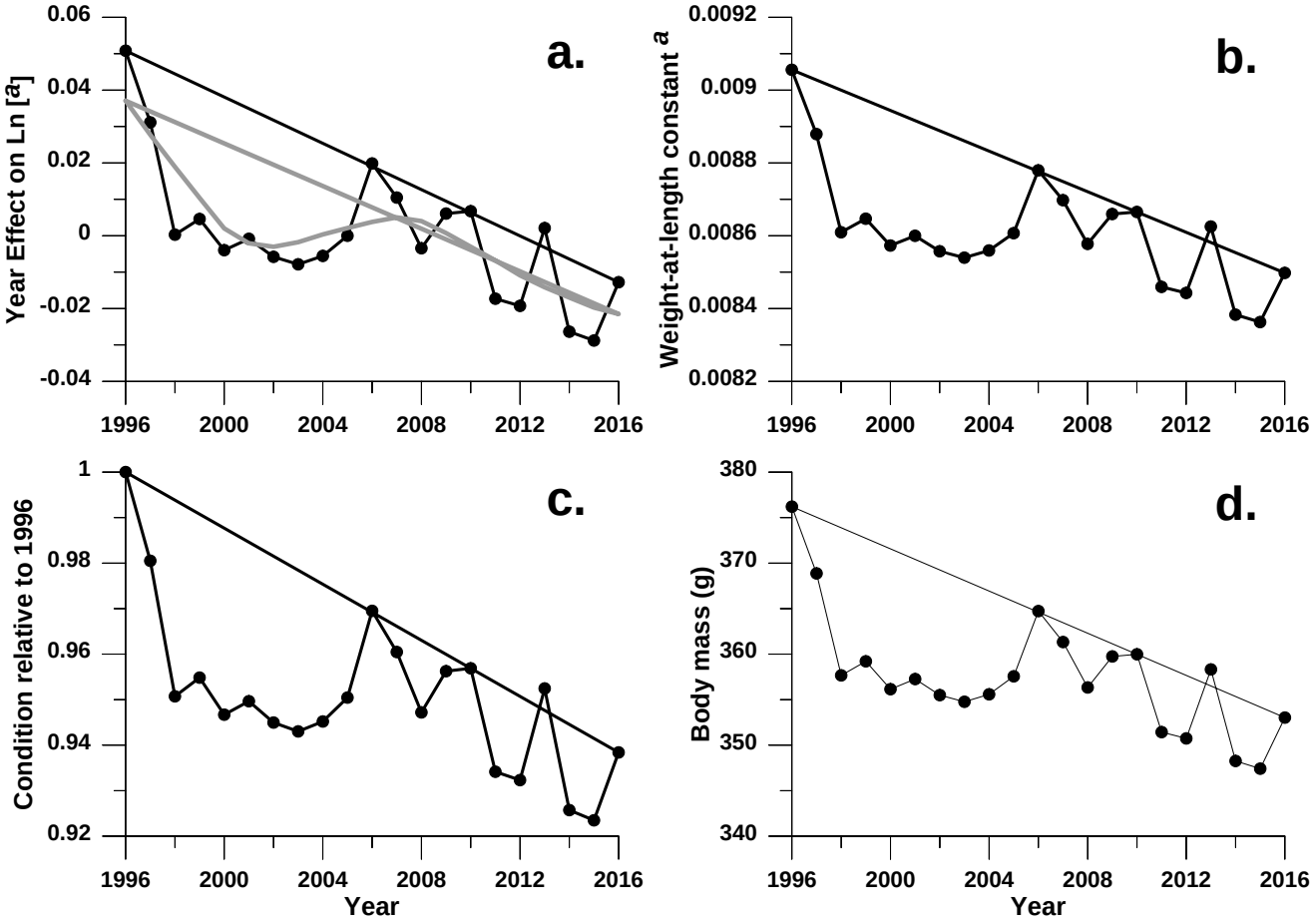

Figure 3.19. Year effect on the Ln [a] parameter relating Ln [weight] to Ln [length] (a) and the consequences of this on the parameter *a* in the standard power function $W=aL^b$ weight-at-length relationship (b), body condition relative to the 1996 reference condition (c), and the body-mass of a 33 cm length plaice (d).

The Dutch beam trawl data also included cohort information, so as well as examining variation in plaice condition as a function of length in each year, it was also possible to track variation in plaice weight-at-length in successive cohorts as they increased in age, length and weight. Since weight-at-length sampling only commenced in 1996, data for cohorts starting life earlier than 1994 were relatively sparse and only included larger sized fish. Similarly, since the available data end in 2016, data for cohorts starting life after 2013 were also sparse and generally only included data for smaller sized individuals. Of the 842 fish sampled belonging to the 2013 cohort, only 13 exceeded 32 cm in length. For that reason, 2013 was considered the latest cohort for which available weight-at-length data were deemed adequate. Figure 3.20 repeats the plots shown above in Figure 3.19. Although the general patterns are similar, differences in detail are apparent, generally suggesting a lag with changes in body condition evident among individual cohorts about one to two years earlier than suggested in the annual data.

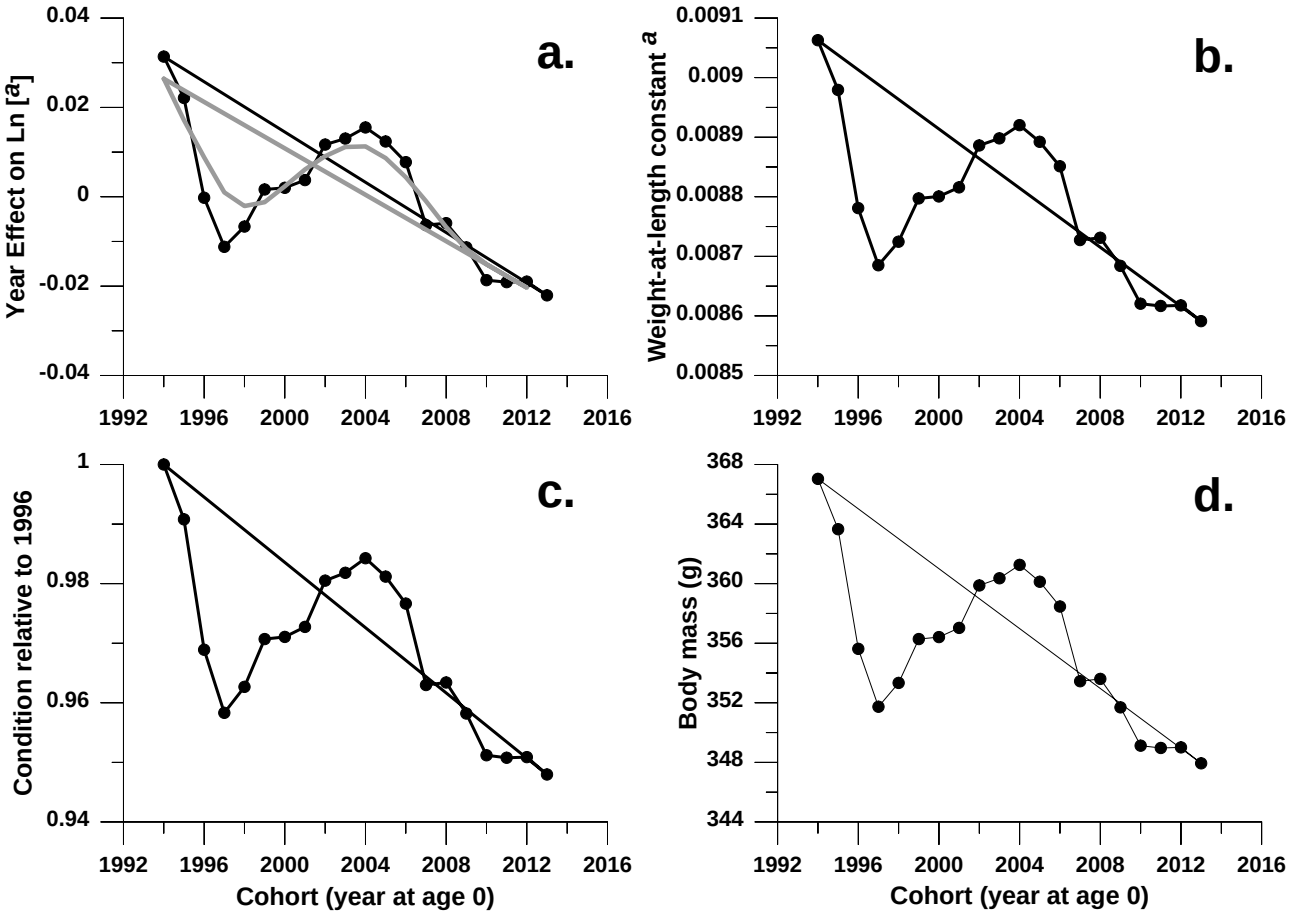

Figure 3.20. Cohort effect on the Ln [a] parameter relating Ln [weight] to Ln [length] (a) and the consequences of this on the parameter *a* in the standard power function $W=aL^b$ weight-at-length relationship (b), body condition relative to the 1994 cohort reference condition (c), and the body-mass of a 33 cm plaice (d).

3.5.5 Trends in growth taking account of changes in body condition

The similarity of the results shown in Figures 3.17 and 3.18 suggests perhaps that the reduction in body condition was insufficient to account for all the decline in weight-at-age observed in the stock assessment data. Some reduction in length-at-age also occurred; the reduction in asymptotic body length may be real, although perhaps not to the same extent as suggested in Figure 3.13. This possibility was examined by again using the Petersen method to estimate the von Bertalanffy growth equation parameter for each plaice cohort, but this time using the Dutch beam trawl weight-at-length relationships determined for each year to account for the post 1996 decline in body condition.

Given that sampling of weight-at-length is undertaken on an annual and fish length basis, rather than targeted sampling of fish of different age, plus the fact that the weight-at-age data provided in the stock assessment are also based on length-based samples rather than age-based samples, the data depicted in Figure 3.19 were used to control for variation in body condition prior to re-estimating the plaice cohort von Bertalanffy growth equation parameters. Given the relative consistency in the earlier estimates of asymptotic body length derived for cohorts originating (age 1) between 1957 and 1997, it seemed reasonable to use an average of the 1996 and 1997 Dutch beam trawl weight-at-length relationship parameters for the whole of this period, and then to use the observed Dutch beam trawl relationships in each subsequent year up to 2016. In 2017, no Dutch data weight-at-length data were available, so for this year, the average of the Dutch parameter values for 2014 to 2016 were applied (Table 3.5). Figure 3.21 shows the revised trends in

the von Bertalanffy asymptotic body length and growth term parameters after accounting for the decline in body condition inferred in the Dutch beam trawl weight-at-length sampling. The 5% to 7% decline in body condition is insufficient to account for the marked decline in weight-at-age observed in the stock-assessment output. The strong decline in asymptotic body length from 1998 onwards is still evident, although the difference between the average values calculated for the periods 1957 to 1997 (6.53 cm) and 1998 to 2008 (5.95 cm) is slightly reduced. In this reanalysis, however, a step function increase in the growth term is perhaps more evident than previously.

Table 3.5. Weight-at-length relationship parameters used to convert estimates of weight-at-age provided in the plaice stock assessment (ICES, 2018) to estimates of length-at-age.

Period/Year	W@L *a*	W@L *b*
1957 to 1997	0.008967	3.041460
1998	0.008609	3.041460
1999	0.008647	3.041460
2000	0.008573	3.041460
2001	0.008600	3.041460
2002	0.008557	3.041460
2003	0.008540	3.041460
2004	0.008559	3.041460
2005	0.008607	3.041460
2006	0.008780	3.041460
2007	0.008698	3.041460
2008	0.008578	3.041460
2009	0.008660	3.041460
2010	0.008665	3.041460
2011	0.008459	3.041460
2012	0.008443	3.041460
2013	0.008625	3.041460
2014	0.008383	3.041460
2015	0.008363	3.041460
2016	0.008498	3.041460
2017	0.008414	3.041460

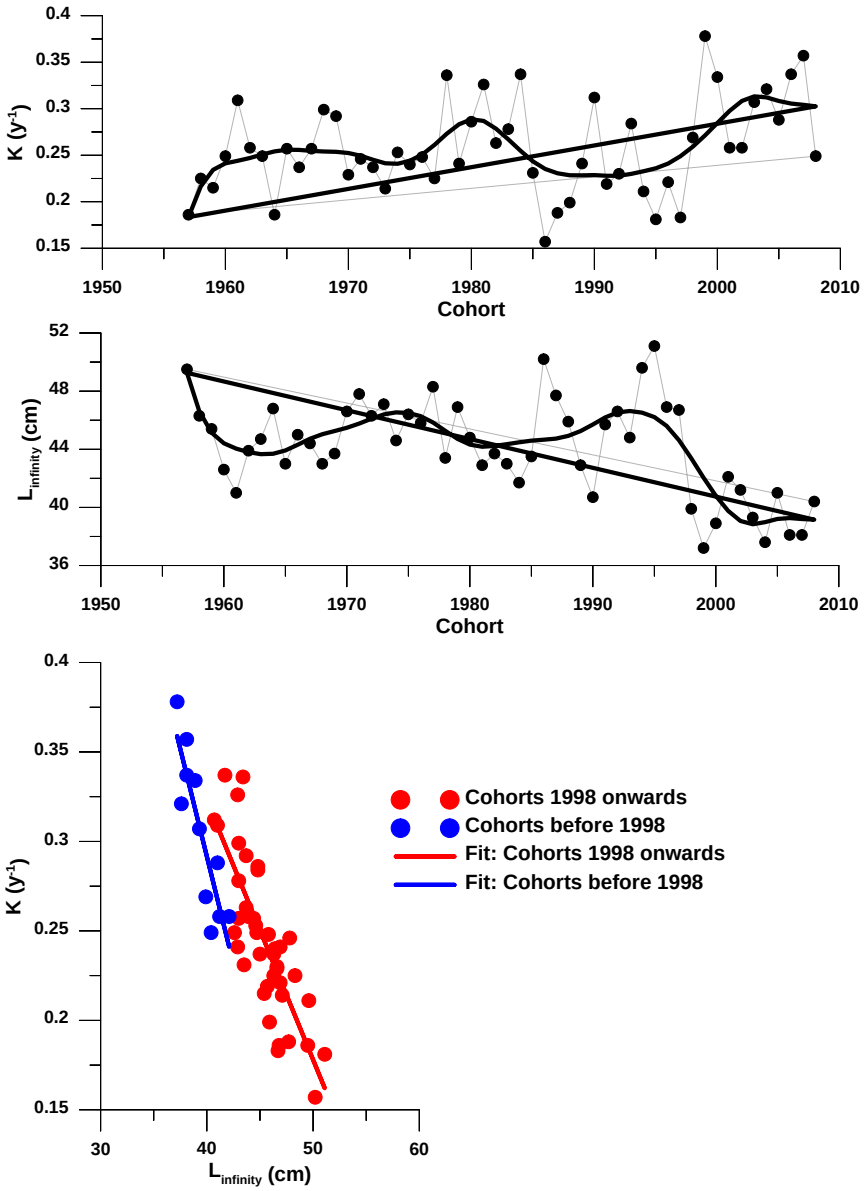

Figure 3.21. Variation in von Bertalanffy growth equation *K* (upper panel) and L_∞ (middle panel) parameter values for plaice cohorts over the period 1952 to 2013. Parameter values for datapoints with a central grey fill are derived from complete weight-at-age data, whilst parameter values for the full black datapoints at the start and end of each time-series are derived from incomplete weight-at-age data. Heavy black lines show fitted loess smooths constructed using a tricubic kernel and second-order polynomial and a fitting window of 40% of the data range. Lower panel shows the relationship between L_∞ and *K*. Linear fits for the whole dataset, and cohorts before and after the apparent change in growth pattern are shown.

3.5.6 An alternative explanation for the changes in plaice growth and condition

The spatial distribution of plaice is examined in Section 5.4. That analysis included plaice in the Kattegat, which is not considered part of the North Sea stock. Therefore, the spatial analyses were repeated for the North Sea proper, excluding the Kattegat component. Results of this reanalysis are qualitatively similar to those presented in Section 5.4 and are therefore not repeated here. As the plaice population increased in abundance, the spatial distribution did not expand, apart from an increased occupancy of marginal areas. The spatial distribution has shifted north-east away from coastal areas into deeper waters. Such shifts have been interpreted as mitigating

against rising seawater temperature, deeper water generally being cooler than shallower waters (Dulvy *et al*., 2008). Over the 35-year survey time-series, significant positive trends in the biomass weighted mean temperatures experienced by each age-class group of plaice occupying the core areas (holding 50% of the population) were evident (Figure 3.22), such that temperatures experienced by plaice in 2017 were generally 1.5°C warmer in summer and 1.0°C warmer in winter. Changes of temperature of this magnitude will have affected plaice food intake rates and metabolic costs.

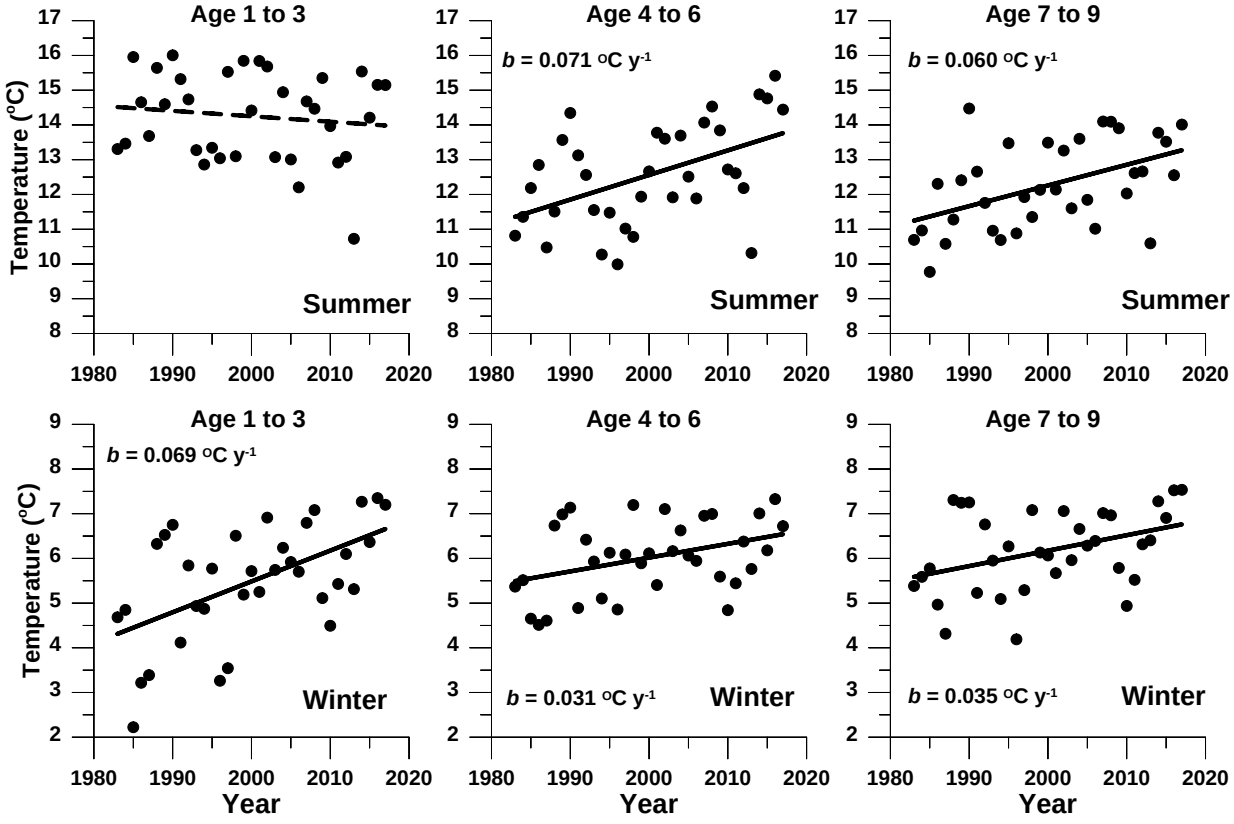

Figure 3.22. Temporal trends in water temperature at the seabed experienced by 50% of North Sea plaice age 1 to 3, 4 to 6 and 7 to 9 occupying the core areas of their distributions in summer (August) and winter (February) each year. Heavy black lines show significant trends in water temperature and annual average rates of increase (regression slope parameter b) are indicated.

3.5.7 Plaice digestion-ingestion model

Basimi and Grove (1985) provide a digestion model for plaice, which relates the time for a meal to be fully digested, the gastric emptying time (T_{GE}), to meal size (M), fish body weight (W), and water temperature (T),

$$\ln[T_{GE}] = 3.68 + 0.49\ln[M] - 0.068\ \ln[W] - 0.086T$$

This equation can be rearranged to describe the digestion rate,

$$0.49\ln[M] - \ln[T_{GE}] = -3.68 + 0.068\ln[W] + 0.068\ln[W] + 0.086T$$

which resolves to

$$\frac{M^{0.49}}{T_{GE}} = -0.025W^{0.068}e^{[0.086T]}$$

If this is the rate that a meal of a given size is digested, then it follows that for a plaice feeding at a specified rate per hour (F_{intake}) and digesting food at a rate (F_{digest}), then the change in stomach contents weight (ΔS_t) in any given hour is

$$\Delta S_t = F_{intake,t} - F_{digest,t}$$

so,

$$S_{t=t+1}^{0.49} = S_{t=t}^{0.49} + F_{intake,t=t}^{0.49} - 0.025W^{0.068}e^{[0.086T]}$$

where $S_{t=t+1}$ is the stomach contents weight at the end of each time-step (beginning of the next time-step) when $S_{t=t}$ is the residual stomach contents weight at the start of each time-step left undigested from the previous time-step. $F_{intake,t=t}$ is the food intake rate, here designated $t=t$ because the model adds the food consumed in any given 1h time-step at the start of the hour, immediately adding this to the undigested food residual from the previous hour, so that both this residual undigested food and the new ingested food are subject to the full hour of the digestion process.

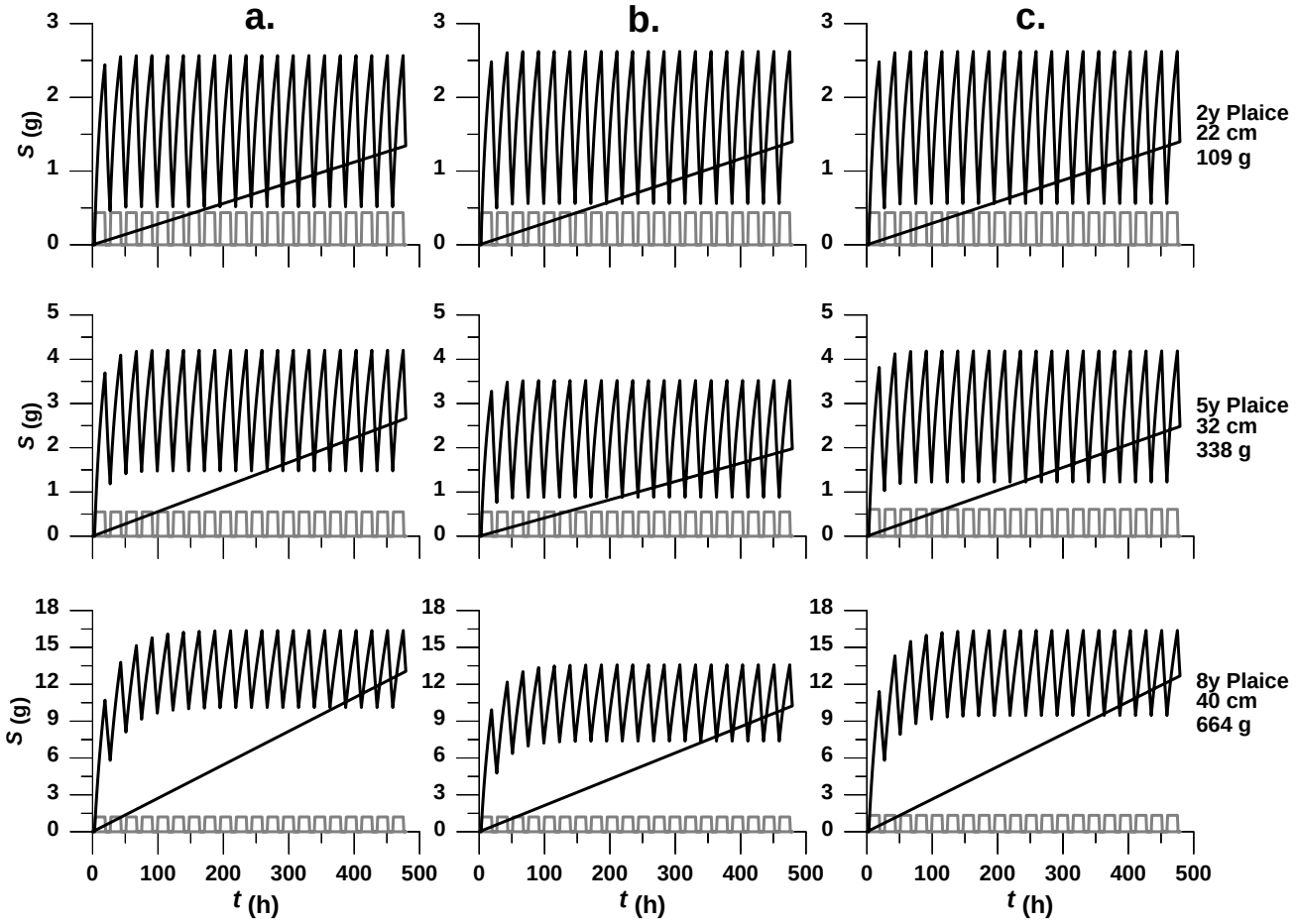

Figure 3.23. Modelled hourly change in stomach contents weight (black lines) of three age/length/body-mass exemplar plaice given 1987 (panels labelled a.) and 2017 (panels labelled b.) water temperature conditions in summer and 'standard' daily food ration consumed at an even rate over a 16 hour daylight feeding period, and (panels labelled c.) under 2017 water temperature conditions when the daily food ration was increased to maintain the same maximum equilibrium stomach contents weight observed in the 1987 model results. See table 3.6 for input parameter values and results summary.

Basimi and Grove (1985) consider plaice to be visual feeders, feeding primarily during daylight hours, although they do acknowledge that some studies have indicated a degree of nocturnal foraging as well. For the purposes of the model presented here, visual searching was assumed

to be the norm, and a 16 hour daylight feeding period in summer, and 10 hour daylight feeding period in winter, were modelled. The model tracks variation in the stomach contents weight of plaice aged 2y, 5y and 8y, i.e. the midpoints of each diet-based age-class groups. The model starts with plaice with completely empty stomachs at the start of either a winter or a summer feeding period. They therefore immediately start feeding at a constant hourly intake rate that accounts for their entire daily food consumption over the full feeding period within each 24 hour day. Thus, for example at the 1987 summer water temperature of 11.67°C, a 5y plaice of length 32 cm and 338 g body mass would consume 8.79 g of food per day, 2.6% of its body mass, over a 16 hour daylight feeding period. This equates to a constant hourly food intake rate of 0.55g h^{1}. The digestion process is assumed to start as soon as food enters the stomach and the model tracks the change in stomach weight as a balance of the two rates: ingestion and digestion. Equilibrium maximum stomach contents weights were achieved within two days in summer (Figure 3.23a) and three days in winter (Figure 3.24a). Basimi and Grove (1985) suggest that the stomach capacity of plaice is small compared with other flatfish, being only 2.4 ml per 100 g of body weight. Assuming prey to have the same density as water, this implies that plaice can only accommodate a stomach contents weight of approximately 2.4% of their body mass. In fact, the density of polychaete and mollusc prey is likely to be slightly greater than that of water, so they could probably accommodate a stomach contents weight to body weight ratio slightly higher than this. Nevertheless, none of the model scenarios indicated a maximum equilibrium stomach contents weight that exceeded this. The food intake rates and feeding patterns portrayed in the simulations were therefore entirely plausible.

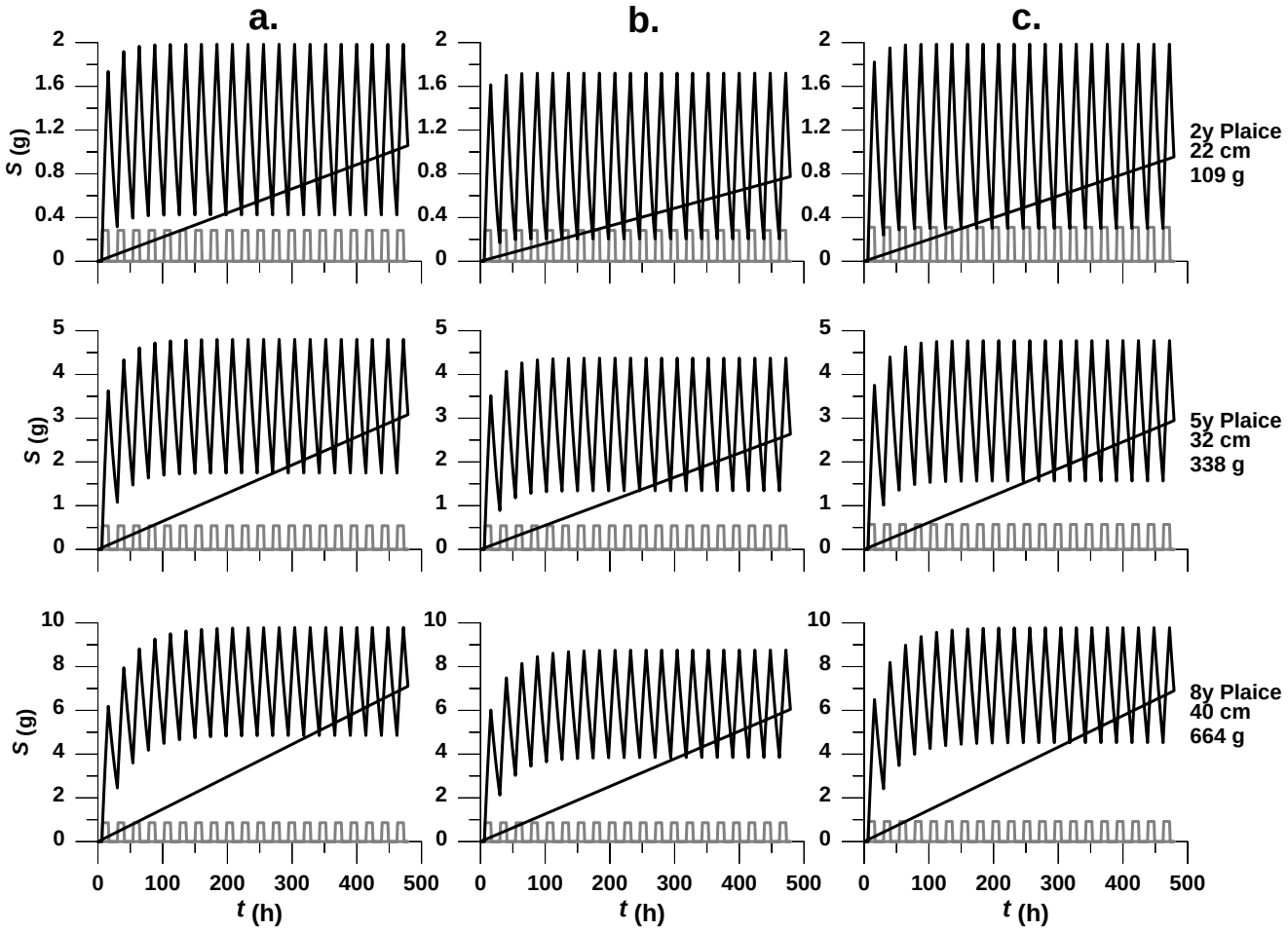

Figure 3.24. Modelled hourly change in stomach contents weight (black lines) of three age/length/body mass exemplar plaice given 1987 (panels labelled a.) and 2017 (panels labelled b.) water temperature conditions in winter and 'standard' daily food ration consumed at an even rate over a 10 hour daylight feeding period, and (panels labelled c.) under 2017 water temperature conditions when the daily food ration was increased to maintain the same maximum equilibrium stomach contents weight observed in the 1987 model results. See table 3.6 for input parameter values and results summary.

Holding food ingestion rates constant, the effects of the changes in temperature indicated in Figure 3.22 on the maximum stomach contents weight at modelled 2017 temperatures are explored in panels b of Figures 3.23 and 3.24. Effects of this rise in temperature on maximum stomach contents weights were apparent in all age-class groups in both seasons, except for the model age-2 plaice in summer because Figure 3.22 suggests that this age-class group experienced no significant trend in summer temperatures over the 35-year survey period. Holding satiation levels constant, i.e. if maximum stomach-content weight observed in the 1987 simulations were forced on the 2017 simulations, the model was then used to explore the increase in food intake rates that would be possible as a consequence of the temperature-related increase in digestion rates. With the exception of the modelled age-2 plaice in summer, which experienced no change in summer temperatures, increases in food ingestion rates of between 5.6% and 6.7% in winter and 9.9% and 11.0% in summer were indicated (Figures 3.23c and 3.24c). Table 3.6 gives all the model input parameter values and summarises the output results.

Table 3.6. Plaice ingestion/digestion model input parameter values and output results: age, length and weight of exemplar fish, giving data for the summer and winter seasons; daily rations as wet-weight per day and percentage these values represent of predator body-mass; water temperature at the seabed experienced by these ages of fish in 1987 and 2017 (derived from the regression equations obtained in 3.22), and the difference (ΔT) in these temperatures; maximum equilibrium stomach contents weight predicted by the model, and the percentage these values represent of predator body mass, when consuming the daily ration at an even rate over a 16 hour daylight feeding period in summer, and over a 10 hour day light feeding period in winter, under 1987 (Figures 3.23 and 3.24, panels a) and 2017 (Figures 3.23 and 3.24, panels b) water temperature conditions; daily ration that plaice would have to consume under 2017 water temperature conditions and still maintain their 1987 stomach contents weight level (Figures 3.23 and 3.24, panels c), and the difference this ration represents shown as a percentage change over the original daily ration.

Age (y)	Length (cm)	Weight (g)	Season	Daily Ration		Temperature (°C)			Maximum S (T_{1987})		Maximum S (T_{2017})		Daily Ration to maintain S	
				($g\ d^{-1}$)	%BW	1987	2017	ΔT	(g)	%BW	(g)	%BW	($g\ d^{-1}$)	ΔR %
2	22	109	Summer	6.98	6.4	13.30	13.13	-0.17	2.565	2.35	2.622	2.41	**6.98**	0%
			Winter	2.83	2.6	5.03	6.54	+1.51	1.984	1.82	1.721	1.58	3.11	+9.89
5	32	338	Summer	8.79	2.6	11.67	13.05	+1.38	4.204	1.24	3.520	1.04	9.72	+10.58
			Winter	5.41	1.6	5.62	6.46	+0.84	4.802	1.42	4.373	1.29	5.71	+5.55
8	40	664	Summer	19.2	2.9	11.38	12.71	+1.33	16.375	2.47	13.582	2.05	21.38	+11.01
			Winter	8.63	1.3	5.71	6.61	+0.90	9.789	1.47	8.757	1.32	9.21	+6.72

Figure 3.25a shows variation in the mean water temperature experienced by each cohort over its entire lifetime. Given that available temperature data were obtained in February and August, average temperature in each year was estimated as: $(T_{Feb,y} + 2T_{Aug,y} + T_{Feb,y+1})/4$. Annual average temperature values for each of the nine annual time-steps were then summed and this total was divided by 9 to give an estimate of lifetime mean temperature. After an initial rise and subsequent decline, annual lifetime temperature exposure increased steadily between 1993 and 2009 and from 1997 has been higher than at any previous time in the available time-series. Cohorts from 1997 onwards experienced lifetime temperature exposures of, on average, 9.8°C compared with a value of 9.2°C for cohorts starting life prior to this date; a difference of 0.6°C. Estimates of cohort asymptotic body length, derived taking account of the reduction in plaice body condition observed in the Dutch Beam trawl data, was significantly negatively correlated with cohort lifetime temperature exposure (Figure 3.25b).

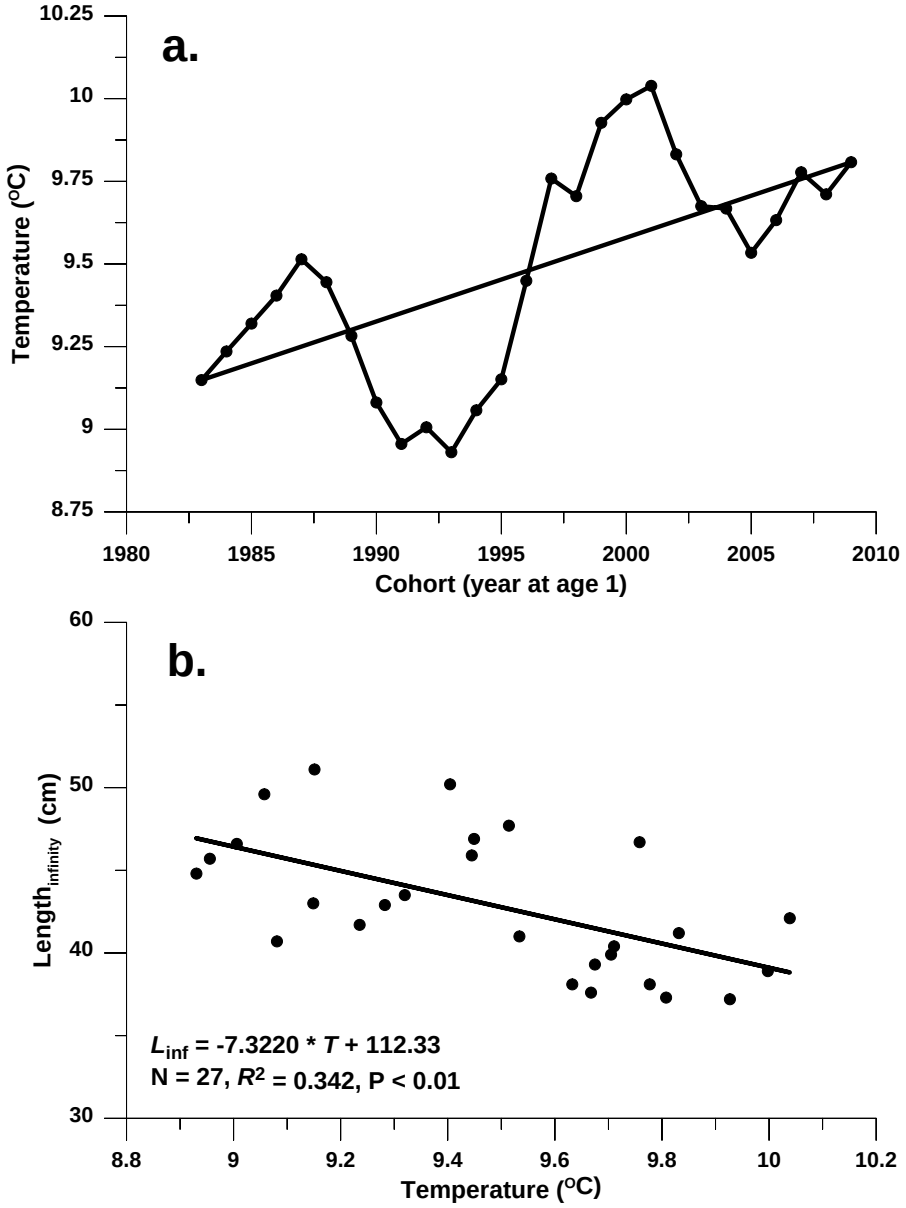

Figure 3.25.a. Trends in average water temperature experienced by plaice over the full lifetime of each successive cohort from 1983 to 2009. b: Relationship between *L*inf and the average water temperature experienced by each cohort.

3.6 Comparing the footprints of predation pressure to the footprints of bottom trawling, including the effects of fish predation mortality in the assessment of bottom-trawling impact on the seafloor

In recent years, a framework for the impact of fishing on seafloor integrity has been developed, first within the BENTHIS FP7 project and the Trawling Best Practice project, and later in the ICES workshops WKBENTH, WKSTAKE and WKTRADE, and the WGFBIT working group. This framework uses the longevity of benthic species to quantify their recovery rates after trawling, and the seabed penetration depth of the fishing gear to quantify the benthic mortality per unit effort. These two parameters are used to calculate the equilibrium benthic abundance relative to its maximum (carrying capacity) given long-term exposure to the current trawling intensity. Subsequently, this quantity is used as an indicator of fishing impact on the benthos. The indicator has the value of 1 if there is no fishing, as the benthic biomass is at its carrying capacity but decreases linearly towards zero as trawling intensity increases (Hiddink *et al*., 2017). This framework considers the mortality effect of trawling on benthos in isolation. However, the primary purpose of bottom-trawl fishing is the removal of fish from the ecosystem, and the primary food for many of these fish are the same benthic invertebrates directly affected by the trawling.

There are indications that this relationship can fundamentally alter the response of the benthos to bottom trawling (van Denderen *et al*., 2013; Johnson *et al*., 2015). In the extreme case, the benthic mortality, which is prevented by the trawl-induced removal of fish, could exceed the direct mortality of trawling on the benthos. This could lead to a net positive relationship between bottom trawling and benthos abundance being observed. However, empirical data generally show a negative relationship between trawling intensity and benthos abundance (van Denderen *et al*., 2014; Johnson *et al*., 2015; van Denderen *et al*., 2015; Sciberras *et al*., 2018). A number of mechanisms may lead to this observation, the most obvious being that the indirect effect of bottom trawling on benthos (reduced feeding by fish) is actually small compared to the direct effects. A second possibility is that this relationship is generally assessed on a small spatial scale, because there is no large-scale benthos sampling, especially not long term. Fish are mobile predators so local fish removal is not necessarily related to the local reduction in consumption induced by trawling. Furthermore, many benthic species are also either mobile or have pelagic larval stages. Hence, the lack of observations of positive net effects on local scales should not be taken as proof of their insignificance.

WGECO recommends that WGFBIT takes-up this issue in its assessment framework, as such indirect effects through feeding are essential in moving towards ecosystem-based management. In the WGFBIT framework, this could be accomplished by adding a second loss term, analogous to that used for trawling. This loss term then could depend on fish abundance, which in turn depends on fishing intensity. This would require re-estimating the carrying capacities used in the FBIT work, because the current carrying capacities include the abundance reduction by fish.

3.7 Distribution of stomach-content data across species and size classes

A table was presented that summarizes the distribution of stomach-content data across species and size classes (See table here). Entries with 0 data show species and/ or size classes that were caught in the Greater North Sea otter trawl data in quarter 1 (i.e. the International Bottom Trawl Survey) but do not appear in DAPSTOM or ICES year-of-the-stomach data. Many countries collect stomach-content data, but these are often not collated despite surveying the same ecosystems

and/or species, and there is no consensus on exactly what information should be collected. Much could be gained from collating data, and remaining information gaps could be systematically addressed via international collaboration. This would mean future stomach contents sampling could be coordinated to best address policy needs cost effectively. Our aim therefore is to integrate these data with other stomach-content data to improve understanding of fundamental and realised diets of marine organisms. Contact Murray Thompson (murray.thompson@cefas.co.uk) for more information.

3.8 References

Anon. 2010. Manuals for the Icelandic bottom-trawl surveys. Hafrannsóknir nr. 156.

Azarovitz, T.R. 1981. A brief historical review of the Woods Hole Laboratory trawl survey time-series. In: Doubleday WG; Rivard D., eds. Bottom trawl surveys. Can Spec. Publ. Fish. Aquat. Sci. 58; p 62–67.

Basimi, R.A. and D.J. Grove. 1985. Estimates of daily food intake by an inshore population of *Pleuronectes platessa* L. off eastern Anglesey, North Wales. J. Fish Biol. 27:505–520.

Belleggia, M., Mabragaña, E., Figueroa, D.E., Scenna, L.B., Barbini, S.A., Díaz de Astarloa, J.M. 2008. Food habits of the broad nose skate, *Bathyraja brachyurops* (Chondrichthyes, Rajidae), in the south-west Atlantic. Sci. Mar. 72:701–710.

Cormon, X., B. Ernande, A. Kempf, Y. Vermard and P. Marchal. 2016. "North Sea saithe *Pollachius virens* growth in relation to food availability, density-dependence and temperature." Marine Ecology Progress Series 542: 141–151.

Durbin, E.G., Durbin, A.G., Langton, R.W., Bowman, R.E. 1983. Stomach contents of silver hake, *Merluccius bilinearis*, and Atlantic cod, *Gadus morhua*, and estimation of their daily rations. Fish. Bull. 81:437–454.

Eggers, D.M. 1977. Factors in interpreting data obtain by diel sampling of fish stomachs. J. Fish. Res. Board Can. 34:290–294.

Elliot, J.M., Persson, L. 1978. The estimation of daily rates of food consumption for fish. J. Anim. Ecol. 47:977–991.

Gulland, J.A. 1983. Fish stock assessment. Wiley, Chichester, UK.

Hermsen, J.M, Collie, J.S., Valentine, P.C. 2003. Mobile fishing gear reduces benthic megafaunal production on Georges Bank. Mar. Ecol. Prog. Ser. 260:97–108.

Hiddink, J. G., S. Jennings, M. Sciberras, C. L. Szostek, K. M. Hughes, N. Ellis, A. D. Rijnsdorp, R. A. McConnaughey, T. Mazor, R. Hilborn, J. S. Collie, C. R. Pitcher, R. O. Amoroso, A. M. Parma, P. Suuronen and M. J. Kaiser. 2017. Global analysis of depletion and recovery of seabed biota after bottom trawling disturbance. Proceedings of the National Academy of Sciences of the United States of America 114(31): 8301–8306.

ICES. 2018. Report of the working group on Ecosystem Effects of Fishing Activities (WGECO). ICES CM 2018 / ACOM: 27, 65 pp.

Jaworski A, Ragnarsson SA. 2006. Feeding habits of demersal fish in Icelandic waters: a multivariate approach ICES Journal of Marine Science, 63: 1682–1694 (2006)

Johnson, A. F., G. Gorelli, S. R. Jenkins, J. G. Hiddink and H. Hinz. 2015. Effects of bottom trawling on fish foraging and feeding. Proceedings of the Royal Society B: Biological Sciences 282.

Jónsson, S., Valdimarsson, H. 2012. Water mass transport variability to the North Icelandic shelf, 1994–2010. ICES J. Mar. Sci. 69, 809–815. https://doi.org/10.1093/icesjms/fss024

Koen Alonso, M., Crespo, E.A., García, N.A., Pedraza, S.N. 2002. Fishery and ontogenetic driven changes in the diet of the spiny dogfish, *Squalus acanthias*, in Patagonian waters, Argentina. Environ. Biol. Fish. 63:193–202.

Latour, R.J., Gartland, J., Bonzek, C.F., Johnson, R.A. 2008. The trophic dynamics of summer flounder (*Paralichthys dentatus*) in Chesapeake Bay. Fish. Bull. 106:47–57.

Link, J.S., Almeida, F.P. 2000. An overview and history of the food web dynamics program of the Northeast Fisheries Science Center, Woods Hole, MA. NOAA Tech. Memo. NMFS-NE-159, 60 p.

Lorenzen, K. and K. Enberg. 2002. Density-dependent growth as a key mechanism in the regulation of fish populations: evidence from among-population comparisons. Proceedings of the Royal Society of London Series B-Biological Sciences 269(1486): 49–54.

Moriarty, M., Greenstreet, S.P.R., Rasmussen, J. and de Boois, I. 2019. Assessing the state of demersal fish to address formal ecosystem based management: making fisheries independent data 'fit for purpose'. Frontiers in Marine Science. 6:162, 10 pp. Doi 10.3389/fmars.2019.00162.

Northeast Fisheries Center (NEFC). 1988. An evaluation of the bottom trawl survey program of the Northeast Fisheries Center. NOAA Tech. Memo. NMFS-F/NEC-52, 83 p.

Reid, R.N., Almeida, F.P. and Zetlen, C.A. 1999. Essential fish habit source document: fishery-independent surveys, data sources, and methods. NOAA Tech. Memo. NMFS-NE-122, 39 p.

Richardson, D.E., Palmer, M.C. and Smith, B.E. 2014. The influence of forage fish abundance on the aggregation of Gulf of Maine Atlantic cod (*Gadus morhua*) and their catchability in the fishery. Can. J. Fish. Aquat. Sci. 71:1349–1362.

Sciberras, M., J. G. Hiddink, S. Jennings, C. L. Szostek, K. M. Hughes, B. Kneafsey, L. J. Clarke, N. Ellis, A. D. Rijnsdorp, R. A. McConnaughey, R. Hilborn, J. S. Collie, C. R. Pitcher, R. O. Amoroso, A. M. Parma, P. Suuronen and M. J. Kaiser. 2018. "Response of benthic fauna to experimental bottom fishing: A global meta-analysis." Fish and Fisheries 19(4): 698–715.

Smith, B.E., Collie, J.S., Lengyel, N.L. 2013. Effects of chronic bottom fishing on the benthic epifauna and diets of demersal fishes on northern Georges Bank. Mar. Ecol. Prog. Ser. 472:199–217.

Smith, B.E., Collie, J.S. and Lengyel, N.L. 2014. Fish trophic engineering: ecological effects of the invasive ascidian *Didemnum vexillum* (Georges Bank, Northwestern Atlantic). J. Exp. Mar. Biol. Ecol. 461:489–498.

Smith, B.E. and Link, J.S. 2010. The trophic dynamics of 50 finfish and 2 squid species on the Northeast US continental shelf. NOAA Tech Memo. NMFS-NE-216, 640 p.

Taylor, M.H. and Bascuñán, C. 2000. CTD data collection on Northeast Fisheries Science Center Cruises: Standard Operating Procedures. NEFSC Ref. Doc. 00-11; 28 p.

Taylor, M.H. and Bascuñán, C., Manning, J.P. 2005. Description of the 2004 oceanographic conditions on the northeast continental shelf. NEFSC Ref. Doc. 05-03; 90 p.

Temming, A. and Herrmann, J. -P. 2003. Gastric evacuation in cod: Prey-specific evacuation rates for use in North Sea, Baltic Sea and Barents Sea multi-species models. – Fish. Res 63: 21–41.

Tsou, T.S. and Collie, J.S. 2001a. Estimating predation mortality in the Georges Bank fish community. Can. J. Fish. Aquat. Sci. 58:908–922.

Tsou, T.S. and Collie, J.S. 2001b. Predation-mediated recruitment in the Georges Bank fish community. ICES J. Mar. Sci. 58:994–1001.

van Denderen, P. D., N. T. Hintzen, A. D. Rijnsdorp, P. Ruardij and T. van Kooten. 2014. Habitat-Specific Effects of Fishing Disturbance on Benthic Species Richness in Marine Soft Sediments. Ecosystems 17(7): 1216–1226.

van Denderen, P. D., S. G. Bolam, J. G. Hiddink, S. Jennings, A. Kenny, A. D. Rijnsdorp and T. van Kooten. 2015. Similar effects of bottom trawling and natural disturbance on composition and function of benthic communities across habitats. Marine Ecology Progress Series 541: 31–43.

van Denderen, P. D., T. van Kooten and A. D. Rijnsdorp. 2013. When does fishing lead to more fish? Community consequences of bottom trawl fisheries in demersal food webs. Proceedings of the Royal Society of London B: Biological Sciences 280(1769): 2013.1883.

van Gemert, R. and K. H. Andersen. 2018. Challenges to fisheries advice and management due to stock recovery. ICES Journal of Marine Science 75(6): 1864–1870.

Zimmermann, F., D. Ricard and M. Heino. 2018. Density regulation in Northeast Atlantic fish populations: Density-dependence is stronger in recruitment than in somatic growth. Journal of Animal Ecology 87(3): 672–681.

4 ToR b: Use empirical data and available multi-species models to examine how the degree of fisheries balance relates to ecosystem status

4.1 General comments

This ToR followed a multiannual workplan, initiated at WGECO 2017, with the three following objectives:

a) Compare the length composition of total catch (landings and discards) to the length composition in the survey for one region (e.g. Irish Sea);
b) Use multispecies models (developed by WGSAM) to identify targets for ecological indicators of state (i.e. status) that relate to an acceptable risk of species diversity loss; and
c) Use output of multispecies models to investigate how proposed management strategies affect fisheries balance.

4.2 Foodweb indicators

4.2.1 Two fish community indicators investigated by WGECO

Species composition within fish communities (measured by the biomass weighted mean maximum length, MML, [cm]) where B_{total} is the estimated total biomass of fish within the community of n species, B_j is the biomass of species j and $L_{\max j}$ is the maximum length per species j and used to rank species from large-bodied and likely sensitive to fishing to small-bodied and likely resilient to fishing. OSPAR (2017) used the maximum observed length ever recorded for each species in any ICES otter or beam trawl survey to determine L_{max}. Ideally, L_{max} would be the growth-model asymptote known as length-at-infinity:

$$MML = \frac{1}{B_{total}} \sum_{j=1}^{n} \left(B_j L_{max,j} \right)$$

Size structure within fish communities (Typical length, TyL [cm]), measured by the geometric mean of all length measurements irrespective of their species identity), where B_i is the biomass and L_i is the observed length of fish i in a sample of N fish:

$$TyL = \exp\left\{ \frac{1}{B_{total}} \sum_{i=1}^{N} \left(B_i \ln L_i \right) \right\}$$

The indicators were tested on six different areas using survey data: the Narragansett Bay (1959–2018, weekly data), the North Sea (1983–2017, International Bottom Trawl Survey in Q1, ICES area 4 and 3a), the Irish Sea (1992–2016, N. Irish groundfish surveys in Q1 and Q4 and the English beam trawl survey in Q3, ICES area 7a) and the Celtic Seas (2003–2016, Rep. of Ireland groundfish survey in Q4, split into 3 areas: West of Scotland ICES area 6a, West of Ireland ICES 7b and northern Celtic Sea ICES 7gj; additional data for the northern Celtic Sea study for the period 1998–2016 and a wider area ICES 7ghj was investigated using the French EVHOE groundfish survey in Q4). Quality assured survey data were obtained from the Marine Scotland Science analysis of ICES DATRAS data http://data.marine.gov.scot/dataset/derivation-groundfish-survey-monitoring-and-assessment-data-product-northeast-atlantic-area (Moriarty *et al.* 2017).

4.2.2 Species composition of demersal fish communities

The mean maximum length metric (MML) has been trialled by OSPAR (2017) as an indicator to represent change in the species composition of fish communities. The indicator is high when the community is dominated by relatively large-bodied fish species (including elasmobranchs) that are particularly vulnerable to the effects of fishing. The pilot assessment of this indicator within the OSPAR Intermediate Assessment in 2017 was based on trends and relative changes with no assessment target identified from which "good" status could be inferred. All regional seas within the ICES area are impacted by human activities and thus the species composition during pristine conditions cannot be observed. An empirical approach was developed by WGECO (2018) to identify baselines for the MML indicator. This empirical approach for MML is further explored here for Narragansett Bay.

Given the long history of fishing in the regional seas within the ICES area and general depletion of large predatory fish (e.g. large sharks, skates and rays), it is reasonable to assume that each of these ecosystems can support large-bodied demersal fish species at their recently observed high (75th percentile) biomass levels simultaneously. If this is not the case currently, it can be considered as a suitable aim for management (termed a "Recovery Goal" by WGECO, 2017) for the species-specific abundance metric-level target within the sensitive species indicator. A system in which large species are heavily depleted cannot be considered to meet Good Environmental Status and further decline of vulnerable species should be avoided (i.e. species biomasses should be above the 25th percentile of observed biomass).

WGECO 2018 proposed that the MML_{75} value for the community based on all species at their 75th percentile biomass, as calculated for the whole dataset and based on survey catch rates, would represent a system with a species composition in an acceptable state. Conversely, a community in which large species (those with $L_{max} \geq MML_{75}$) are depleted in biomass (to their 25th percentile levels) yet small species (those with $L_{max} < MML_{75}$) are abundant (i.e. at their 75th percentiles) was proposed as a threshold for poor status for species composition and termed $MML_{depleted}$ (i.e. a state in which a high abundance of prey is available, but the system does not support a high abundance of predators).

To determine the area and survey-specific value of MML_{75}, the distribution of biomass across species and the length at which species were considered "large" was investigated through the calculation of cumulative distribution functions (cdf) of biomass against L_{max} (Figure 4.1), where the acceptable single biomass values per species are calculated from the 75th percentile of the species' biomass over the whole time-series. This approach was trailed by WGECO 2018 for the North Sea (Figure 4.1), Irish Sea and three distinct areas in the Celtic Sea (West of Ireland, West of Scotland and south of Ireland). For the North Sea IBTS Q1, the approach yielded the value of MML_{75} = 77 cm. For the Irish Sea, MML_{75} = 80 cm using the N. Irish survey in Q1 (see WGECO 2018, for the full set of figures, including cdfs for the 3 case study areas based on the Republic of Ireland survey in Q4).

The North Sea species composition appeared to have stabilised near the threshold for an acceptable status, whereas the Irish Sea showed a positive trend in MML since the mid-2000s indicating that recovery in species composition is underway, but incomplete. Based on the Republic of Ireland survey in Q4, the West of Scotland and northern Celtic Sea areas demonstrated acceptable species composition since 2010 and 2013 respectively, while the West of Ireland indicated low values in 2013–2015 but with great fluctuations without trend (see WGECO 2018, and also Figure 4.18).

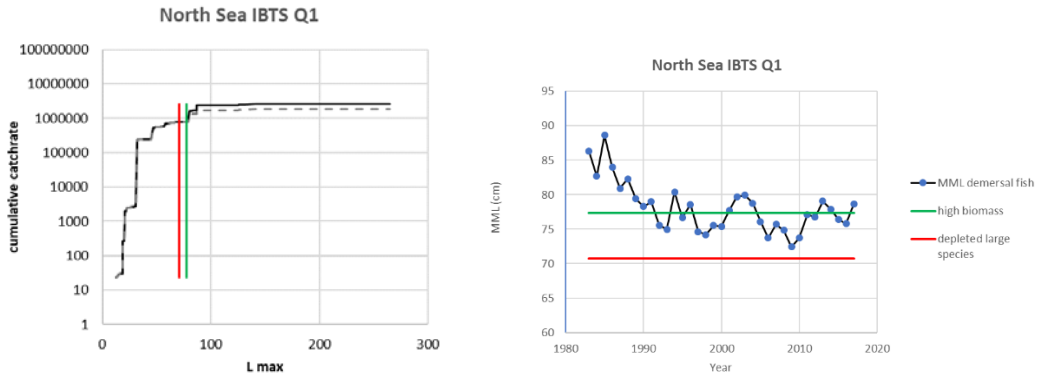

Figure 4.1. Cumulative catch distributions (left) showing the depleted community (dashed lines, with corresponding $MML_{depleted}$ red) relative to the high biomass community (solid lines with corresponding MML_{75} in green). Time-series of MML (right) shown with upper and lower baselines. Above the green line, the species composition is considered in acceptable status and below the red area is a situation to avoid. Replotted from WGECO 2018.

4.2.3 Case study area: Narragansett Bay Fish Trawl

The Graduate School of Oceanography conducts a weekly bottom-trawl survey at two stations in Narragansett Bay (web.uri.edu/fishtrawl). The Fox Island station is located in the mid-bay, whereas the Whale Rock station is at the bay mouth. MML was calculated for the subset of 25 species that have been numerically dominant over time and account for a high percentage (96%) of the total numbers. This subset includes 14 demersal fish, four pelagic fish, and seven invertebrate species. Though the species list is the same for both stations, the relative numerical abundance differs. MML was calculated based on mean catch per tow (standardized by tow duration) in numbers, as weights were not measured until 1994.

At the Whale Rock station, MML started above 55 cm, when the community had large numbers of silver hake and red hake (Figure 4.2). Since 1980, MML has fluctuated around the upper reference level of 39 cm. MML was never below the lower reference level of 29 cm. At the Fox Island station, MML started at a lower level of about 45 cm before declining in the 1970s (Figure 4.2). Since then MML has fluctuated at or below the upper reference level of 40 cm, with a gradual increase since 2000. MML fell below the lower reference level of 29 cm in 1995 when sea stars peaked in abundance.

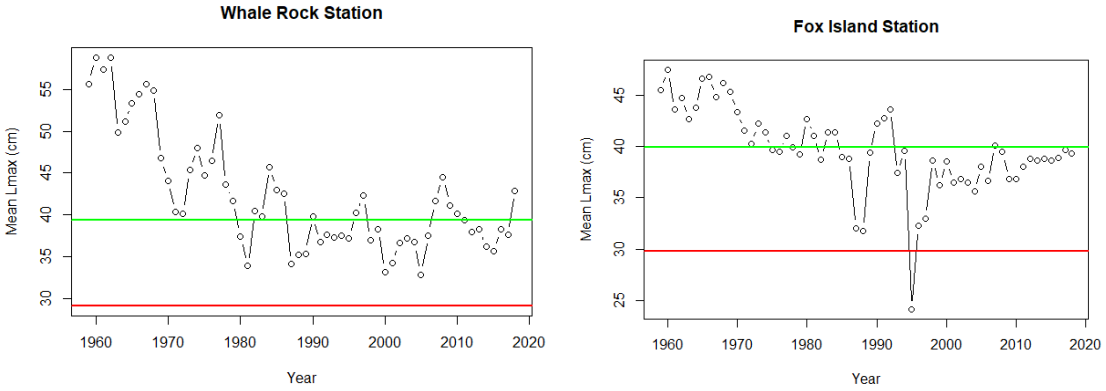

Figure 4.2. MML of 25 species in the GSO fish trawl survey, showing the empirical baselines for the upper reference level MML_{75} (green) and the lower reference level $MML_{depleted}$ (red).

To remove the effects of variable pelagic and invertebrate species, calculations were repeated for the 14 most abundant demersal species. These subsets account for 64% of total numbers at the Fox Island Station and 45% of total numbers at the Whale Rock station. The overall MML is higher because the demersal species are larger. At the Whale Rock station, MML declined during the first three decades, varied between the upper and lower reference levels during the next two decades, and fell below the lower reference level in the 2010s (Figure 4.3). At the Fox Island station MML started at a lower level (~50 cm) and declined throughout the time-series, falling below the lower reference level between 2014 and 2017 (Figure 4.3). When considering only the demersal species, the difference between the upper and lower reference levels is smaller than when considering all species because the demersal species are much more similar in their L_{max} values.

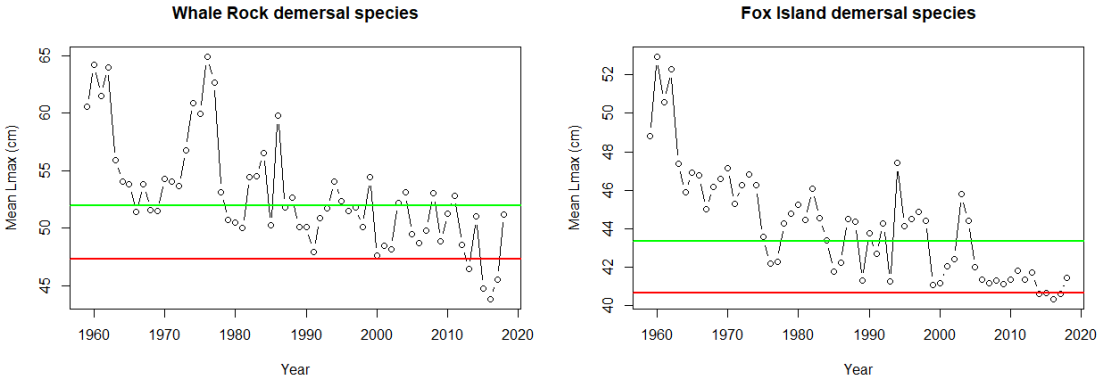

Figure 4.3. MML of 14 demersal species in the GSO fish trawl survey, showing the empirical baselines for the upper reference level MML_{75} (green) and the lower reference level $MML_{depleted}$ (red).

4.2.4 Sensitivity analysis of the upper reference level for the species composition indicator

Here we focus on the sensitivity of the indicator threshold method to the choice of percentile level and the duration of time-series. Further investigation could assess the sensitivity of the indicator to the abundance of single species.

For the North Sea and Irish Sea, as the percentile choice increases, the community MML based on these high biomasses increases (Figure 4.4). However, in the West of Scotland and West of Ireland areas the opposite is true, while in the northern Celtic Sea the indicator is largely insensitive to the choice of percentile. The difference between the case study areas is clearly linked to the relative dominance of large vs. small species in the survey. Given the different patterns across the areas, the pragmatic option is to continue with the 75th percentile as the level at which acceptable biomasses and species composition is determined for all areas, seems the best approach unless further information becomes available (e.g. for the North Sea see Section 4.4).

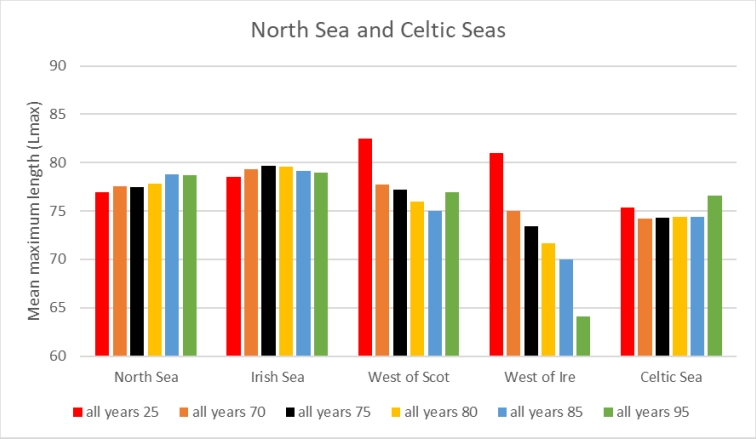

Figure 4.4. Sensitivity of the baseline to the choice of percentile level (red bar 25th, orange 70th, black 75th, yellow 80th, blue 85th, and green 95th applied to the catch rates by species) upon which to determine the baseline for MML, here calculated using the maximum observed length in the data product consistent with OSPAR (2017). Data were used from the North Sea IBTS Q1 (1983–2017), the Irish Sea N. Irish Q1 survey (1992–2016) and the Celtic Seas Republic of Ireland Q4 survey (2003–2016).

For the North Sea, a restriction in the time-series to the period 2006–2015 or 2010–2015 leads to a lower MML for demersal fish since the high biomasses of the early 1980s are missed (Figure 4.5). This is a classic case of shifting baselines, to which all empirical approaches are susceptible. The difference in the indicator between 2006–2015 and 2010–2015 is small in most instances except for the low percentile level (25th) in the West of Scotland area. Therefore, the choice of percentile is a greater issue than the number of years themselves as long as the major changes in the system have been recorded. The pragmatic option is to use the whole time-series and update with each assessment, while acknowledging the issue of shifting baselines for this surveillance approach. This analysis indicates that MML is relatively insensitive to the number of years included in its calculation.

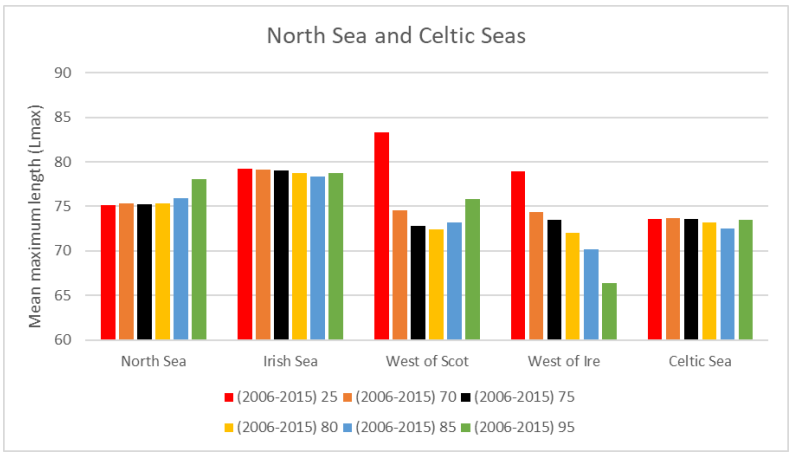

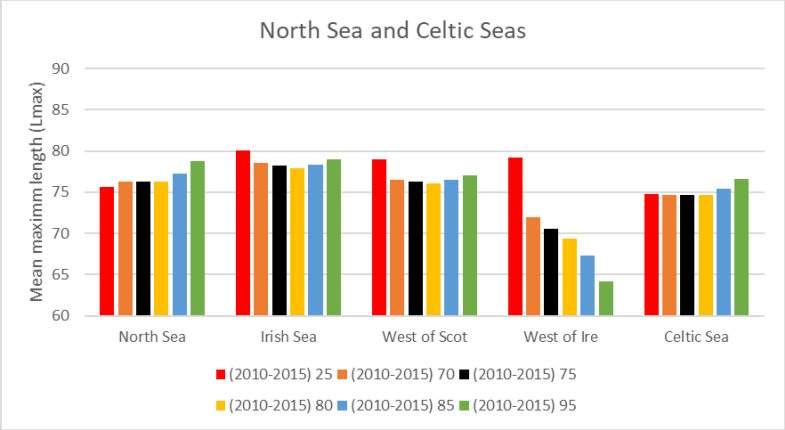

Figure 4.5. Sensitivity of the baseline to time period (2006–2015 above and 2010–2015 below) and the choice of percentile level (25th, 70th, 75th, 80th, 85th and 95th applied to the catch rates by species). Data were used from the North Sea IBTS Q1, the Irish Sea N. Irish Q1 survey and the Celtic Seas Rep. of Ireland Q4 survey.

4.2.5 Size–structure

The Typical Length indicator (TyL) measures the change in size–structure within communities. High values of the indicator represent a high biomass of predators in the ecosystem relative to the prey available, since body size is an excellent predictor of trophic level in fish communities (Jennings *et al.*, 2001; 2008). Size–structure of fish communities can change in two main ways:

1. The community becomes more or less dominated by small species due to fishing impacts or climate change for example;
2. The community becomes more or less dependent on new recruits to support its biomass, potentially due to overexploitation.

Clearly changes due to the first condition should be captured by the indicator on species composition (Mean maximum length) above. Therefore, the baseline and lower limit for the size–structure indicator should be made independent of the species composition, as far as possible, and as highly dependent on the size–structure as possible. The target or goal for the indicator should be based on the expected structure of the system when species have recovered from overexploitation, which is best informed through multispecies modelling.

WGECO proposes that a fish community with biomass highly dependent on recruitment events (condition 2 above) is a depleted community and should be classified as *not in good environmental status*. While recruitment events can be large, a diverse and well-functioning ecosystem should be represented by a sufficient biomass of large individuals that are reproductively active. Each species (sp) should have a large proportion of its biomass composed of mature fish, such that its population geometric mean length (TyL_{sp}), weighted by biomass, is greater than the length-at-maturity ($L_{m.sp}$) times a multiplier dependent on productivity of the system and species interactions. So, overall the Typical Length of the community (TyL) should be greater than the community-averaged length-at-maturity (L_m) times a scale factor dependent on the species present. As the species composition changes, the reference value, L_m, also changes and in this way the assessment of the size–structure indicator is specific to the current species composition. As a result, a reduction in the MML indicator and a poor status for species composition does not necessarily result in a poor status of the size–structure. This was further investigated through multispecies modelling; see Section 4.4 below.

4.3 Fisheries-dependent data and pressure indicators

WGECO 2018 analysed fisheries-dependent data from UK(E&W) and Republic of Ireland to explore the evolution of catch length structure through time and compare it with the survey length structures. WGECO 2019 updated the Irish fisheries data and added French fisheries data to the dataset. The pressure analysis was restricted to four regions, namely the West of Scotland (6a), Irish Sea (7a), West of Ireland (7b) and northern Celtic Sea (7fghj) and two groups, the demersal bony fish and elasmobranchs.

Catch composition data from commercial fisheries were collated from the Observer Programmes (collected under the EU data collection framework (Council regulation (EC) No 199/2008)) for UK (England and Wales), France, and Republic of Ireland for the period 2007–2017. For each sampled haul the following information is collected: gear type and mesh size, tow duration, shot and haul position, species catch composition and quantity and length of fish landed and discarded. Observer data were aggregated per species, region (6a, 7a, 7b and 7fghj), year and gear type to produce total catch volumes and length structures.

Discard volumes were estimated by raising the proportion of discards to landings observed during the sampled trips (numbers of fish landed and discarded were converted into volumes using length–weight relationships) to the total landing recorded for the strata. When no landings were reported, effort (number of trips in stratum UK(E&W) and hours fished IRL) was used to raise the discard data.

Length structures of landings and discards were estimated by raising observed length structures of discarded and landed fish on sampled trips to the total volumes of landings and discards per strata. Only the strata where >25 (UK(E&W) & IRL) or >30 (FR) individuals over 3+ trips (FR) were measured, were considered. More information on each country's observer programmes and raising procedures can be found in Cornou *et al.* (2018), Dubroca *et al.* (2016), Borges *et al.* (2004); Enever, Revill, and Grant (2007). Tables 4.1 and 4.2 show the total landings per country and per year in the four regions for demersal bony fish and demersal elasmobranchs separately. For bony fish, the catch in the northern Celtic Sea is well sampled in the observer data by all three countries (at least 70% of landings represented). In the West of Scotland area, only the Irish fleet is well sampled, and here the analysis is missing an important component of the catch from Scotland. Similarly, in the Irish Sea, an important proportion of the international catch by UK(NI) was not available for this analysis. The West of Ireland area is well represented by the Irish fleet only. A similar pattern is seen between areas in the elasmobranch data. However in all areas, the catch of elasmobranchs is less well represented in the observer data than bony fish. Since 2010 for the Irish Sea and since 2012 in the northern Celtic Sea, UK(E&W) data and Irish observer data do represent a substantial proportion of the country level landings of elasmobranchs.

Table 4.1. Landings of demersal bony fish per country and regions in tonnes (top), and percentage of the country's landings represented in the catch length structure (bottom in italic). Percentages were calculated by summing up the landings of the gear strata for which length structures could be inferred from the observer data.

			2007	2008	2009	2010	2011	2012	2013	2014	2015	2016	2017
6a	UK-E&W	t	376	55	98	1	0	16	81	180	207	216	45
		%	0	0	0	0	0	0	0	0	0	0	0
	IR	t	2288	2115	1875	2766	2054	2244	2101	1887	2129	2886	2254
		%	89	87	93	93	95	94	92	92	82	44	50
	FR	t	21176	25157	18340	20544	16477	12329	15651	19486	18685	17336	19425
		%	0	11	11	16	21	26	74	60	60	61	58
7a	UK-E&W	t	650	475	480	418	257	331	130	102	140	114	84
		%	84	74	42	34	32	52	69	55	49	45	56
	IR	t	2641	1760	1215	1158	1288	1139	1020	1145	1194	1623	1889
		%	57	48	62	75	69	50	70	68	59	50	70
	FR	t	61	14	17	14	19	7	4	10	6	1	8
		%	0	0	0	0	0	0	0	0	0	0	0
7b	UK-E&W	t	384	311	250	188	289	326	176	324	705	1010	734
		%	0	0	0	0	0	0	0	0	0	0	0
	IR	t	1640	1379	1713	1981	1951	2032	2260	2570	1927	1861	1929
		%	74	71	71	75	82	79	70	67	72	65	80
	FR	t	2885	3801	2492	2277	1316	2421	3068	4078	2832	3968	2864
		%	0	0	0	0	0	0	0	0	0	0	0
7fghj	UK-E&W	t	7320	5997	6444	6804	7632	8207	10495	10208	8857	9443	8181
		%	72	72	58	85	87	84	90	47	84	68	74
	IR	t	14645	11223	13209	15646	17105	21002	20441	18762	17545	19924	18191
		%	85	82	90	85	92	94	88	94	76	82	93
	FR	t	29301	27002	24408	25047	31448	40532	40008	39840	42831	41349	40050
		%	76	70	76	77	78	82	79	76	78	76	74

The total annual catch, combined landings and discards by fleet and catch per 20 cm size categories were explored for the observed strata for demersal fish and elasmobranchs (Figures 4.6 to 4.9). The combined change in observed catch and size–structure within the catch from all countries is shown in Figure 4.10. For the demersal bony fish species data, the contribution of each species to the total raised biomass was calculated (Figure 4.11). As before, the UK(E&W), Irish and French combined dataset was analysed based on area fished (6a – West of Scotland, 7a – Irish Sea, 7b – West of Ireland, 7fghj – northern Celtic Sea).

To the west of Ireland, data from Ireland only were considered informative. These data arise solely from otter trawlers with little change evident in the proportions of each size class in the catch (Figure 4.6). For the West of Scotland area, the largest proportion of the total catch in the dataset is from bottom otter trawlers (OTB) and these are monitored in all years from 2007 with

catch by this component fluctuating over time. Set longlines (LLS) and twin-otter trawlers (OTT) are observed from 2011 onwards and pairtrawlers (PTB) from 2015 (Figure 4.7). Overall, the proportion of large fish (especially in the 100–119 cm range) increases post-2013.

Table 4.2. Landings of demersal elasmobranchs per country and regions in tonnes, and percentage of the country's landings represented in the catch length structure. Percentages were calculated by summing up the landings of the gear strata for which length structures could be inferred from the observer data.

			2007	2008	2009	2010	2011	2012	2013	2014	2015	2016	2017
6a	UK-E&W	t	5	5	2	0	0	0	0	0	0	0	0
		%	0	0	0	0	0	0	0	0	0	0	0
	IR	t	145	128	122	174	223	136	183	228	229	350	398
		%	46	39	36	34	27	55	41	32	38	32	32
	FR	t	1291	1207	983	638	406	431	405	336	321	292	266
		%	0	0	0	0	0	0	0	0	5	6	5
7a	UK-E&W	t	444	254	237	159	141	261	198	156	260	155	98
		%	21	60	68	80	67	76	85	95	96	93	80
	IR	t	413	311	268	536	522	506	414	445	384	238	233
		%	2	4	1	80	88	89	97	44	22	31	66
	FR	t	92	32	10	10	19	4	6	4	1	2	2
		%	0	0	0	0	0	0	0	0	0	0	0
7b	UK-E&W	t	50	75	23	16	14	33	12	12	34	30	22
		%	0	0	0	0	0	0	0	0	0	0	0
	IR	t	306	112	158	122	123	141	121	123	120	132	124
		%	21	10	28	37	26	40	51	46	52	59	58
	FR	t	222	270	172	162	58	72	68	63	65	74	46
		%	0	0	0	0	0	0	0	0	0	0	0
7fghj	UK-E&W	t	1247	1255	1199	1433	1380	1272	1040	842	931	1124	1035
		%	4	39	63	49	47	59	66	15	23	54	52
	IR	t	569	618	480	424	447	366	504	477	614	537	459
		%	7	3	8	22	47	80	59	58	38	58	90
	FR	t	4866	4780	4527	4485	4304	3906	3519	3737	3545	3362	3262
		%	0	0	0	0	0	0	0	0	15	26	23

In the northern Celtic Sea, a great variety of fleets are observed (Figure 4.8). Again, otter trawlers (single OTB and twin OTT) account for the greatest proportion of the catch and they are observed in all years, with increasing catch over time for twin otter trawlers and a decrease in the proportion of the catch composed of small fish post-2011. Gillnets (GNS), trammelnets (GTR) and beam trawlers (TBB) were also observed in all years. In the Irish Sea, otter trawlers dominate the catch of demersal fish and elasmobranchs with clear decreases in catch over time (Figure 4.9 and 4.10).

For each area, the proportion of the raised biomass estimates within each size class was calculated per species, per year. Species that contributed less than 10% of the biomass within any size category were removed from the analyses to allow for the identification of the species that contributed most to catches. The proportion of each of these abundant species, in relation to the total catch, across all size classes, was also calculated to identify which components of the catches were driving temporal trends in the observer data in each region.

Table 4.3. Codes and gear types present in the combined observer dataset.

Code	Gear type
DRB	*Boat dredges*
FPO	*Pots*
GN	*Other gill/driftnets*
GNS	*Set gillnets (anchored)*
GTR	*Trammelnets*
LHP	*Handlines and pole-lines (hand-operated)*
LLS	*Set longlines*
LTL	*Troll lines*
OTB	*Bottom otter trawl*
OTM	*Midwater otter trawl*
OTT	*Otter twin trawl*
PS	*Purse-seines*
PTM	*Pelagic pair trawl*
SDN	*Danish seines*
SSC	*Scottish seines*
TBB	*Beam trawl*

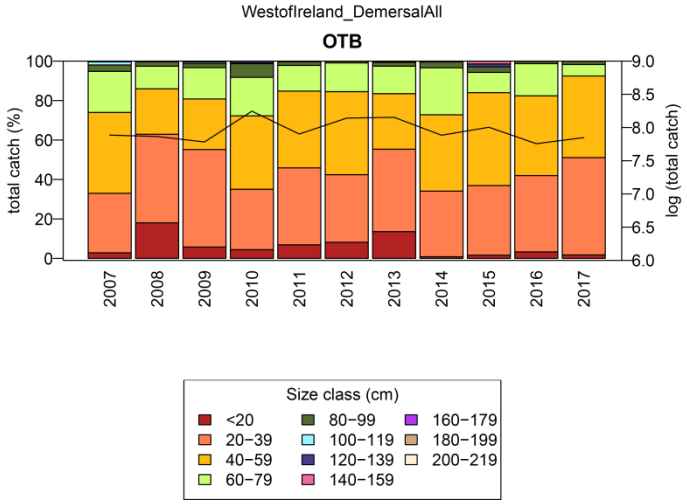

Figure 4.6. Catch of demersal fish and elasmobranchs from Irish commercial fisheries measured as raised weight (t) for West of Ireland (7b) per gear. Bars represent percentages per size class for each year (left y-axis) and lines represent natural log-transformed total tonnage (right y-axis) for observed strata per year. See Table 4.3 for the gear codes and types.

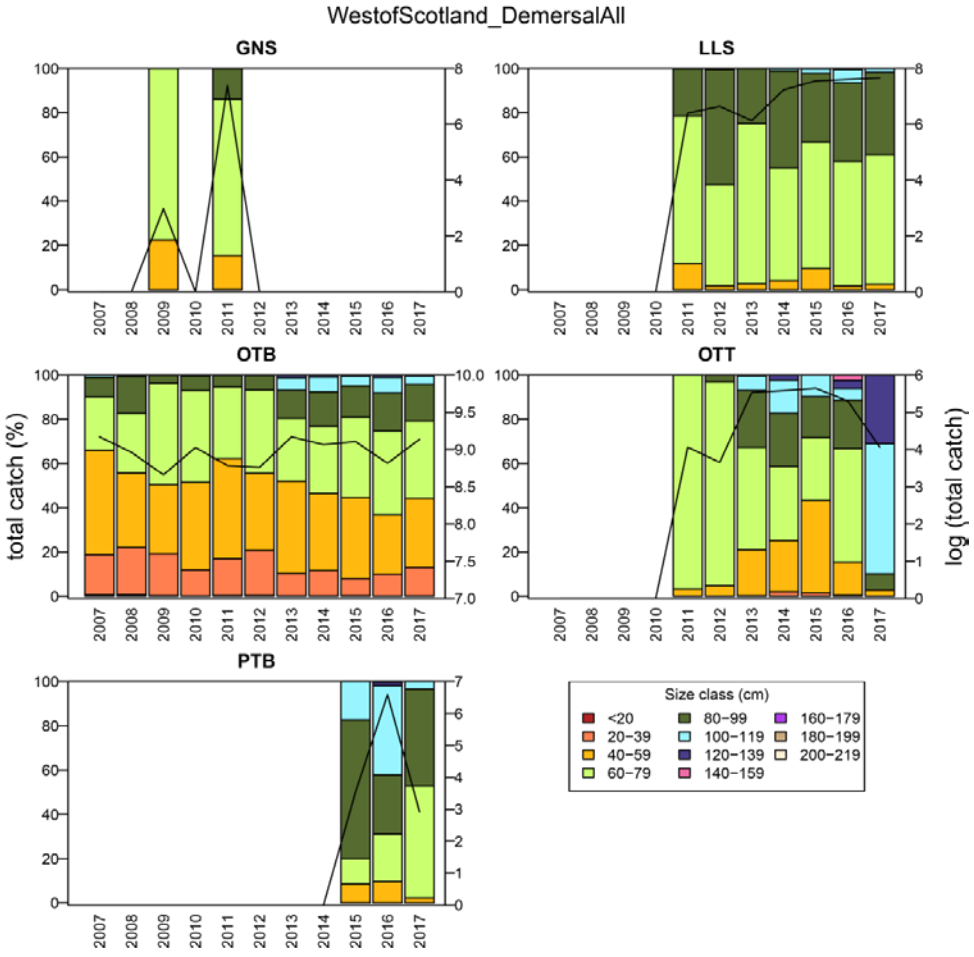

Figure 4.7. Catch of demersal fish and elasmobranchs from collated Irish and French commercial fisheries measured as raised weight (t) for West of Scotland (6a) per gear. Bars represent percentages per size class for each year (left y-axis) and lines represent natural log-transformed total tonnage (right y-axis) for observed strata per year. See Table 4.3 for the gear codes and types.

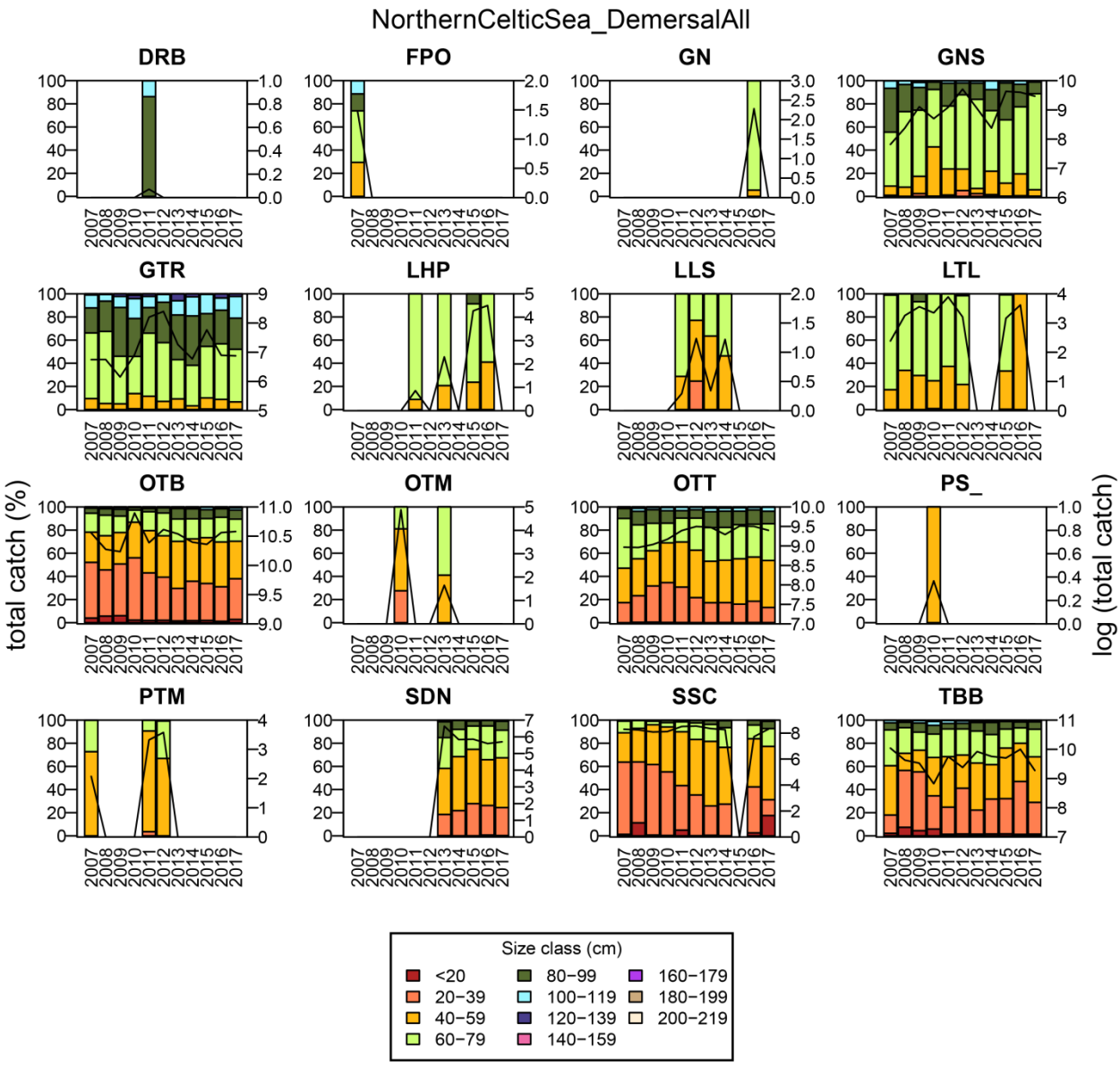

Figure 4.8. Catch of demersal fish and elasmobranchs from collated UK(E&W), Irish and French commercial fisheries measured as raised weight (t) for northern Celtic Sea (7fghj) per gear. Bars represent percentages per size class for each year (left y-axis) and lines represent natural log-transformed total catch (right y-axis) for observed strata per year. See Table 4.3 for the gear codes and types.

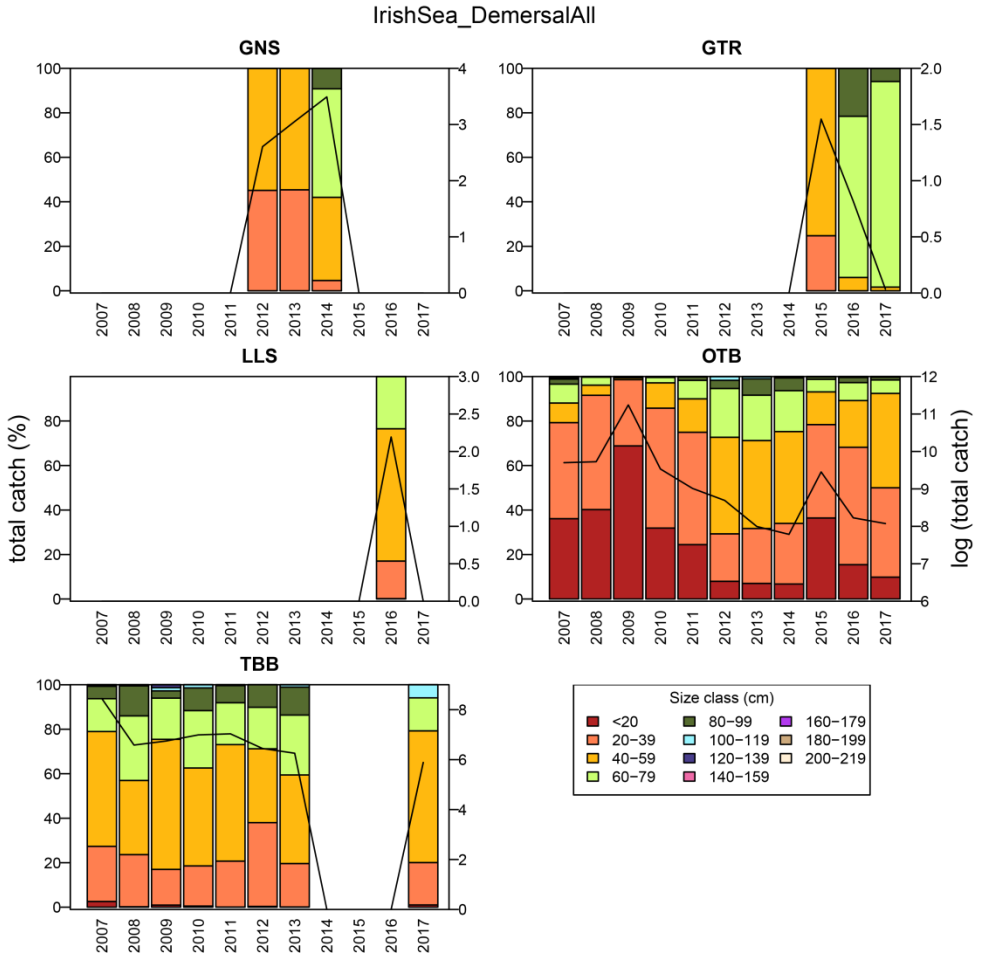

Figure 4.9. Catch of demersal fish and elasmobranchs from collated UK(E&W) and Irish commercial fisheries measured as raised weight (t) for the Irish Sea (7a) per gear. Bars represent percentages per size class for each year (left y-axis) and lines represent natural log-transformed total catch (right y-axis) for observed strata per year. See Table 4.3 for the gear codes and types.

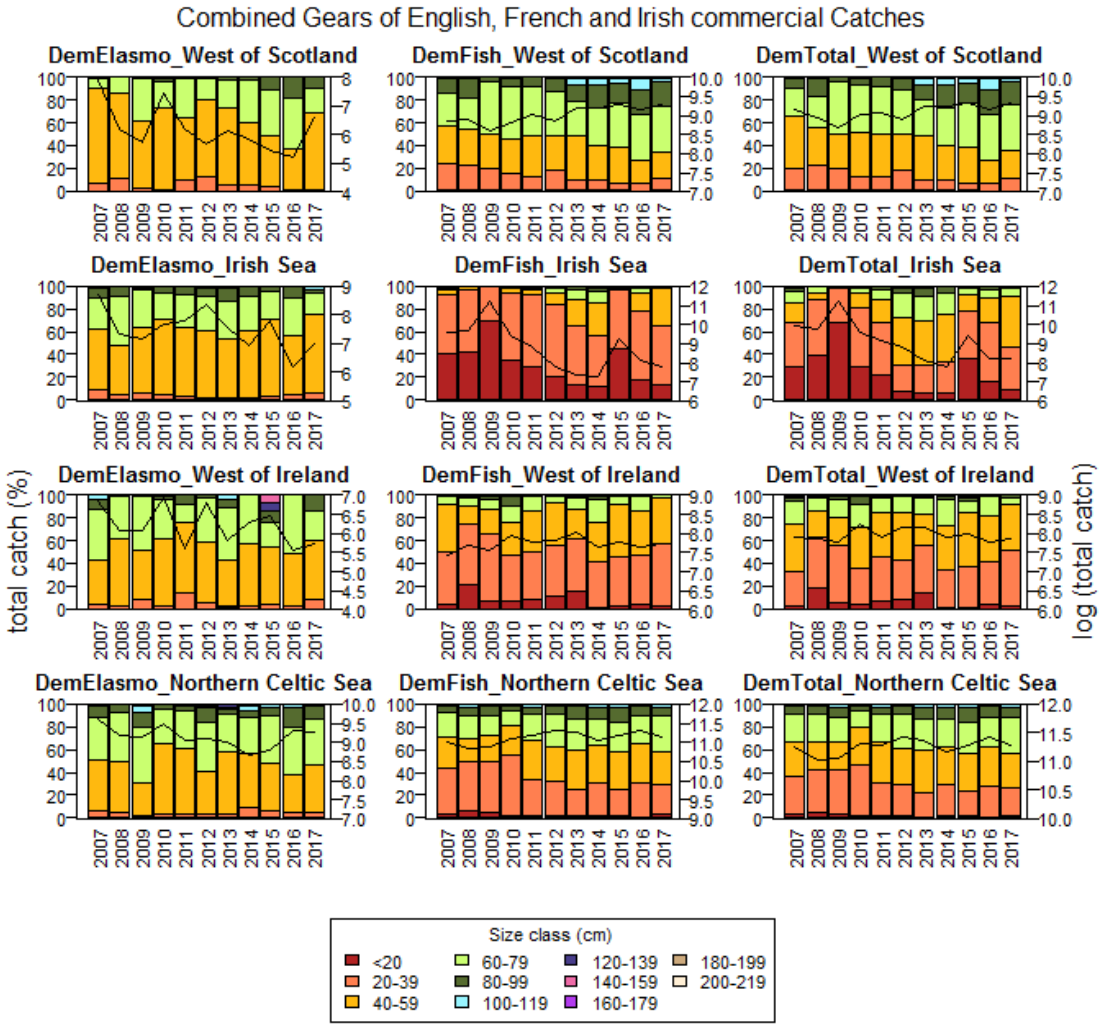

Figure 4.10. Catch of demersal elasmobranchs (DemElasmo), demersal fish (DemFish) and combined (DemTotal) from collated UK(E&W), Irish and French commercial fisheries measured as raised weight (t) for the northern Celtic Sea (7fghj), West of Ireland (7b), the Irish Sea (7a) and West of Scotland (6a). Bars represent percentages per size class for each year (left y-axis) and lines represent natural log-transformed total catch (right y-axis) for observed strata per year.

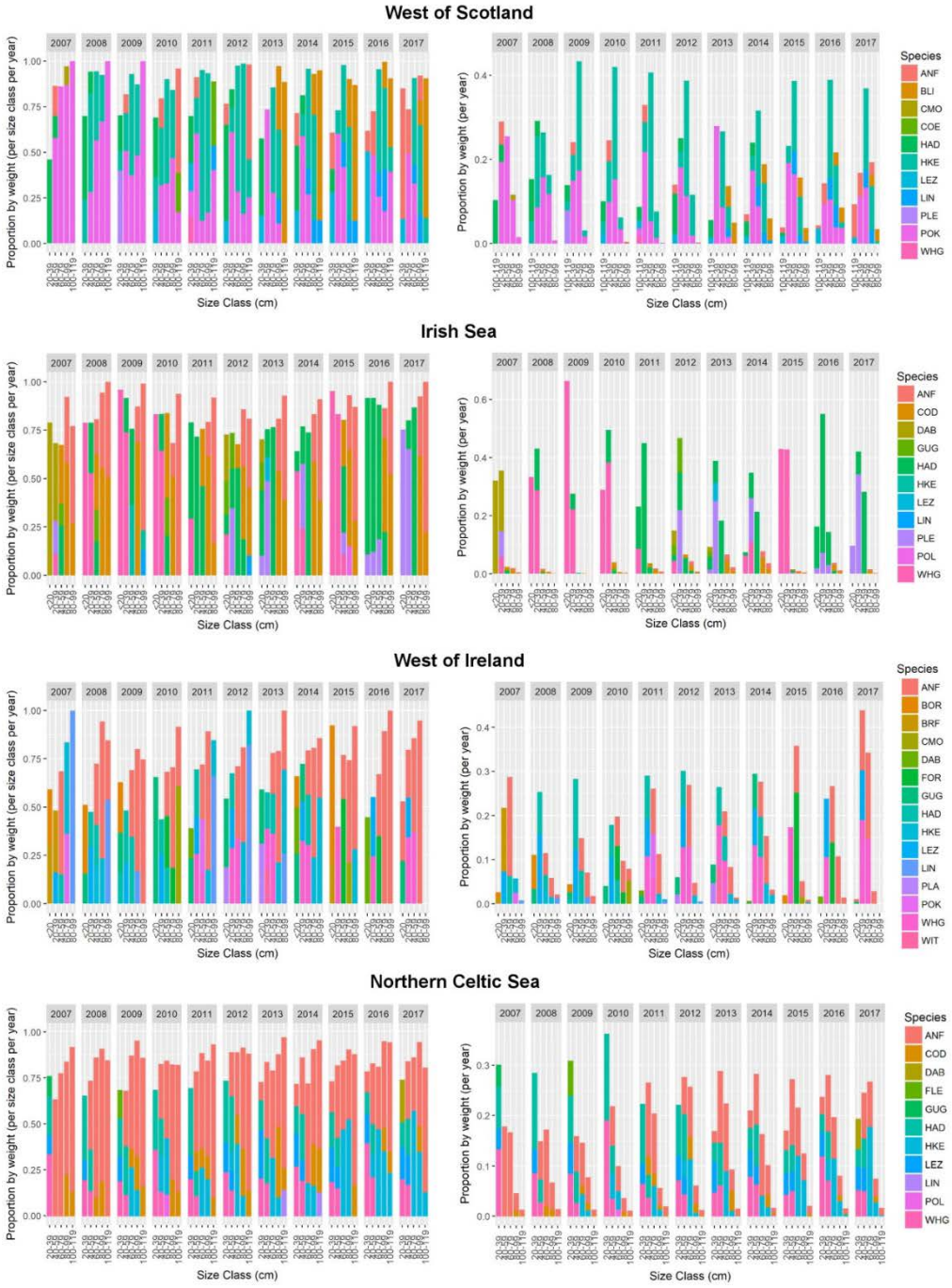

Figure 4.11. Proportion by total biomass per 20 cm size category (all figures on the left) and proportion by total biomass per year (all figures on the right) for species which contributed to at least 10% biomass of at least one size class for the West of Scotland, Irish Sea, West of Ireland and northern Celtic Sea. (The key species identified in the analyses were ANF-*Lophius* spp, BLI - *Molva dyptergia*, BOR - *Capros aper*, BRF - *Helicolenus dactylopterus*, CMO - *Chimaera monstrosa*, COD - *Gadus morhua*,COD - *Conger conger*, DAB - *Limanda limanda*, FLE - *Plactichthys flesus*, FOR - *Phycis phycis*, GUG - *Eutrigla gurnardus*, HAD - *Melanogrammus aeglefinus*, HKE - *Merluccius merluccius*, LEZ - *Lepidorhombus whiffiagonis*, LIN - *Molva molva*, PLA - *Hippoglossoides platessoides*, PLE - *Pleuronectes platessa*, POK - *Pollachius virens*, POL - *Pollachius pollachius*, WHG - *Merlangius merlangus*, WIT - *Glyptocephalus cynoglossus*).

4.3.1 Results – pressure indicators

When examining the combined catch of demersal fish and elasmobranchs by otter trawlers (OTB) for all three countries in each of the four fishing areas (Figure 4.10), the northern Celtic Sea, West of Ireland and the West of Scotland fishing grounds show fairly stable catch patterns over the study period. The area West of Scotland displays a variability of species composition from 2013. In contrast, the catches from the Irish Sea show a steady decrease in tonnage over the study period (Figure 4.10). In this case, the reduction in catch is driven by a significant reduction in the available quota for the key commercial species in this area (Figures 4.11 and 4.12). Cod, whiting and sole quotas in ICES Division 7a, in particular, have seen dramatic reductions since 2007, with cod quotas in 2017 being reduced to just 10% of what was available in 2007 as part of the EU's cod recovery plan (Kraak *et al.*, 2013). Smaller size classes of fish contribute much more to the tonnage caught in the Irish Sea compared to other areas. Peaks in the total catch in 2009 and 2015 in the Irish Sea are associated with large proportions of small (<20 cm) whiting in the catch, thus the total tonnage caught shows deviations from the trend in available TAC (Figures 4.11, 4.12 and 4.13). There are also oscillations between the species constituting the majority of the catch in the Irish Sea over time, with the main species alternating between whiting, haddock and plaice for the two smaller size classes (<40 cm), whilst cod and anglerfish dominate the larger size classes throughout the time-series (Figure 4.11). Overall, the commercial fleet is now catching larger fish and an increased dominance of demersal species that grow large (Figure 4.13).

There is much greater consistency in the size and species compositions of catches West of Scotland and in the northern Celtic Sea, with fish <20 cm in length having a negligible contribution to the overall biomass in both areas. Although the West of Scotland is lacking data from the Scottish fleet, saithe and hake dominate catches across size classes (Figure 4.11). While these species remain dominant in the catches from 2013, more species including *Molva* spp. contribute to the majority of the biomass caught between 2013 and 2017, reflecting the contribution of French data in this area during this period. The catch composition in the northern Celtic Sea displays the greatest stability over time. Whiting, haddock and megrim are evident in size classes below 60 cm throughout the study period, while hake and anglerfish dominate the larger size classes in this area. Cod significantly contributes to catches, but there is variation in the size class in which it is more dominant, with smaller cod (<80 cm) being less evident from 2013 onward. The largest number of species, contributing to the majority of the biomass, occurs in the area to the west of Ireland (7b). Angler and megrim species remain fairly dominant in the larger size classes throughout. For fish below 60 cm in length there are oscillations between the dominance of whiting, haddock and hake throughout the study period, with a number of other species contributing to the overall biomass caught in individual years (Figure 4.11).

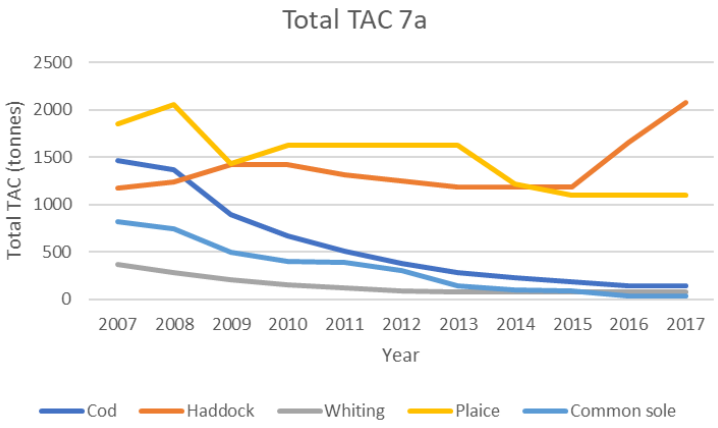

Figure 4.12. Total international TAC limits for five main commercial species within the Irish Sea (ICES 7a) from 2007 to 2017.

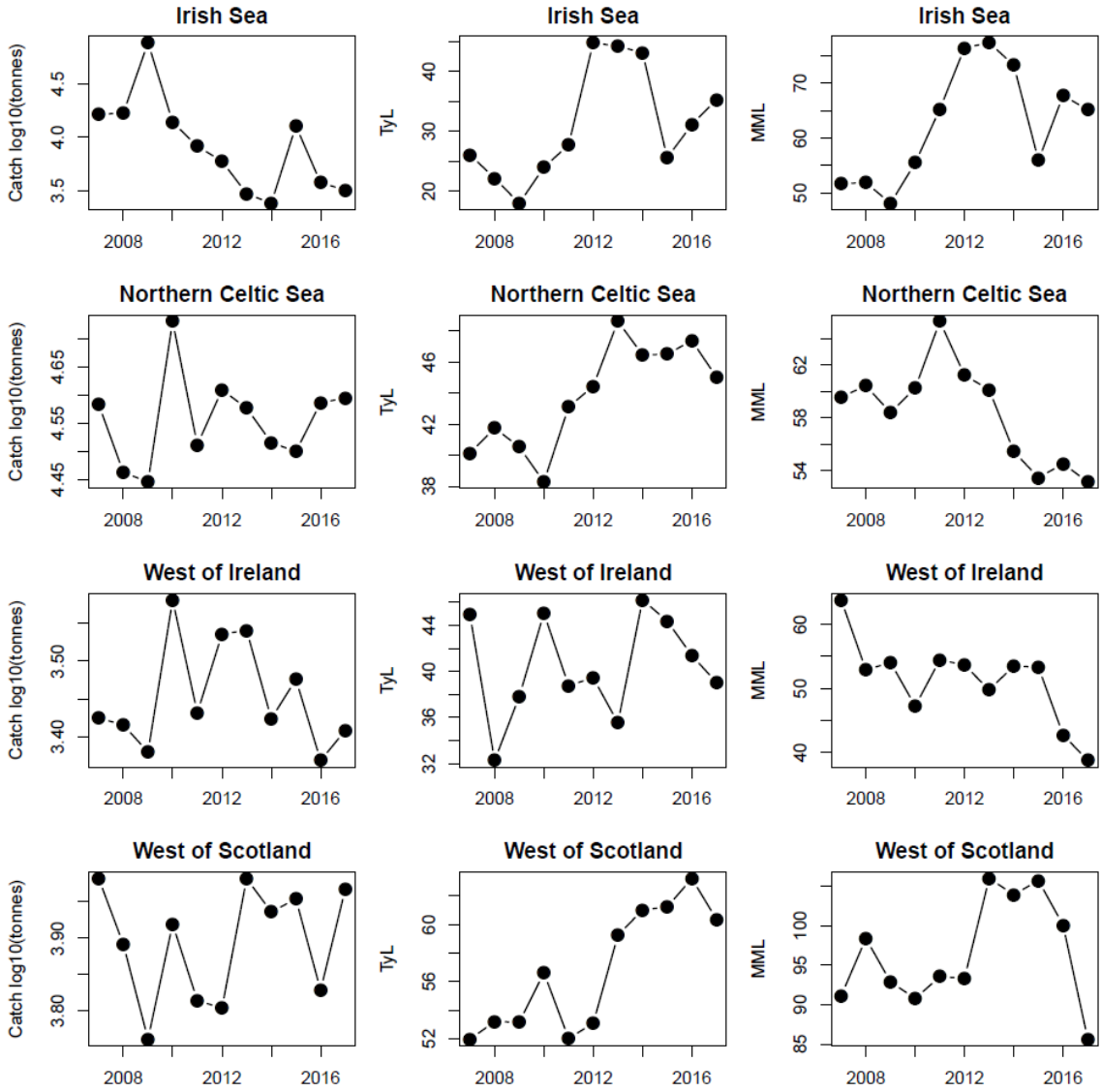

Figure 4.13. Pressure indicators from a combined analysis of observer data from UK(E&W), Ireland and France for otter trawlers (OTB) fishing for demersal fish and elasmobranchs.

4.3.2 Comparison between size–structure in the commercial catch and surveyed size–structure in the ecosystem

In the northern Celtic Sea and West of Scotland areas, the commercial fleets generally catch fish of a much larger size than those that are available in the ecosystem as measured by the surveys (Figures 4.14 and 4.15). This pattern is similar in the West of Ireland area (Figure 4.16) but generally less pronounced. In contrast, in the Irish Sea in some years (e.g. 2007 and 2011) the commercial fleets capture fish across the vast majority of the size range as seen in the ecosystem (Figure 4.17). This result is consistent when compared to each of three surveys in the area (the two Northern Irish groundfish surveys and the English beam trawl survey). This difference in the size–structure in the catch observed per region is summarised by the typical length indicator based on commercial data (Figure 4.13), which fluctuates in the region 25–30 cm in the period 2007–2011 for the Irish Sea data, similar to the typical length in the surveys (Figure 4.18). Elsewhere, the typical length indicator based on commercial data varies between 30 and 65 cm while the survey varies around values lower than this (Figures 4.13 and 4.18). The species composition indicator (MML) demonstrates the demersal species fished in the Irish Sea are generally similarly sized species relative to those in the observer data elsewhere, with the exception of the West of Scotland where the species can attain a larger body size. Notably, increases in surveyed biomass in all areas are generally evident since 2005 (Figure 4.18).

In the northern Celtic Sea, there is an increase in the typical length in the commercial catch (from about 40 to 46 cm), but a decrease in the species composition in the commercial catch over time (from 60 to 54 cm) (Figure 4.13). The French survey fluctuates without trend in this area, whereas the Irish survey does also demonstrate an increase in the individual size over the period (from 25 to 30 cm) and a slight shift toward species that attain larger ultimate body size (increase in MML from about 70 to 80 cm) (Figure 4.18). Together with the increase in surveyed biomass in the northern Celtic Sea since the early 2000s, the indicators suggest a potential improvement in the demersal fish community.

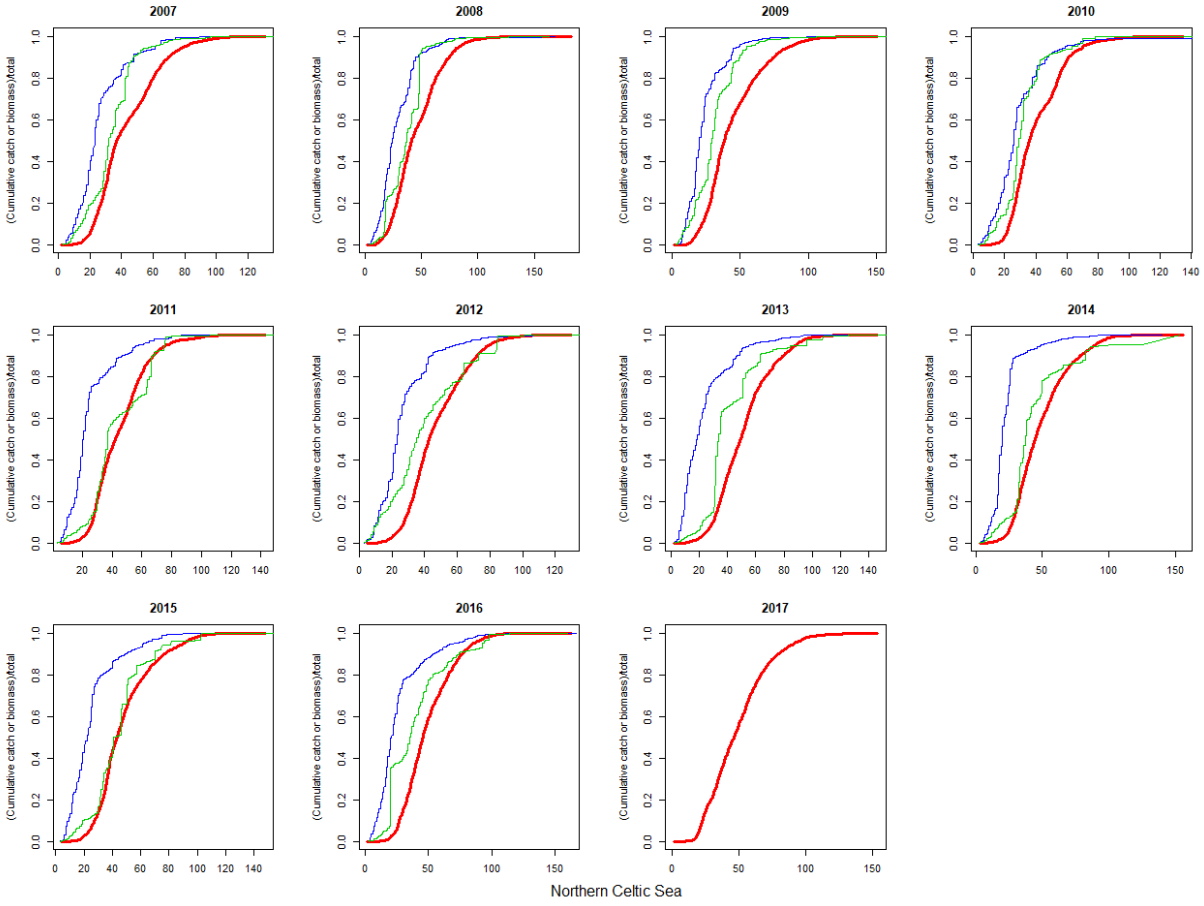

Figure 4.14. Northern Celtic Sea. Annual fisheries balance in terms of size–structure from a combined analysis of observer data from UK(E&W), Ireland and France otter trawlers (OTB) fishing for demersal fish and elasmobranchs. Commercial data from the observer programme is shown in red and surveyed size–structure in the demersal community in blue for the Irish Q4 survey and in green for the French Q4 survey (survey data were not available for 2018).

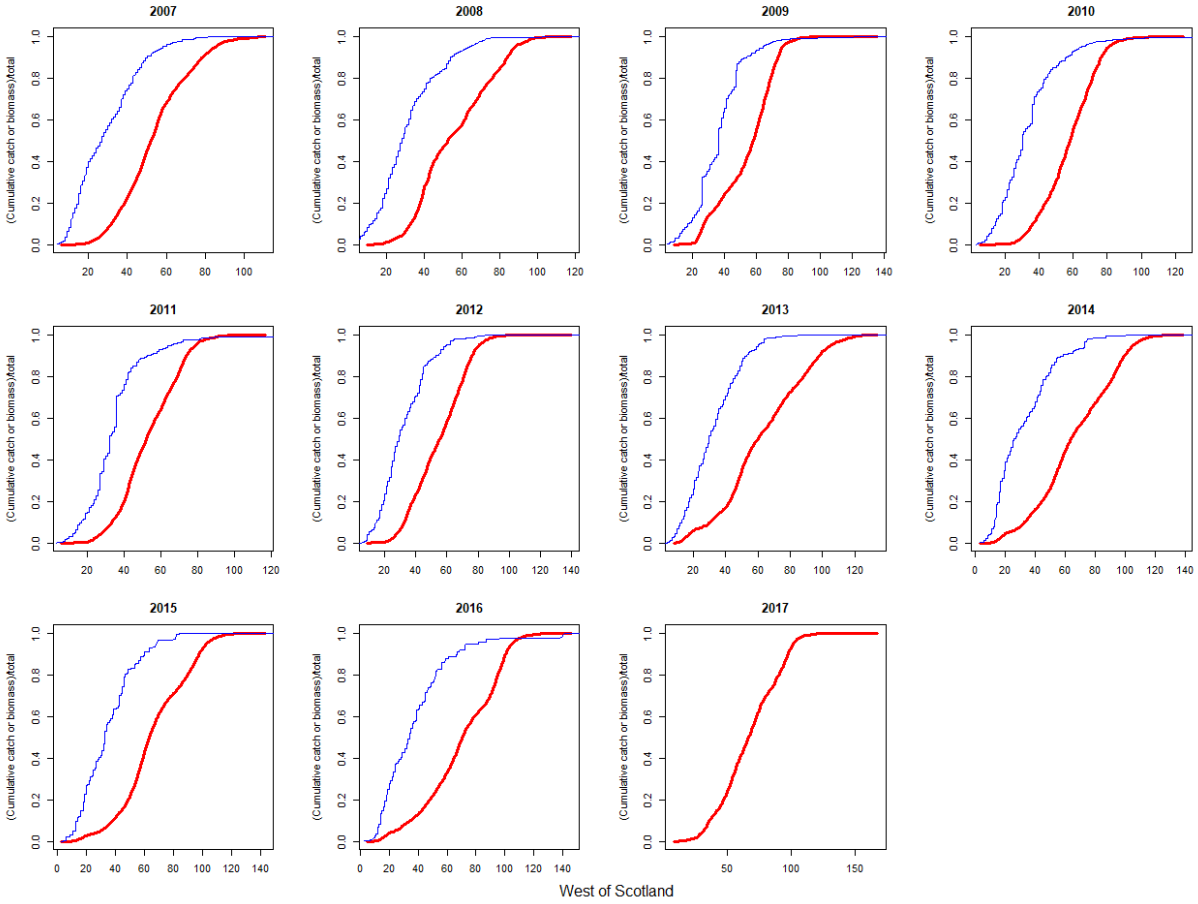

Figure 4.14. West of Scotland. annual fisheries balance in terms of size–structure from a combined analysis of observer data from Ireland and France otter trawlers (OTB) fishing for demersal fish and elasmobranchs. Commercial data from the observer programme are shown in red and surveyed size–structure in the community in blue for the Irish Q4 survey (survey data were not available for 2018).

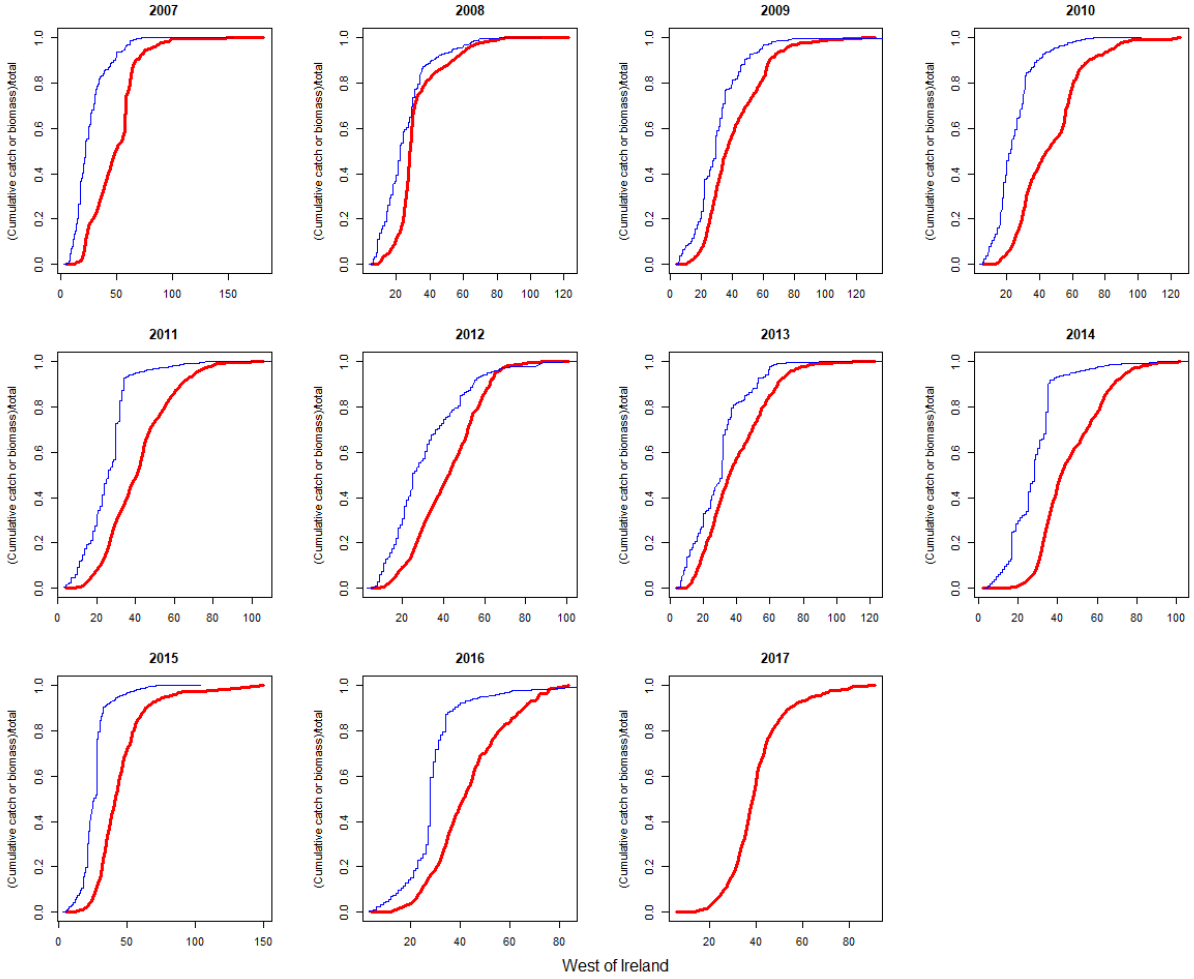

Figure 4.15. West of Ireland. annual fisheries balance in terms of size–structure from a combined analysis of observer data from Ireland otter trawlers (OTB) fishing for demersal fish and elasmobranchs. Commercial data from the observer programme are shown in red and surveyed size–structure in the community in blue for the Irish Q4 survey (survey data were not available for 2018).

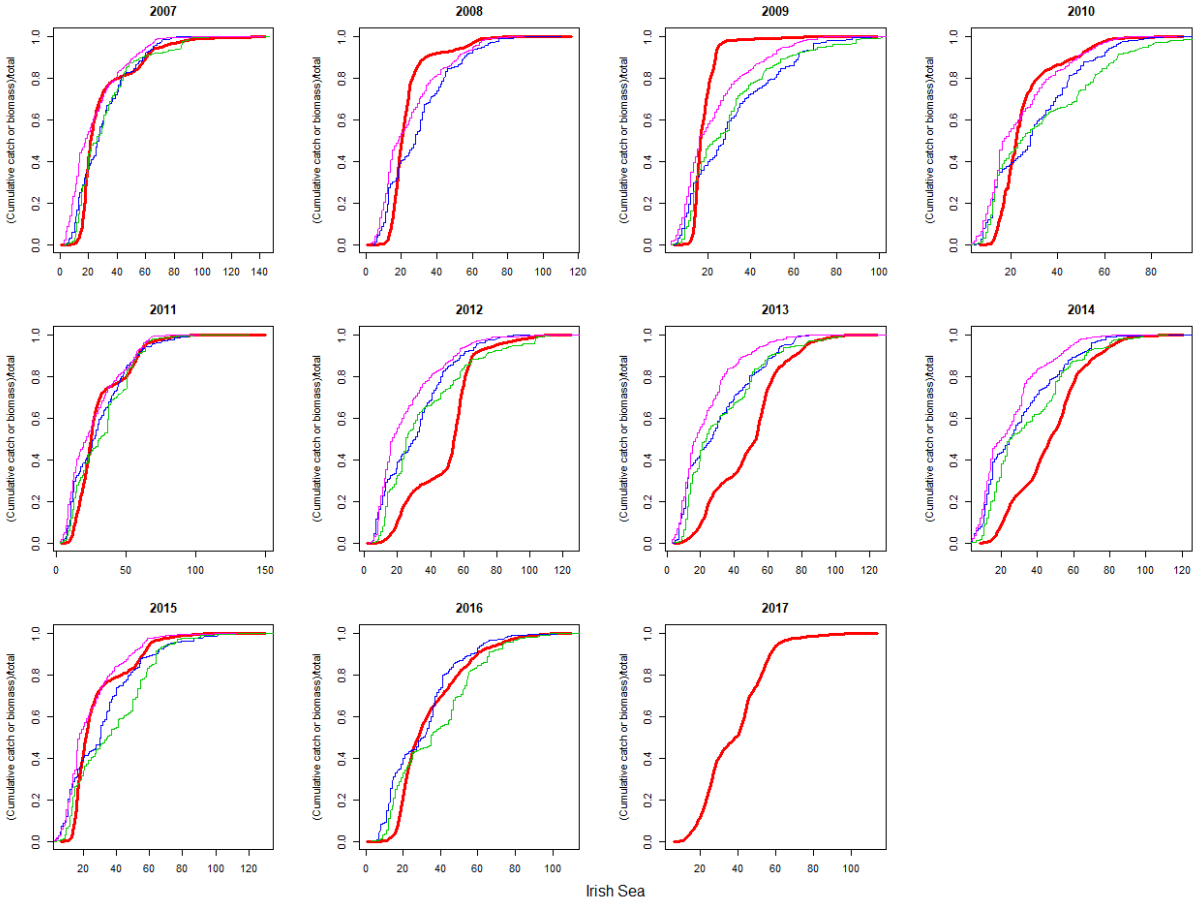

Figure 4.16. Irish Sea. Annual fisheries balance in terms of size–structure from a combined analysis of observer data from UK(E&W) and Ireland otter trawlers (OTB) fishing for demersal fish and elasmobranchs. Commercial data from the observer programme are shown in red and surveyed size–structure in the community in blue. Three survey datasets were available: Northern Irish Q1 survey is shown in blue and Northern Irish Q4 survey is shown in green and English beam trawl Q3 survey is shown in pink.

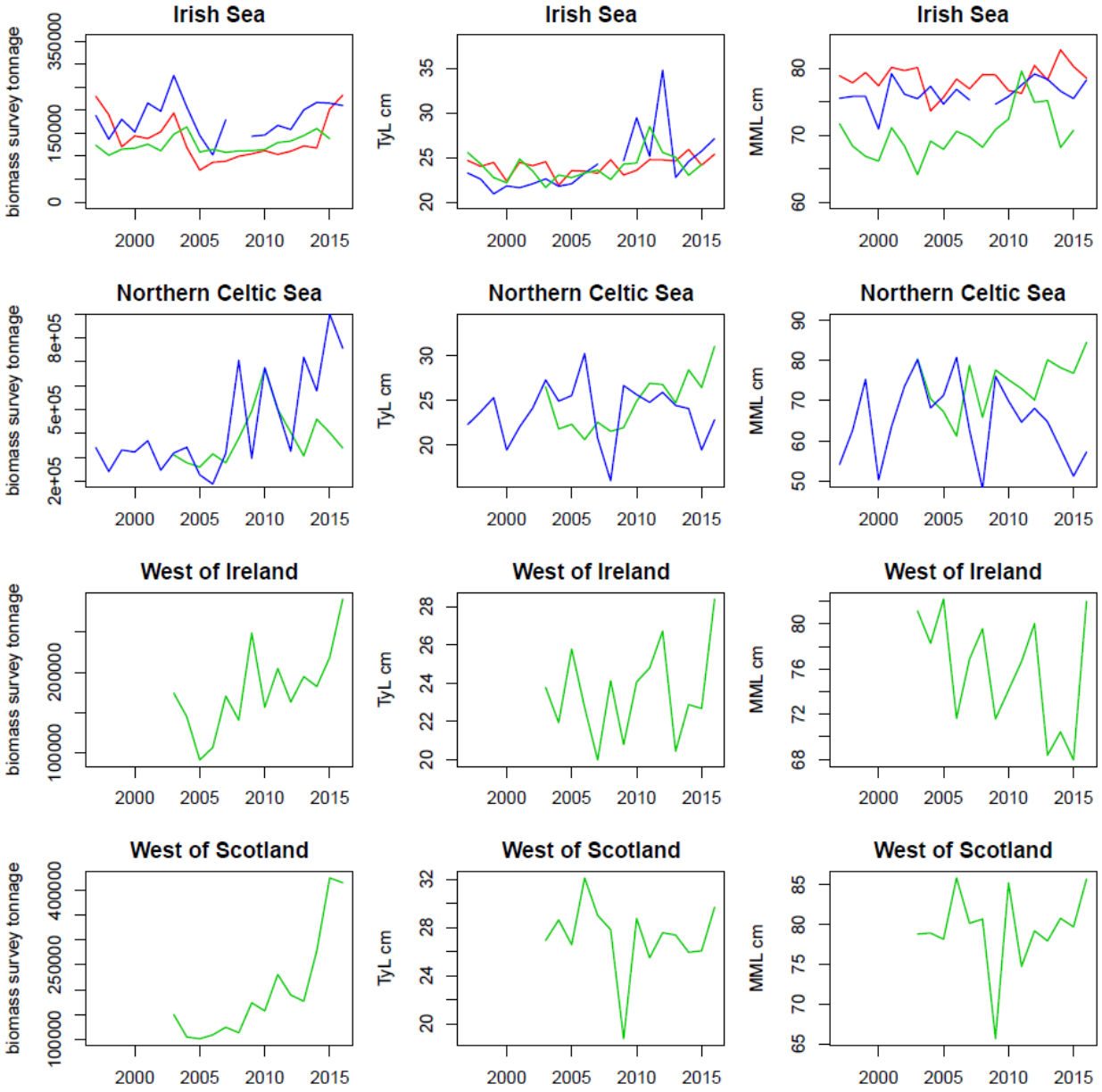

Figure 4.17. State indicators from analysis of otter trawl and beam trawl survey data for demersal fish and elasmobranchs. Three survey datasets were available for the Irish Sea: the N. Irish groundfish survey is shown in red for Q1 data and in blue for Q4, the English beam trawl survey in Q3 is shown in green. Two survey datasets were available for the northern Celtic Sea: Republic of Ireland survey in Q4 is shown in green and French Q4 survey is shown in blue. In the West of Ireland and West of Scotland areas the Republic of Ireland survey in Q4 is shown in green.

4.4 Targets for ecological indicators of state that relate to an acceptable risk of species diversity loss

A multispecies modelling approach was used to identify risk-based assessment thresholds for the North Sea demersal fish community that are applicable to species composition indicators (mean maximum length of fish) and size–structure (typical length) indicators.

Intersessionally, a size–structured multispecies predator–prey model of the North Sea (Thorpe *et al.*, 2015; 2016) was extended to include 27 stocks, food limitation processes and a recent declining trend in primary production (following Capuzzo *et al.*, 2018). In addition to fitting the modelled biomass to single-species stock assessment outputs; this model was further refined by

fitting the length distribution of modelled fish stocks to the observed length distribution data from the available surveys in the North Sea. The survey data used for this purpose were extracted from the processed dataset for otter trawl and beam trawl surveys, quality controlled by Marine Science Scotland (see Greenstreet and Moriarty, 2017 and Moriarty *et al.*, 2017 for further details), and these data were catchability-corrected following Walker *et al.* (2017).

Model simulations were made to investigate the responsiveness and sensitivity of the state indicators (biomass, species composition and size–structure) to increases in fishing effort and fishing pressure. The model was run over 200 model years using the best parameterisation achieved during the fitting process. A range of fishing strategies were simulated including: 'no fishing', 'status-quo fishing effort' and with fishing effort increased up to four times the status quo level. Fishing efforts were varied specifically for each of the four fleet groupings considered: beam, otter, industrial, and pelagic fleets yielding 10 000 different combinations. The resulting fishing pressure was calculated as the annual harvest rate (catch/biomass) per stock and per community (e.g. catch of all demersal stocks/total biomass of all demersal stocks).

The number of stocks with model biomass (representing spawning-stock biomass levels) less than the ICES single species assessment derived limit value of MSY $B_{trigger}$ was counted in each year of each simulation. For model stocks without this biomass reference value (see Table 4.4), a proxy was calculated as a percentage of the modelled virgin biomass per stock prior to fishing. The percentage value (33%) was calculated from the average ratio of known MSY $B_{trigger}$ values to modelled virgin biomass for the following stocks: cod, haddock, herring, hake, Norway pout, saithe, sandeel, sole, whiting. An exception was made for the stock of dab, for which 20% of virgin biomass was chosen, since the model produces an elevated level of biomass of this stock in the historic unfished period. An ICES reference point is available for the spawning–stock biomass of plaice, but it was not used because the current model was unable to reach this value even in unfished scenarios. The proportion of stocks with biomass below MSY $B_{trigger}$ was considered as a simple measure of risk of reduced reproductive capacity within the community.

Table 4.4. Species included in the North Sea multispecies model, the fish community allocation used and the reference point for the lower acceptable limit of biomass below which the stock is at risk of reproductive impairment.

Scientific Name	Common name	Code	Fish community	MSY $B_{trigger}$ or proxy (tonnes)	Origin of reference point
Amblyraja radiata	starry ray	RJR	demersal	3407	Model (33% of B0)
Ammodytidae spp.	sandeel	SAN	not grouped	460 000	ICES
Clupea harengus	herring	HER	pelagic	1 400 000	ICES
Dicentrarchus labrax	bass	BSS	not grouped	-	Model (33% of B0)
Eutrigla gurnardus	grey gurnard	GUG	demersal	132 575	Model (33% of B0)
Gadus morhua	cod	COD	demersal	150 000	ICES
Glyptocephalus cynoglossus	witch	WIT	demersal	2933	Model (33% of B0)
Hippoglossoides platessoides	long rough dab	PLA	demersal	463 277	Model (33% of B0)
Lepidorhombus whiffiagonis	megrim	MEG	demersal	1315	Model (33% of B0)
Leucoraja naevus	cuckoo ray	RJN	demersal	959	Model (33% of B0)
Limanda limanda	dab	DAB	demersal	752 839	Model (20% of B0)
Lophius piscatorius	monkfish	MON	demersal	40 582	Model (33% of B0)
Melanogrammus aeglefinus	haddock	HAD	demersal	132 000	ICES
Merlangius merlangus	whiting	WHG	demersal	166 708	ICES
Merluccius merluccius	hake	HKE	demersal	45 000	ICES
Microstomus kitt	lemon sole	LEM	demersal	41 848	Model (33% of B0)
Molva molva	ling	LIN	demersal	45 140	Model (33% of B0)
Nephrops units 5, 6, 7 ,8, 9, 10, 32, 33, 34	Norway lobster	NEP	*Nephrops*	-	Model (33% of B0)
Pleuronectes platessa	plaice	PLE	demersal	124 413	Model (33% of B0)
Pollachius virens	saithe	POK	demersal	150 000	ICES
Raja clavata	thornback ray	RJC	demersal	734	Model (33% of B0)
Scomber scombrus	mackerel	MAC	pelagic	30 264	Model (33% of B0)
Scophthalmus maximus	turbot	TUR	demersal	8295	Model (33% of B0)
Squalus acanthias	spurdog	DGS	demersal	276	Model (33% of B0)
Solea solea	sole	SOL	demersal	37 000	ICES
Sprattus sprattus	sprat	SPR	pelagic	14 200	ICES
Trachurus trachurus	horse mackerel	HOM	pelagic	27 670	Model (33% of B0)
Trisopterus esmarkii	Norway pout	NOP	demersal	65 000	ICES
Trisopterus minutus	poor cod	POD	demersal	33 406	Model (33% of B0)

In the simulations examined, increases in otter trawl effort led to a decrease in the TyL indicator for demersal fish and a limited (non-significant) decline in the MML indicator for demersal fish. The decrease in the TyL indicator arising from high levels of otter trawling could be reduced to some extent by the cessation of fishing by other fleets. Increases in fishing effort had no clear impact on the total biomass of the demersal fish community, since lightly fished species are able to benefit from a reduction in the biomass of either their predators or their competitors. Fishing effort–indicator relationships were not evident for the pelagic fish community. No direct linear relationship was evident with harvest rate for the TyL of demersal fish despite a clear relationship between TyL and otter trawl effort, suggesting that indirect effects of fishing through predator–prey interactions can alter the size–structure of the community and obscure the direct effects of fishing pressure. In contrast, for each of the pelagic and demersal fish communities, high

harvest rates did correspond to low values of the MML indicator suggesting that species composition within the community does respond directly to fishing pressure. Importantly, both MML and TyL of demersal fish communities showed clear non-linear relationships with the risk of stock depletion below MSY $B_{trigger}$ (Figure 4.19).

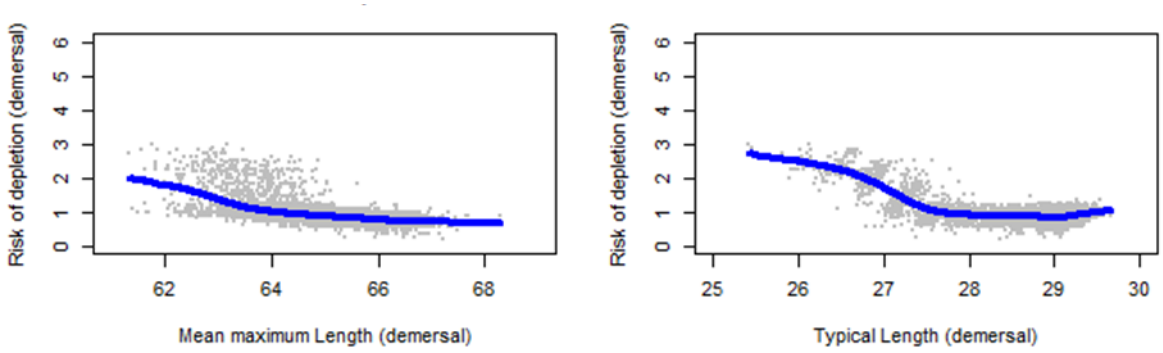

Figure 4.19. Modelled number of stocks depleted below MSY $B_{trigger}$ (or proxies) vs. indicators of species composition (left, MML) and size–structure (right, TyL) for demersal fish.

The likely recovery levels of each of the indicators was averaged over a decade for the two scenarios in which fishing effort for each fleet was set at either zero or maintained at current levels (Table 4.5). These future equilibrium values suggest that the current level of fishing in the North Sea should allow the current fish community to recover to natural levels (as modelled without fishing). Given the strong relationship of the indicators to risk of stock depletion for the demersal fish community, maintaining the TyL indicator (for the model stocks) to above 28 cm (Figure 4.18) and MML (for the model stocks) at or above 65 cm (Figure 4.18 and Table 4.5) should lead to a low risk of depletion of commercial stocks. Management towards these community targets is thus consistent with current targets for commercial fish and shellfish.

Table 4.5. Average indicator values during two possible future scenarios under constant primary production: a 'Recovery' level in the absence of fishing and 'Status Quo' an expected level under current fishing effort levels.

Scenario	Biomass Total (inc *Nephrops*) Mt	MML total cm	TyL total cm	Biomass demersal fish Mt	MML demersal cm	TyL demersal cm	Biomass Pelagic fish Mt	MML Pelagic cm	TyL Pelagic cm
Recovery (no fishing)	10.12	49.7	25.0	4.76	64.7	29.2	4.27	38.8	21.2
Status Quo (current fishing effort levels)	9.84	50.0	24.9	4.72	65.0	29.1	4.09	38.8	21.1

Embedding the model targets within assessments of Good Environmental Status

In order to make the model targets directly comparable to each survey available for the North Sea with the full suite of species, further work is required to rescale the model-based target appropriately. Given that the risk of depletion of commercial stocks is linked to these indicators, the hypothesis is that management of fisheries to achieve the community targets should also provide a level of protection to the non-assessed species within the community.

Indicator assessments of Good Environmental Status for the demersal fish community are typically based on time-series of change in surveys (see OSPAR Intermediate Assessment 2017, https://oap.ospar.org/en/ospar-assessments/intermediate-assessment-2017/). When the MML and TyL indicators are calculated using the species list from the model and the survey data that the model has been fit to, the model-derived targets proposed here to minimize risk of stock depletion (MML_{ref} = 65 cm and TyL_{ref} = 28) can be directly compared to the survey data (Figure 4.20). In 2015 and 2016, the MML for demersal fish has been at or above MML_{ref}, while TyL approached very close to TyL_{ref} in 2016.

Interestingly, the total surveyed biomass fell between 2000 and 2005 and has since been rising. In the period 2000–2005, TyL was much less than the mean community length-at-maturity (contrast the smooth line to the dashed turquoise line in Figure 4.20) suggesting that the high biomass toward the start of the time-series was the result of a high abundance of immature fish. Since 2008, the TyL indicator has been closer to the community mean length-at-maturity and the biomass is following a recovery trajectory. Together with the good status for species composition, these three indicators suggest that the demersal fish community is recovering to good environmental status at the North Sea level. However, at smaller geographic scales issues may still be evident (see MML and TyL assessment by OSPAR 2017).

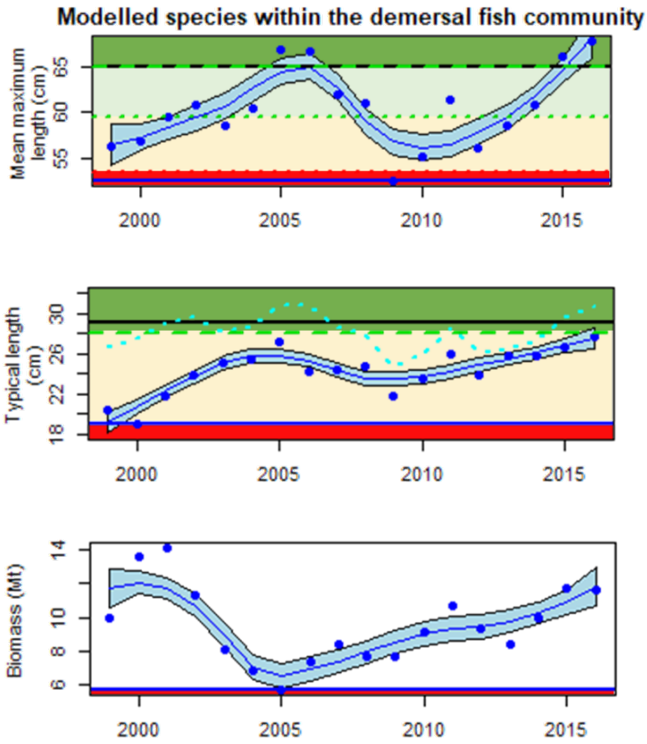

Figure 4.20. Modelled demersal fish community indicators for the North Sea (species composition, top, and size–structure, middle, and modelled biomass, bottom) with risk-based thresholds, dashed green horizontal line and dark green zone, based on minimizing risk of reproductive impairment. The dotted green line for species composition and pale green "acceptable" area is based on the empirically defined level given recent data (MML_{75}) and the percentile method following WGECO (2018). The black horizontal line shows the expected recovery level in the absence of fishing (note that this is plotted underneath the proposed target for mean maximum length indicator, top, as the values are equal). The area below the lower limit, in which management action is likely required, is shown by the red zone (this is either below the minimum observed value, identified by the horizontal blue line, or, for species composition, below the empirically defined minimum $MML_{depleted}$). The yellow zone is an area in which monitoring is the most appropriate action to take. The points are the annual estimated values of the indicators from survey data and the black curves show LOESS smooths fitted to these points with uncertainty (± 1 standard error) represented by the blue band. Also shown in the middle plot, is the community average length-at-maturity, which can be seen to fluctuate around the risk-based target to minimize risk of reproductive impairment.

This assessment outcome above is also in agreement with the current assessment of the Large Fish Indicator for the North Sea for which a target has been based on historical data (https://oap.ospar.org/en/ospar-assessments/intermediate-assessment-2017/biodiversity-status/fish-and-food-webs/proportion-large-fish-large-fish-index/). Historical data such as that investigated for the North Sea LFI indicator by Greenstreet *et al.* (2011) are not available for all ICES areas. However, multispecies models such as that developed here can be developed for each ICES area. So the risk-based approach explored above can be widely applicable in order to determine indicator assessment targets and baselines. In lieu of these model studies, the empirical approach for species composition (the MML indicator) developed by WGECO 2018 (see also Section 4.2 above), can be used to produce baselines for indicators of fish communities solely of observed data within a surveillance approach (Shepherd *et al.*, 2015). Importantly, the risk-based approach attempts to set a target level consistent with minimal risk of depletion of any single commercial stock, whereas the empirical-approach explores the data to determine an acceptable level for the community. Within the empirical-approach for the community, it is acceptable for one large species to replace another.

Compared with the model approach here (and the risk-based target of MML_{ref} = 65 cm), the empirical approach for the demersal species in the model community (which differs from that in

the IBTS survey in section 4.2) suggests the lower value of MML_{75} = 60 cm can be used for "acceptable" status with a lower limit of $MML_{depleted}$ = 54 cm for a community in which large species are depleted. The model-based approach provides strong evidence, given risk to reproductive impairment, that the assessment target could be higher and more ambitious than that determined through the empirical approach for the North Sea.

4.4.1 Model investigation of the sensitivity of the choice of percentile (for surveyed biomass by species) for empirical MML baselines

The empirical approach of WGECO (2018) uses time-series of biomass catch rates of surveyed species in order to identify acceptable and unacceptable levels for species composition *in lieu* of other approaches. As the percentile of surveyed catch rate (where the 75th percentile was chosen to represent each species biomass at an acceptable level) in the demersal fish community in the North Sea is increased towards the 99th percentile, the upper target for species composition increases (see Section 4.2). For the selected demersal species in the multispecies model, the upper baseline for MML approaches closest to the risk-based target at the 95th percentile (Figure 4.21). So for the North Sea, use of a higher percentile in the empirical method represents the higher ambition. However, this result does not appear to be universal given the sensitivity analysis of survey data in other areas (see Section 4.2).

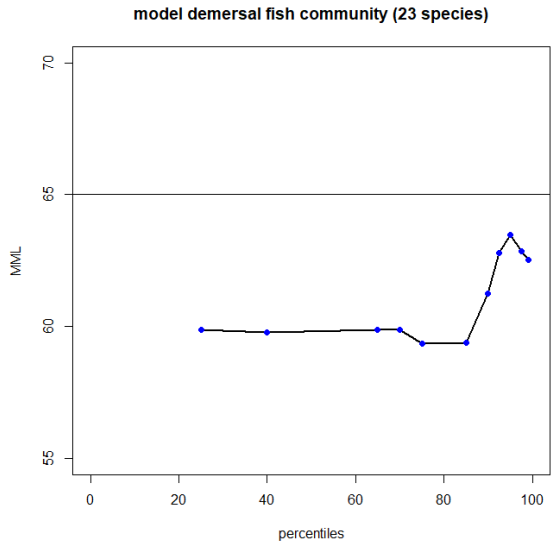

Figure 4.21. Sensitivity of survey derived target (based on percentiles) for MML of demersal fish (modelled community only).

4.4.2 Size–structure target to maintain reproductive capacity

In 4.2.1, we reasoned that a fish community with its biomass highly dependent on immature fish (i.e. recruitment events) is a depleted community and TyL should reflect a poor status in this situation. An increase in TyL towards the mean length-at-maturity is thus an improvement, when the biomass is not decreasing, since this indicates that the dependence of the community on new recruits (immature fish) is decreasing. Interestingly, the average (weighted by species biomass) of the community length-at-maturity values in the time-series shown in Figure 4.20 is equal to the proposed target of 28 cm for the demersal community arising from the model-derived acceptable risk of reproductive impairment (Figure 4.19). This agreement suggests that an empirical target for the TyL indicator can be determined based on community mean length-at-

maturity, with TyL less than this value considered to represent a community in poor status (e.g. Figure 4.22). Such a target would then be specific to current species composition, itself monitored through the MML, such that variation in size–structure can be assessed separately to species composition. However, such a target level would also be expected to vary as a result of change in primary production and predator–prey interactions within feeding guilds. Further exploration of this approach and the assumption that similar taxonomic groups with similar life histories should behave similarly may allow this approach to be applied to the wider surveyed community.

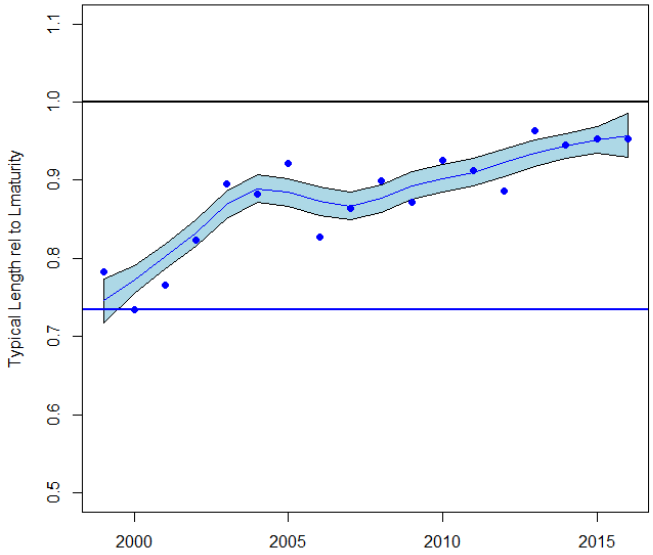

Figure 4.22. Typical length indicator (thin blue line and blue shaded area) for modelled demersal fish species only with LOESS smooth, relative to the expected length distribution at equilibrium (black line) without fishing (based on multi-species modelling) given relative annual biomass of species in the surveyed community.

4.5 Use of multispecies models to investigate proposed management strategies

The model study above was based solely on one recently developed model (unpublished). Here, we use an ensemble model (Spence *et al.*, 2018) to further examine the expected trajectory of fish community indicators with either: no fishing, 'status quo' fishing levels, fishing at single-species F_{msy} levels or fishing at multispecies rates (F_{Nash}). Results from the multi-model study confirm that the fish community should continue to recover, in each scenario considered.

Five different published ecosystem models (listed below) were run and used with empirical data to create an ensemble model. Historical fishing mortalities were applied annually in each model until 2013 and then the future scenarios were run to 2050 with fishing mortalities set constant at 2013 rates (status-quo), zero (no fishing) or at either F_{MSY} or F_{Nash} following Thorpe *et al.* (2017) and Thorpe and de Oliveira (2019). Due to the inherent complexity of fitting multiple models to multiple indicators, a selection of six indicators was modelled: (1) mean maximum length of all fish species (2) typical length of all fish species, (3) large fish indicator for demersal fish, (4) relative biomass of zooplankton, and (5) the biomass of demersal fish and (6) of birds and mammals combined. The ecosystem models employed were:

1. StrathE2E: The Strathclyde end-to-end, marine foodweb model, which has been designed to simulate regional-scale, macroscopic top–down and bottom–up cascading trophic effects (Heath *et al.*, 2014). The model explicitly considers the following functional groups: phytoplankton, omnivorous zooplankton, suspension/deposit feeding benthos, pelagic

fish larvae, demersal fish larvae, carnivorous/scavenge feeding benthos, carnivorous zooplankton, pelagic fish, demersal fish and birds and mammals. StrathE2E modelled the following indicators: zooplankton biomass, fish biomass, and combined biomass of birds and mammals.

2. FishSUMS: A length-based multispecies model of the North Sea (Spiers *et al.*, 2008). The model explicitly considers the following species: sandeel, Norway pout, herring, dab, whiting, grey gurnard, plaice, haddock, cod, saithe and *Nephrops*. FishSUMS modelled the following indicators: large fish indicator, mean maximum length, typical length and fish biomass.
3. mizer: A multispecies size-based model of the North Sea (Blanchard *et al.*, 2009). The model explicitly considers the following species: sprat, sandeel, Norway pout, herring, dab, whiting, sole, grey gurnard, plaice, haddock, cod and saithe. mizer modelled the following indicators: large fish indicator, mean maximum length, typical length and fish biomass.
4. Ecopath with Ecosim: The Ecopath model used in this case is the model of the North Sea (ICES, 2016). It contains >10 fishing fleets and >60 functional groups from benthos to seabirds, some of which (cod, haddock, whiting, saithe, herring) are split into multiple age stanzas (juvenile and adult). Ecopath with Ecosim modelled the following indicators: zooplankton biomass, mean maximum length, fish biomass and the combined biomass of birds and mammals.
5. LeMans: A length-based model for the North Sea (Thorpe *et al.*, 2016) upon which the primary model was based. The original LeMans model explicitly considers the following species: sprat, Norway pout, sandeel, poor cod, long rough dab, dab, herring, horse mackerel, lemon sole, sole, mackerel, whiting, witch, gurnard, plaice, starry ray, haddock, cuckoo ray, monkfish, cod and saithe. LeMans modelled the following indicators: large fish indicator, mean maximum length, typical length and fish biomass.

The parameter uncertainty in each of the ecosystem model's predictions was calculated in Spence *et al.* (2018) for StrathE2E and FishSUMs, in Spence *et al.* (2016) for mizer, in Mackinson *et al.* (2018) for Ecopath with Ecosim and in Thorpe *et al.* (2016) for LeMans. Following the approach of Spence *et al.* (2018), the ecosystem models above are combined with empirical studies in an ensemble model. The ensemble model describes the discrepancies, or biases, in each of ecosystem models and the empirical studies, exploiting strengths whilst discounting weaknesses, to give a single prediction of the future of the indicators with quantifiable uncertainty. Zooplankton biomass data were taken from Continuous Plankton Recorder data (Lynam *et al.*, 2017). The mean maximum length for all species, typical length for all species and the large fish indicator for demersal fish species were calculated from the International Bottom Trawl Survey (IBTS) data used during the OSPAR (2017) assessment. Processed data were obtained from the OSPAR Groundfish Survey Monitoring and Assessment Data Product for the Northeast Atlantic Area (Greenstreet and Moriarty, 2017; Moriarty *et al.*, 2017), which is based on national datasets uploaded to the ICES DATRAS system. The biomass of birds and mammals was obained from species distribution model (SDM) predictions based on ~2 million kilometres of at-sea cetacean and seabird surveys between 1985 and 2015 (Waggitt *et al.*, in prep.). As this analysis is ongoing, predictions should be treated as preliminary. However, qualitative inspection revealed nothing surprising or extreme. We fitted the observation data using a 2nd order polynomial regression with a first order auto-regressive error structure.

Results

The ensemble model demonstrates a recovery of the fish community from the low levels observed in the 1990s (consistent with empirical data and the OSPAR, 2017 assessment). All forecast scenarios suggest continued improvement in the fish community with little difference between

F_{msy} and F_{Nash} scenarios, but a considerable difference between these and the no-fishing and status-quo scenarios (Figures 4.23 and 4.24). All fish community indicators reach higher values in the no-fishing scenario than in any other scenario. It is important to note that the absolute values modelled here are not comparable to the modelling in Section 4.4, since the species composition differs between the models and datasets (and here the models include pelagic species). However, the agreement in the trend between the models is interesting and together they demonstrate that the wider fish community is also recovering.

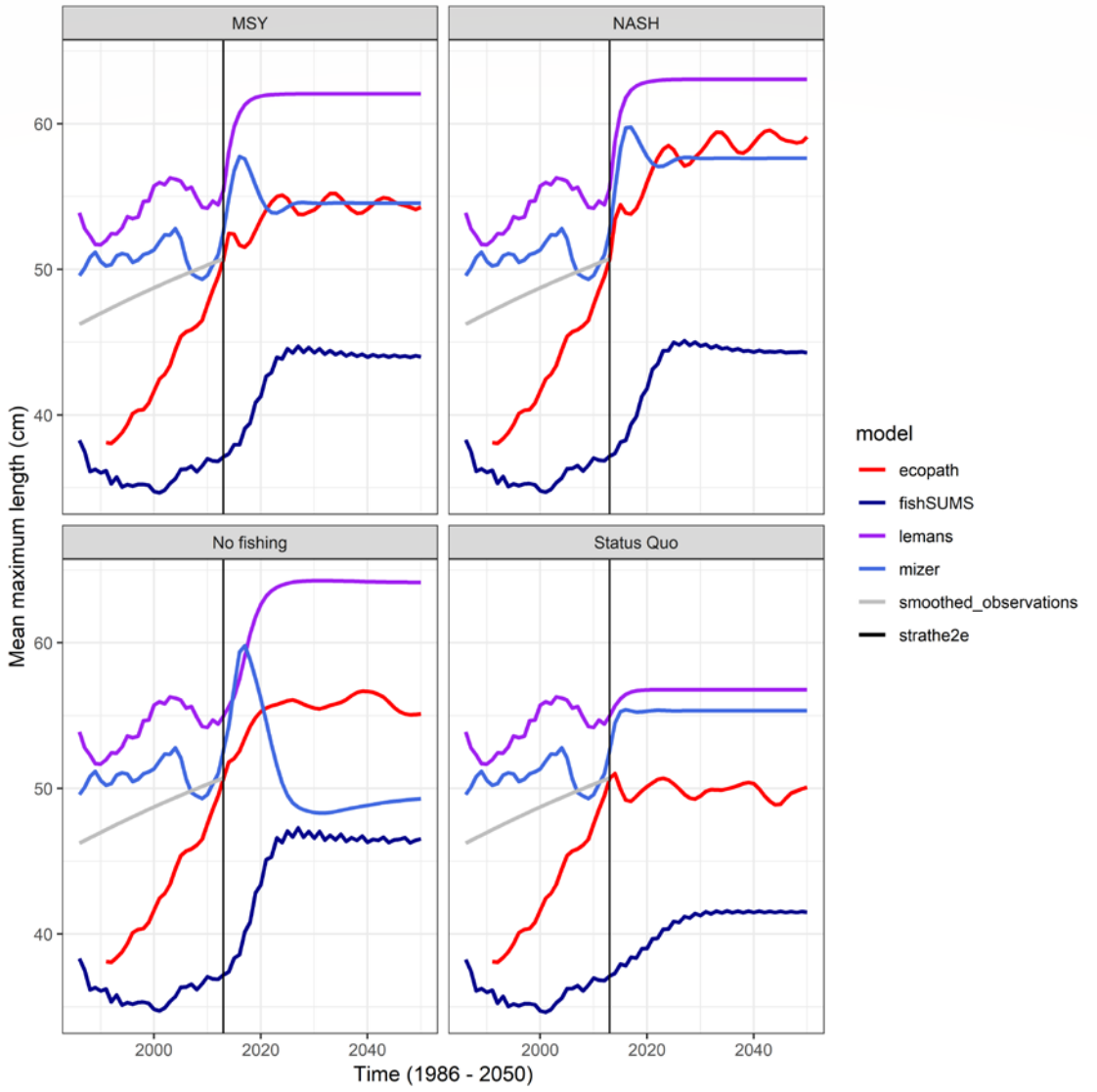

Figure 4.23. Separate model output for the mean maximum length of the total fish community as defined specifically and differently by the data and each foodweb model where the vertical line shows the period in which forecasts begin.

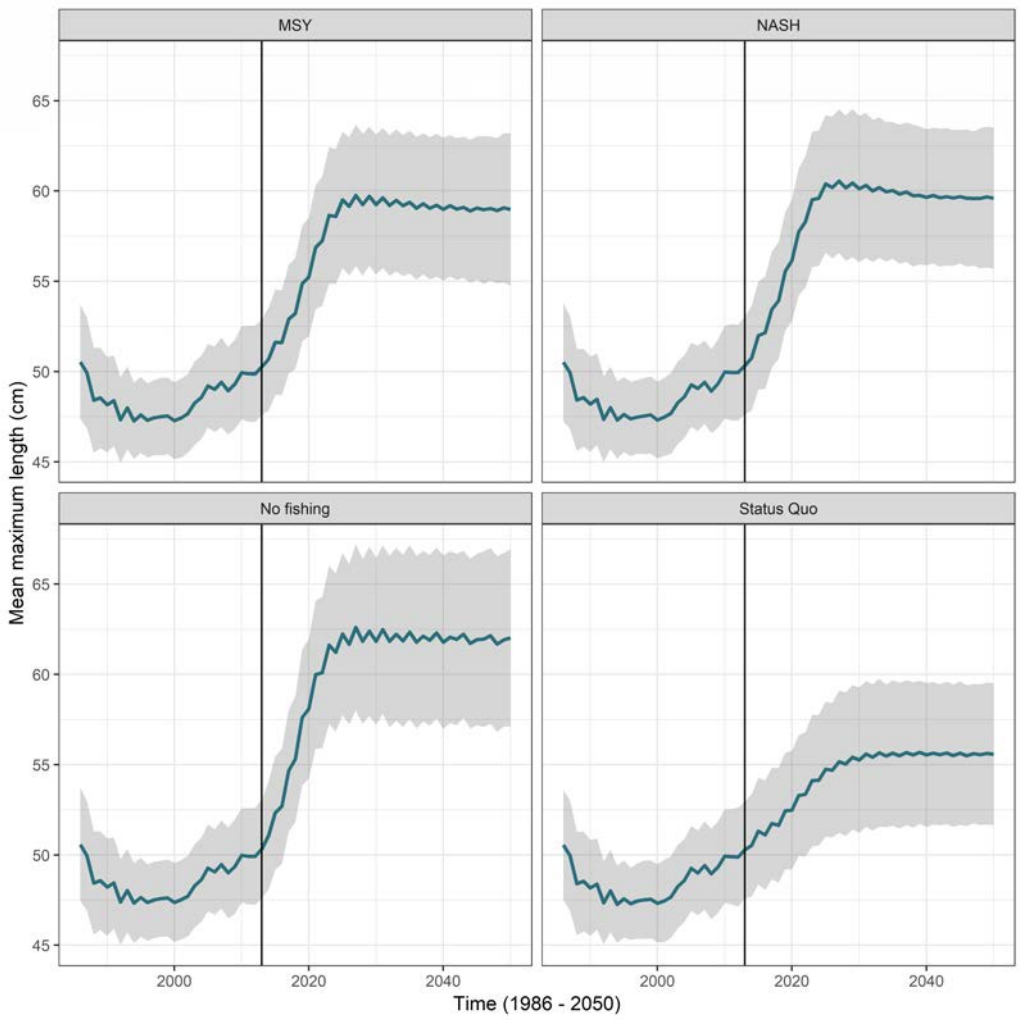

Figure 4.24. Ensemble model output for the demersal fish community (as specifically defined by the dataset and each foodweb model) given a combined analysis of data and five ecosystem models where the vertical line shows the year at which forecasts begin.

4.6 References

Blanchard JL, Andersen KH, Scott F, Hintzen NT, Piet G, Jennings S. 2014. Evaluating targets and trade-offs among fisheries and conservation objectives using multispecies size spectrum model. Journal of Applied Ecology 51(3):612–662 https://doi.org/10.1111/1365-2664.12238

Borges, L., Zuur, A. F., Rogan, E., and Officer, R. 2004. Optimum sampling levels in discard sampling programs. Canadian Journal of Fisheries and Aquatic Sciences, 61, 1918–1928. https://doi.org/10.1139/f04-138

Borges, L., Zuur, A. F., Rogan, E., and Officer, R. 2004. Optimum sampling levels in discard sampling programs. Canadian Journal of Fisheries and Aquatic Sciences, 61, 1918–1928. https://doi.org/10.1139/f04-138

Capuzzo E, Lynam CP, Barry J, Stephens D, Forster RM, Greenwood N, McQuatters-Gollop A, Silva T, van Leeuwen SM, Engelhard G.H. 2018. A decline in primary production in the North Sea over twenty-five years, associated with reductions in zooplankton abundance and fish stock recruitment. Glob Change Biol. 24: e352–e364 https://doi.org/10.1111/gcb.13916

Cornou, AS, Goascoz N, Scavinner M, Prioul F, Sabbio A, Dubroca L, Renaud F, Rochet M.J. 2018. Captures et rejets des métiers de pêche français. Résultats des observations à bord des navires de pêche professionnelle en 2017. OBSMER 2018-10-09.

Dubroca L, Vigneau J, Cornou AS, Demaneche S, Weiss J, Merzereaud M, Vermard Y, Savina-Rolland M, Villanueva CM, Schlaich I, Pawlowski ML, Robert M, Lissardy M, Morandeau G, Drogou M, Fifas S, Gadenne H, Lorance P, Saraux C, Rouyer T, Gontrand F. 2016. Ptyx: data compilation at the edge of automation. ASC 2016 - ICES Annual Science Conference 2016. 19–23 September 2016, Riga.

Enever, R., Revill, A., and Grant, A. 2007. Discarding in the English Channel, Western approaches, Celtic and Irish seas (ICES Subarea VII). Fisheries Research, 86, 143–152. https://doi.org/10.1016/j.fishres.2007.05.013

Greenstreet, S.P.R., Rogers, S.I., Rice, J.C., Piet, G.J., Guirey, E.J., Fraser, H.M., Fryer, R.J. 2011. Development of the EcoQO for fish communities in the North Sea. ICES Journal of Marine Science 68, 1–11.

Greenstreet, SPR, and Moriarty, M. 2017. Manual for version 3 of the groundfish survey monitoring and assessment data product. Scottish Marine and Freshwater Science 8: 77. https://doi.org/10.7489/1986-1

Heath MR, Speirs DC, Steele J.H. 2014. Understanding patterns and processes in models of trophic cascades. Ecology Letters 17: 101–114. https://doi.org/10.1111/ele.12200

ICES. 2016. Report of the Working Group on Multispecies Assessment Methods (WGSAM), 9–13 November 2015, Woods Hole, USA. ICES CM 2015/SSGEPI:20. 206.

Kraak, S. B. M., Bailey, N., Cardinale, M., Darby, C., De Oliveira, J. A. A., Eero, M., … Vinther, M. 2013. Lessons for fisheries management from the EU cod recovery plan. Marine Policy, 37, 200–213. https://doi.org/10.1016/j.marpol.2012.05.002

Lynam CP, Llope M, Möllmann C, Helaouët P, Bayliss-Brown GA, Stenseth N.C. 2017. Interaction between top–down and bottom–up control in marine food webs. Proceedings of the National Academy of Sciences 114 (8) 1952–1957. https://doi.org/10.1073/pnas.1621037114

Mackinson S, Platts M, Garcia C, Lynam C.P. 2018. Evaluating the fishery and ecological consequences of the proposed North Sea multi-annual plan. PLoS One, 13(1): e0190015. https://doi.org/10.1371/journal.pone.0190015

Moriarty, M, Greenstreet, SPR, Rasmussen, J. 2017. Derivation of groundfish survey monitoring and assessment data product for the Northeast Atlantic Area. Scottish Marine and Freshwater Science, 8: 240. https://doi.org/10.7489/1984-1

OSPAR. 2017. Intermediate Assessment (2017) Available at: https://oap.ospar.org/en/ospar-assessments/intermediate-assessment-2017

Shephard, S., Greenstreet, S. P. R., Piet, G. J., Rindorf, A., and Dickey-Collas, M. 2015. Surveillance indicators and their use in implementation of the Marine Strategy Framework Directive. ICES Journal of Marine Science, 72: 2269–2277.

Speirs D, Guirey E, Gurney W, Heath M. 2010. A length-structured partial ecosystem model for cod in the North Sea. Fisheries Research 106(3):474–494.

Spence MA, Blanchard JL, Rossberg AG, Heath MR, Heymans JJ, Mackinson S, Serpetti N, Speirs DC, Thorpe RB, Blackwell P.G. 2018. A general framework for combining ecosystem models. Fish and Fisheries 19:1031–1042 https://doi.org/10.1111/faf.12310

Thorpe RB, De Oliveira J.A.A. 2019. Comparing conceptual frameworks for a fish community MSY (FCMSY) using management strategy evaluation — an example from the North Sea, ICES Journal of Marine Science, fsz015. https://doi.org/10.1093/icesjms/fsz015

Thorpe RB, Le Quesne WJF, Luxford F, Collie JS, Jennings S. 2015. Evaluation and management implications of uncertainty in a multispecies size–structured model of population and community responses to fishing. Methods in Ecology and Evolution 6(1):49–58. https://doi.org/10.1111/2041-210X.12292

Thorpe, R. B., Dolder, P. J., Reeves, S., Robinson, P., and Jennings, S. 2016. Assessing fishery and ecological consequences of alternate management options for multispecies fisheries (2016) ICES Journal of Marine Science 73 (6) 1503–1512. https://doi.org/10.1093/icesjms/fsw028

Waggitt JJ, Evans PGH, Hiddink JG *et al.* In prep. Mapping of cetacean and seabird distributions in the North-East Atlantic.

Walker, ND, Maxwell, DL, Le Quesne, WJF, and Jennings, S. 2017. Estimating efficiency of survey and commercial trawl gears from comparisons of catch-ratios. ICES Journal of Marine Science, 74(5) 1448–1457. https://doi.org/10.1093/icesjms/fsw250

5 ToR c: Review the knowledge of spatial distribution indicators for fish and benthos

5.1 Approach and general remarks

The review was structured into three subsections:

1. Recommendations on which indicators to develop, considering both how useful/important these are, and with respect to simplicity of use and clarity of communication;
2. Test the performance of several candidate spatial distribution indicators;
3. Initial consideration of methods to integrate indicators.

5.2 Recommendations on which indicators to develop, considering both how useful/important these are, and also simplicity of use and clarity of communication

To complete this task, the review of potential indicators from WGECO 2016 and literature published since then was reviewed to identify whether new indicators had been suggested which were not already part of the indicator list. There did not appear to be any necessary additions, and hence the work continued based on the list from 2016 (Table 5.1). In 2018, WGECO noted that all the spatial metrics reviewed may respond to changes in total abundance as well as to climate change and fishing.

5.2.1 Restrictions on possible analyses due to data characteristics

Most of the analyses of distribution in the literature concern a single fish species within a surveyed area. However, this is due to the availability of fish trawl data rather than a reflection of the greater importance of distributional changes in fish compared to benthos. As data become available for benthos, the analyses should be conducted for these taxa.

The lack of complete standardisation in time and gear among surveys has generally led to analyses of individual survey areas to avoid the issue of standardising between surveys. This type of analysis may lead to the conclusion that there is no change in spatial distribution even if there is a substantial change in the relative importance of two surveyed areas. Furthermore, the analyses should be life-stage specific, as changes in only some life stages may tell us about the causes of change. For example, changes may occur in juvenile distribution if spawning or juvenile survival changes, whereas changes in the distribution of adults only may reflect the spatial distribution of fishing mortality.

On applying the indicators, it is necessary to attend to the issue of how sampling scale affects the indicators. For example, survey catch rates of fish appear to be correlated at spatial scales from 5 to 10 km (Stelzenmüller *et al.*, 2005), implying that the scale of individual patches is below 5–10 km. In general, survey hauls in the Northeast Atlantic cover between 3.7 and 7.4 km (30–60 min at 4 knots) and the recommended minimum distance between hauls is 18.5 km. Hence, it is likely that patches and the associated spatial correlation occurs at spatial scales less than the distance between hauls and possibly at scales smaller than the length of the individual hauls. In this case, the data will not provide sensible information on the size, frequency and distance between individual patches.

5.2.2 Simplicity of use and communication

WGECO rated all metrics for simplicity of use and ease of communication to non-experts. The simplicity rating is meant to reflect the ease of use from acquisition of the data to producing repeated estimates of the metric, preferably including the uncertainty of these estimates. The communication rating is focused on non-experts and includes describing the biological meaning a change in the metric will have. All the suggested measures can be used for scientific purposes, as is demonstrated by their repeated use in the literature, and therefore a low rating should not be interpreted as the metric being irrelevant from a scientific point of view. The resulting consideration is given in Table 5.1.

Overall, the metrics that include aspects of latitude, longitude or depth (range extremes, average, 5% and 95%tiles of latitude, longitude and depth of recorded specimens) were considered easy to use and communicate. These metrics are frequently used in terrestrial studies and in communication to the public (e.g. climate-induced shifts).

The "centre of gravity metric" can be misleading for coastal species and for sea areas containing land masses. For areas with a large land mass in the middle, the centre of gravity may often move around in the middle of the land mass due to changes in the distribution of a species dispersed around the land mass. Conversely, in a large area of open sea, such as the North Sea, the centre of gravity of a coastal species may move about in the middle of the area where no fish are present. Such plots, while perhaps useful to scientists, could easily lose credibility with stakeholders and managers. Instead, weighted-mean latitude and weighted-mean longitude plotted separately as time-series can convey compelling information demonstrating clear changes in species' distributions.

The area containing a fixed percentage of the population, also termed the core area, and area occupied (surface area of potential and realised occupied areas) are easy to use and communicate. However, both are sensitive to abundance at low sampling densities and are therefore likely to be most reliable for abundant species, unless based on modelled surfaces. It is not clear how to define the area occupied from a fitted surface (which generally predicts a very low mean but not zero) in a way that avoids the inherent link with abundance; hence, the area containing a fixed percentage of the population seems the most promising of the two.

The indicators referring to identified patches are challenged both by the sampling scale issue mentioned under 5.2.1 and by the requirements for specific software, expertise and subjective decisions to be made in the process. Further, while it is easy to explain what the metric measures, it is difficult to explain how it relates to the ecology of organisms and particularly management measures. However, not including any indicators on splitting or merging distributions, will not allow such changes to be identified. One approach to rectify this would be to investigate the number of large-scale aggregations rather than specifically estimate patch characteristics.

Table 5.1. Aspects important to analysis of distribution, possible metrics, caveats and examples of drivers and pressures to which the metric may respond.

High level aspect	detailed level aspect	Possible Metrics	Caveats	Responsive to which drivers and pressures	Simple to use?	Easy to communicate to the non-expert?
Geographical range	Latitude and longitude of distribution area Depth in distribution area Temperature in distribution area	Extreme, 5% and 95%tiles of latitude, longitude, depth and temperature of recorded specimens.	Highly dependent on surveyed area and hence not comparable if surveyed area has changed The accuracy of the estimated distribution relies on catchability being independent of place, depth and temperature	Responsiveness to climate change is likely to be greatest for temperature based metrics and metrics which are highly correlated to the limiting factor. Responsive to spatially targeted fishing pressure and in species which are not highly mobile, the most appropriate metric depends on how the fishing pressure is aggregated (by latitude, longitude, depth or temperature). Geographical extent can change without a concurrent change in other aspects of distribution. Can be used to detect: Parallel shift and contraction/expansion	Yes. Especially the measures based on latitude, longitude and depth. Temperature related measures require reliable information on temperature and a decision on which temperature to use (which depth and which days/months) and hence are somewhat more complicated to use.	Yes, provided results are not illustrated with ranges or centre of gravity plotted on land in maps.
Geographical average location	Latitude and longitude of distribution area Depth in distribution area Temperature in distribution area	Average of latitude, longitude, depth and temperature of recorded specimens.	Highly dependent on surveyed area and hence not comparable if surveyed area has changed The accuracy of the estimated distribution relies on catchability being independent of place, depth and temperature	Responsiveness to climate change is likely to be greatest for temperature based metrics and metrics which are highly correlated to the limiting factor. Responsive to spatially targeted fishing pressure and in species which are not highly mobile, the most appropriate metric depends on how the fishing pressure is aggregated (by latitude, longitude, depth or temperature). Geographical extent can change without a concurrent change in other aspects of distribution.	Yes. Especially the measures based on latitude, longitude and depth. Temperature related measures require reliable information on temperature and a decision on which temperature to use (which depth and which days/months) and hence are somewhat more complicated to use.	Yes, provided results are not illustrated with centre of gravity plotted on land in maps.

High level aspect	detailed level aspect	Possible Metrics	Caveats	Responsive to which drivers and pressures	Simple to use?	Easy to communicate to the non-expert?
				Can be used to detect: Parallel parallel shift and contraction/expansion		
Occupied area	Potential and realised occupied area	Surface area of empty areas (potential and realised) Surface area of near-empty areas (5% lowest abundance) (potential and realised) Surface area of occupied areas (potential and realised) Realised occupied area relative to potential occupied area	The occupied area when measured directly from the number of empty samples recorded is highly statistically dependent on abundance, survey effort and assessment scale. If this effect is not desired, modelled probability of observing the species can be used together with a threshold defining empty areas (e.g. probability of observing the species is less than 10%). This can remove the effect of survey effort but will not remove the inherent link with abundance.	Responsive to habitat loss (including that induced by climate change) and a general decline in habitat suitability which may lead to poorer habitat being vacated. Can be responsive to spatially targeted fishing pressure in species which are not highly mobile. All metrics may be responsive to changes in total abundance. Occupied area can change without a concurrent change in geographical distribution. However, most aggregation measures depend on the amount of empty habitat and hence are related to occupied area. Can be used to detect: Contraction/expansion	Yes, occupied area from observations directly is easily estimated while model predictions require more consideration and work.	Yes, but requires explanation of caveats for mobile creatures and of scale dependence
Aggregation	Surface area of high and low density areas	Area containing a fixed percentage of the population (both high and low) standard deviation of average latitude, longitude, depth and temperature	Area containing a fixed percentage of the population is statistically dependent on abundance at low density unless data are model smoothed before estimation.	Can be responsive to spatially targeted fishing pressure in species which are not highly mobile. All metrics may be responsive to changes in total abundance. Indicative of stock sensitivity to potential changes in overlap with the fishery as a highly aggregated species will experience	Yes. Aggregation directly from observations is easily estimated for abundant species while model predictions require more consideration and work. Model predictions must be	Yes, areas containing a fixed percentage is easy to explain. Standard deviation of latitude etc. are not easy to explain.

High level aspect	detailed level aspect	Possible Metrics	Caveats	Responsive to which drivers and pressures	Simple to use?	Easy to communicate to the non-expert?
				a large increase in pressure if aggregation areas become targeted by the fishery. Aggregation can change without a concurrent change in geographic aspects of distribution. However, most aggregation measures depend on the amount of empty habitat and hence are related to occupied area. Can be used to detect: Contraction/expansion and splitting/merging	used for less abundant species and these are more labour intensive. Standard deviation of latitude etc. is easy to estimate.	
	Patchiness	Lloyd's patchiness index/Negative binomial k	Patchiness indices require a substantial number of non-zero observations to be reliable	As above	Yes	Not without substantial explanation.
Pattern description	Number of patches Distance between patches Size/area of individual patches Density in patches Variance in density on different spatial scales/Evenness of patches	Number of patches Number of isolated patches Distance between patches Size/area of individual patches Density in patches Persistence of patch locations Variance in density on different spatial scales/ Evenness of patches	Patch definition is still very much a subjective decision and spatial extent and distance between observed patches is highly dependent on sampling distribution relative to patch size. The spatial scale of sampling is crucial to the determination of patch size, as the minimum size is determined by the min-	Patch number, size and density depend on patch 'birth' and 'dead' rate. Distance between patches and number of isolated patches are both related to number of patches, whereas variance in density in patches at larger spatial scales is related to aggregation. Pattern can potentially change without a concurrent change in geographic aspects of distribution. Aggregation and occupied areas are related to pattern if measured at the same spatial scale. However, the spatial scale of patterns if often less than	Requires specific software, expertise and subjective decisions.	Easy to explain what the metric measures but difficult to explain how it relates to the ecology of organisms. The density and variance in density on different spatial scales/Evenness of patches is difficult to explain.

High level aspect	detailed level aspect	Possible Metrics	Caveats	Responsive to which drivers and pressures	Simple to use?	Easy to communicate to the non-expert?
			imum distance between sampling locations.	that investigated for aggregation and occupied area. Can be used to detect: not simply related to any of the types Parallel shift, Contraction/expansion or splitting/merging		
Pattern dynamic	Within and between patch dynamics	Connectivity/contagion between patches/areas Increase or decrease of individual patches	Patch definition is still much a subjective decision and spatial extent and distance between observed patches is highly dependent on sampling distribution relative to patch size. The temporal scale of sampling determines which temporal scale of dynamics can be investigated.	Connectivity is related to species dispersal (including in the larval phase), mobility and distance between patches. Increase and decrease of individual patches is related to patch density and size/area. Can be used to detect: not simply related to any of the types Parallel shift, Contraction/expansion or Splitting/Merging	Requires specific software, expertise and subjective decisions.	Difficult to explain what the metric measures and how it relates to the ecology of organisms.

5.3 Test several candidate spatial distribution indicators

5.3.1 Candidate spatial distribution indicators testing

An examination of some attributes of distributions of marine species, which ideally would be monitored, and their value to management are presented herein. Challenges in applying distribution indicators have been identified in Section 5.2.1. These include the sampling effects particularly with relation to rare species, the complexity of metrics currently available to assess distributional changes (Table 5.1) and the geographical scales needed to assess distributions, which generally do not fit with management regions for many species. Mapping the distribution of organisms, especially at spatial scales relevant to the species concerned, provides an indication of a species distributional range and the pattern of variation in density within this range. However, common practice is to assess distributional changes at the level at which data are collected (e.g. Petitgas and Poulard, 2009; Lewy and Kristensen, 2009). A few authors have assessed changes in distribution over larger spatial scales (e.g. Hughes *et al.*, 2014; Thorson *et al.*, 2016).

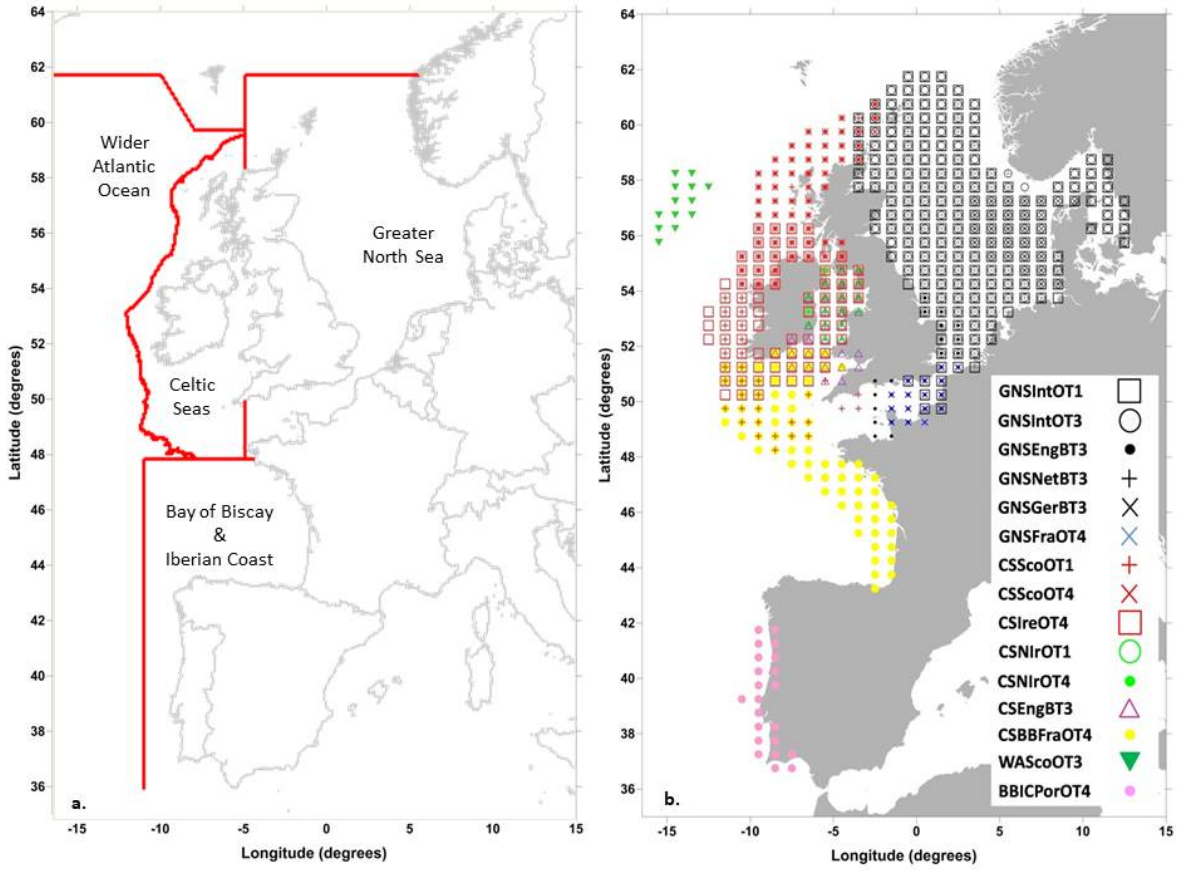

Figure 5.1a. The subregions of the Northeast Atlantic Ocean Region; The Greater North Sea (including the Kattegat and English Channel), the Celtic Seas, the Bay of Biscay and Iberian Coast, and the wider Atlantic Ocean. b. Survey coverage of the 15 published datasets across the Northeast Atlantic. See Moriarty *et al.* (2019) for explanation of survey acronyms. (From Moriarty *et al.*, 2019).

Potentially useful distributional indicators of good environmental health or Good Environmental Status (GES) in the context of ecosystem-based management (e.g. Marine Strategy Framework Directive (MSFD)) are applied to simulated data at the scale of the Northeast Atlantic (Figure 5.1a) to test for accuracy and potential biases in use of the indicators.

5.3.2 Data generation process

A zero-inflated Poisson distribution was used to simulate the distribution of species at the scale of the Northeast Atlantic (Figure 5.1a). We limited the lower depth range to 250 m and applied the substratum map from the EU seamap. We generated data to fulfil six potential scenarios:

- Scenario 1: weak space-time-trend in distribution for a relatively common species: Fish are moving in a north–east direction, with no change in abundance over time.
- Scenario 2: strong space-time-trend), for a relatively common species: Fish are moving in a south–east direction, with no change in abundance over time.
- Scenario 3: strong space-time-trend with a preference for a given substratum, for a relatively common species: Fish are moving in a south–east direction with a strong habitat preference for course and mixed habitat types, with no change in abundance over time.
- Scenario 4: weak space-time-trend in distribution for a rare species: Fish are moving in a north–east direction, with no change in abundance over time.
- Scenario 5: strong space-time-trend for a rare species: fish are moving in a south–easterly direction, with no change in abundance over time.
- Scenario 6: strong space-time-trend with a preference for a given substratum, for a rare species: Fish are moving in a north–westerly direction with a strong habitat preference for course and mixed habitat types, with no change in abundance over time.

We drew random sample data locations (n = 2100) for ten years from the simulated dataset. We modelled the sampled data using a Generalised Additive Mixed Model (GAMM) approach, producing a predictive abundance surface to test several candidate distribution indicators for bias and accuracy. Table 5.3.2.1 below supplies the coefficients used to generate the data. Comparisons were made between the expected result in the simulated dataset and the predicted result in the modelled data, as well as between the simulated dataset and the raw survey data. As this was a preliminary study and scoping exercise, we performed a single iteration of each scenario.

Table 5.3.2.1. Table of simulated data function arguments for each of the six scenarios.

Data Generation Function Arguments	Scenario 1	Scenario 2	Scenario 3	Scenario 4	Scenario 5	Scenario 6
M: Number of spatial replicates	10 800	10 800	10 800	10 800	10 800	10 800
N: Number of sample sites	2100	2100	2100	2100	2100	2100
J: Number of temporal replicates (years)	10	10	10	10	10	10
$\bar{\lambda}$: Mean abundance at value 0 of abundance covariates	20	20	20	0.2	0.2	0.2
B_1: Main effect of X on abundance	1	3	3	1	3	3
B_2: Main effect of Y on abundance	1	-4	-4	1	-4	-4
B_3: Interaction effect on abundance of X and Y	1	2	2	1	2	2
$\bar{\theta}$: Mean detection prob. at value 0 of detection covariates	0.3	0.3	0.3	0.3	0.3	0.3
A_1: Main effect of X on detection probability	1	2	2	1	2	2
A_2: Main effect of time (in quarters) on detection probability	1	2	2	1	2	2
A_3: Interaction effect on detection of X and time	1	2	3	1	2	3
A_4: Effect on abundance of substratum	All =1	All =1	Coarse = 5 Mixed = 5 Other =1	All =1	All =1	Coarse = 5 Mixed = 5 Other =1

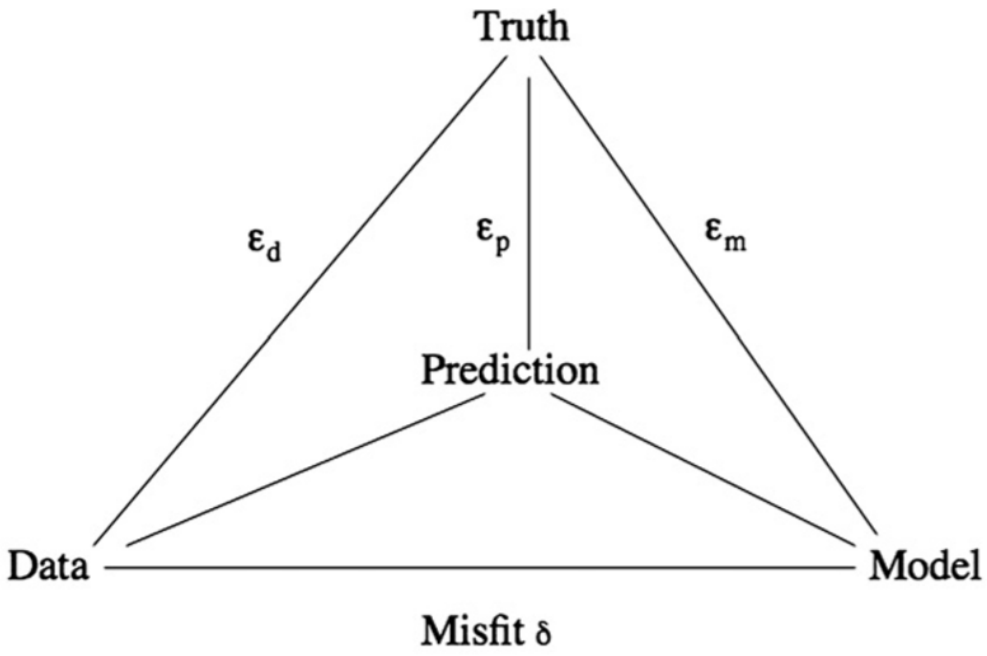

Figure 5.2. Conceptual diagram of truth, observed data and model results, showing the associated errors from each component and the truth. We make a distinction between error and misfit (from Lynch *et al.*, 2009).

In trying to understand marine ecosystems we observe and measure data, then make hypotheses and predictions on these observations (Figure 5.2). Real fisheries data are incomplete and imperfect samples, so much of the truth goes unobserved. Using simulations allows us to try to explain what is happening in a population in the hope that we might get a better understanding of the associated error between our data, models, predictions and the truth. In the simulations described below, the population simulated with the operating model represents "Truth"; the raw data are obtained by sampling from the true population with errors similar to the trawl survey; the modelled data are obtained by fitting the spatial model to the raw data.

Visualisation of species data

To identify metrics that could perform distribution indicator functions, we looked for patterns in the data by visualization of distribution maps. We plotted maps of the six simulated scenarios (See Section 5.3.2 for details). Summing across all points provided a relative abundance estimate for our six simulated scenarios across the surveyed area.

Indicator development and testing

To find patterns within the point estimate of relative abundance from our simulated data, maps were produced on a spatial grid of 5 km by 5 km for each scenario. During the development stage, we described elements of these maps and the best way to capture this information in a univariate metric, which we felt captured elements of interest to managers, policy-makers and stakeholders (Table 5.1). Taking a subset of these metrics, we tested for potential bias between the estimated distributional indicators and the real distributional trend in the data by looking at the standardized mean relative error between them.

Generalised Additive Mixed Models (GAMM) were used to account for non-linear spatial and temporal trends in simulated density using a modelling framework adapted from Moriarty *et al*. (Accepted ICES JMS). Simulated survey catches were modelled as count data. The simulated data are modelled as zero–inflated Poisson distributions; thus, we cast all models as zero-inflated Poisson GAMMs. The global model had the form:

$$\log(C_{i,s}) \sim te(X_i, Y_i, t_i, bs = \text{cs}) + te(d_i, bs = \text{cs}) + substrate + offset(\log(E_i))$$

where $C_{i,s}$ is the total number of fish of a given species (s) in a given length category caught in each sample (i). Spatial (X_i,Y_i) and temporal trends (t_i), are estimated with a multivariate tensor smoother (te), which accommodates data on different scales. The relationship of abundance with depth (d_i), was also estimated with a tensor smoother, the smooth term (bs) used was a cubic regression spline with shrinkage (cs). Substratum was a categorical variable in the model with eight levels from the EMODnet seabed substrata map (EMODnet Geology 2016). To account for simulated variations in fishing effort (E), the log swept-area was included as an offset in the model. The spatio-temporal smoothers describe the underlying estimated distribution of species across space and time, which is the ecological process of interest here. No model selection was carried out at this time, as this was a scoping exercise.

5.3.3 Metrics of distributional range and pattern within the range

Total area occupied

We interpret distributional range to mean the 'total area occupied' by a species at any single point in time; defined as the number of 5 km by 5 km pixels occupied by the species (i.e. with a density estimate >0 km^{-2}). This metric can be used to monitor interannual change in the extent of the distributional range of our species.

Geographic Range

Metrics of 'range geolocation' and 'core area geolocation' are necessary to differentiate between the various scenarios relating to inter annual variations or systematic shift. To look for a systematic shift in the geolocation of the entire range, the minimum and maximum latitude, longitude and depth were calculated (See Section 5.3.4 for results). This metric checked for change in the location of the entire range, rather than any change in distributional pattern within the range.

Occupied core area geolocation

To assess shifts in the distribution of the occupied core area of the range region, each core area's centre of mass in terms of latitude, longitude and depth were calculated. This metric checked for geographic change in the distributional pattern within the range (See Section 5.3.4 for results).

Core area fraction of the range

Managers and scientists alike are primarily concerned about identifying core areas of a species distribution or areas of essential fish habitat. Metrics that quantify the fraction of the population located within the core area are therefore needed. As an example, we may calculate the smallest area holding 50% of the fish population, i.e. the core area. The minimum proportion of the range with the highest densities of individuals (y-axis) that holds stipulated proportions of the population (x-axis) is plotted (See Section 5.3.4 for results).

Aggregation

The degree of aggregation in the distribution was calculated using the Lloyd's patchiness index estimated by the moment estimator as $L = 1 + \frac{variance(P)}{mean(P)^2} - \frac{1}{mean(P)}$ where P is of the population of interest. If the value is less than one this indicates a totally random distribution, as it increases the level of aggregation of fish in the population gets higher (See Section 5.3.4 for results).

5.3.4 Simulation studies: Preliminary results

This section summarizes the results of the simulation studies. The full set of diagnostic figures is provided in Annex 3. In the graphs that follow, time is measured in quarter years.

Simulation 1: weak space-time-trend distribution, for a relatively common species

Expected output: In this simulation, we have imagined a common species that was moving in a north–east direction, with no change in abundance over time. We expect that it will be difficult to make inference about the species' core areas as this species doesn't have a habitat preference but should be able to define the range and the total occupied space with relatively high accuracy.

Realised output: To help visualise the data, a sample time frame (year 10) of the simulated data (i.e. the truth), the sample and the modelled output is provided in Figure 5.3. The model performed moderately well, explaining 47.4% of the deviance in the raw data. For the occupied area, precision was poor with mean relative error of -87.6% between the "truth" and sampled data and of 119.3% between "truth" data and modelled data (Figure 5.4). The prediction of the trend in area occupied was fairly accurate for the core areas (Figure 5.5), and the resultant maps provided the same general spatial trend as the simulated dataset (Annex 3). The Lloyd's index for the simulated dataset was 3.39, for the raw survey data it was 3.38 and for the modelled survey data it was 2.21. The mean relative error for the total area occupied by 50% of the population (i.e. the "core area") between the "truth" and the modelled data was -25.5%. The mean relative error increased as we increased the proportion of the population for 75% (i.e. "prime), with the mean relative error of 85.1%. Including the sub-prime (i.e. 95% of the population) raised the mean relative error to 98.5% (Figure 5.5).

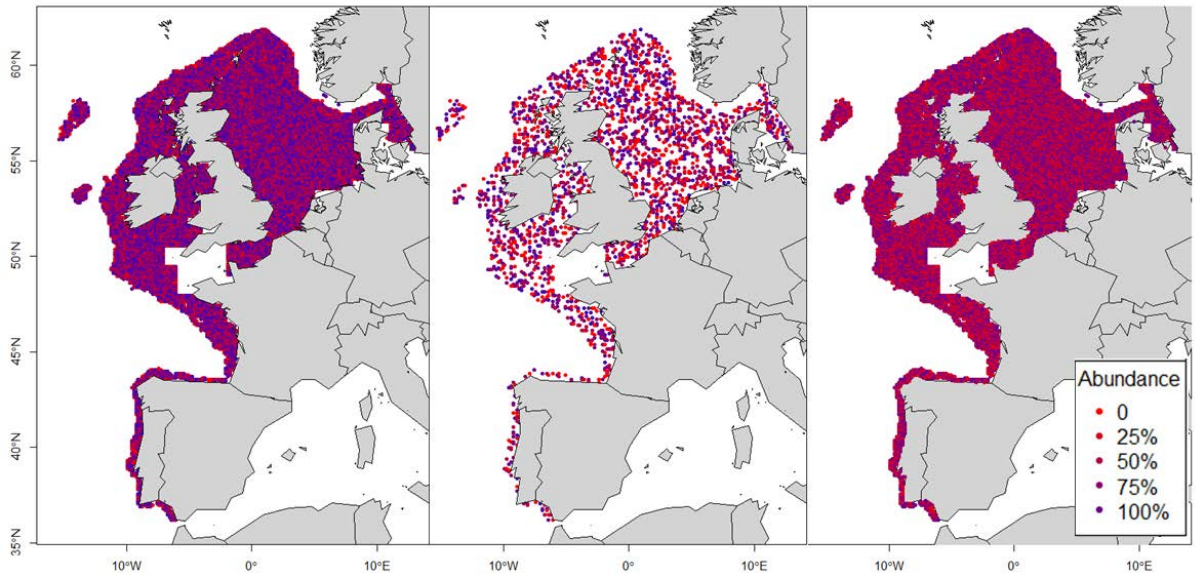

Figure 5.3. The simulated data (truth) for the final year of within the sampling time frame (left). The 2100 samples randomly chosen for the final year of within the sampling time frame (middle) and the modelled output generated from the 2100 samples (right).

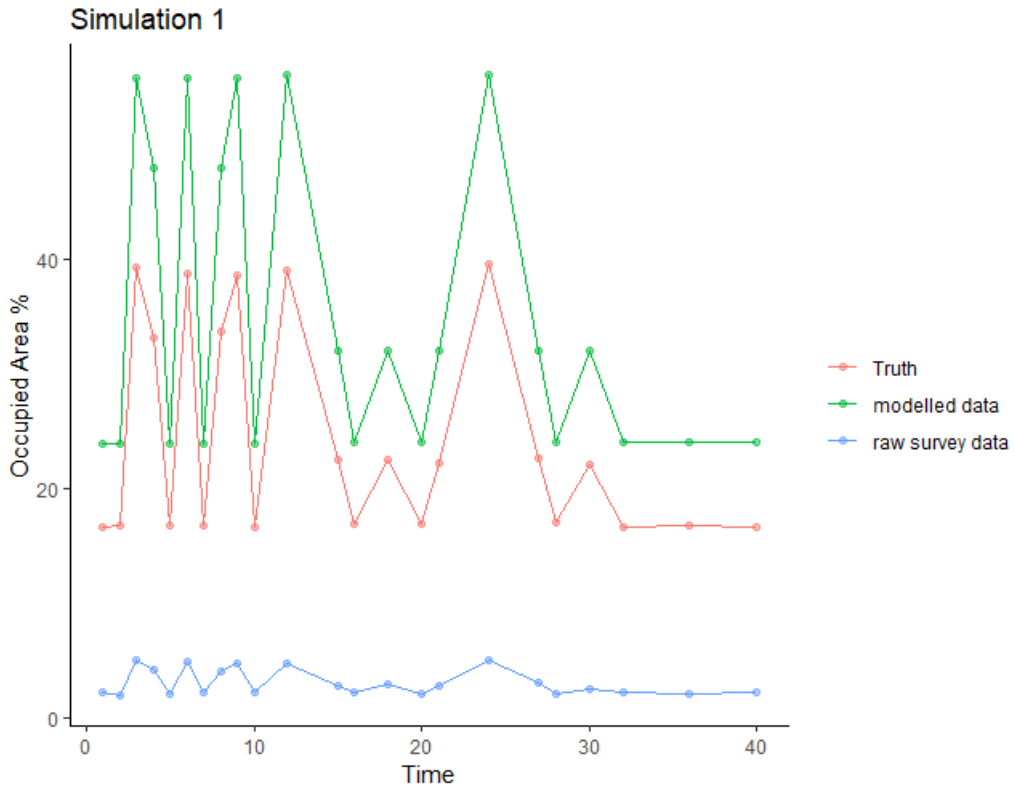

Figure 5.4. Total percentage of occupied area in our study domain in each dataset with mean relative error of -87.6% between simulated data (the truth) and raw survey data and of 119.3% between simulated data (the truth) and modelled survey data.

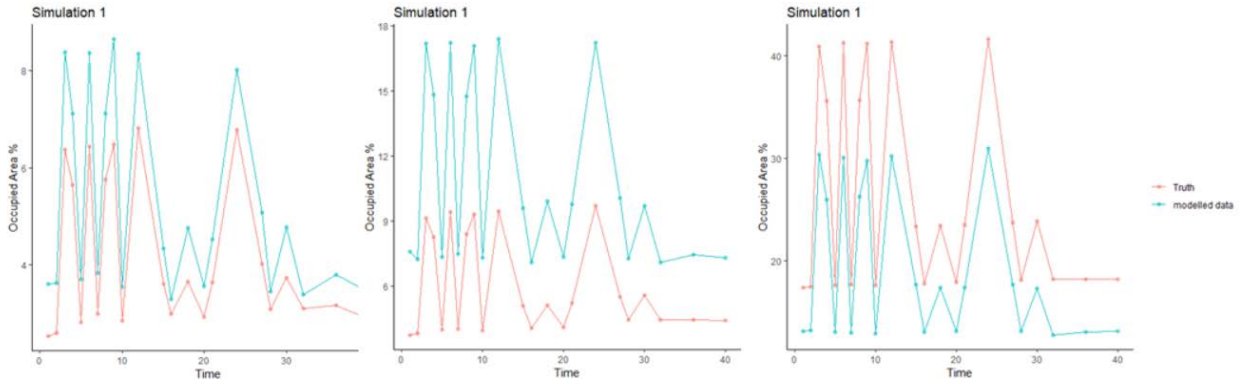

Figure 5.5. Amount of total area occupied by 50% (i.e. the "core area") (left), 75% (i.e. "prime" (middle) and 95% (i.e. sub-prime) of the population in the simulated data (the truth) and the modelled survey data with mean relative error of -25.5%, 85.1%, and 98.5%, respectively.

Simulation 2: strong space-time-trend, for a relatively common species

Expected output: In this simulation, we have imagined a common species that has no particular preference for any substratum and that shows a strong space-time-trend. Here the fish are moving in a south–east direction with no change in abundance over time. We expect to be able to make inferences about the species core areas, the range and the occupied space with relatively high accuracy.

Realised output: To help visualise the data, a sample time frame (year 10) of the simulated data (i.e. the truth), the sample and the modelled output is provided in Figure 5.6. The model explained 80.5% of the deviance in the raw data. It performed moderately well in capturing the

range parameters, and it could capture the general pattern of the core areas, but again, the precision was poor in predicting the total occupied area (Figures 5.7 and 5.8). The resultant maps provided the same general spatial trend as the simulated dataset (Annex 3). The Lloyd's index for the simulated dataset was 27.29, for the raw survey data, it was 26.99 and for the modelled survey data it was 18.14.

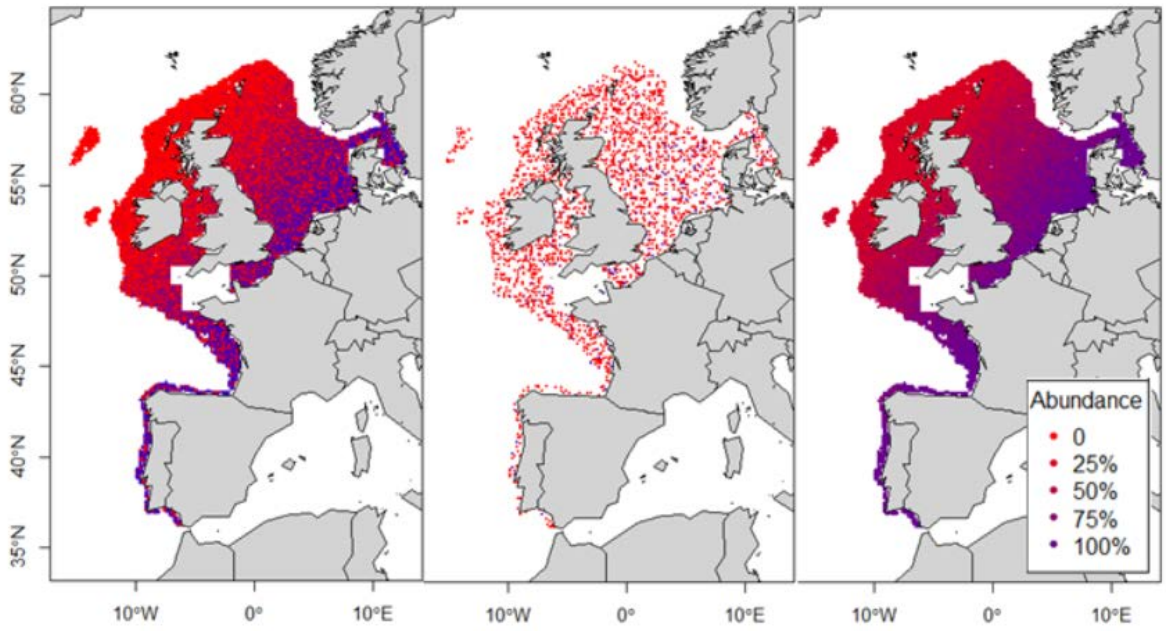

Figure 5.6. The simulated data (truth) for the final year of within the sampling time frame (left). The 2100 samples randomly chosen for the final year of within the sampling time frame (middle) and the modelled output generated from the 2100 samples (right).

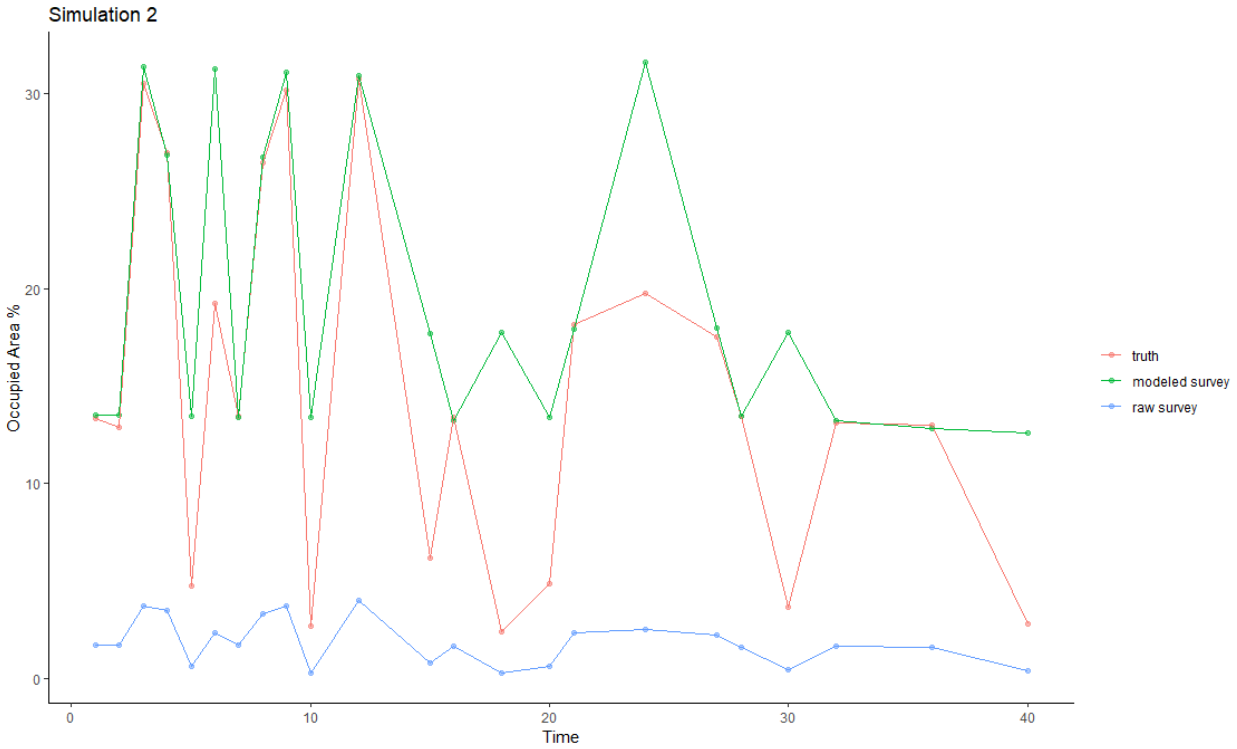

Figure 5.7. Total percentage of occupied area in our study domain in each dataset with mean relative error of -87.8% between simulated data and raw survey data and of 179.5% between simulated data and modelled survey data.

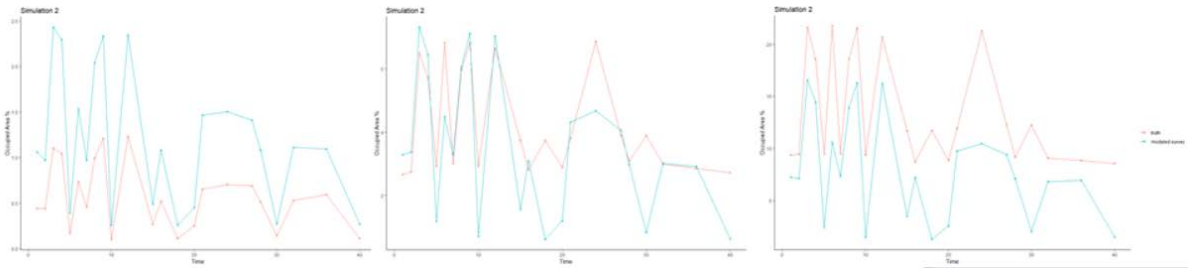

Figure 5.8. Amount of total area occupied by 50% (i.e. the "core area") (left), 75% (i.e. "prime" (middle) and 95% (i.e. sub-prime) of the population in the simulated data and the modelled survey data with mean relative error of -53.1%, 211%, and 325%, respectively.

Simulation 3: strong space-time-trend, with a preference for mixed sediments, for a relatively common species

Expected output: In this simulation, we have imagined a common species that has a habitat preference for coarse and mixed sediments, the fish are moving in a south–east direction with no change in abundance over time. We expect to be able to make inferences about the species core areas, the range and the occupied space with relatively high accuracy.

Realised output: To help visualise the data a sample time frame (year 10) of the simulated data (i.e. the truth), the sample and the modelled output is provided in Figure 5.9. The model performed well, explaining 84.9% of the deviance in the raw data, and the resultant maps (Annex 3) provided the same general spatial trend as the simulated dataset, though precision in capturing absolute extent of occupied areas was poor (Figures 5.10 and 5.11). The Lloyd's index for the simulated dataset was 18.8, for the raw survey data it was 24.6 and for the modelled survey data it was 21.8.

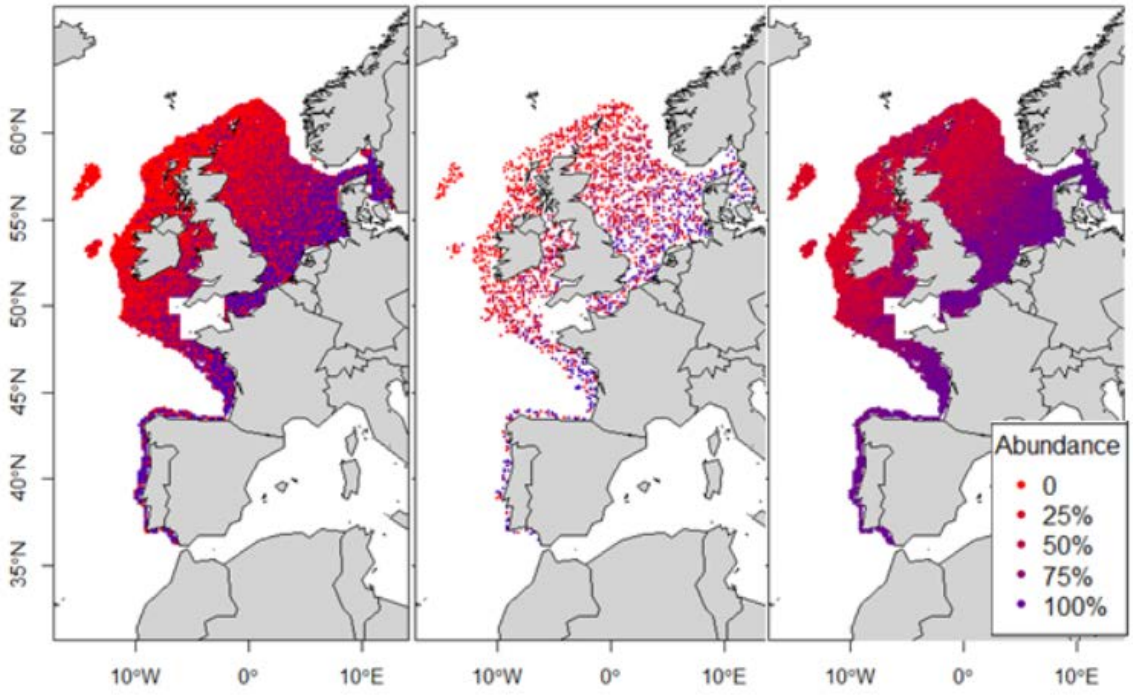

Figure 5.9. The simulated data (truth) for the final year of within the sampling time frame (left). The 2100 samples randomly chosen for the final year of within the sampling time frame (middle) and the modelled output generated from the 2100 samples (right).

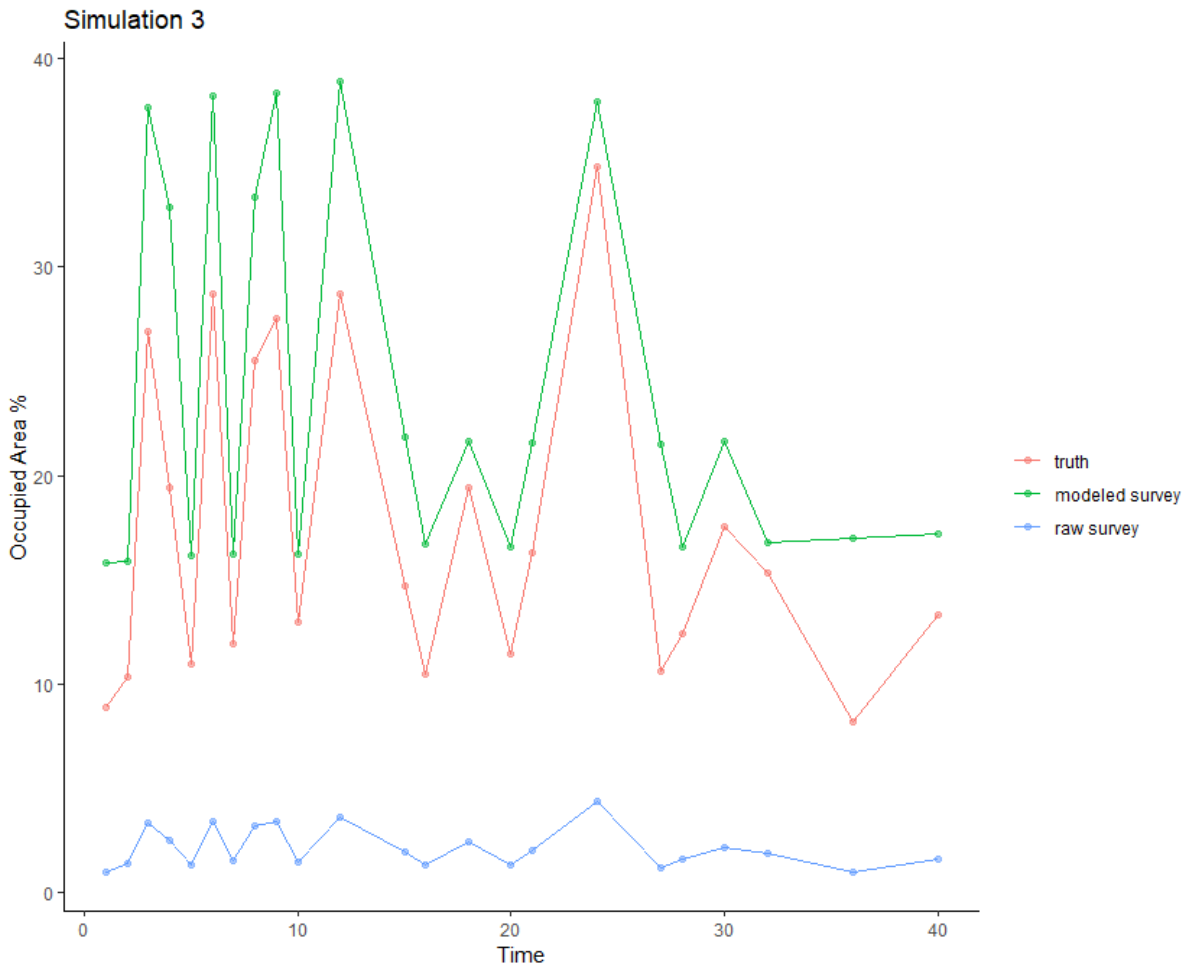

Figure 5.10. Total percentage of occupied area in our study domain in each dataset with mean relative error of -87.6% between simulated data and raw survey data and of 45.6% between simulated data and modelled survey data.

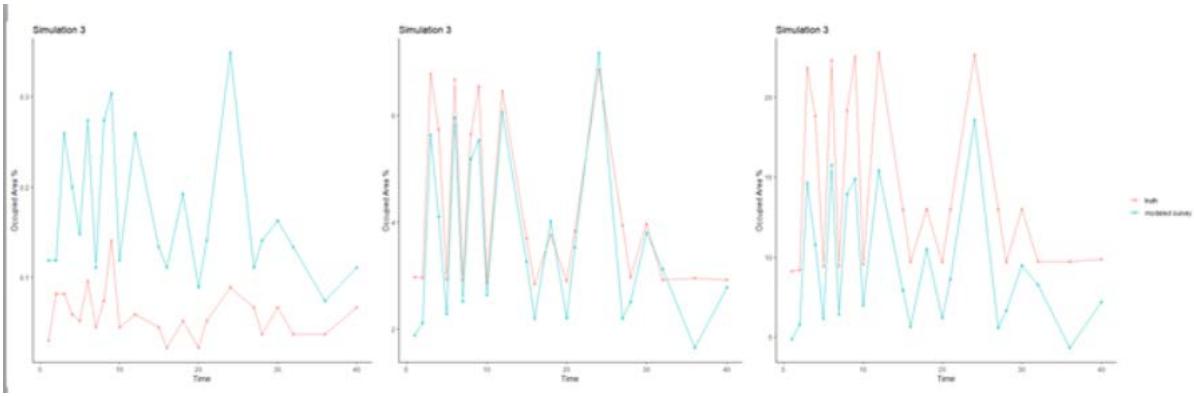

Figure 5.11. Amount of total area occupied by 50% (i.e. the "core area",left), 75% (i.e. "prime" (middle) and 95% (i.e. sub-prime, right) of the population in the simulated data and the modelled survey data. The mean relative error was -45.3%, 23.1%, and 50.3%, respectively.

Simulation 4: fully random latent distribution, for a rare species

Expected output: In this simulation we have imagined a rare species that has a weak space-time-trend in distributed in space and time. Fish are moving in a north–east direction, with no change in abundance over time. We expect that it will be difficult to make inferences about the species core areas. It may also be difficult to define the range and the occupied space.

Realised output: To help visualise the data a sample time frame (year 10) of the simulated data (i.e. the truth), the sample and the modelled output is provided in Figure 5.12. The model explained 30.1% of the deviance in the raw data, and the resultant maps provided the same general spatial trend as the simulated dataset (Annex 3). The model could predict the abundance well, but prediction of range with regard to geolocation was relatively poor (Annex 3). With respect to occupied area, the survey and the modelled data preformed similarly, neither was successful at accurately capturing the total occupied area (Figure 5.13). Furthermore, core areas could not be calculated likely due to the scarcity of the simulated species. The Lloyd's index for the simulated dataset was 3.30, for the raw survey data it was 3.34 and for the modelled survey data, it was -3.36.

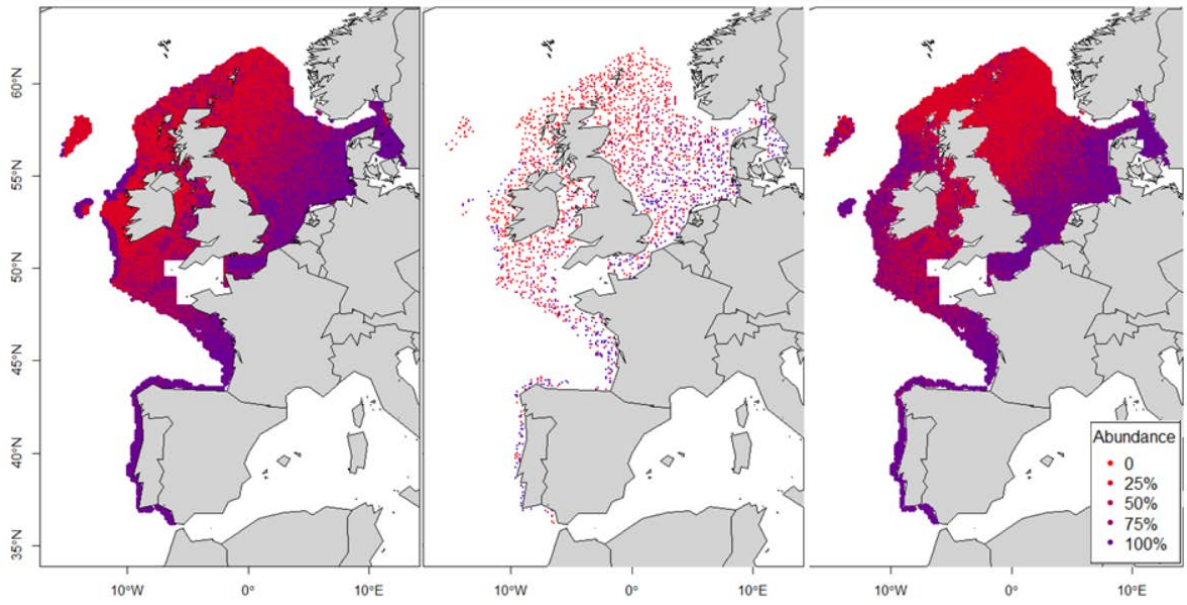

Figure 5.12. The simulated data (truth) for the final year of within the sampling time frame (left). The 2100 samples randomly chosen for the final year of within the sampling time frame (middle) and the modelled output generated from the 2100 samples (right).

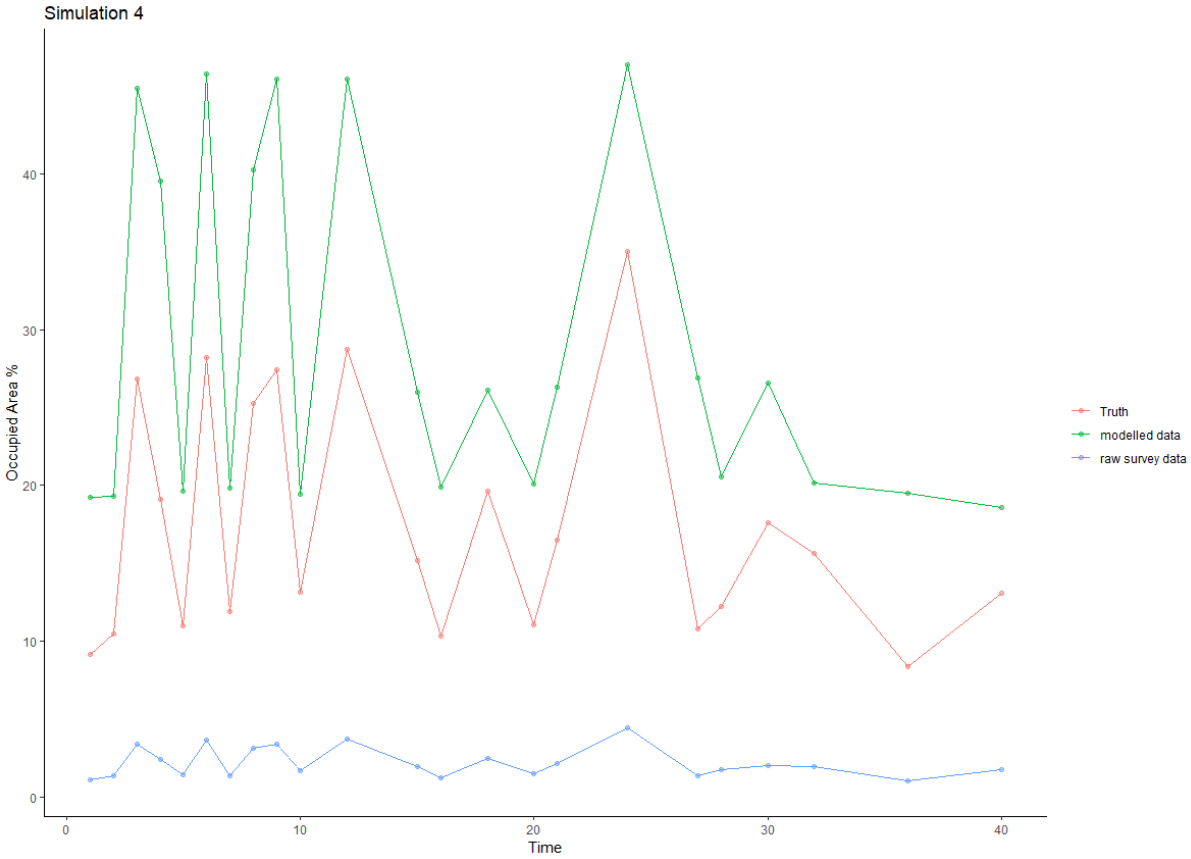

Figure 5.13. Total precentage of occupied area in our study domain in each dataset with mean relative error of -87.9% between simulated data and raw survey data and of -95.1% between simulated data and modelled survey data.

Simulation 5: strong space-time-trend, for a rare species

Expected output: In this simulation, we have imagined a rare species with a strong space-time-trend that has a no particular preference for any substratum. Fish are moving in a south–easterly direction with no change in abundance over time. We expect that we will not be able to make inferences about the species core areas with a high level of confidence, but we expect that we should pick up the range and the occupied space with a moderate level of accuracy.

Realised output: To help visualise the data a sample time frame (year 10) of the simulated data (i.e. the truth), the sample and the modelled output is provided in Figure 5.14. The model explained 72.1% of the deviance in the raw data. However, while it could predict the abundance relatively well, it was poor in predicting the range of the total occupied area (Figure 5.15). It was not possible to calculate core areas, most likely due to the scarcity of the simulated species. The Lloyd's index for the simulated dataset was 26.8, for the raw survey data it was 29.5 and for the modelled survey data, it was -2.3.

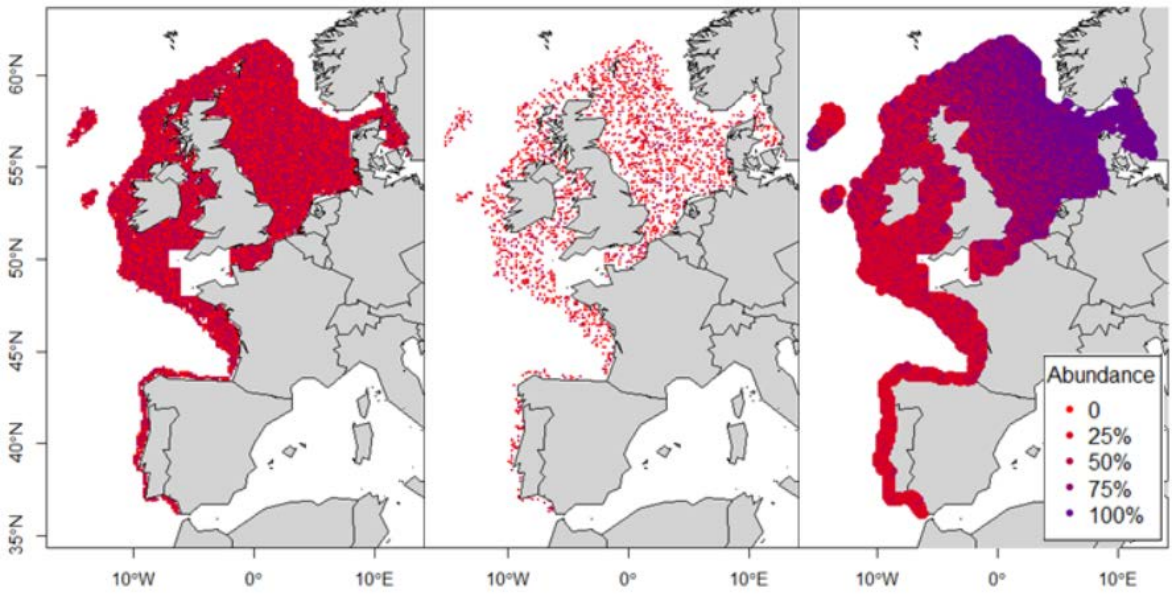

Figure 5.14. The simulated data (truth) for the final year of within the sampling time frame (left). The 2100 samples randomly chosen for the final year of within the sampling time frame (middle) and the modelled output generated from the 2100 samples (right).

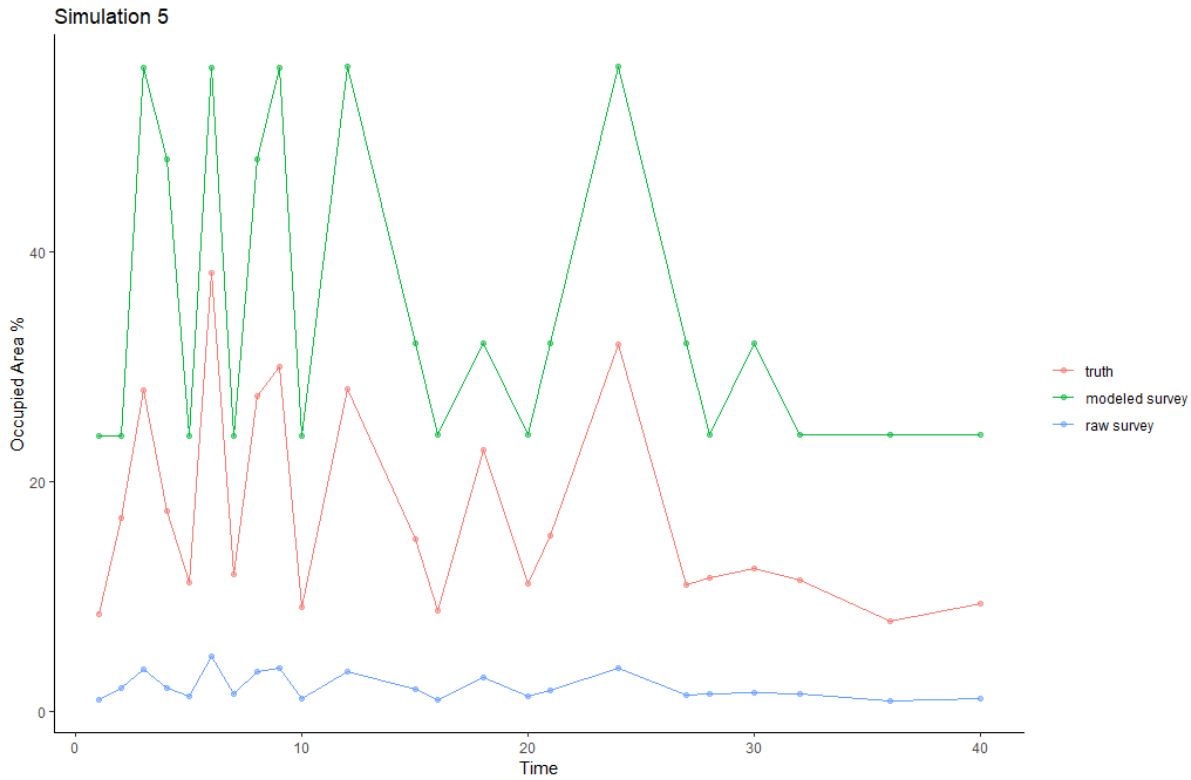

Figure 5.15. Total percentage of occupied area in our study domain in each dataset with mean relative error of -87.2% between simulated data and raw survey data and of -78.1% between simulated data and modelled survey data.

Simulation 6: strong space-time-trend, with a preference for sandy substrata, for a rare species

Expected output: In this simulation we have generated data for a rare species that has a habitat preference for a given sediments. Fish are moving in a north–westerly direction with a strong habitat preference for course and mixed habitat types, no change in abundance over time. We

expect to be able to make inference about the species core areas, the range and the occupied space with moderate accuracy.

Realised output: To help visualise the data a sample time frame (year 10) of the simulated data (i.e. the truth), the sample and the modelled output is provided in Figure 5.16. The model explained 56.8% of the deviance in the raw data. The resultant figures provided similar trends for abundance and geolocation. The model captured the general pattern of the total occupied area (Figure 5.17) and the core are with 50% of the population (Figure 5.18), though the precision was poor. It was not possible to calculate core areas for 75% and 95% of the population, respectively, likely due to the scarcity of the simulated species. The Lloyd's index for the simulated dataset was 31.7, for the raw survey data, it was 33.5 and for the modelled survey data, it was 22.3.

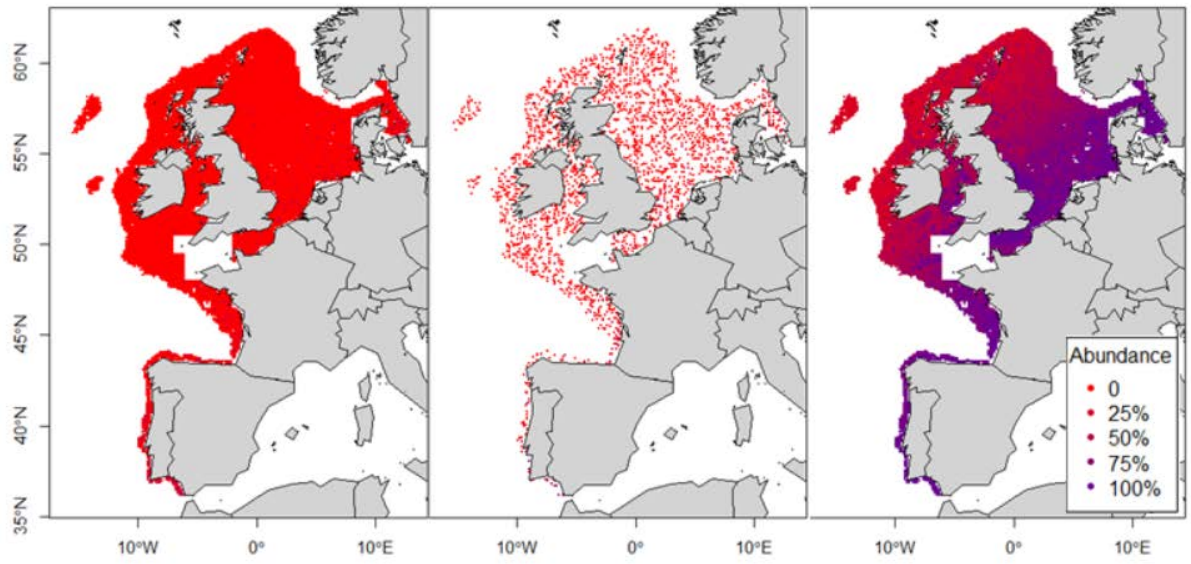

Figure 5.16. The simulated data (truth) for the final year of within the sampling time frame (left). The 2100 samples randomly chosen for the final year of within the sampling time frame (middle) and the modelled output generated from the 2100 samples (right).

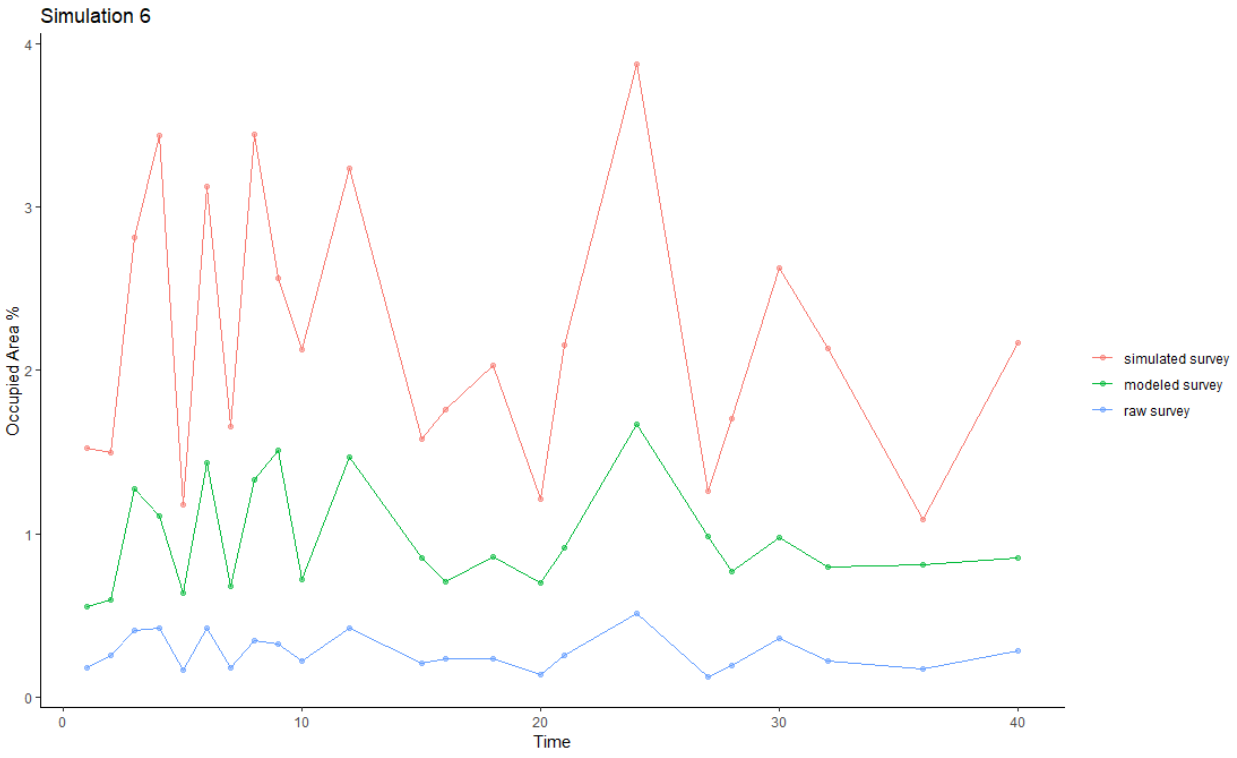

Figure 5.17. Total precentage of occupied area in our study domain in each dataset with mean relative error of -87.9% between simulated data and raw survey data and of -54.5% between simulated data and modelled survey data.

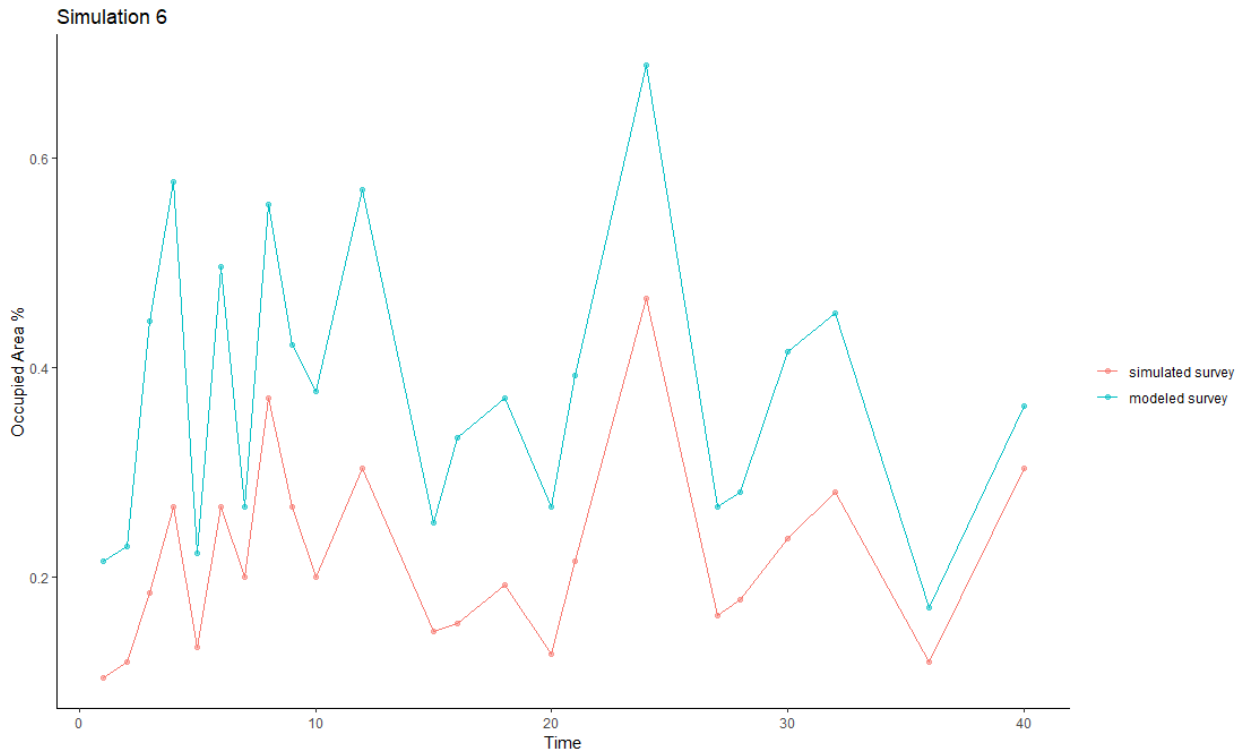

Figure 5.18. Amount of total area occupied by 50% (i.e. the "core area") of the population in the simulated data and the modelled survey data with mean relative error of -38.8%. Amount of area occupied by 75% and 95% of the population could not be calculated.

Summary of results from simulation studies

In this preliminary simulation, we have begun to test some of the potential indicators for distributional range and pattern within the range. We are firstly interested to test if the maps produced from the sample data and modelled surface accurately predict the simulated maps. We then tested whether the metrics produced from the raw survey data and modelled data accurately reflect the metrics produced by the simulated data. We have summarised the mean relative error between the simulated data and the modelled data to describe the potential bias in the sampled results (Table 5.2). When modelling a common species, we are better able to produce metrics that reflect the pattern seen in the simulated data than we can for rare species. For the common species, the model generally smooths the values in the survey data, which means that we predict a higher survey abundance than the realised abundance in the simulated data. The scaled abundance trend generally match with high accuracy, the raw data tend to underestimate slightly, whereas the modelled data tend to overestimate slightly. Both the modelled and raw data generally produce the expected change in the centre of mass with high accuracy. Furthermore, they tend to do better in the Y-axis than the X-axis, which is not surprising given the error associated with having to "empty" sampling spaces for the land masses of Ireland and the UK in the middle of the area. The percent of occupied area is generally accurate in its trend when there is a strongly aggregated population whereas classifying occupied area is more complicated when the population is more dispersed.

Table 5.2 Summary of the accuracy of our raw survey data and our predicted modelled data in indicating the trend in our simulated data for three potential distributions for a common species ($\bar{\lambda}$= 20) and a rare species ($\bar{\lambda}$= 0.2): 1 and 4. weak change in spatial pattern over time; 2 and 5. A strong change in spatial pattern over time; 3 and 6. A generated spatial pattern, with a strong habitat preference changing over time. The % mean relative error (MRE) proves a simple metric to assess the performance of the distributional metrics.

Simulation	Datasets compared	% MRE: Scaled Abundance	% MRE: Centre of Mass (X)	% MRE: Centre of Mass (Y)	% MRE: % Occupied Area
1 Random distribution, common population	Raw	13	0.017	0.008	-87.6
	Modelled	10	0.025	0.006	119.3
2. Strong space time-trend, common population	Raw	-18	-4.31	0.084	-87.8
	Modelled	5	-4.54	0.96	179.5
3. Strong space time-trend and habitat preference, common population	Raw	3.8	-2.7	2.1	-87.6
	Modelled	10.6	-0.55	2.1	45.6
4. Random distribution, rare population	Raw	9.7	0.03	0.008	-87.9
	Modelled	20.1	-0.07	-0.004	-95.1
5 Strong space time-trend, rare population	Raw	-5.1	1.86	2.84	-87.2
	Modelled	5.7	0.831	-8.72	-78.1
6. Strong space time-trend and habitat preference, rare population	Raw	-3.5	-0.45	-1.77	-87.9
	Modelled	0.29	-1.17	-1.82	-54.5

For the rare species the model generally smooths the abundance in the survey data, which means that we predict a higher survey abundance than the realised abundance in the simulated data, except for when the species is randomly distributed. The scaled abundance trend generally matches with relatively high accuracy, but lower precision than in the simulated data for more common species. Similar to the common species, the modelled and raw data generally produce the expected change in the centre of mass with high accuracy. The percent of occupied area is generally accurate in its trend but has low precision in its estimated occupied area.

The degree of spatial patchiness, as measured with Lloyd's index, was fairly accurate for the raw survey data, but was consistently underestimated by the modelled survey due to the smoothing provided by the GAMM. This preliminary analysis provides the context for analysing distributional metrics at the scale of large marine ecosystems. There are many elements of the distributional pattern that we have not included. This simulation requires further exploration to answer questions about the utility and application of metrics derived from survey-based, modelled abundance surfaces; for example, what is the rarest species abundance for which we can infer the distribution?

5.4 Case Study: Changes in the distribution of plaice in the North Sea, Kattegat and Skagerrak

This case study uses data collected by the First Quarter (Q1) International Bottom Trawl Survey (IBTS) carried out in January and February each year by up to ten different participating nations and coordinated by ICES. The survey data, stored on the ICES DATRAS database, have been downloaded to produce a quality assured and quality audited GNSIntOT1 data product (Moriarty *et al*., 2019). The analyses presented here, are based on this data product.

The objectives of this study are:

1. To describe the distribution of three age-class groupings of plaice in the North Sea, Kattegat and Skagerrak in each of the 35 years, 1983 to 2017; this constitutes the full time-series of data held in the GNSIntOT1 data product.

- Plaice are primarily benthivorous throughout their lifetime, but some ontogenetic change in their diet occurs at ages 4 and 7 (Basimi and Grove, 1985), giving three diet groups: age 1 to 3, corresponding approximately to fish of ≤30 cm in length; age 4 to 6, corresponding approximately fish of length >30 cm to ≤ 37 cm; and age 7 to 10 corresponding to fish of length >37 cm. Fish with different diets may have different distributions and fish of different age, size, maturity status, and growth rates may respond in different ways to changes in water temperature. The survey data were partitioned by length, to approximate these age groupings and each age-class grouping within the population was examined separately.

2. To derive some simple indicators that capture different attributes of the distributions of the three plaice age-class groups, and which can be used to demonstrate change in these distributions over time.

- Currently there is some concern that climate change, which is generally driving an increase in water temperature in the region, is causing species' distributions to change. The possibility that plaice are responding to rising water temperatures by shifting their distributions is explored.

5.4.1.1 Methods and distributions

A 60-km radius knife-edge equal weighting interpolation procedure was applied to the data product trawl density-at-length data to derive estimates of the biomass density-at-length (kg km^2) in each quarter ICES statistical rectangle (0.5°latitude by 1.0°longitude), henceforth referred to as quadrants (0.25°latitude by 0.5°longitude). These quadrant density estimates were multiplied by the sea area of each quadrant in question to derive estimates of the biomass of each age-class group present in each quadrant in each year. For each year, and for each age-class group, summing across all quadrants provided an estimate of the total annual surveyed biomass; the proportion of this total population resident in each quadrant could therefore be determined. Quadrants were then ranked according to the proportion of the population of each age-class group they contained. The top ranked quadrants holding 50% (core quadrants), 75% (prime quadrants), and 95% (sub-prime quadrants) of the surveyed population of each age-class group in each year could then be determined. The remaining marginal quadrants hold the last 5% of each age-class group. For each year, quadrants identified as core, prime, sub-prime, and marginal, were mapped for the 1 to 3 age-class group (Figure 5.14), the 4 to 6 age-class group (Figure 5.15), and the 7 to 10 age-class group (Figure 5.16).

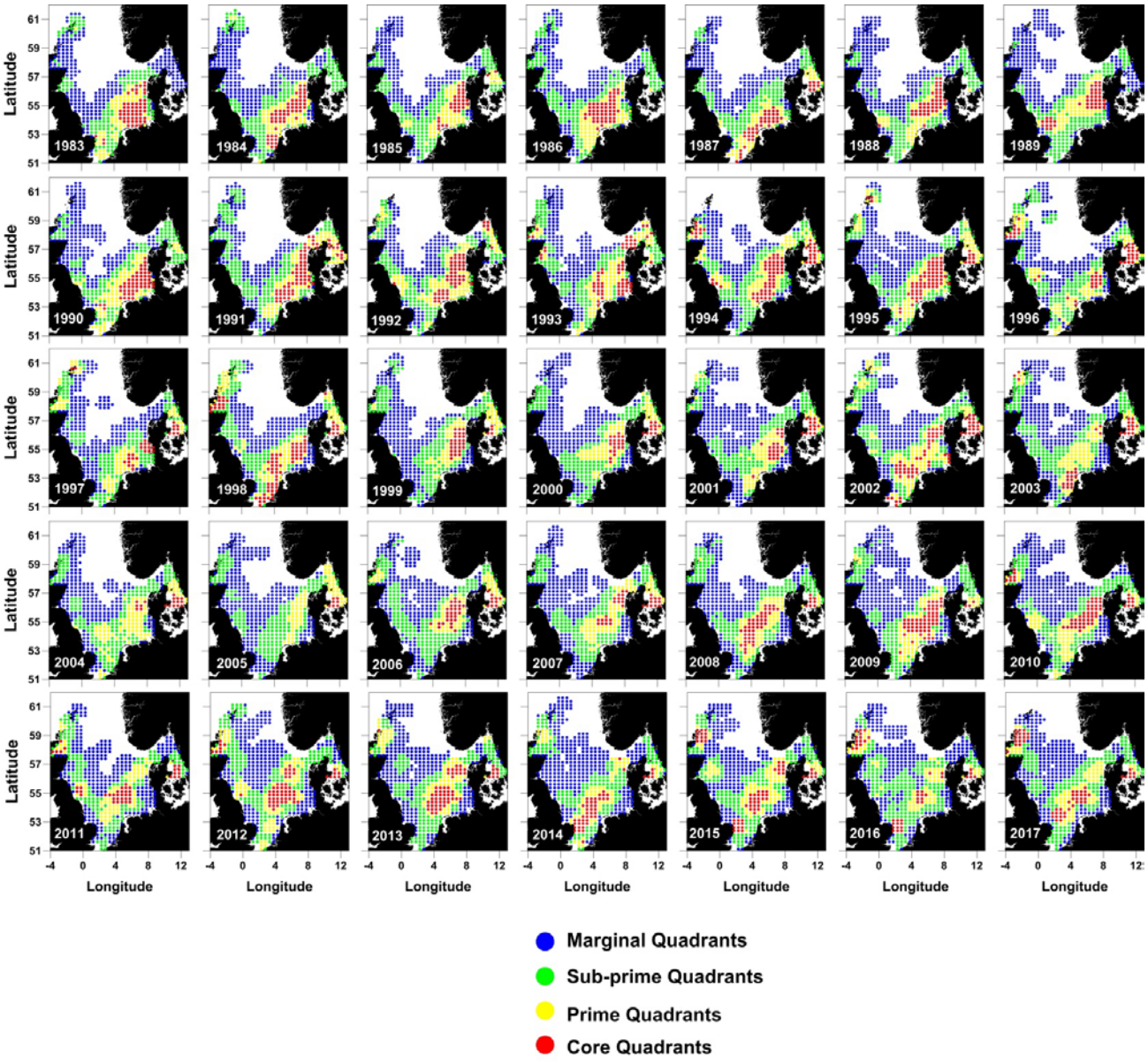

Figure 5.14. Distributions of plaice aged 1 to 3 in each year. Core quadrants were the highest ranked quadrants accounting for 50% of the population. Prime quadrants were the highest ranked of the remaining quadrants accounting for the next 50% to 75% of the population. Sub-prime quadrants were the highest ranked of the remaining quadrants accounting for the next 75% to 95% of the population. Marginal quadrants were the lowest ranked quadrants accounting for the final 5% of the population.

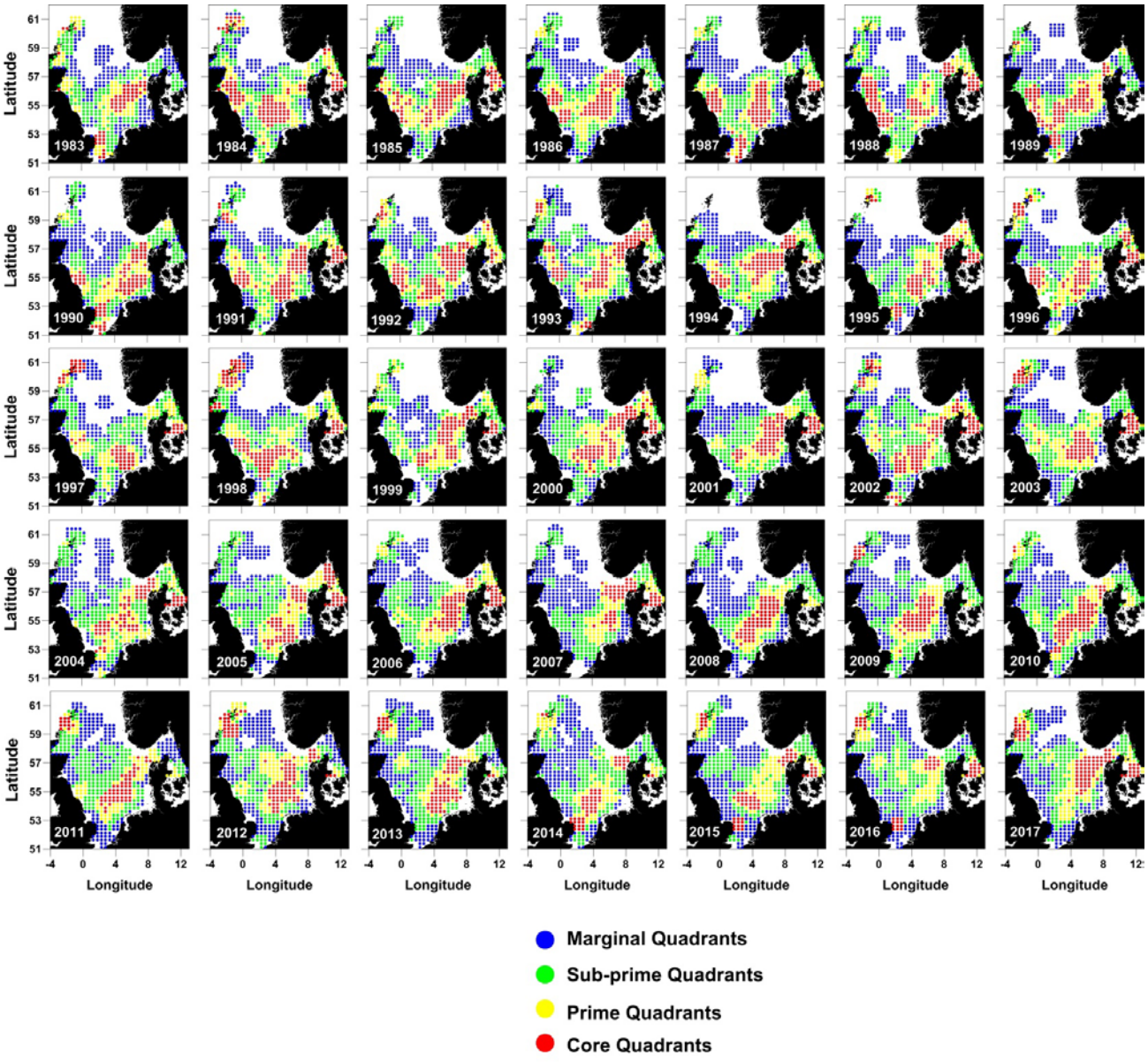

Figure 5.15. Distributions of plaice aged 4 to 6 in each year. Core quadrants were the highest ranked quadrants accounting for 50% of the population. Prime quadrants were the highest ranked of the remaining quadrants accounting for the next 50% to 75% of the population. Sub-prime quadrants were the highest ranked of the remaining quadrants accounting for the next 75% to 95% of the population. Marginal quadrants were the lowest ranked quadrants accounting for the final 5% of the population.

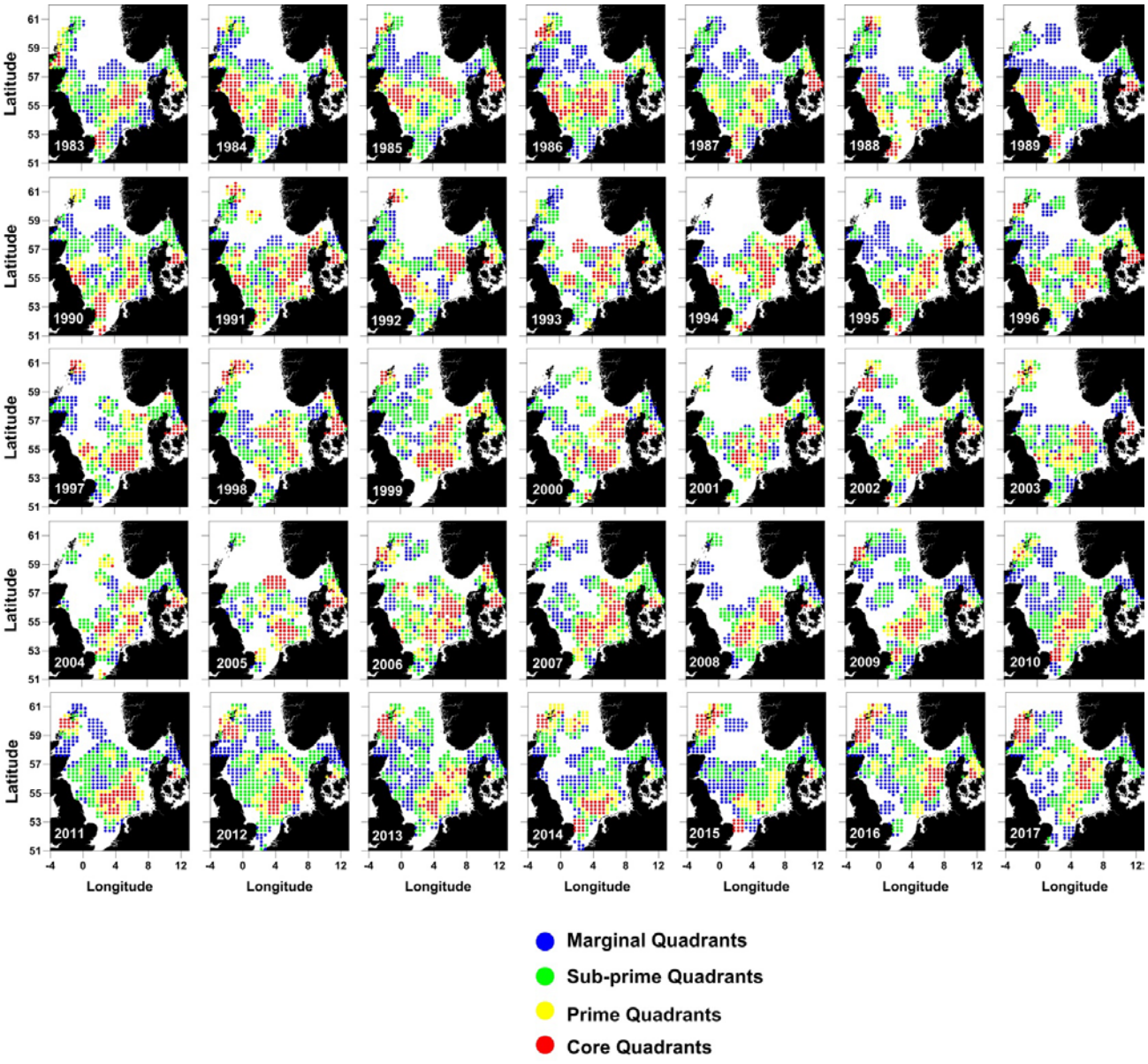

Figure 5.16. Distributions of plaice aged 7 to 10 in each year. Core quadrants were the highest ranked quadrants accounting for 50% of the population. Prime quadrants were the highest ranked of the remaining quadrants accounting for the next 50% to 75% of the population. Sub-prime quadrants were the highest ranked of the remaining quadrants accounting for the next 75% to 95% of the population. Marginal quadrants were the lowest ranked quadrants accounting for the final 5% of the population.

5.4.1.2 Range extent indicators

The first distribution indicator examined was the total area occupied by the whole population of each age-class group. The total area of core, prime and sub-prime area holding, respectively, 50%, 75% and 95% of the population of each age-class group in each year is also worthy of consideration. Such "range extent" indicators are generally closely related to variation in population abundance; increase in the number of individuals in the population is normally associated with an increase in population "range extent". This follows theoretical expectations derived from, for example, the ideal free distribution (Fretwell and Lucas, 1970). Here the effect of variation in population biomass on variation in the "range extent" of the whole population of each age class of plaice and the "range extent" of core area, prime area and subprime area, holding 50%, 75% and 95% of the population of each age-class group in each year respectively, is shown (Figure

5.17). The population biomass data used as the explanatory variable are the stock biomass at age data provided in the recent assessment working group report (ICES, 2018). As the biomass of plaice aged 4 to 6 and aged 7 to 10 increased, the "range extent" of the whole population expanded as expected. However, no significant relationships between population biomass and "range extent" of core, prime, or subprime area were detected for any of the three age-class groups.

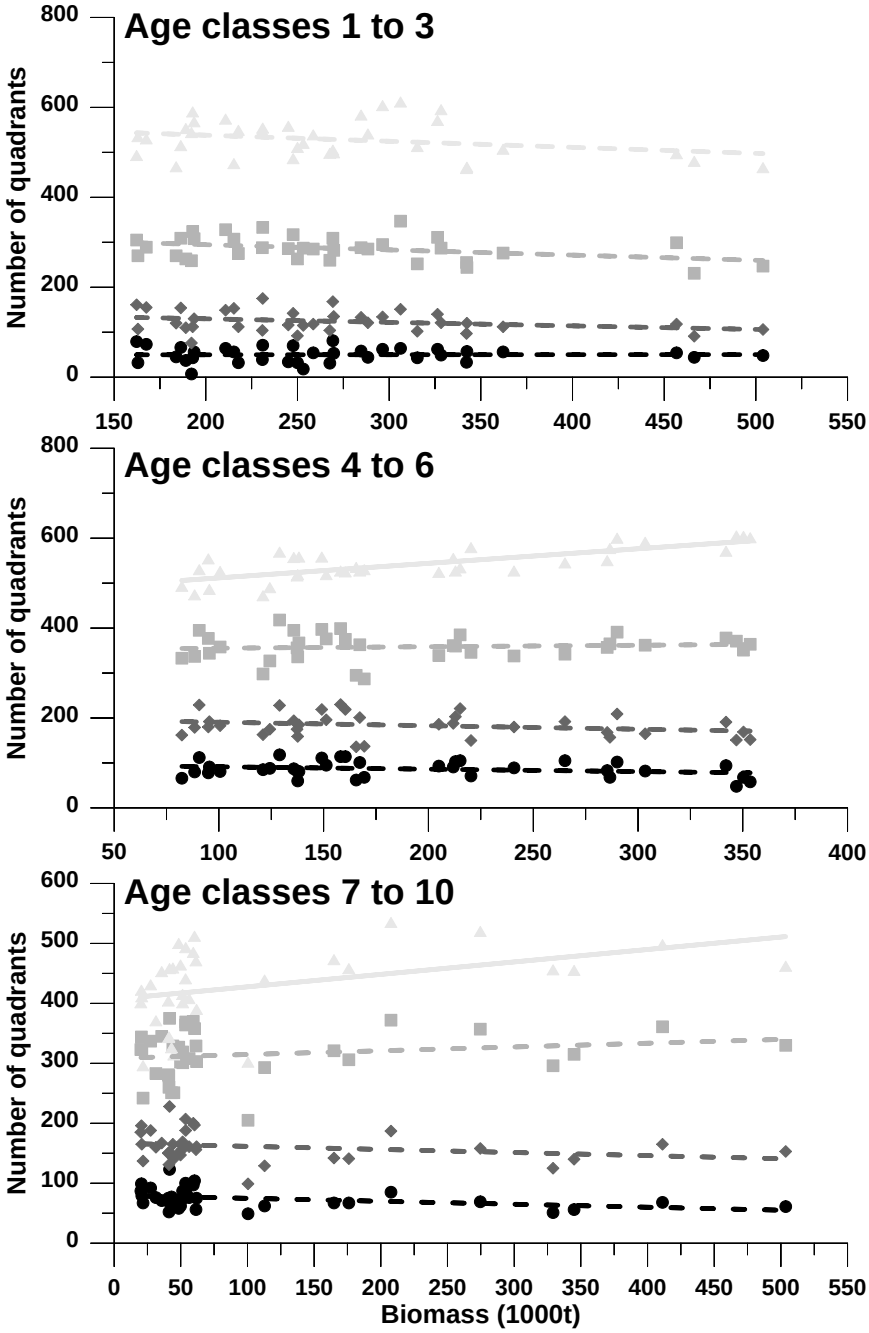

Figure 5.17. Relationships between population biomass of 1y to 3y, 4y to 6y, and 7y to 10y aged plaice and the "range extent" of core area (black circles and lines), prime area (dark grey squares and lines), sub-prime area (medium grey diamonds and lines), and marginal area (light grey triangles and lines). Dashed lines indicate non-significant correlations and full lines indicate non-significant correlations.

5.4.1.3 Average location indicators

Clear latitudinal and longitudinal shifts are apparent in the distribution of each age group of plaice in the North Sea. Marked shifts north and east in recent years are particularly evident among the 7 y to 10 y age-class group (Figure 5.18). A strong easterly shift in distribution has also occurred in 1y to 3 y aged plaice (Figure 5.19). Dulvy *et al*. (2008) suggest that fish are shifting their distributions towards deeper, cooler waters in order to mitigate the detrimental effects of warming sea temperatures caused by climate change. The recent northerly and easterly shifts in North Sea plaice distribution certainly seem to conform to this hypothesis; the biomass-weighted mean depth of 1 y to 3 y and 7 y to 9 y plaice has increased in recent years (Figure 5.20).

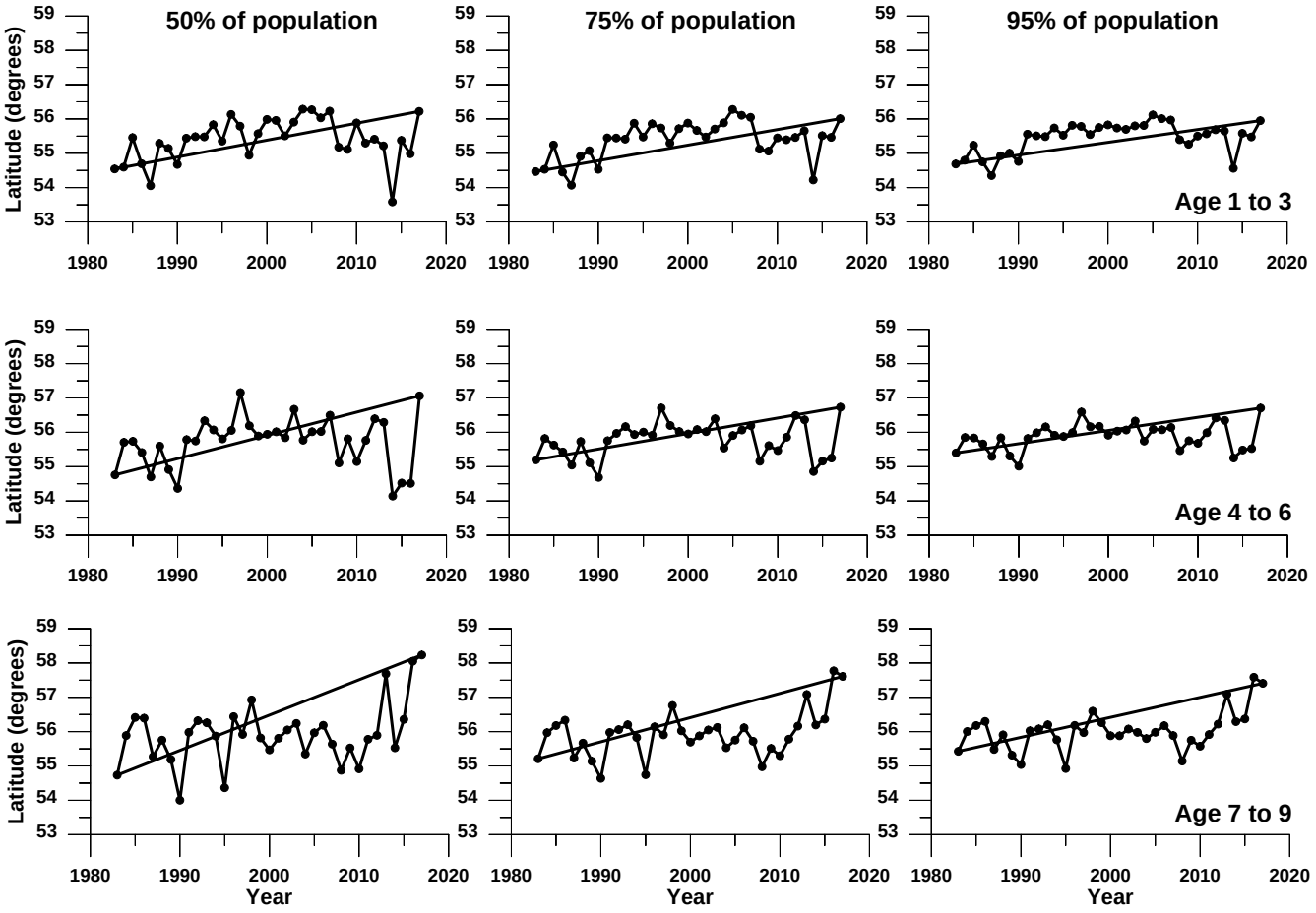

Figure 5.18. Temporal trends in the biomass-weighted mean latitude of 50%, 75% and 95% of the population of 1 y to 3 y aged, 4 y to 6 y aged and 7 y to 9 y aged plaice in the North Sea.

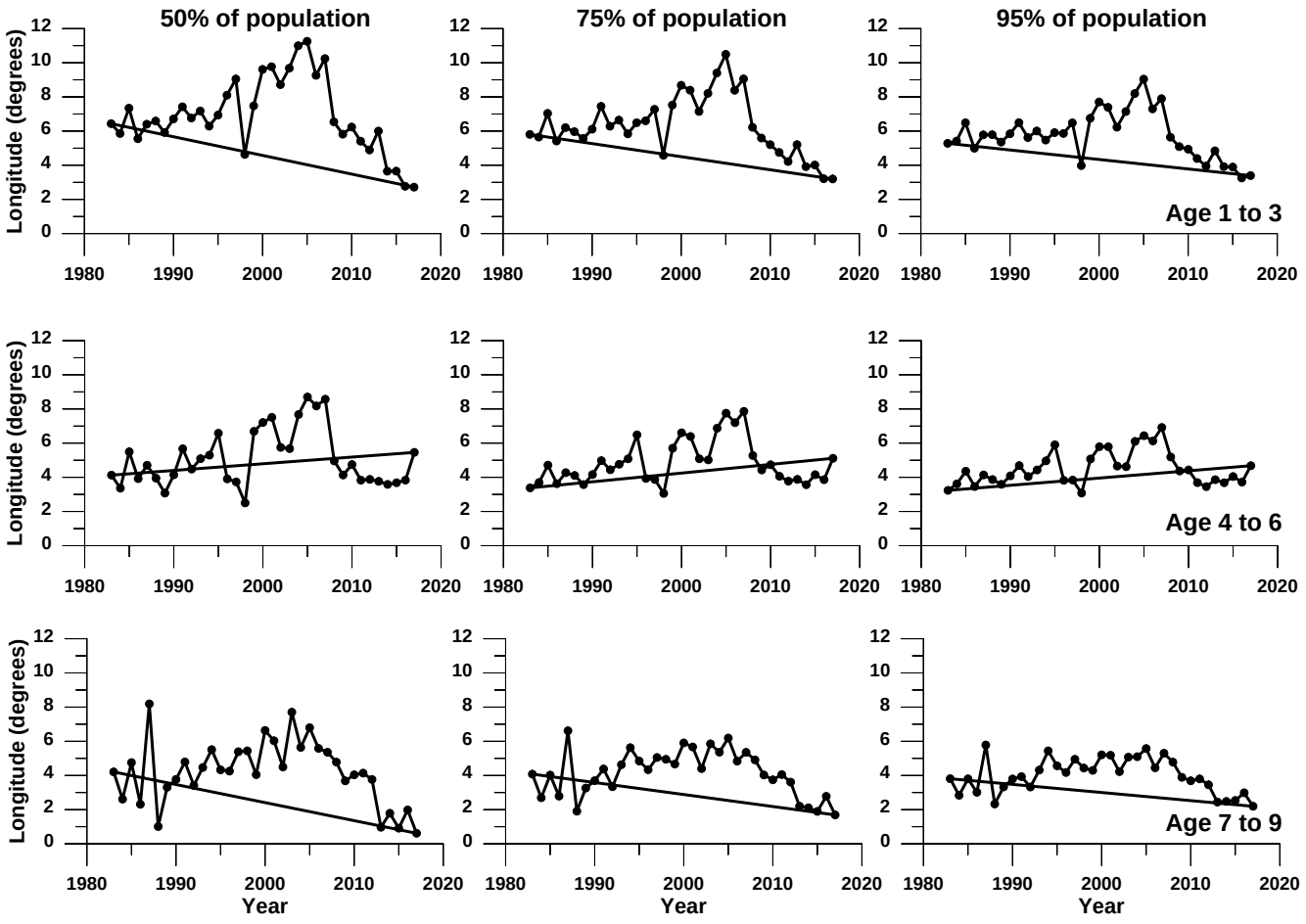

Figure 5.19. Temporal trends in the biomass-weighted mean longitude of 50%, 75% and 95% of the population of 1 y to 3 y aged, 4 y to 6 y aged and 7 y to 9 y aged plaice in the North Sea.

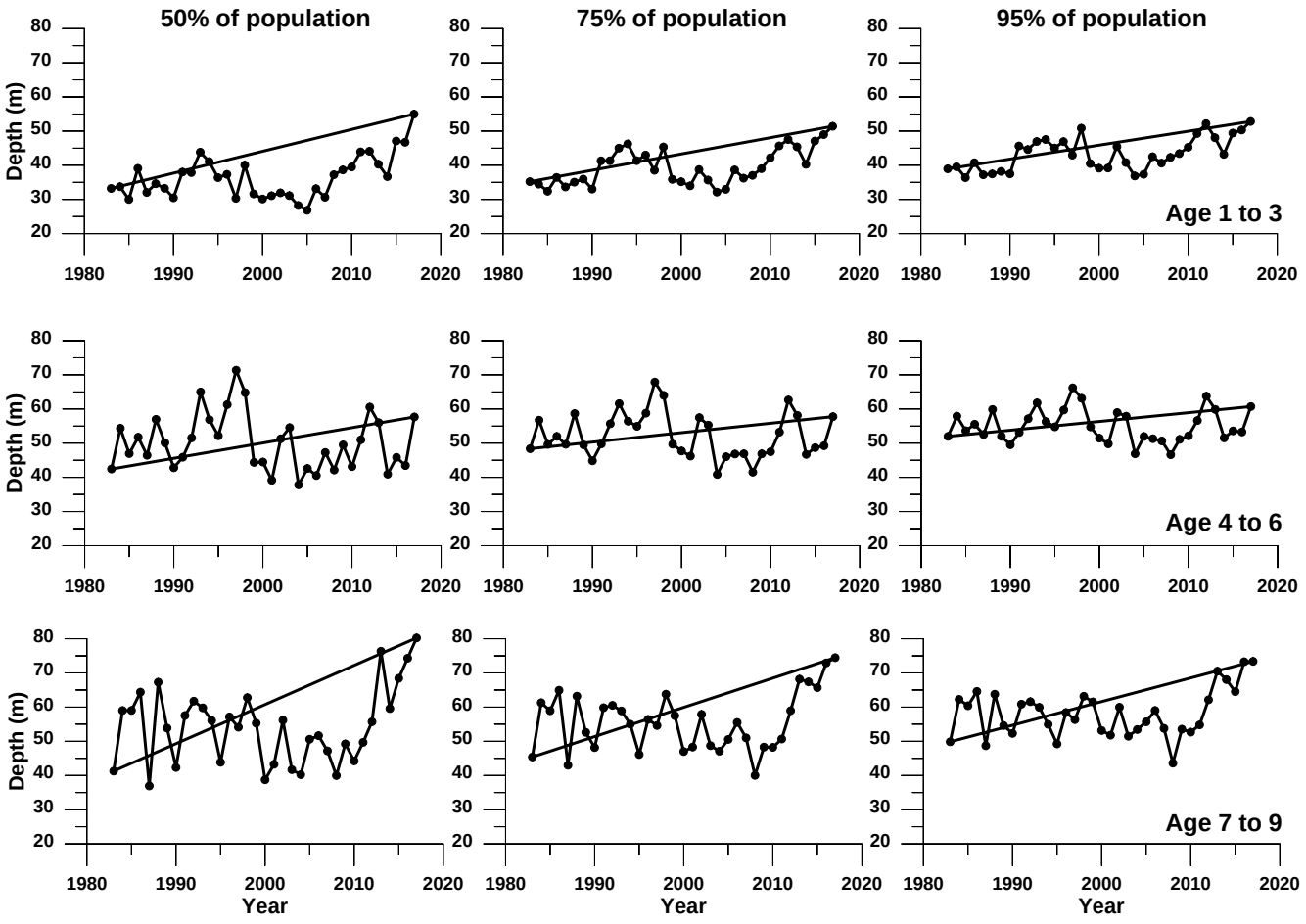

Figure 5.20. Temporal trends in the biomass-weighted mean depth of 50%, 75% and 95% of the population of 1 y to 3 y aged, 4 y to 6 y aged and 7 y to 9 y aged plaice in the North Sea.

5.4.1.4 Consistency of use indicators

Consistency in the use of space is another key aspect of species' distributions likely to be of interest to managers, for example in informing the designation of marine protected areas aimed at protecting fish biodiversity. Figure 5.21 demonstrates this aspect for the three age-class groups of plaice. Core area consistency was relatively low. The area holding 50% of the plaice population in any given year seemed to vary from year to year such that the number of quadrants considered part of the core area in, for example, 60% (21 y) of years was low. Consistency in prime area was much higher. A much greater number of quadrants fell into this category in a higher percentage of years. Consistency in sub-prime area was even higher. Most of the quadrants occupied by plaice at any time were considered sub-prime area in at least 60% of occasions. In trying to identify a critical area used consistently by plaice, which might be considered for particular spatial management measures, the core area grade would seem to be too sharp and the sub-prime area grade too blunt. The prime area grading would appear to be the optimal category for defining a critical area for plaice, and a definition of critical area along the lines of "quadrants occupied by 75% of the plaice population in 60% of years". Such a definition identifies 80 quadrants for the 1 y to 3 y age-class group, 130 quadrants for the 4 y to 6 y age-class group, and 82 quadrants for the 7 y to 9 y age-class group, covering areas of 70 621 km^2, 113 001 km^2, and 72 383 km^2 respectively. Figure 5.22 shows variation in the proportion of the plaice population using this consistent critical area in each year of the survey. Clear trends area are apparent up to around 2008, where the proportion of each age-class group population using these areas has generally increased, but then has subsequently sharply declined.

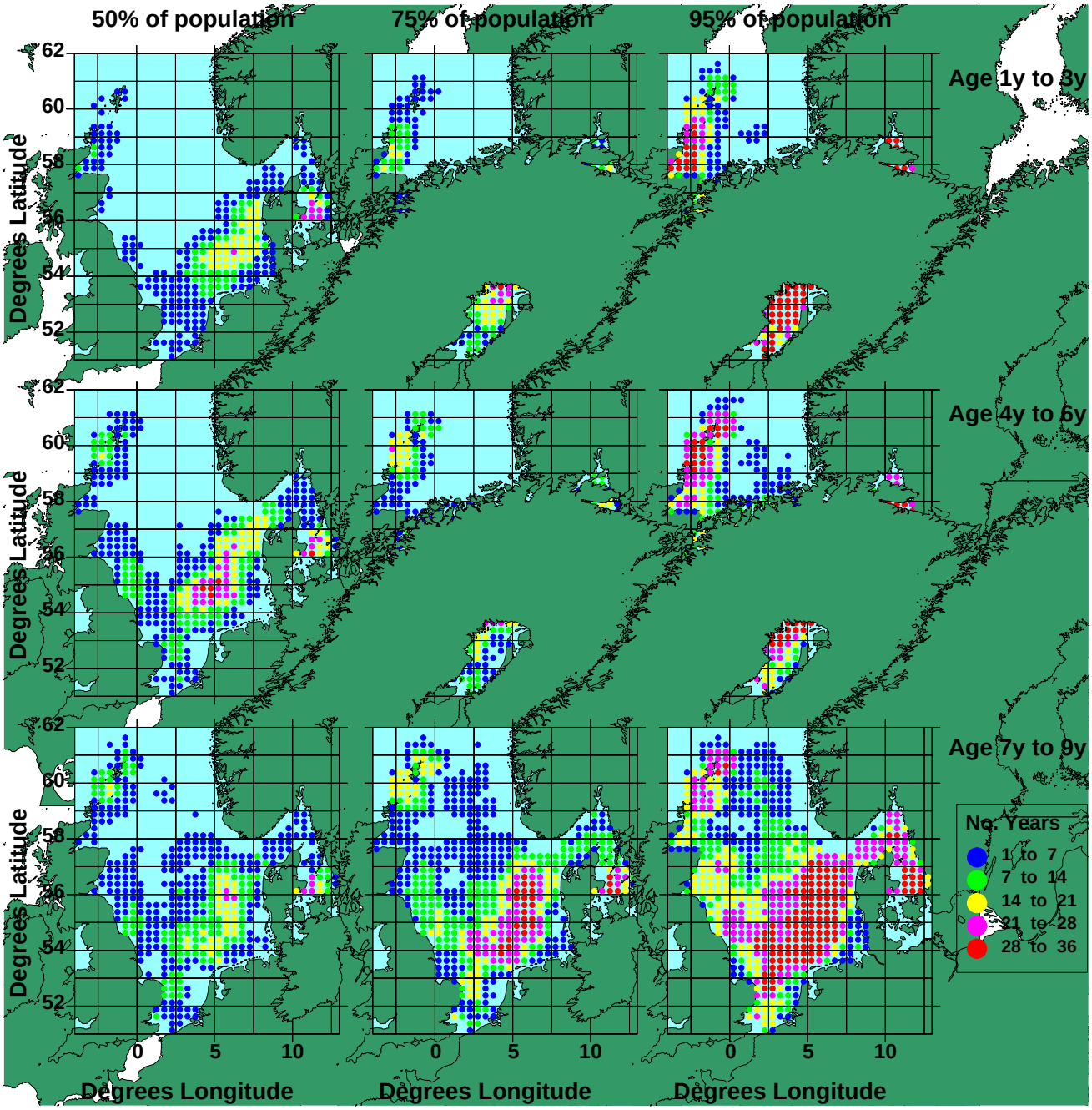

Figure 5.21. Consistency of quadrant occupancy grading measured as the number of years (out of a possible total of 35 y) that each quadrant was considered to be core area (holding 50% of the plaice population), core and prime area (holding 75% of the plaice population) and core, prime and subprime area (holding 95% of the plaice population).

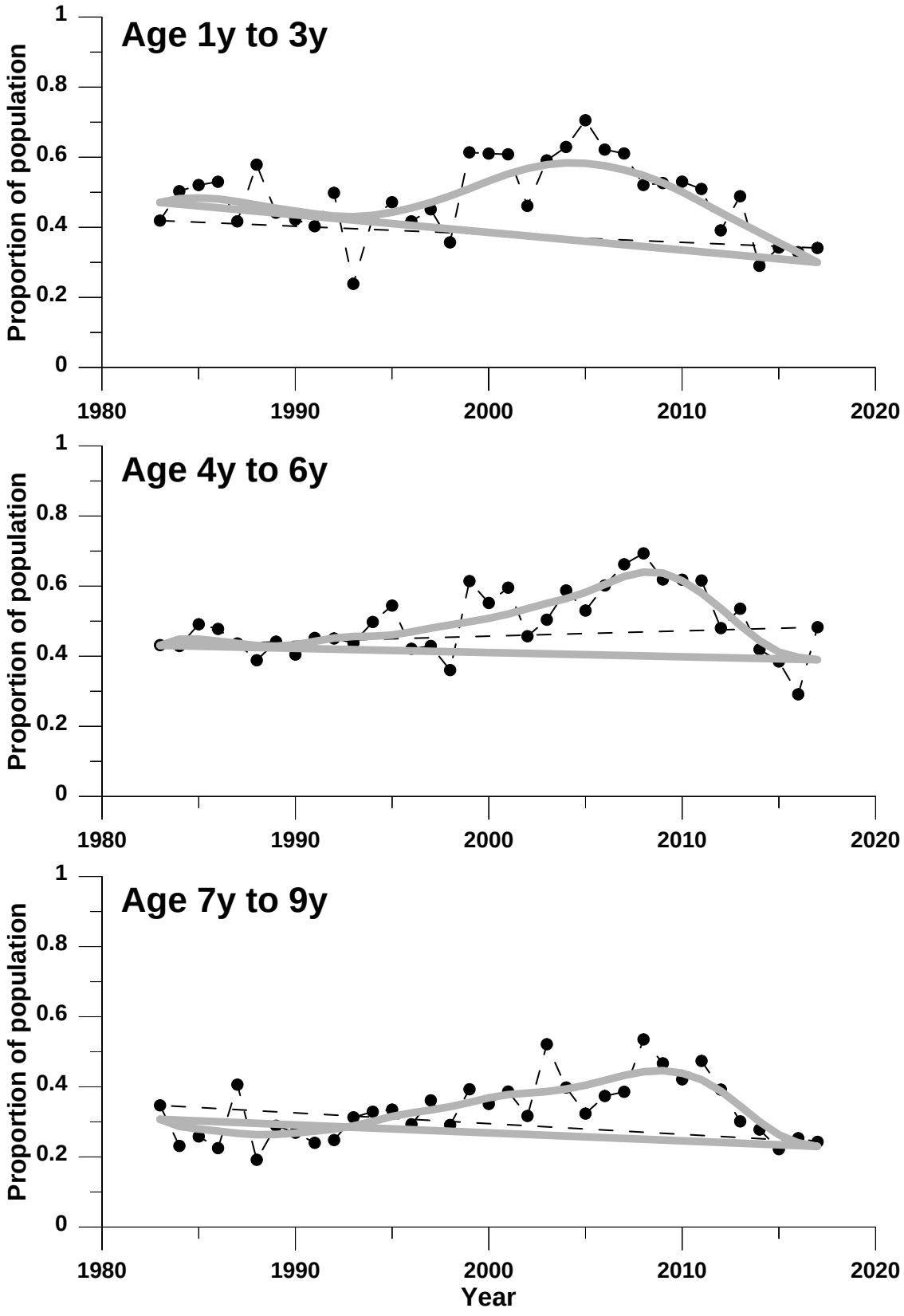

Figure 5.22. Temporal trends in the proportion of the population of plaice using the 'critical areas', defined as quadrants occupied by 75% of the plaice population in 60% of years. The numbers of critical quadrants are 89 for ages 1 to 3, 130 for ages 4 to 6, and 82 for ages 7 to 9.

5.5 References

Basimi, R.A. and D.J. Grove, 1985. Estimates of daily food intake by an inshore population of *Pleuronectes platessa* L. off eastern Anglesey, North Wales. J. Fish Biol. 27:505–520.

Dulvy, N.K., Rogers, S.I., Jennings, S., Stelzenmüller, V., Dye, S. R., and Skjoldal, H.R. 2008. Climate change and deepening of the North Sea fish assemblage: a biotic indicator of warming seas. Journal of Applied Ecology, 45: 1029–1039.

EMODnet. Geology 2016 Seabed substrate 1:1000000 – Europe. EMODnet Geology, European Commission. Available at http://emodnet-geology.eu.Accessed 10th April 2019.

Fretwell, S.D. and Lucas, H.L. 1970. On territorial behaviour and other factors influencing habitat distribution in birds. Acta Biotheoretica, 19, 16–36.

Hughes, K. M., Dransfeld L, and Johnson M.P. 2014. "Changes in the Spatial Distribution of Spawning Activity by North-East Atlantic Mackerel in Warming Seas: 1977–2010." *Marine Biology* 161(11):2563–76.

ICES. 2018. Report of the Working Group on the Assessment of Demersal Stocks in the North Sea and Skagerrak (WGNSSK), 24 April–3 May 2018, Oostende, Belgium. ICES CM 2018/ACOM:22.

Lewy P and Kristensen K. 2009. Modelling the Distribution of Fish Accounting for Spatial Correlation and Overdispersion. Canadian Journal of Fisheries and Aquatic Sciences 66(10:1809–20. (http://www.nrcresearchpress.com/doi/pdf/10.1139/F09-114).

Lynch, D.R., McGillicuddy, D.J., and Werner, F.E. 2009. Skill assessment for coupled biological/physical models of marine systems. Journal of Marine Systems, 79, 1–3.

Moriarty, M., Greenstreet, S.P.R., Rasmussen, J. and de Boois, I. 2019. Assessing the state of demersal fish to address formal ecosystem based management: making fisheries independent data 'fit for purpose'. Frontiers in Marine Science. 6:162, 10pp. Doi 10.3389/fmars.2019.00162.

Petitgas P and Poulard J-C. 2009. A Multivariate Indicator to Monitor Changes in Spatial Patterns of Age-Structured Fish Populations. Aquatic Living Resources 22(2):165–71.

Stelzenmüller, V., Ehrich, S., and & Zauke, G. P. 2005. Effects of survey scale and water depth on the assessment of spatial distribution patterns of selected fish in the northern North Sea showing different levels of aggregation. Marine Biology Research, 1(6), 375–387.

Thorson, James T., Malin L. Pinsky, and Eric J. Ward. 2016. "Model-Based Inference for Estimating Shifts in Species Distribution, Area Occupied and Centre of Gravity" edited by O. Gimenez. *Methods in Ecology and Evolution* 7(8):990–1002. Retrieved April 5, 2017 (http://doi.wiley.com/10.1111/2041-210X.12567).

6 ToR d: Conduct a “reality check” and horizon scanning survey within WGECO

The aim of this ToR is to develop a consensus view of the major emerging issues in relation to fisheries and ecosystems, and on which WGECO could focus future work. WGECO members will provide a list of emerging issues (horizon scanning), that would benefit from scrutiny by WGECO. This list will be collated and used as material for a plenary discussion, and with the aim of producing a perspectives paper in the ICES JMS or Fish and Fisheries.

WGECO decided to table this ToR until 2020 in order to concentrate work on the other ToRs. Two plenary discussions were held to scope topics and issues to address in 2020. A high-level question is how humans relate philosophically with the ocean? Does our cultural association extend beyond goods and services? Do these perspectives lead to different ocean futures? Other topics include but are not limited to: accurate verifiable catch data, undersea noise, rise of recreational fisheries, microplastics in the ocean, cumulative effects on the marine environment, functional diversity, use of multispecies models, and socio-economic issues.

7 ToR e: Review the sensitive species list prepared by WGBYC

This year, WGBYC evaluated the list of species to be monitored under protection programmes in the European Union or under international obligations (COMMISSION IMPLEMENTING DECISION (EU) 2016/1251) to determine which of the bony fish species are considered sensitive bycatch and hence relevant to the work of WGBYC. This list will be included in the fisheries overviews. WGECO is requested to compare the resulting list to sensitive species identified using methods reviewed previously in WGECO and to comment on any discrepancies.

7.1 Approach

WGECO considered two relevant issues: which European fish species are considered sensitive to fishing and which are the species identified by WGBYC among the species expected to be sensitive to fishing. To address the first question, two methods to identify sensitive species were considered. One method, Greenstreet *at al*., 2012 evaluates sensitivity based on a ranking according to life-history traits (Greenstreet *et al*., 2012) whereas the other method, Gislason *et al*. (in prep.) considered at the WGECO 2018 meeting, is based on the life-history trait model of Le Quesne and Jennings (2012) combined with evaluation of the catchability of the species in demersal fisheries from Walker *et al*. (2017). Further, the IUCN rating of the species was examined. Only species caught in surveys that were found in the DATRAS database, were included.

The resulting list of sensitive species and vulnerable/endangered/critically endangered species is given in Table 7.1 and the sensitivity of the species considered by WGBYC for monitoring is given in Table 7.2. Only one of the listed species is considered sensitive to fishing (halibut, *Hippoglossus hippoglossus*), while the remaining species, with the exception of the two *Hippocampus* species, are diadromus species likely to be most sensitive to deterioration of their freshwater habitat.

Of the species listed in Table 7.1, Table 7.3 lists species that either do not appear in the COMMISSION IMPLEMENTING DECISION (EU) 2016/1251 or appear in the list only for a very limited area that does not cover their distribution. **WGECO recommends** that these species should be added to the Commission list to provide information on sensitive and vulnerable species. Further, several of the scientific names given in the list are not the currently accepted names (e.g. *Psetta maxima*) and should be updated to avoid confusion.

Among the sensitive species in Table 7.1, only 20% are required to be returned to the sea upon catching while 30% have a defined TAC in at least one area (Council Regulation (EU) 2018/2025, Council Regulation (EU) 2019/124). Though some species are listed as required to be returned live to the sea as quickly as possible, the requirement is often only stated for part of EU waters (e.g. *Rostroraja alba*), and in the rest of EU waters, the species will be under an obligation to land. **WGECO recommends** that the requirement to return species to the sea for endangered and critically endangered species should apply to all EU waters.

The remaining species listed in Table 7.1 (50%) can be landed without specific limits for the individual species. Some species are allocated to grouped TACs (e.g. deep-water sharks, rays and skates). Limits to grouped landings are not necessarily sufficient to avoid decline of the individual sensitive species. **WGECO recommends** that the status of sensitive species identified is monitored regularly and species-specific landing restrictions are advised in case of decline of one or more species.

Table 7.1. Species occurring in DATRAS and identified as sensitive or vulnerable/endangered/critically endangered by IUCN. IUCN ratings: CR: Critically endangered, EN: Endangered, VU: Vulnerable, NT: Near threatened, LC: Least concern, DD: data deficient. Sensitive to fishing: N: not sensitive, Y: sensitive, -: not evaluated.

Scientific name	Common name	IUCN rating	Sensitive according to Gislason *et al*. (in. prep)	Sensitive according to Greenstreet *et al*. (2012)
Alopias vulpinus	Thresher	EN	N	-
Amblyraja hyperborea	Arctic skate	LC	Y	-
Amblyraja radiata	Starry ray	LC	Y	N
Anarhichas lupus	Wolffish	DD	Y	Y
Anarhichas minor	Spotted wolffish	NT	Y	Y
Anguilla anguilla	European eel	CR	Y	Y
Argyrosomus regius	Meagre	LC	Y	-
Balistes capriscus	Grey triggerfish	VU	N	Y
Beryx decadactylus	Alfonsino	LC	Y	-
Brama brama	Atlantic pomfret	LC	Y	Y
Brosme brosme	Cusk	LC	N	Y
Cetorhinus maximus	Basking shark	EN	N	-
Chelidonichthys lucerna	Tub gurnard	LC	N	Y
Chimaera monstrosa	Rabbit fish	NT	Y	Y
Conger conger	Conger eel	LC	Y	Y
Coryphaenoides rupestris	Roundnose grenadier	EN	Y	-
Cyclopterus lumpus	Lumpfish	NT	N	Y
Dalatias licha	Kitefin shark	EN	Y	-
Dasyatis pastinaca	Common stingray	VU	Y	-
Deania calcea	Birdbeak dogfish	EN	Y	-
Dipturus batis	Common skate	CR	Y	Y
Dipturus oxyrinchus	Longnosed skate	NT	Y	-
Dipturus nidarosiensis	Norwegian skate	NT	Y	-
Etmopterus princeps	Great lanternshark	LC	Y	-
Gadus morhua	Atlantic cod	LC	N	Y
Galeorhinus galeus	Tope shark	VU	Y	Y

Scientific name	Common name	IUCN rating	Sensitive according to Gislason *et al*. (in. prep)	Sensitive according to Greenstreet *et al*. (2012)
Galeus melastomus	Blackmouth cat-shark	LC	Y	-
Helicolenus dactylopterus	Blackbelly rose-fish	LC	N	Y
Hexanchus griseus	Bluntnose sixgill shark	LC	Y	-
Hippoglossus hippoglossus	Halibut	VU	Y	Y
Labrus bergylta	Ballan wrasse	LC	N	Y
Lamna nasus	Porbeagle	CR	N	-
Lepidorhombus whiffiagonis	Megrim	LC	N	Y
Leucoraja circularis	Sandy ray	EN	Y	Y
Leucoraja fullonica	Shagreen ray	VU	Y	Y
Leucoraja naevus	Cuckoo ray	LC	Y	Y
Lophius budegassa	Blackbellied angler	LC	Y	Y
Lophius piscatorius	Angler	LC	Y	Y
Merluccius merluccius	European hake	LC	N	Y
Molva dypterygia	Blue ling	VU	Y	Y
Molva macropthalma	Spanish ling	LC	Y	-
Molva molva	Ling	LC	Y	Y
Mustelus asterias	Starry smooth-hound	VU	Y	Y
Mustelus mustelus	Smooth-hound	VU	Y	Y
Myliobatis aquila	Common eagle ray	VU	N	-
Petromyzon marinus	Sea lamprey	LC	N	Y
Phycis blennoides	Greater forkbeard	DD	Y	N
Polyprion americanus	Wreckfish	NT	Y	-
Pollachius pollachius	Pollack	LC	N	Y
Pollachius virens	Saithe	LC	N	Y
Raja brachyura	Blonde ray	NT	Y	Y
Raja clavata	Thornback ray	NT	Y	Y

Scientific name	Common name	IUCN rating	Sensitive according to Gislason *et al*. (in. prep)	Sensitive according to Greenstreet *et al*. (2012)
Raja microocellata	Small-eyed ray	NT	Y	-
Raja montagui	Spotted ray	NT	Y	Y
Raja undulata	Undulate ray	NT	Y	Y
Rajella bathyphila	Deep-water ray	LC	Y	-
Rajella lintea	Sailray	LC	Y	-
Rostroraja alba	White skate	CR	Y	-
Salmo salar	Atlantic salmon	VU	N	-
Scophthalmus maximus	Turbot	VU	N	N
Scyliorhinus canicula	Lesser spotted dogfish	LC	Y	Y
Scyliorhinus stellaris	Nursehound	NT	Y	Y
Sebastes marinus	Golden redfish	VU	N	Y
Sebastes mentella	Beaked redfish	VU	N	Y
Sebastes viviparus	Norway redfish	LC	N	Y
Somniosus microcephalus	Greenland shark	NT	Y	Y
Squalus acanthias	Picked dogfish	EN	Y	Y
Torpedo marmorata	Marbled electric ray	LC	Y	-
Zoarces viviparous	Eelpout	LC	N	Y

Table 7.2. Species identified by WGBYC together with IUCN rating and sensitivity to fishing. IUCN ratings: CR: Critically endangered, EN: Endangered, VU: Vulnerable, NT: Near threatened, LC: Least concern, DD: data deficient. Sensitive to fishing: N: not sensitive, Y: sensitive, -: not evaluated.

Scientific name	IUCN	Sensitive according to Gislason *et al*. (in. prep)	Sensitive according to Greenstreet *et al*. (2012)
Acipenser spp.	CR	-	-
Alosa alosa	LC	N	-
Alosa fallax	LC	N	-
Coregonus balticus	not accepted by WORMS		
Coregonus lavaretus	LC	N	-
Coregonus maraena	VU	-	-
Coregonus pallasii	LC	-	-
Hippocampus guttulatus	DD	N	-
Hippocampus hippocampus	DD	N	-
Hippoglossus hippoglossus	VU	Y	Y
Lampetra fluviatilis	LC	N	N
Petromyzon marinus	LC	N	Y

Table 7.3. Species that either do not appear in the COMMISSION IMPLEMENTING DECISION (EU) 2016/1251 or appear in the list only for a very limited area that does not cover their distribution. Gislason *et al*., 2019 (in prep.), Greenstreet *et al.,* 2012.

Species	Identified as sensitive, vulnerable (VU), near threatened (NT) or data deficient (DD) by:
Balistes capriscus	IUCN (VU)
Myliobatis aquila	IUCN (VU)
Anarhichas lupus	Gislason *et al*., Greenstreet *et al*., (IUCN DD)
Anarhichas minor	Gislason *et al*., Greenstreet *et al*., IUCN (NT)
Dipturus oxyrinchus	Gislason *et al*., IUCN (NT)
Leucoraja naevus	Gislason *et al*., Greenstreet *et al*.
Raja brachyura	Gislason *et al*., Greenstreet *et al*., IUCN (NT)
Raja microocellata	Gislason *et al*., IUCN (NT)
Rajella bathyphila	Gislason *et al*.
Rajella lintea	Gislason *et al*.
Scyliorhinus stellaris	Gislason *et al*., Greenstreet *et al*., IUCN (NT)

7.2 References

Council Regulation (EU) 2018/2025 of 17 December 2018 fixing for 2019 and 2020 the fishing opportunities for Union fishing vessels for certain deep-sea fish stocks.

Council Regulation (EU) 2019/124 of 30 January 2019 fixing for 2019 the fishing opportunities for certain fish stocks and groups of fish stocks, applicable in Union waters and, for Union fishing vessels, in certain non-Union waters.

Gislason, H. Rindorf, A, Burns, F, and Reid, D. 2019. Are fish sensitive to trawling recovering in European waters? In prep.

Greenstreet, S. P., Rossberg, A. G., Fox, C. J., Le Quesne, W. J., Blasdale, T., Boulcott, P., ... and Moffat, C. F. 2012. Demersal fish biodiversity: species-level indicators and trends-based targets for the Marine Strategy Framework Directive. ICES Journal of Marine Science, 69(10), 1789–1801.

Le Quesne, W. J., and Jennings, S. 2012. Predicting species vulnerability with minimal data to support rapid risk assessment of fishing impacts on biodiversity. Journal of Applied Ecology, 49(1), 20–28.

Walker, N. D., Maxwell, D. L., Le Quesne, W. J., and Jennings, S. 2017. Estimating efficiency of survey and commercial trawl gears from comparisons of catch-ratios. ICES Journal of Marine Science, 74(5), 1448–1457.

Annex 1: List of Participants

Name	Institute	Country	E-mail
Julia Calderwood Chair-invited	Marine Institute Rinville	Ireland	Julia.calderwood@marine.ie
Jeremy Collie Chair	Graduate School of Oceanography	USA	jcollie@gso.uri.edu
Jasper Croll Chair-invited	University of Amsterdam Faculty of Science Institute for Biodiversity and Ecosystem Dynamics	Netherlands	j.c.croll@uva.nl
Simon Greenstreet	Marine Laboratory	UK	S.Greenstreet@MARLAB.AC.UK Simon.greenstreet@gov.scot
Chris Griffiths	Centre for Environment, Fisheries and Aquaculture Science Lowestoft Laboratory	UK	chris.griffiths@cefas.co.uk
Ellen Kenchington by correspondence	Fisheries and Oceans Canada Bedford Institute of Oceanography	Canada	Ellen.kenchington@dfo-mpo.gc.ca
Tobias van Kooten	Wageningen University	Netherlands	tobias.vankooten@wur.nl
Chris Lynam	Centre for Environment, Fisheries and Aquaculture Science Lowestoft Laboratory	UK	chris.lynam@cefas.co.uk
Meadhbh Moriarty	Centre for Environment, Fisheries and Aquaculture Science Lowestoft Laboratory	UK	m.moriarty@marlab.ac.uk
Stefán Áki Ragnarsson Chair	Marine Research Institute of Iceland	Iceland	steara@hafro.is
David Reid By correspondence	Marine Institute Rinville	Ireland	David.Reid@Marine.ie
Anna Rindorf	DTU Aqua - National Institute of Aquatic Resources	Denmark	ar@aqua.dtu.dk
Marie Savina-Rolland	Ifremer Lorient Station	France	Marie.Savina.Rolland@ifremer.fr
Victoria Sarrazin	University of Hamburg	Germany	victoria.sarrazin@uni-hamburg.de
Sam Shephard	Inland Fisheries Ireland	Ireland	Sam.Shephard@fisheriesireland.ie

Name	Institute	Country	E-mail
Brian Smith	NOAA Fisheries Woods Hole	USA	Brian.smith@noaa.gov
Murray Thompson Chair-invited	Centre for Environment, Fisheries and Aquaculture Science Lowestoft Laboratory	UK	murray.thompson@cefas.co.uk

Annex 2: Meeting Agenda

	Tuesday April 9th
9:30	Opening of the meeting
	Adoption of ToRs and Agenda
	Assignment of ToR leaders and subgroups formed Overview of presentations
11:00	Coffee
11:30	Initial discussion of ToR b
12:30	Lunch
14:00	Initial discussions on ToR a
15:00	Initial discussions on ToR c
16:00	Initial discussion on ToR d and ToR e: review WGBYC sensitive species list
17:00	Coffee
17:30	Preliminary workplan presented
1800+	Adjourn
	Wednesday April 10th
09:00	Plenary: ToR e overview
1100	Coffee
11:30	Subgroup work
12:30	Lunch
14:00	Subgroup work
15:00	Continued discussion on ToR C
1600	Subgroup work
17:00	Coffee
1800+	Adjourn

	Thursday April 11th
09:00	Subgroup reporting ToRs a–c
10:00	Subgroup work
10:30	Mikael van Deurs: Presentation on stock recruitment density-dependence
11:00	Coffee
11:30	Subgroup work
12:30	Lunch
14:00	Subgroup work
15:00	Subgroup b meeting
16:30	Subgroup work
1800+	Adjourn
	Friday April 12th
09:00	Plenary: initial discussion of ToRs, scheduling of 2020 WGECO meeting and next chair, ICES vision, name change?
11:00	Coffee
11:30	ToRa subgroup meeting
12:30	Lunch
14:00	Review sensitive species lists (Anna and Simon)
15:00	ToR c Subgroup meeting
14:00	Drafting session/subgroup work
1800+	Adjourn
	Saturday April 13th
09:00	Plenary: subgroup reporting ToRs a–c
11:00	Coffee
11:30	Drafting session/plenary/subgroup work
13:00	Lunch
14:00	WGECO excursion

	Sunday April 14th
09:00	Drafting session/plenary/subgroup work
11:00	Coffee
11:30	Drafting session/plenary/subgroup work
12:30	Lunch
15:00	Subgroup work
16:00	Coffee
16:30	Subgroup work
18:00	Adjourn
19:00	WGECO Dinner
	Monday April 15th
09:00	Plenary to review draft report sections
11:00	Coffee
11:30	Presentation on feeding guilds/workplan
12:30	Lunch
14:00	Plenary: discussion of ToR d
15:00	ToRs and scheduling of 2019 WGECO meeting and select chair
16:00	Coffee
16:30	Drafting session/subgroup work
18:00+	Adjourn
	Tuesday April 16th
09:00	Plenary to review draft report sections
11:00	Coffee
11:30	Tidy up loose ends—final edits
1300+	Adjourn

Annex 3: Supplementary figures from simulations of spatial indicators

Simulation 1: fully random latent distribution, for a relatively common species

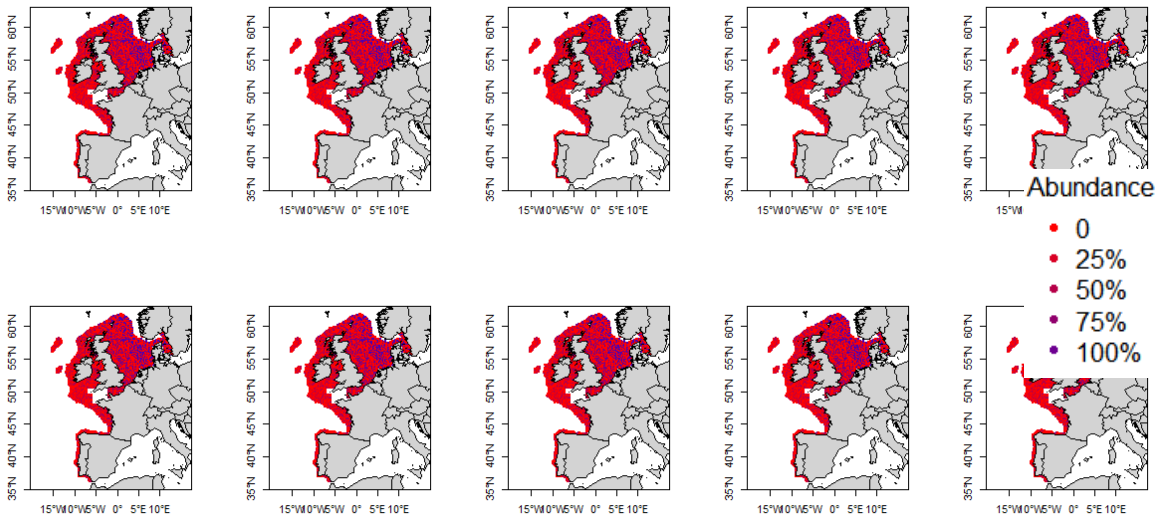

Figure A3.1. Simulated surface from data generating process for scenario 1, a common species (mean lambda = 20) where we have simulated a random latent distribution showing data for ten years.

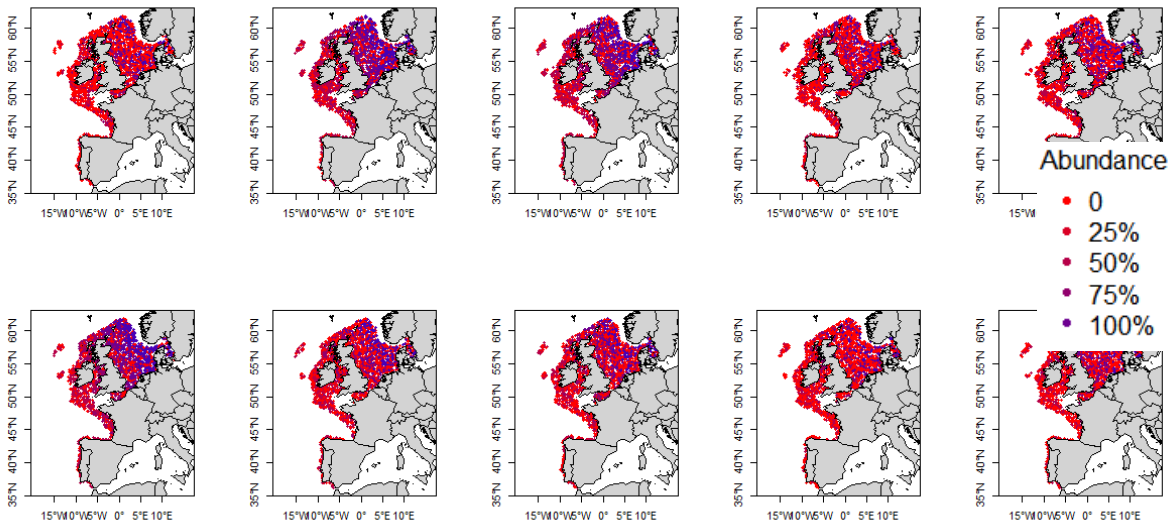

Figure A3.2. Yearly random survey samples (n=2100) taken from the simulated surface.

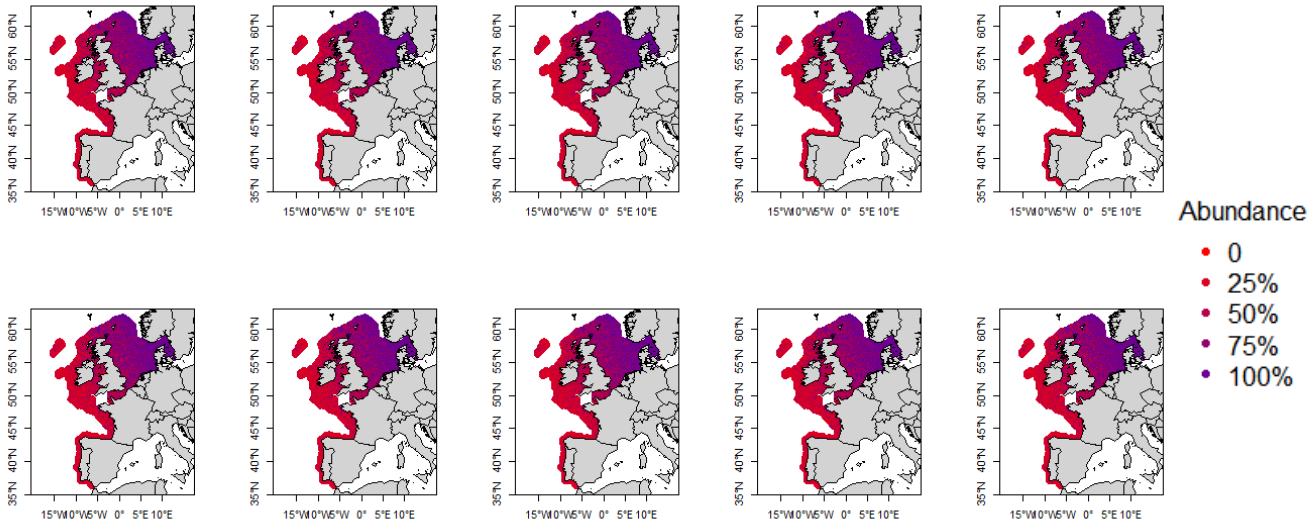

Figure A3.4. Yearly modelled surface generated from the random survey samples.

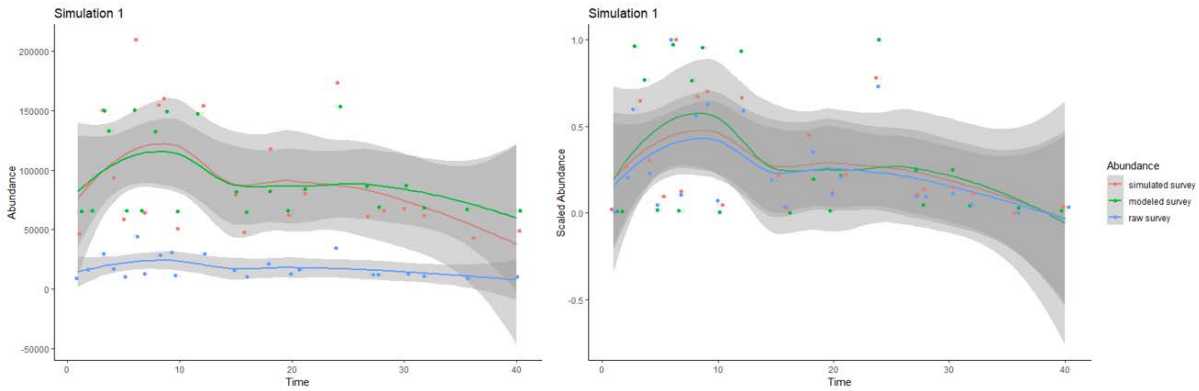

Figure A3.5. Abundance estimates (left) and scaled abundance (right) from the simulated data (red), the raw survey data (blue) and the modelled survey data (green). The mean relative error between the scaled abundance from the simulated data and the scaled abundance from the raw survey data was -13%. The mean relative error between the scaled abundance from the simulated data and the scaled abundance from the modelled survey data was 10%.

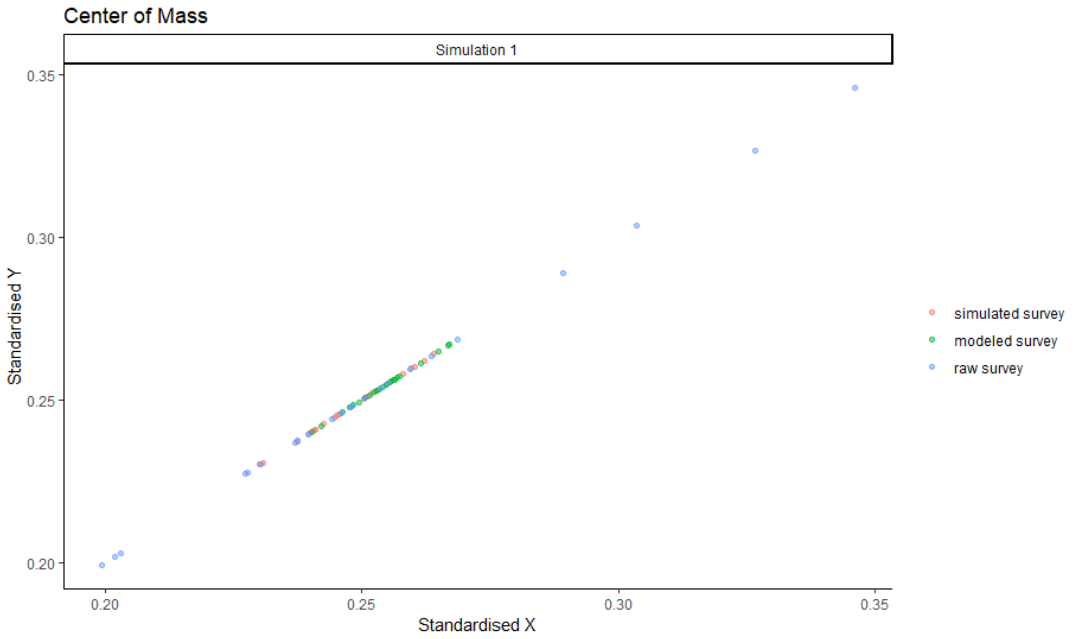

Figure A3.6. Standardised centre of mass estimates from the three datasets. The mean relative error of standardised centre of mass between the simulated data and the raw survey data was 0.017% in the X-axis and 0.008% in the y-axis. The mean relative error of the standardised centre of mass between the simulated data and the modelled survey data was 0.025% in the X-axis and 0.006% in the y-axis.

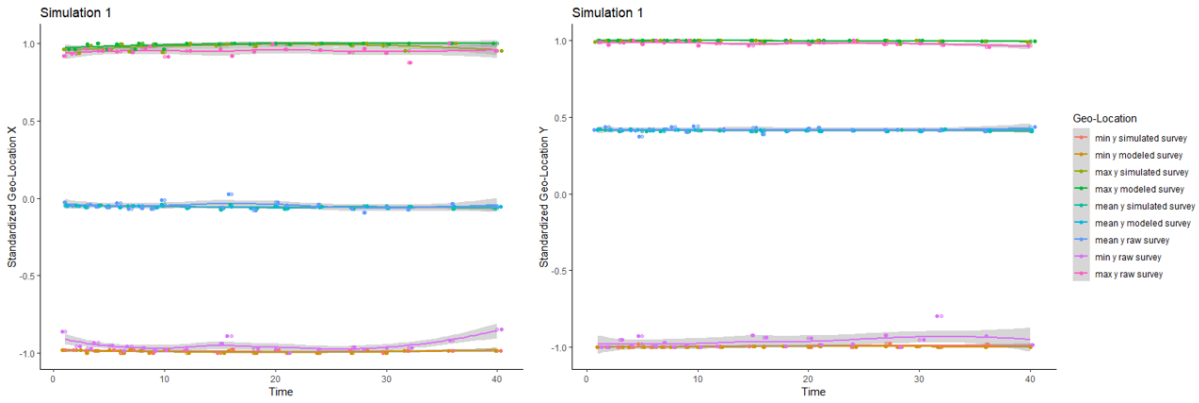

Figure A3.7. Changes in geographical extent or range in X and y-axis from the three datasets.

Simulation 2: strong space-time-trend, for a relatively common species

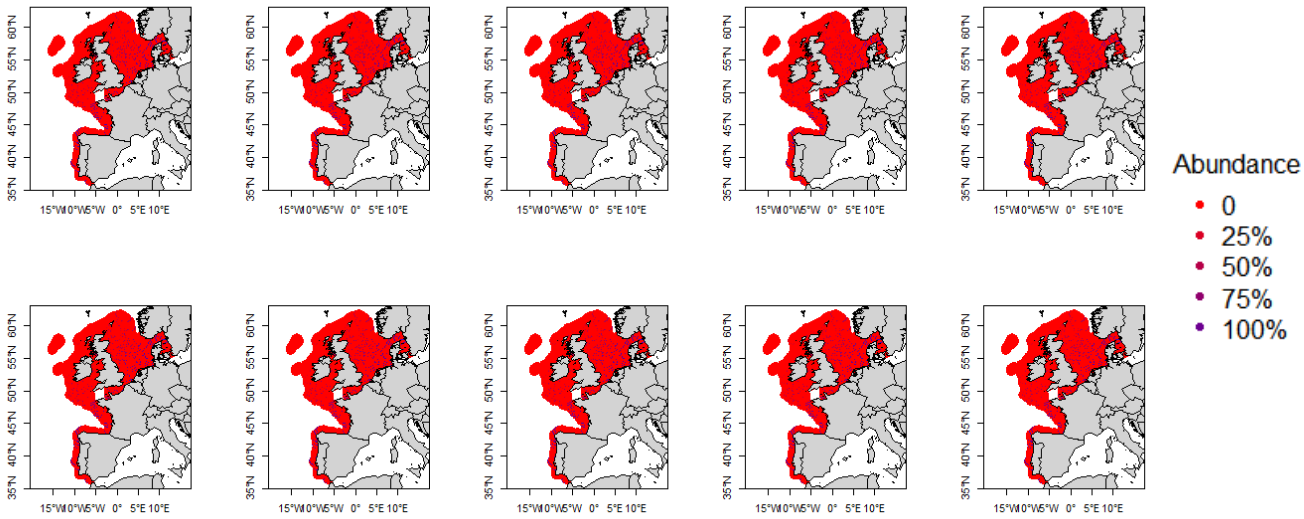

Figure A3.8. Simulated surface from data generating process for scenario 2, a common species (mean lambda = 20) where we have simulated a distribution with strong space–time-trend.

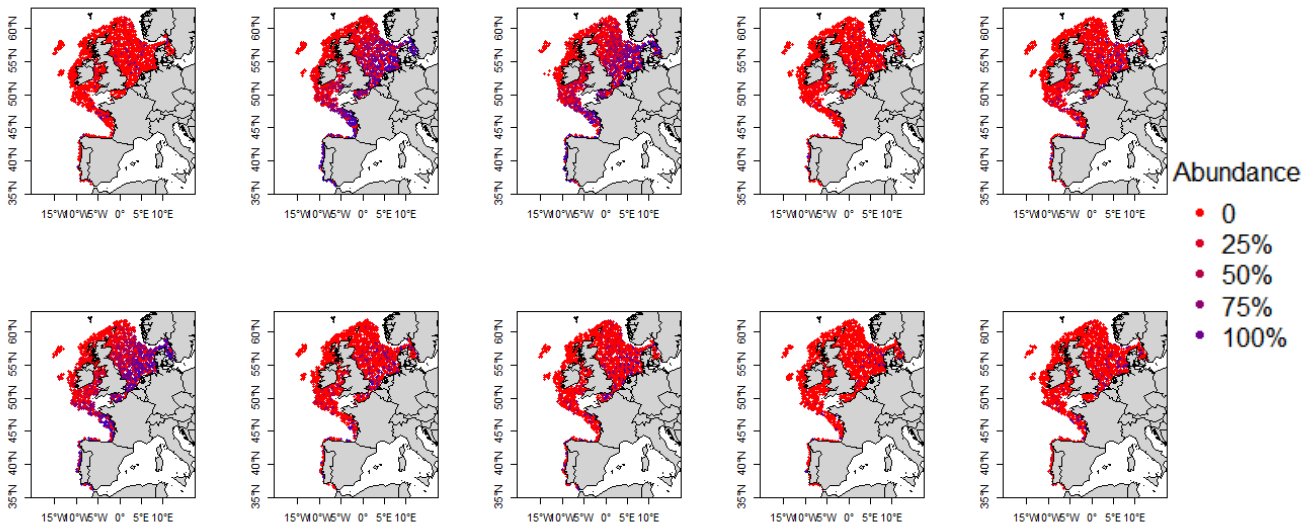

Figure A3.9. Yearly random survey samples (n=2100) taken from the simulated surface.

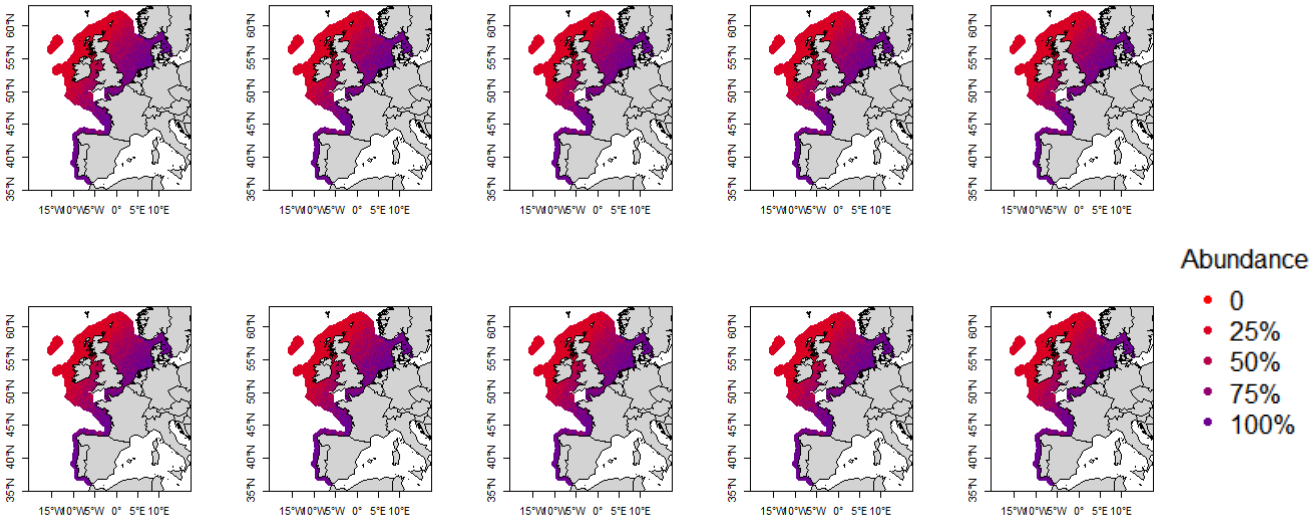

Figure A3.10. Yearly modelled surface generated from the random survey samples.

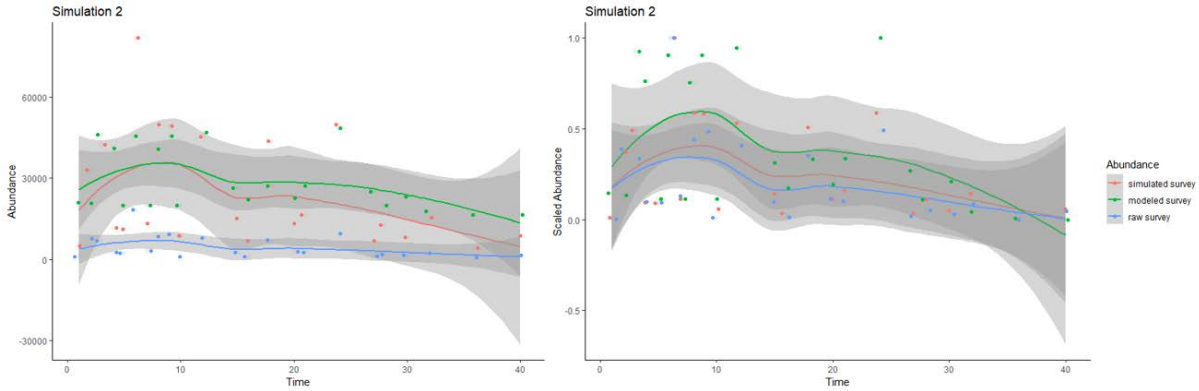

Figure A3.11. Abundance estimates (left) and scaled abundance (right) from the simulated data (red), the raw survey data (blue) and the modelled survey data (green). The mean relative error between the scaled abundance from the simulated data and the scaled abundance from the raw survey data was -18%. The mean relative error between the scaled abundance from the simulated data and the scaled abundance from the modelled survey data was 50%.

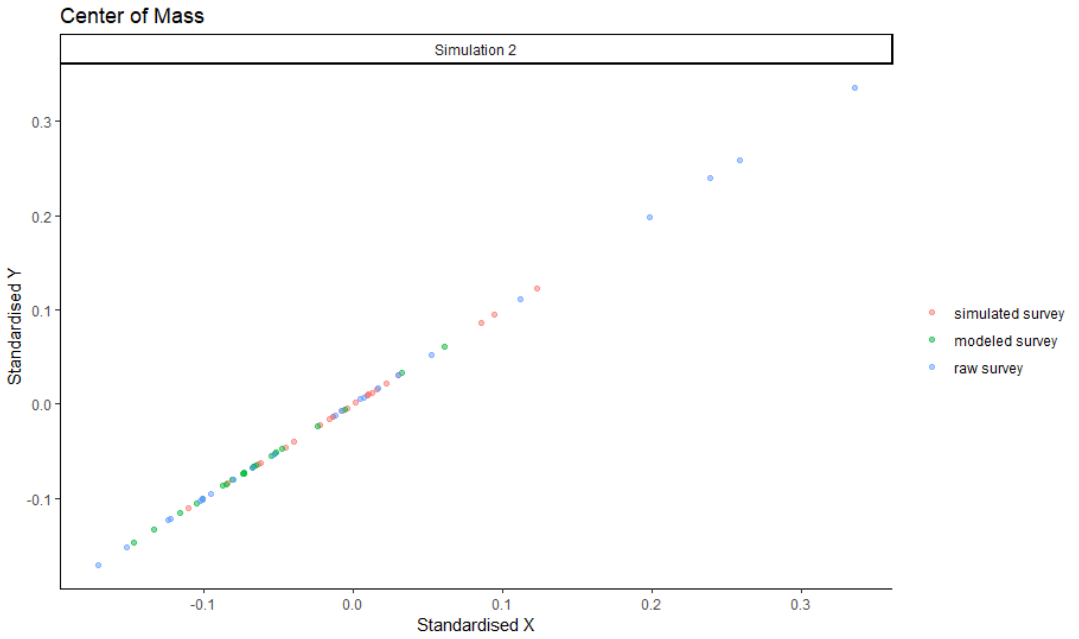

Figure A3.12. Standardised centre of mass estimates from the three datasets. The mean relative error of standardised centre of mass between the simulated data and the raw survey data was -4.31% in the X-axis and 0.084% in the y-axis. The mean relative error of the standardised centre of mass between the simulated data and the modelled survey data was -4.54% in the X-axis and 0.96% in the y-axis.

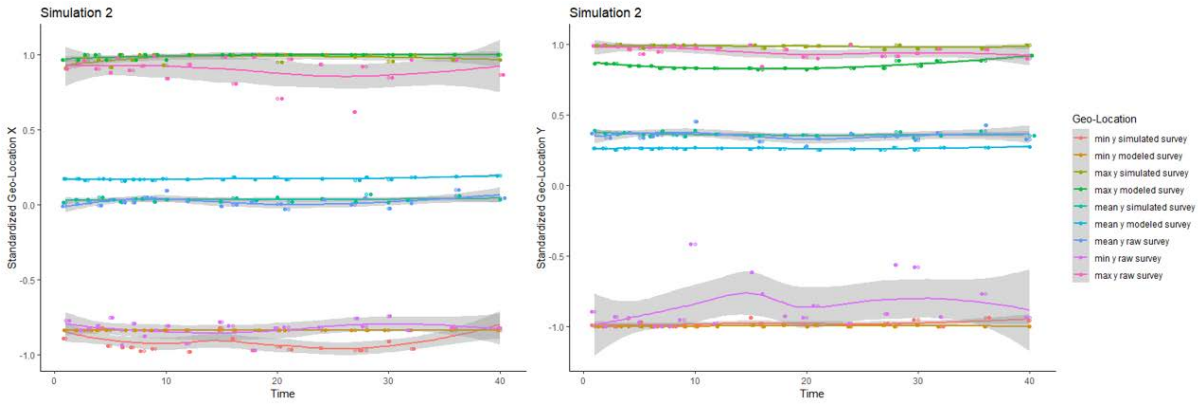

Figure A3.13. Changes in geographical extent or range in X and y-axis from the three datasets.

Simulation 3: strong space–time-trend, with a preference for mixed sediments, for a relatively common species

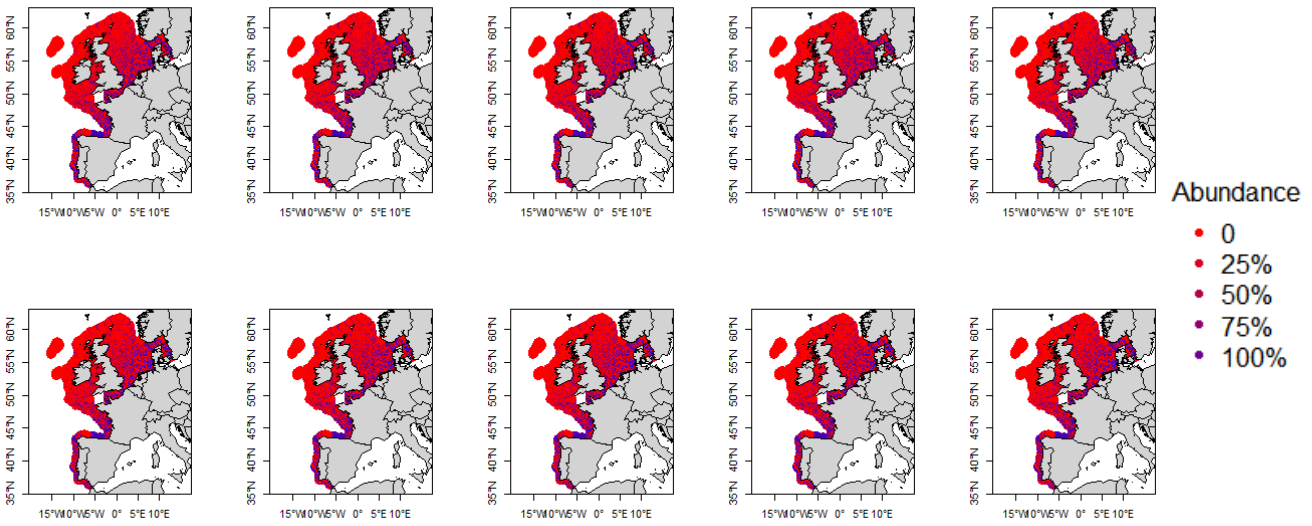

Figure A3.14. Simulated surface from data generating process for scenario 3, a common species (mean lambda = 20) where we have simulated a strong spatial response with a preference for coarse and mixed substrata, but which may be found in "sub prime" habitats in smaller numbers.

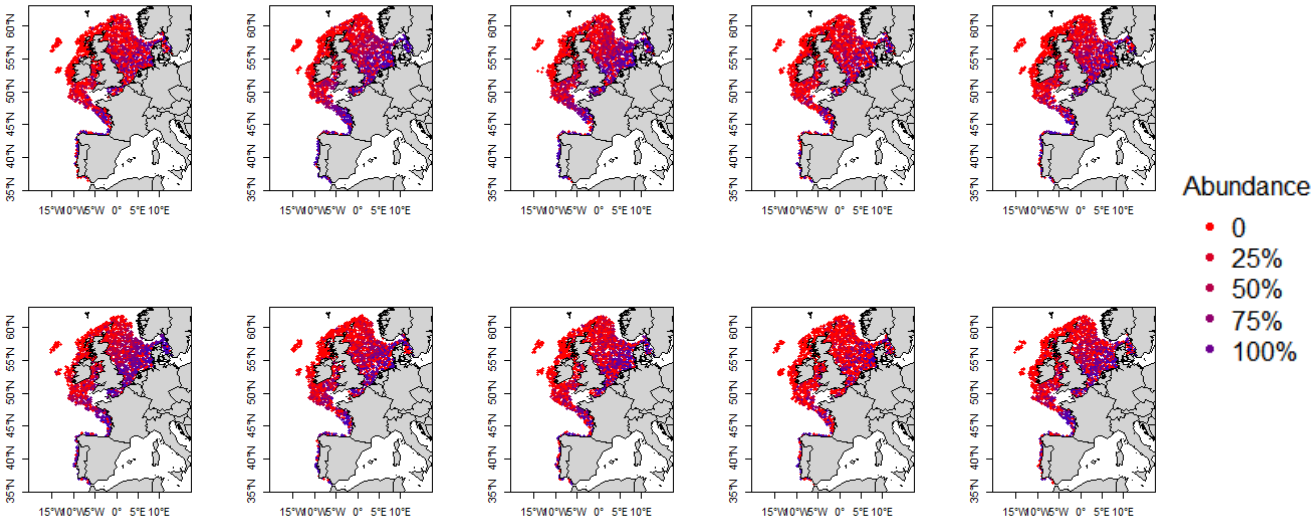

Figure A3.15. Yearly random survey samples (n=2100) taken from the simulated surface.

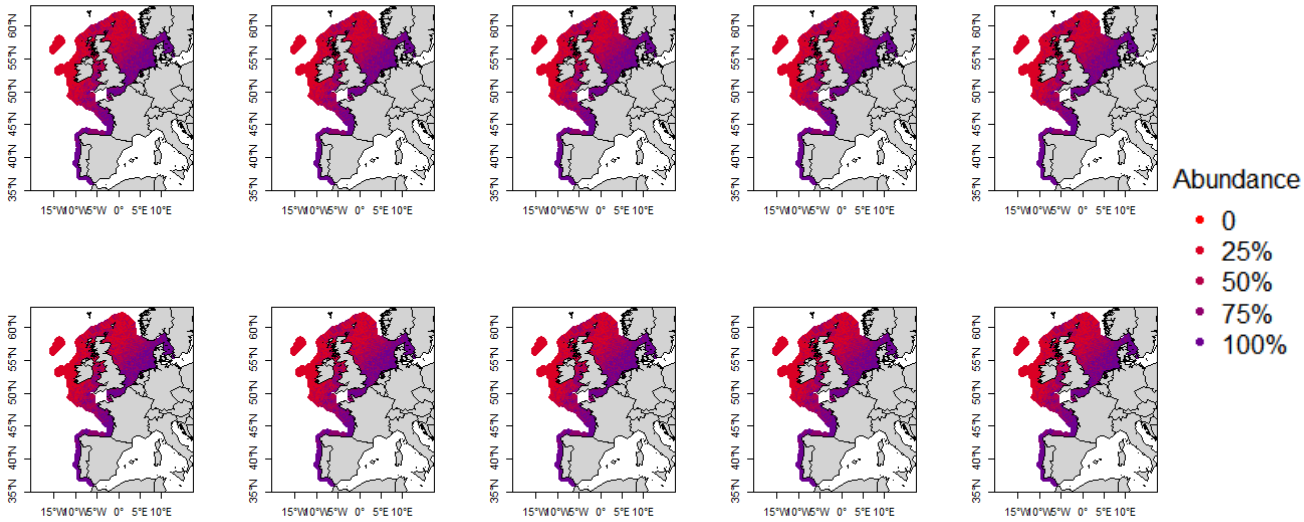

Figure A3.16. Yearly modelled surface generated from the random survey samples.

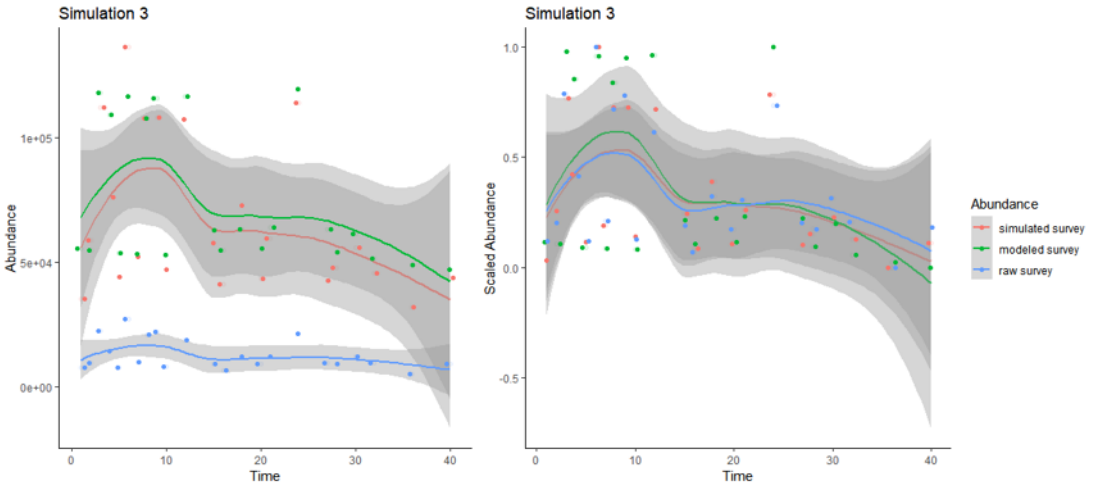

Figure A3.17. Abundance estimates (left) and scaled abundance (right) from the simulated data (red), the raw survey data (blue) and the modelled survey data (green). The mean relative error between the scaled abundance from the simulated data and the scaled abundance from the raw survey data was 3.8%. The mean relative error between the scaled abundance from the simulated data and the scaled abundance from the modelled survey data was 10.6%. The total abundance in the simulated data was 1 539 711 fish while the model predicted a total of 1 698 118 fish.

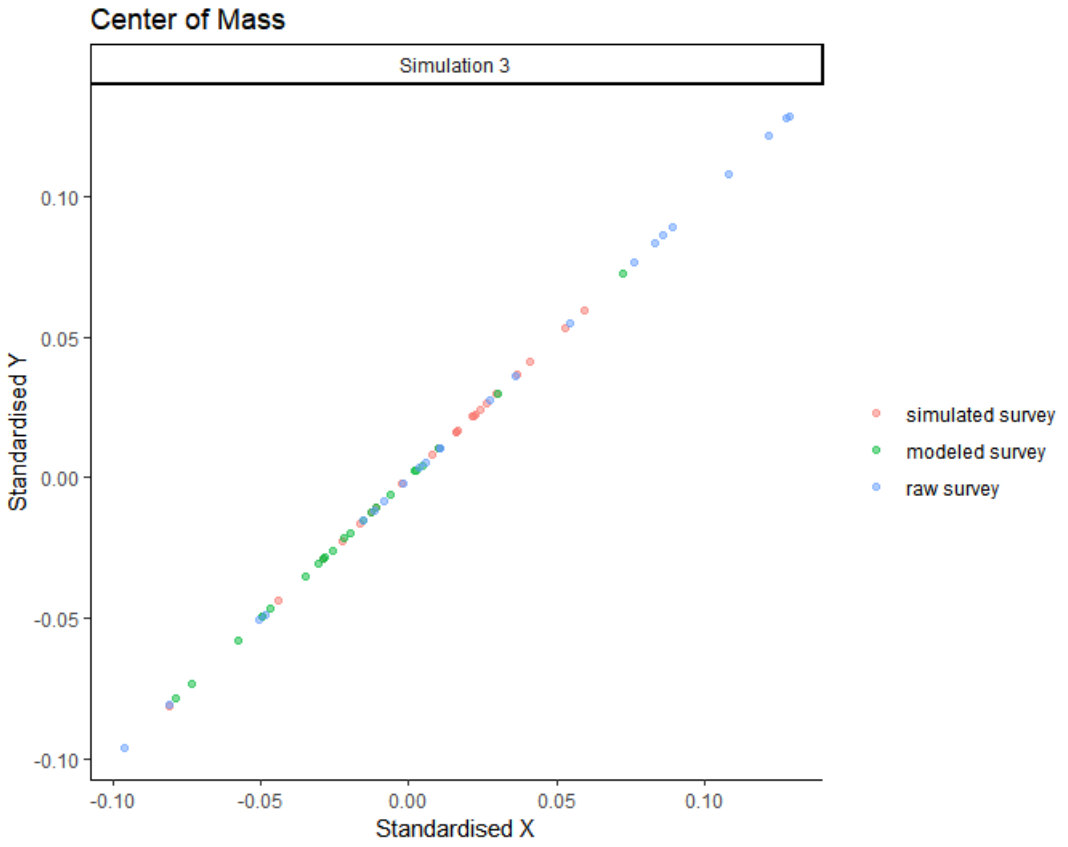

Figure A3.18. Standardised centre of mass estimates from the three datasets. The mean relative error of standardised centre of mass between the simulated data and the raw survey data was -2.7% in the X-axis and 2.1% in the y-axis. The mean relative error of the standardised centre of mass between the simulated data and the modelled survey data was -0.55% in the X-axis and 2.1% in the y-axis.

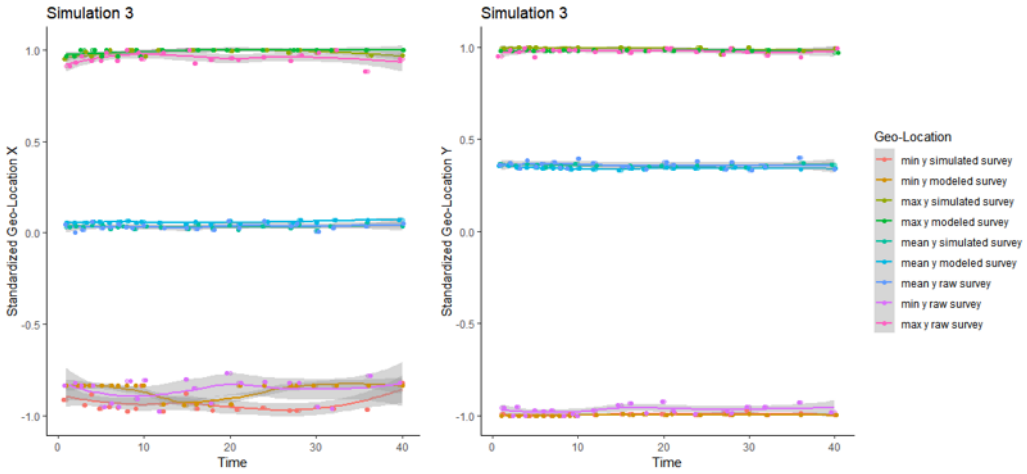

Figure A3.19. Changes in geographical extent or range in X and y-axis from the three datasets.

Simulation 4: fully random latent distribution, for a rare species

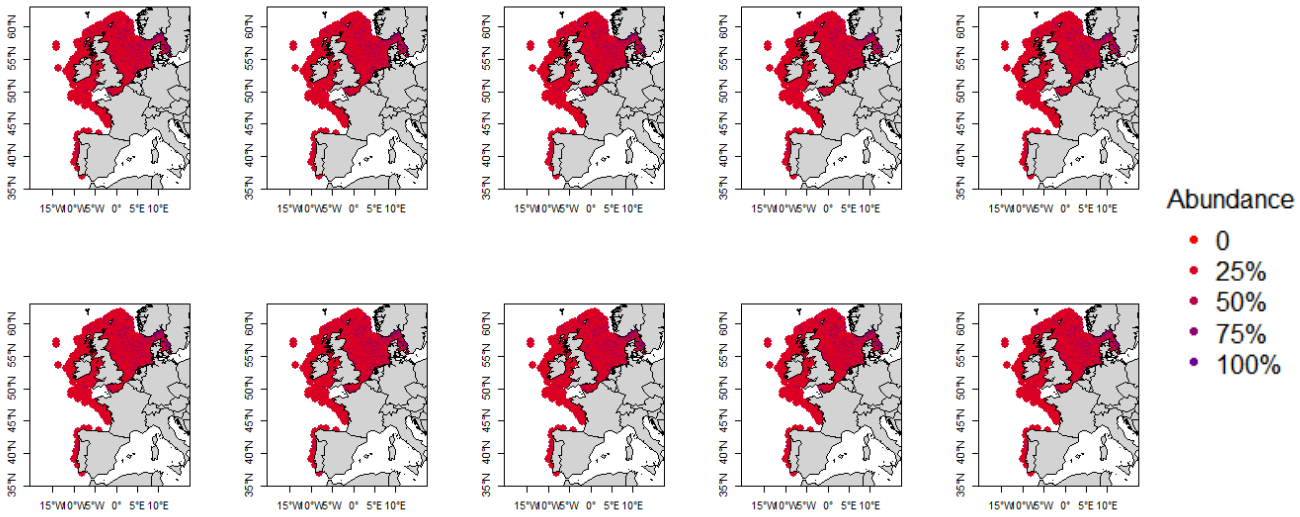

Figure A3.20. Simulated surface from data generating process for scenario 4, a rare species (mean lambda = 0.2) where we have simulated a random latent distribution showing data for ten years.

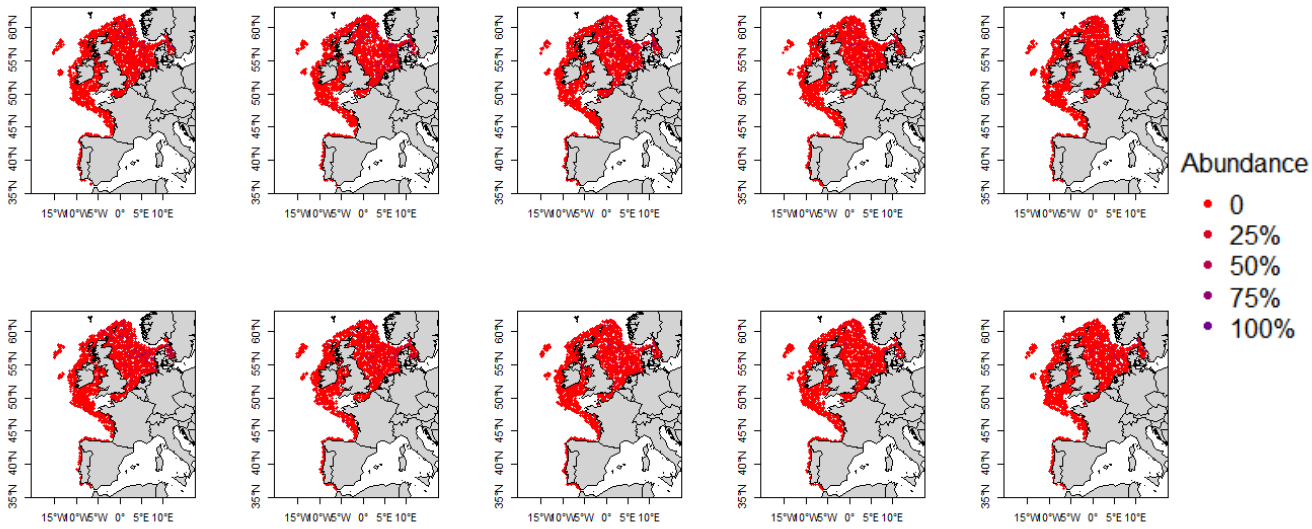

Figure A3.21. Yearly random survey samples (n=2100) taken from the simulated surface.

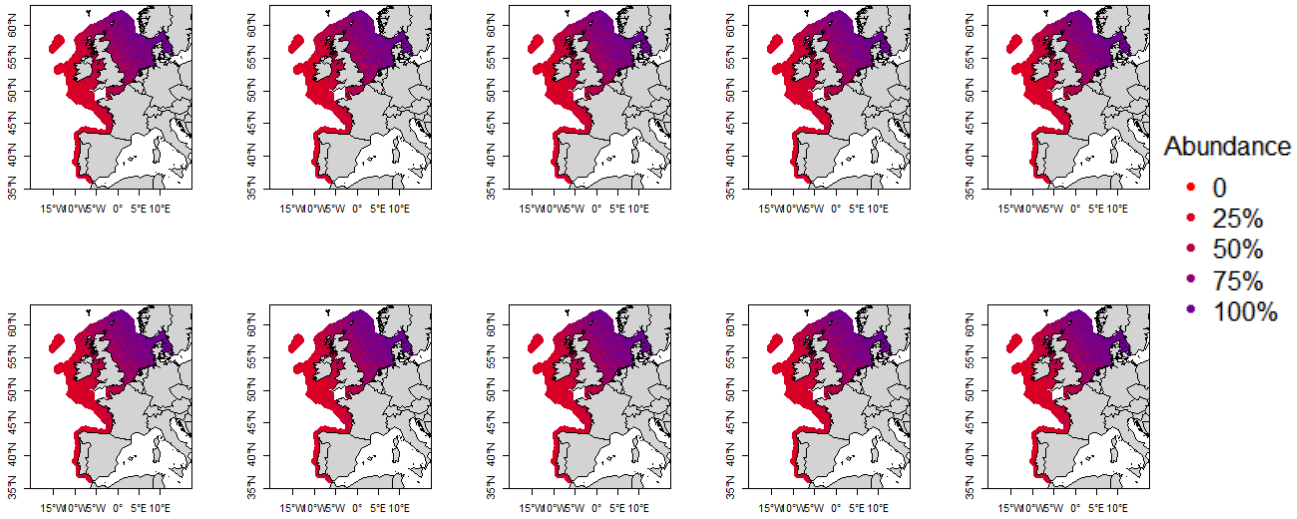

Figure A3.22. Yearly modelled surface generated from the random survey samples.

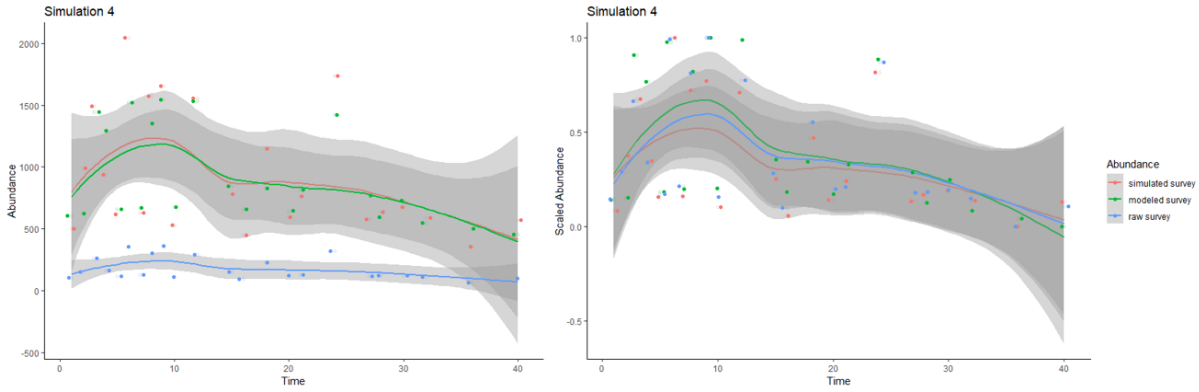

Figure A3.23. Abundance estimates (left) and scaled abundance (right) from the simulated data (red), the raw survey data (blue) and the modelled survey data (green). The mean relative error between the scaled abundance from the simulated data and the scaled abundance from the raw survey data was 9.7%. The mean relative error between the scaled abundance from the simulated data and the scaled abundance from the modelled survey data was 20.1%.

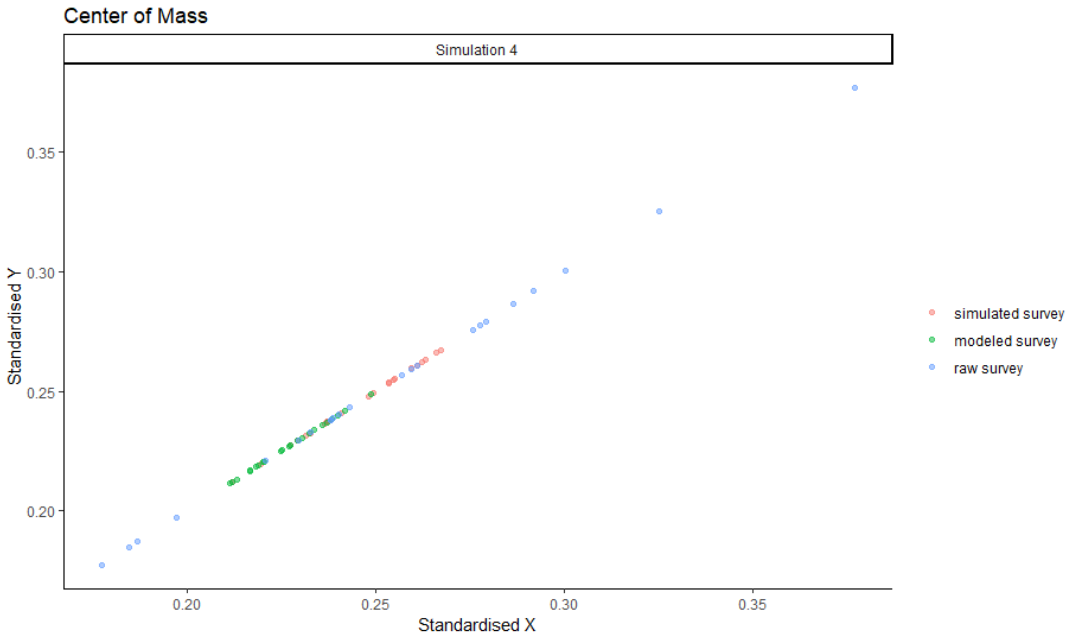

Figure A3.24. Standardised centre of mass estimates from the three datasets. The mean relative error of standardised centre of mass between the simulated data and the raw survey data was 0.030% in the X-axis and 0.008% in the y-axis. The mean relative error of the standardised centre of mass between the simulated data and the modelled survey data was -0.07% in the X-axis and -0.004% in the y-axis.

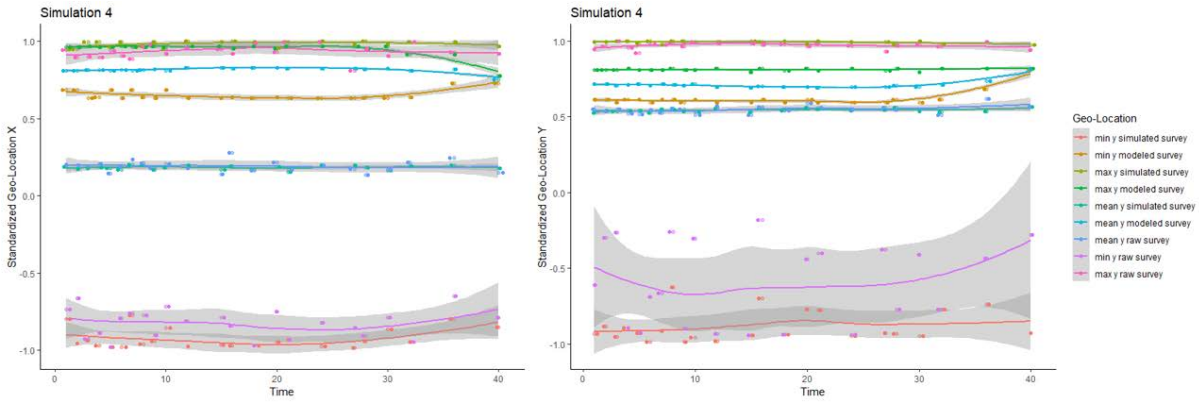

Figure A3.25. Changes in geographical extent or range in X and y-axis from the three datasets.

Simulation 5: strong space-time-trend, for a rare species

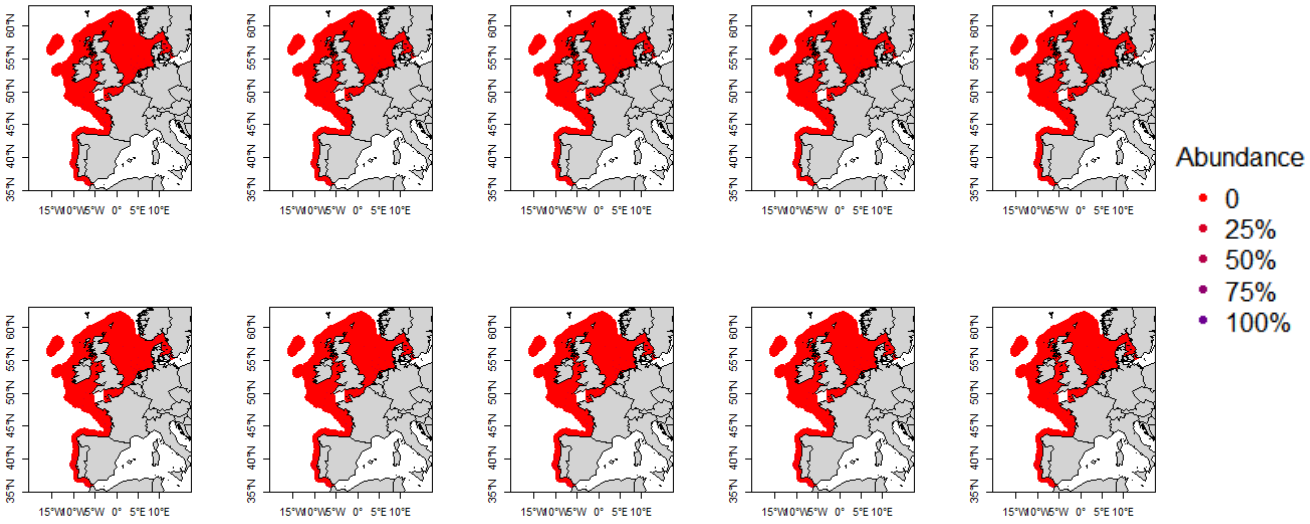

Figure A3.26. Simulated surface from data generating process for scenario 5, a rare species (mean lambda = 0.2) where we have simulated both a spatial and temporal trend in the distribution for ten years.

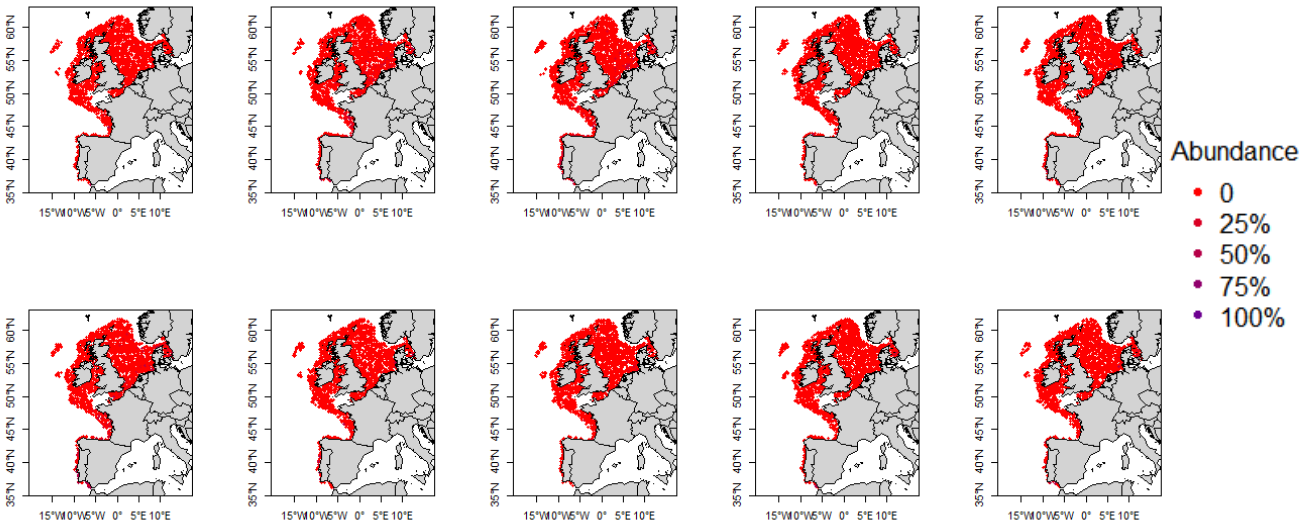

Figure A3.27. Yearly random survey samples (n=2100) taken from the simulated surface.

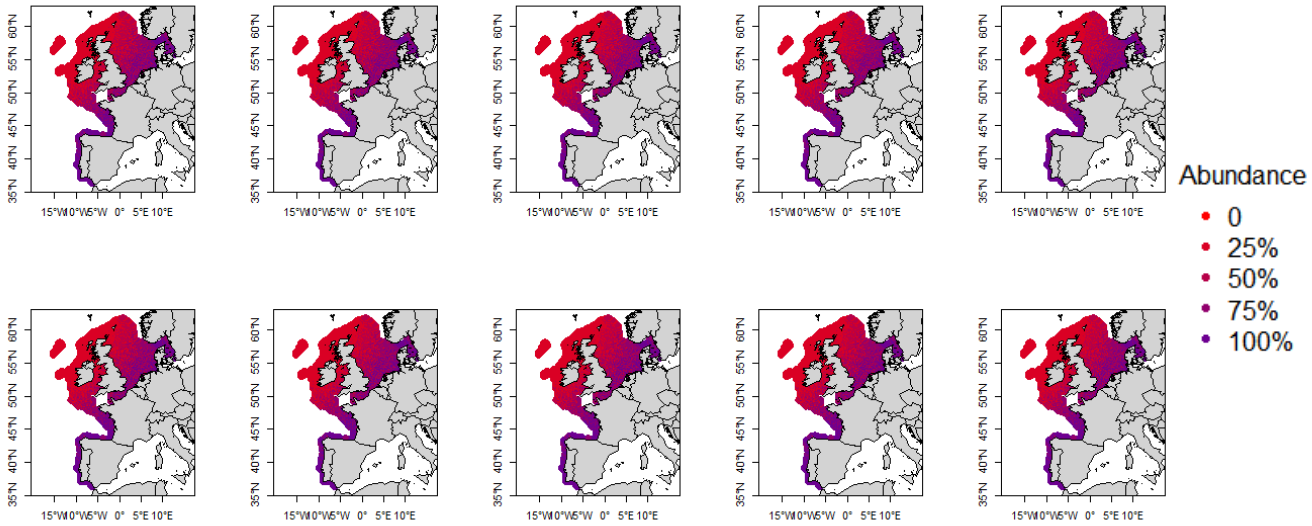

Figure A3.28. Yearly modelled surface generated from the random survey samples.

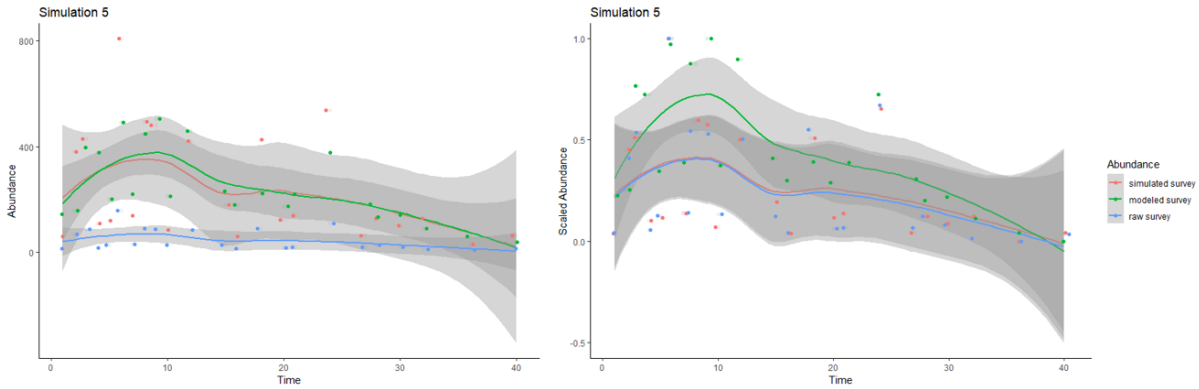

Figure A3.29. Abundance estimates (left) and scaled abundance (right) from the simulated data (red), the raw survey data (blue) and the modelled survey data (green). The mean relative error between the scaled abundance from the simulated data and the scaled abundance from the raw survey data was -5.1%. The mean relative error between the scaled abundance from the simulated data and the scaled abundance from the modelled survey data was 5.7%.

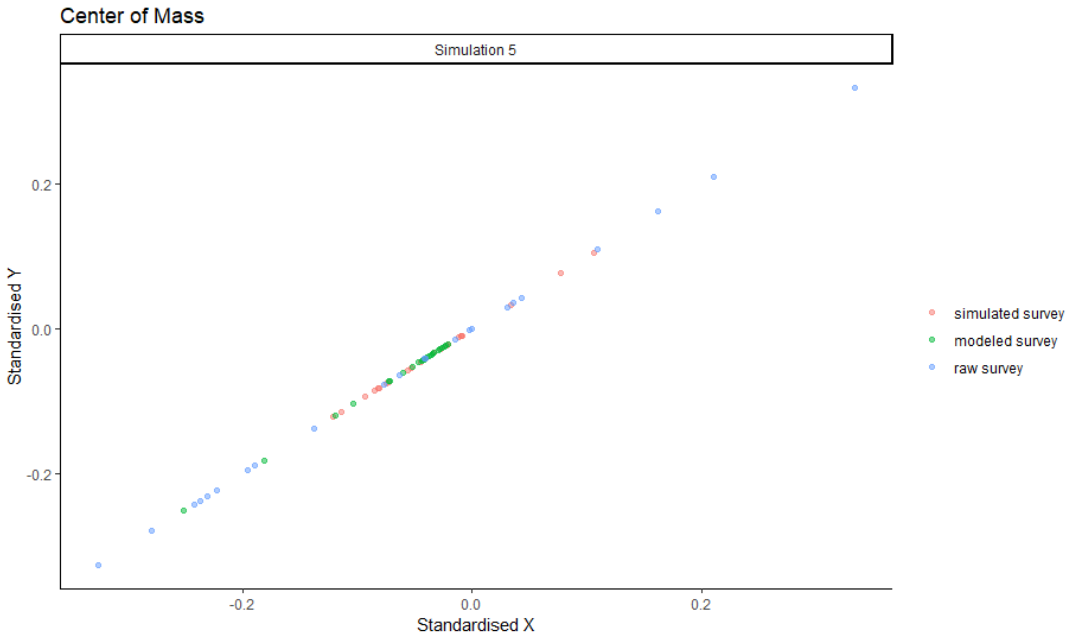

Figure A3.30. Standardised centre of mass estimates from the three datasets. The mean relative error of standardised centre of mass between the simulated data and the raw survey data was 1.86% in the X-axis and 2.84% in the y-axis. The mean relative error of the standardised centre of mass between the simulated data and the modelled survey data was 0.831% in the X-axis and -8.72% in the y-axis.

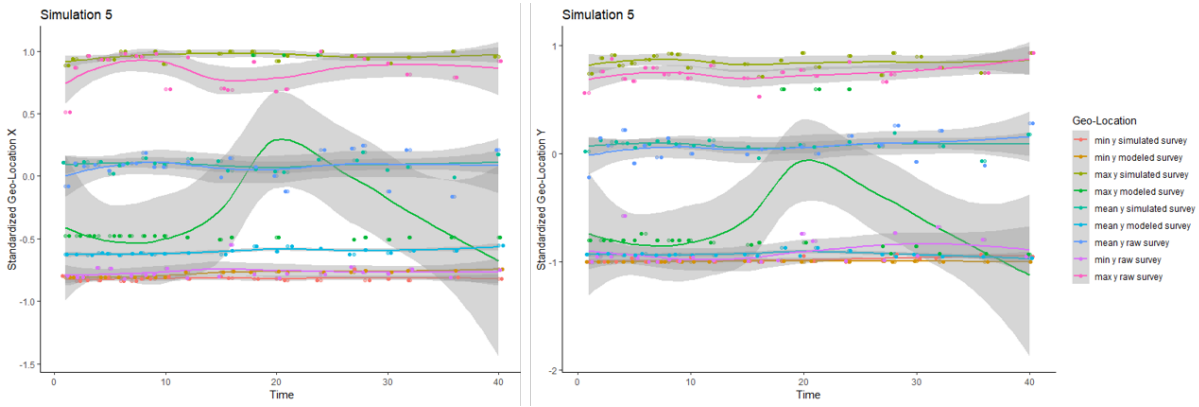

Figure A3.31. Changes in geographical extent or range in X and y-axis from the three datasets.

Simulation 6: strong space-time-trend, with a preference for sandy substrata, for a rare species

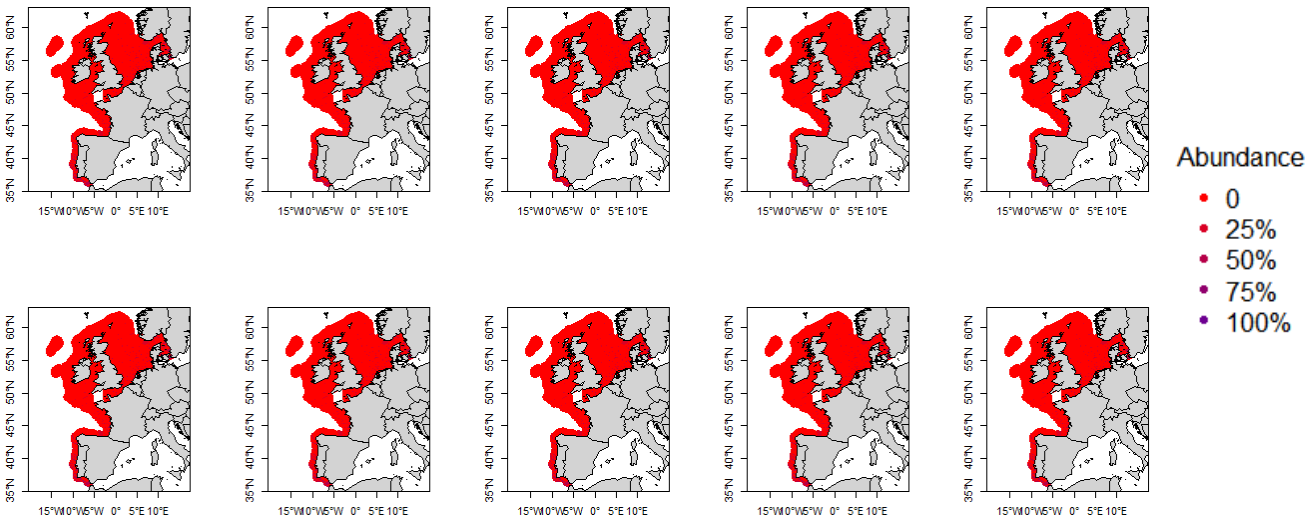

Figure A3.32. Simulated surface from data generating process for scenario 6, a rare species (mean lambda = 0.2) with preference for coarse and mixed sediments where we have simulated a space-time-trend in the distribution showing data for ten years.

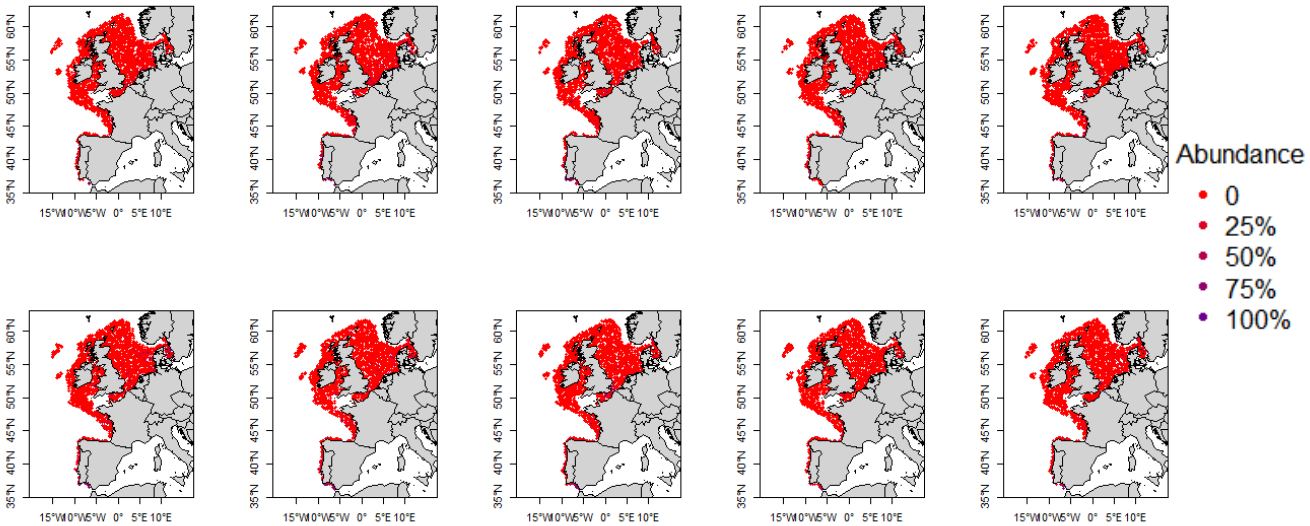

Figure A3.33. Yearly random survey samples (n=2100) taken from the simulated surface.

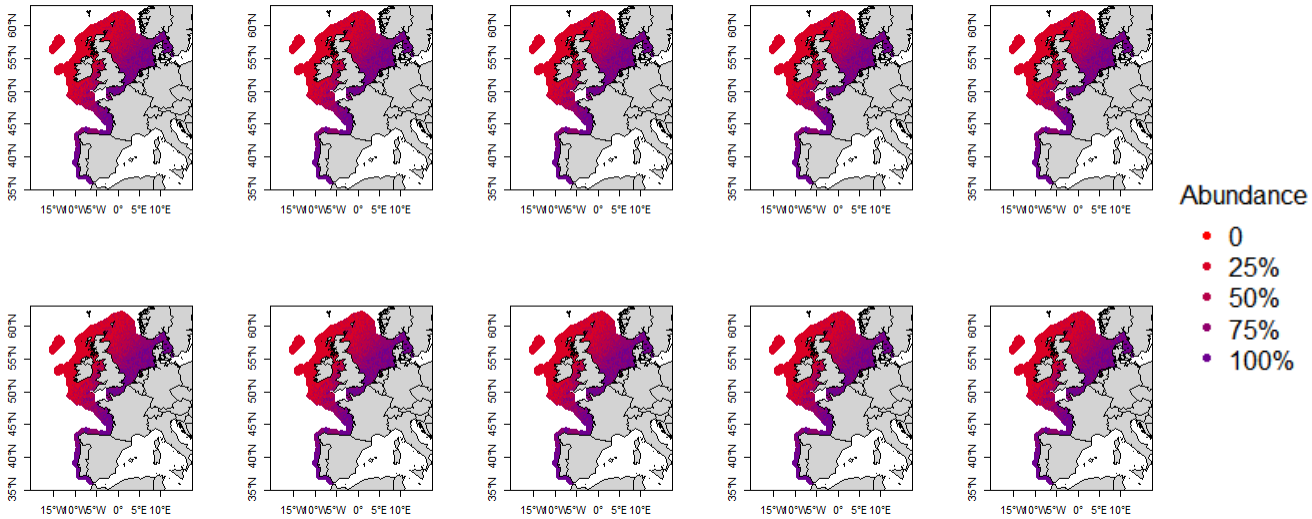

Figure A3.34. Yearly modelled surface generated from the random survey samples.

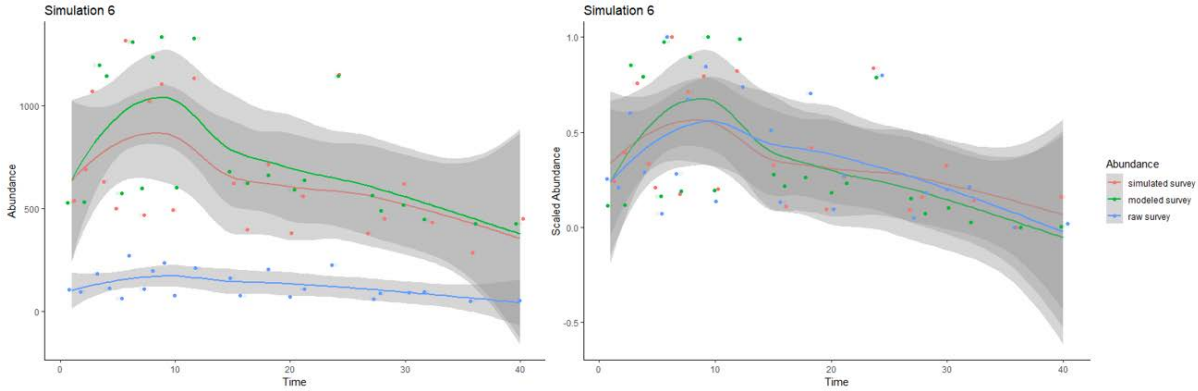

Figure A3.35. Abundance estimates (left) and scaled abundance (right) from the simulated data (red), the raw survey data (blue) and the modelled survey data (green). The mean relative error between the scaled abundance from the simulated data and the scaled abundance from the raw survey data was -3.5%. The mean relative error between the scaled abundance from the simulated data and the scaled abundance from the modelled survey data was 0.29%.

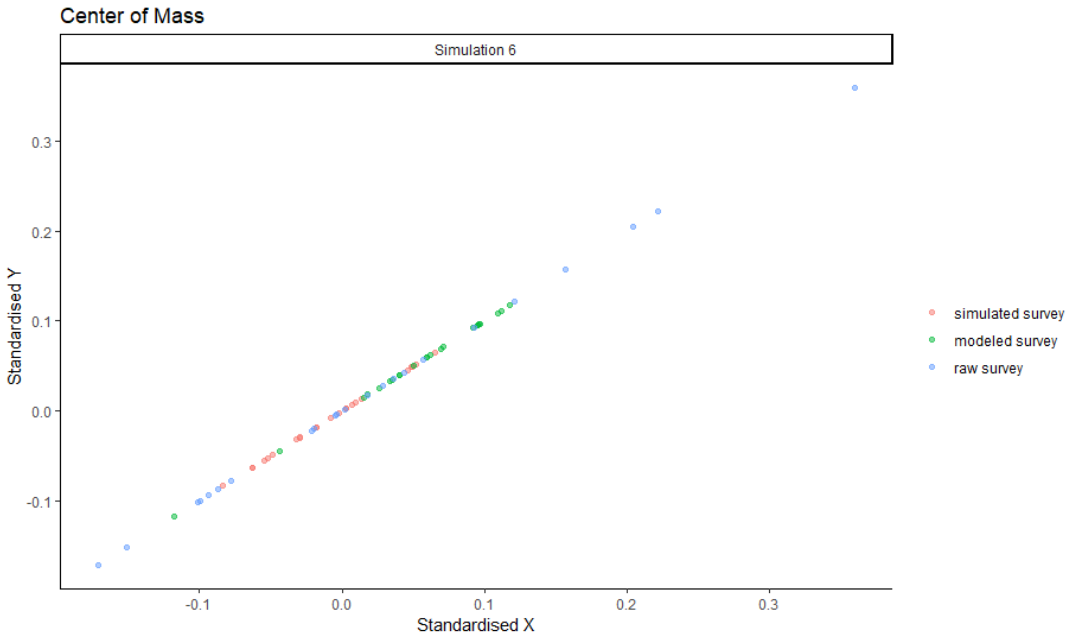

Figure A3.36. Standardised centre of mass estimates from the three datasets. The mean relative error of standardised centre of mass between the simulated data and the raw survey data was -0.45% in the X-axis and -1.77% in the y-axis. The mean relative error of the standardised centre of mass between the simulated data and the modelled survey data was -1.17% in the X-axis and -1.82% in the y-axis.

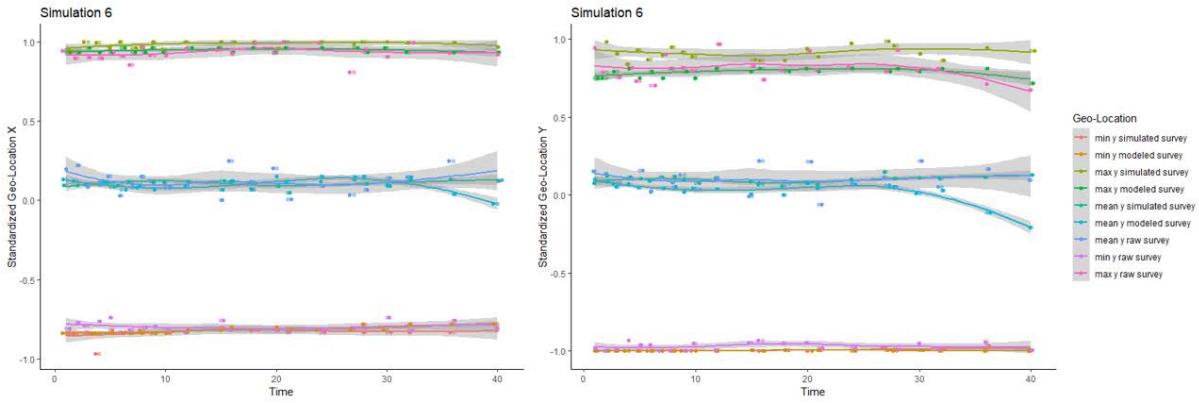

Figure A3.37. Changes in geographical extent or range in X and y-axis from the three datasets.

Annex 4: WGECO terms of reference for the next meeting

WGECO–Working Group on the Ecosystem Effects of Fishing Activities

2020/ /ACOM The **Working Group on the Ecosystem Effects of Fishing Activities** (WGECO), chaired by Tobias van Kooten, NL and Brian Smith, US, will meet in IJmuiden, Netherlands, 31 March–7 April 2020 to:

a) Investigate the ecological consequences of stock rebuilding, with particular emphasis on benthivorous fish and invertebrates.
   1. Make first-order estimates of predation pressure on benthos;
   2. Examine evidence of food limitation and density-dependent growth;
   3. Compare the footprints of trawling to the footprints of predation pressure on benthos.

b) Apply spatial distribution indicators to survey data (fish and benthos) across marine ecosystems. Analyse temporal trends in spatial indicators in relation to potential drivers and pressures (e.g. climate change, abundance changes).

c) Conduct a "reality check" and horizon scanning survey within WGECO. The aim is to develop a consensus view of the major emerging issues in relation to fisheries and ecosystems, and on which WGECO could focus future work. WGECO members will provide a list of emerging issues (horizon scanning), that would benefit from scrutiny by WGECO. This list will be collated and used as material for a plenary discussion, and with the aim of producing a perspectives paper in the ICES JMS or Fish and Fisheries.

WGECO will report by 30 April for the attention of the Advisory Committee.

Supporting Information

Priority	The current activities of this Group will enable ICES to respond to advice requests from member countries. Consequently these activities are considered to have a very high priority. It will also lead ICES into issues related to the ecosystem affects of fisheries, especially with regard to the application of the Precautionary Approach. Consequently, these activities are considered to have a very high priority.
Scientific justification	Term of Reference a) Many stocks are rebuilding and will likely have higher abundance and biomass than we have seen in recent times. This in turn will likely have effects through trophic interactions both up and down the foodweb. At ICES, WGECO and WGSAM have been tasked previously with similar ToRs. WGECO will investigate the potential consequences of stock recovery of benthivorous fish and invertebrates, their ensuing risks for fish stock management and the use of MSFD indicators. It is hypothesized that a large increase in benthivorous fish will have an impact on benthic productivity and biodiversity. This ToR requires data on the spatial distribution of benthivorous predators, their prey consumption rates and diet composition. It also requires data on the abundance and production of benthic faunal. This ToR links to ToR c. Term of Reference b) WGECO has traditionally had a leading role in developing and testing indicators, and their use for provision of advice. The work of this ToR facilitates operationalization of these indicators, by identifying data sources, refining, evaluating their strengths and weaknesses and gaps in indicator availability. Indicators that are evaluated to be promising will be applied to fish and benthic invertebrates species in the ICES region. Term of Reference c) The ICES Strategic Plan seeks to incorporate a wider range of scientific knowledge into advice to inform decision-makers and society about the state of our seas and oceans, the consequences of human use, and option for conservatoin and mangement. This ToR will allow WGECO to contribute strongly to the development of future ICES strategy. We intend to seek input across the national and disciplinary range of WGECO members, many of whom are operating at a high level in the field and in the home institutes. We aim to publish the results of this initiative as a perspective paper in one of the key journals, and this will be available to inform future progress for this important and centrally positioned Expert Group.
Resource requirements	The research programmes which provide the main input to this group are already underway, and resources are already committed. The additional resource required to undertake additional activities in the framework of this group is negligible.
Participants	The Group is normally attended by some 20–25 members and guests.
Secretariat facilities	None.
Financial	No financial implications.
Linkages to advisory committees	There are no current direct linkages with the advisory committees.
Linkages to other committees or groups	There is a very close working relationship with the groups of the Fisheries Technology Committee, WGBIRD, BEWG, WGBIODIV, WGBYC, WGFBIT and WGSAM.
Linkages to other organizations	OSPAR, HELCOM